EXCITED STATE CARBON ACIDITY OF THE BENZYLIC POSITION OF DIBENZANNELATED CYCLOHEPTATRIENES

By

David Patrick Budac
B.Sc., University of Victoria, 1988
M.Sc., University of Victoria, 1990

A Dissertation Submitted in Partial Fulfilment of the
Requirements for the Degree of

DOCTOR OF PHILOSOPHY

in the Department of Chemistry

We accept this dissertation as conforming
to the required standard

Dr. P. C. Wan, Supervisor (Department of Chemistry)

Dr. A. Fischer, Departmental Member (Department of Chemistry)

Dr. C. Bohne, Departmental Member (Department of Chemistry)

Dr. R. D. Burke, Outside Member (Department of Biology)

Dr. C. O. Bender, External Examiner (University of Lethbridge)

University of Victoria

Supervisor: Dr. P. C. Wan

ABSTRACT

The excited state carbon acidity of the benzylic position of *5H*-dibenzo[a,d]cycloheptene (**5**) and *5H*-dibenzo[a,c]cycloheptene (**6**) and a number of their derivatives has been studied in the presence of a variety of bases by the measurement of kinetic isotope effects and structure-reactivity relationships. The purpose of the study was to determine the factors which control the excited state carbon acidity of **5** and **6**. Previous research in this group demonstrated that both **5** and **6** exhibited enhanced carbon acidity in the excited singlet state when irradiated in the presence of a base. It has been proposed that the unprecedented facile ionization of the C-H bond of these systems in S_1 occurs because the incipient carbanion, which has an 8π (4n) internal cyclic array of electrons, is a stabilized species on the S_1 surface, as opposed to the analogous 6π (4n+2) system. A variety of derivatives of **5** and **6** were therefore studied to further probe the mechanism responsible for the substantially enhanced carbon acidity of these systems.

Primary kinetic isotope effects were measured for fluorescence quenching of **5** by H_2O and other bases using the deuterated derivative, 5,5-dideuterio-dibenzo[a,d]cycloheptene (**91**). With bases such as H_2O or EtOH, a kinetic isotope effect of 2.8 ± 0.4 was observed. Use of ethanolamine as base gave a lower isotope effect of 1.4 ± 0.2. The magnitude of these isotope effects suggest that the transition state for C-H bond ionization moves closer to the reactant when a

stronger base is used. A Brønsted β coefficient of 0.07 ± 0.02 determined for general base catalysis of the excited state deprotonation of **5** by a series of primary amines is consistent with an early transition state in these deprotonation.

Substitution of the 5-position of compound **5** with methyl or phenyl was found to reduce the acidity substantially. A stereoelectronic effect has been proposed to account for this decrease in reactivity. Support for such an effect on excited state carbon acidity was obtained by studying *3H*-cyclohepta[2,1-a:3,4-a']dinaphthalene (**88**). Axial and equatorial protons at the site of proton exchange in this system were differentiable by ^{1}H NMR at room temperature. Deuterium incorporation on photolysis was observed predominantly at the axial position. An isomeric system, *3H*-cyclohepta[2,3-a:3,2-a']dinaphthalene (**89**), exhibited efficient formal di-π-methane rearrangement with no evidence for excited state carbon acidity.

Photolysis of 7-deuterio-*5H*-dibenzo[a,c]cycloheptene (**87**) revealed that in conjunction with the excited state acidity observed for **6**, a competitive base catalyzed [1,3] hydrogen shift also takes place. Substitution of **6** at the 6-position with methyl and phenyl reduced the excited state acidity of this system. An enhanced rate of internal conversion has been proposed to account for this effect.

The results of this study substantially increases our understanding of carbon acid behaviour in the excited state, a process discovered only recently in this laboratory.

Examiners:

Dr, P. C. Wan, Supervisor (Department of Chemistry)

Dr. A. Fischer, Departmental Member (Department of Chemistry)

Dr. E. Bohne, Departmental Member (Department of Chemistry)

Dr. R. D. Burke, Outside Member (Department of Biology)

Dr. C. O. Bender, External Examiner (University of Lethbridge)

TABLE OF CONTENTS

List of Tables

List of Figures

Acknowledgements

As a long standing member of Dr. Peter Wan's group I have seen many people come and go. All have indicated how enjoyable it was to work for Peter. I leave this group grudgingly knowing that it does not get any better. Thank you Peter for all you have done and for providing me with such a bright future.

Thanks also to all the people I have enjoyed working with: Erik Krogh, Deepak Shukla, Barb Hall, Chris Lee, Li Diao, Yijian Shi, Beverly Barker, Renee Pollard, Almira Blazek, Carolyn Moorlag, Sukumaran Muralidharan, Xigen Xu, Bing Guan, Cheng Yang, Geoff Zhang, Pin Wu, C.-G. Huang, Wayne Ingham, Ellen Comeau, Francis DeRege and Thao Ho.

To Ian and Liz a special thanks for helping me through a very rough time in my life and best wishes for their future together. Also to all my friends especially Mark Kleinman for editing my introduction.

Finally, thanks to my numerous family members for their support even though they had no idea what I was doing.

Dedication

To my three angels.

CHAPTER 1

INTRODUCTION

Photochemical reactions involving cleavage of bonds in organic compounds can produce different reactive intermediates depending on the type of bond cleavage observed. The most common type is homolytic bond cleavage, where the electrons of the broken bond are equally apportioned to the atoms which originally formed the bond. The radical intermediates produced can either recombine or react further to form products. Norrish Type I and II cleavage of carbonyl compounds are examples of photochemical reactions of this type (Scheme 1.1)[1]. Organic photochemical reactions which produce intermediates

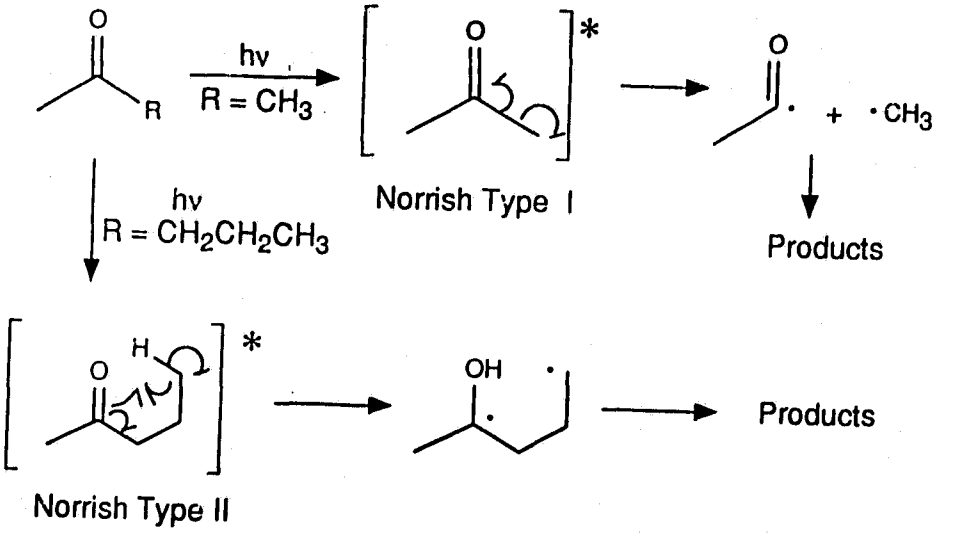

Scheme 1.1

with negative or positive charges via heterolytic bond cleavage are much less common.

The predominance of homolytic cleavage in organic photochemistry is

believed to be due to the use of non-polar solvents for the study of most photochemical processes[2]. In non-polar solvents, homolytic cleavage of bonds is more likely since homolytic bond dissociation energies are lower than heterolytic bond dissociation energies (80 versus 170 Kcal/mol for the C-Cl bond in the gas phase)[2]. However, in a polar solvent the heterolytic bond dissociation energy can be lowered by solvation of the ionic intermediates formed. The use of more polar solvents in photochemical studies has resulted in the discovery of many examples of reactions involving carbocation intermediates. However, significantly fewer examples of reactions involving carbanion intermediates have been found[2,3].

The photoheterolysis observed in the triarylmethyl leuco dye **1** provided one of the first examples of a photogenerated carbocation intermediate[2] (Scheme 1.2). Photolysis of **1** in cyclohexane resulted in homolytic cleavage of the methyl

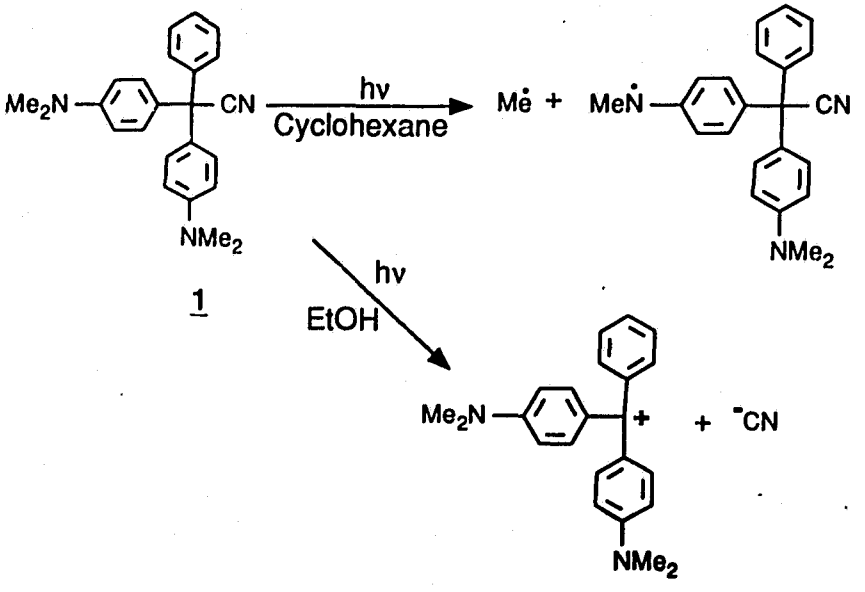

Scheme 1.2

nitrogen bond. However, photolysis in ethanol resulted in predominantly heterolytic cleavage of the benzyl-cyano bond, producing a triarylmethyl cation and cyanide ion.

Photolysis of nitrophenyl acetates (e.g., 2) in aqueous solution provided the first example of photogenerated carbanions, some of which have been spectrophotometrically characterized[4]. Photodecarboxylation occurs to produce the carbanion intermediate 3 which can be protonated to yield the final product 4 (eq. 1.1). Photogeneration of nitrobenzyl carbanions via other routes has also been demonstrated by others[3].

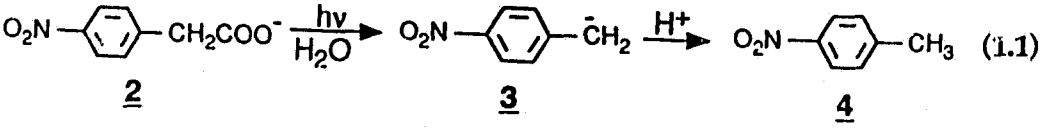

2 3 4 (1.1)

Very little information concerning carbocations and carbanions in photochemical reactions exists compared to the results accumulated for ground state reactions involving these ions. In the ground state, carbanions and carbocations have been studied extensively to provide mechanistic and kinetic data on reactions in this state. Studies of these ions in the excited state should provide similar information on photochemical reactions and the factors which influence them. The majority of the research carried out on the photochemistry of carbocations[5] and carbanions[6], involves excitation of ions generated in the ground state. However, studies have been performed where the required ions are formed in the excited state after excitation of the appropriate substrate[2,3] (e.g.,

photodecarboxylation of **2** to generate **3**).

The influence of aromaticity on excited state reactions involving cyclic arrays of π electrons is one factor which has been studied using photogenerated carbocations and carbanions (*vide infra*). A portion of these studies involve the study of a series of dibenzannelated hydrocarbons which led to discovery of the first types of excited state carbon acids[7,8]. Irradiation of either *5H*-dibenzo[a,d]-cycloheptene (suberene) (**5**) (eq. 1.2) or the isomeric system *5H*-dibenzo[a,c]cyclo-heptene (**6**) (eq. 1.3) in D_2O/ACN (where ACN is CH_3CN) led to incorporation of deuterium at the 5-position. These systems are believed to form carbanion

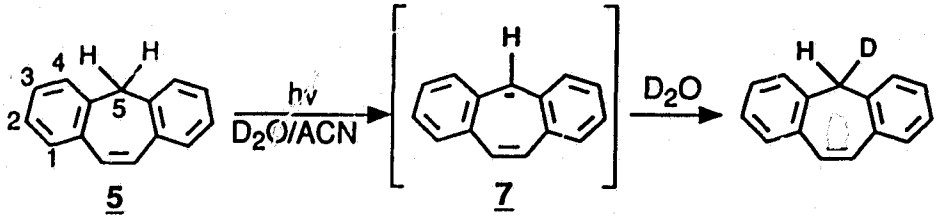

5 **7** (1.2)

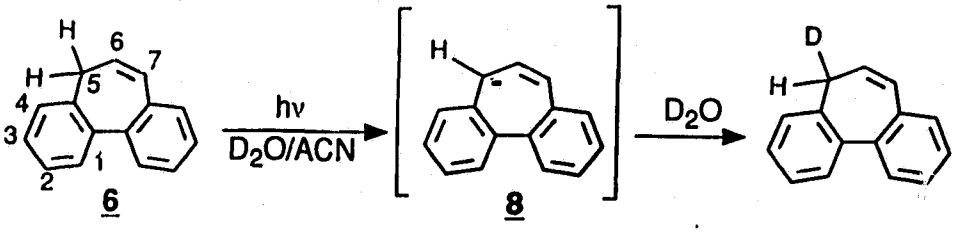

6 **8** (1.3)

intermediates **7** and **8** respectively after deprotonation of the 5-position. These intermediates are formally antiaromatic in the ground state and would therefore not be favoured in this state. The high pK_a of these systems (≈32-38)[9] support this expectation. When the 9-position of fluorene (**9**) is deprotonated a carbanion intermediate (**10**), which is formally aromatic, is formed. In the ground state **9** has a much lower pK_a (≈20-25)[10] than **5** or **6** and is readily deprotonated.

However, photolysis of **9** in D_2O does not result in deuterium incorporation. The facile photodeprotonation of **5** and **6** compared to **9** suggests that carbanion intermediates with cyclic arrays of π electrons having antiaromatic character are favoured in excited state reactions. This result is not unexpected since Dewar[11], Zimmerman[12] and Woodward and Hoffmann[13] have predicted similar behaviour for pericyclic reactions involving transition states consisting of cyclic arrays of orbitals with 4n+2 vs 4n electrons.

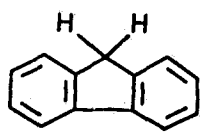

9

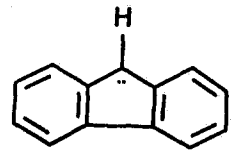

10

The purpose of this research is to further study the reactions of these dibenzannelated systems through structure reactivity relationships and to determine the effect of various amine bases on the excited state carbon acidity of **5** and **6**. The remainder of this Introduction will cover topics relevant to the photochemistry of these compounds. Included will be discussions of: (a) a review of previous studies from this group concerning the excited state carbon acidities of **5** and **6**; (b) aromaticity and antiaromaticity; (c) the Brønsted catalysis law; (d) excited state acid-base chemistry; and (e) di-π-methane rearrangements and photochemical sigmatropic shifts.

1.1 Aromaticity and Antiaromaticity in the Excited State

According to Hückel's rule[12], in the ground state (S_0) a cyclic array of

orbitals with 4n+2 π electrons (where n=0,1,2,...) has special stability ascribed to aromaticity. Systems containing such an array are said to be aromatic (e.g., benzene (11)). Systems with a cyclic array of 4n π electrons which are destabilized relative to acyclic analogs, are said to be antiaromatic according to Breslow[14]. Cyclobutadiene (12), with a 4n cyclic array of π electrons, demonstrates this concept as it is substantially less stable than 1,3-butadiene (13) in S_0.

11

12

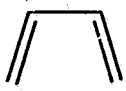

13

Ground state reactions involving intermediates or transition states with cyclic arrays of π electrons are governed by the concepts of aromaticity and antiaromaticity. Excited state reactions are also influenced by these factors but not in the same way. Examples are described in the following section.

1.1.1 Excited State Behaviour of Aromatic and Antiaromatic Species

Wan and Krogh[15] studied the photosolvolysis of a series of dibenzannelated alcohols (14-17). By comparison of the reactivity of each system towards photosolvolysis (e.g., eq. 1.4), they observed a trend in reactivity which is the reverse of that expected in S_0 (based on the relative stabilities of the carbocation intermediates proposed (e.g., 18)). The predicted relative reactivity in S_0 of these compounds was determined by comparison of π electron counts in the centre ring of the charged intermediates. This count determines the nature of the internal

cyclic array (ICA) associated with the intermediate (i.e., for conjugated arrays aromatic (4n+2 electrons) or antiaromatic (4n electrons)). The suberenyl (19) and fluorenyl (18) carbocations which are generated during solvolysis are formally aromatic and antiaromatic, respectively. In S_0, suberenol (17) is more reactive than fluorenol (14). However, in the first singlet excited state (S_1) 14 was found to be more reactive than 17[15].

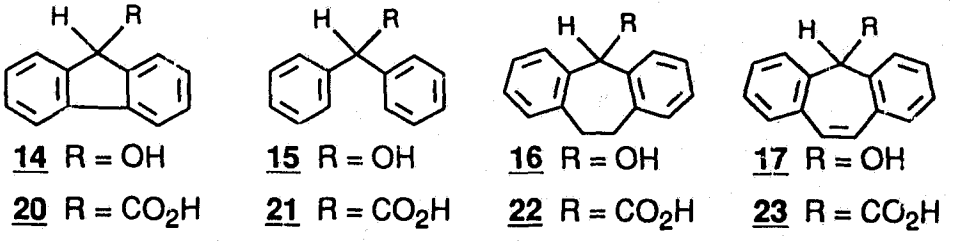

14 R = OH 15 R = OH 16 R = OH 17 R = OH

20 R = CO_2H 21 R = CO_2H 22 R = CO_2H 23 R = CO_2H

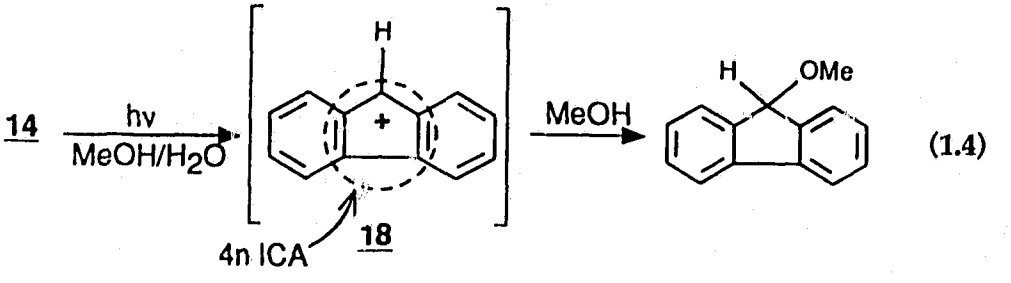

(1.4)

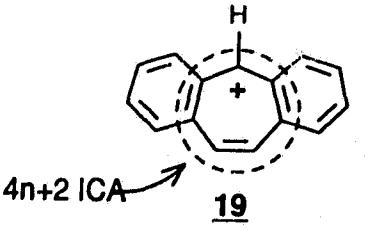

Wan and Krogh[16] also studied the photodecarboxylation of a series of dibenzannelated carboxylic acids (20-23). As observed for the alcohols, the relative reactivity of the acids in S_1 was the reverse of that in S_0. The carbanion intermediates generated by decarboxylation of 23 (eq. 1.5) and 20 (eq.1.6) (7 and

10) are formally antiaromatic and aromatic, respectively in S_0. In the excited state reaction the system able to form an intermediate with a 4n ICA, 23, was more reactive.

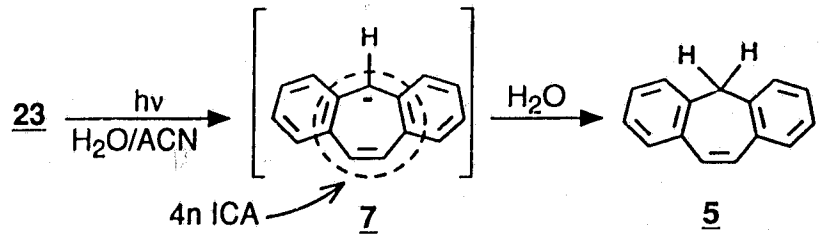

(1.5)

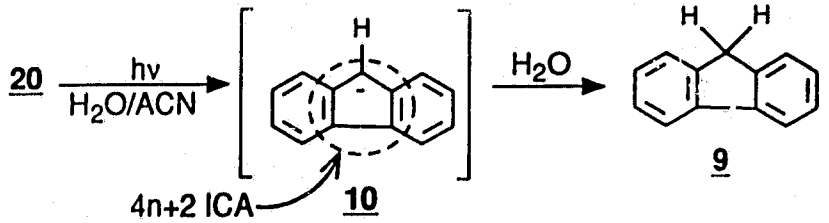

(1.6)

The relative reactivity of the suberene and fluorene systems towards photodecarboxylation and photosolvolysis agrees with the results obtained for the excited state carbon acids 5 and 6 (i.e., excited state reactions involving formally ground state antiaromatic intermediates are more efficient than reactions involving aromatic intermediates). Other compounds in the alcohol and carboxylic acid series do not form conjugated ICAs and have reactivities between that of the fluorene and suberene systems.

The contrasting photochemistry of benzene (11) and cyclobutadiene (12) has also been used to suggest a change in the significance of ground state aromatic and antiaromatic species in the excited state[17]. Benzene (11) as stated is aromatic

in S_0 and stabilized due to delocalization of π electrons in a 4n+2 cyclic array[18]. Photoreactions of **11** suggest a change in the properties of this system in the excited state (eq. 1.7)[19]. However, only minor yields of these products are observed[19]. Cyclobutadiene (**12**) is antiaromatic and rapidly dimerizes in S_0 (eq. 1.8)[19-21]. Dimerization products are not observed after generation of **12** in the excited state, instead acetylene is formed[20]. The product observed after photolysis of **12** cannot be used to suggest a change in the properties of this system in the excited state since these studies were carried out in matrices[20] which would favour unimolecular reactions. The photodecomposition behaviour observed for **11** and **12** does not necessarily indicate a change in ground state aromatic or antiaromatic character in the excited state.

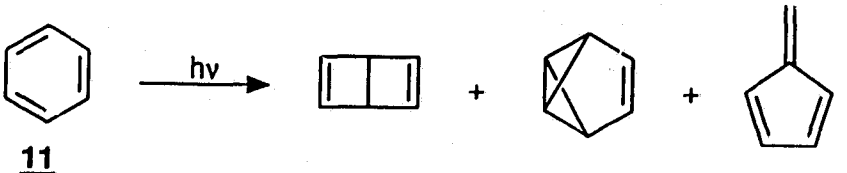

11 (1.7)

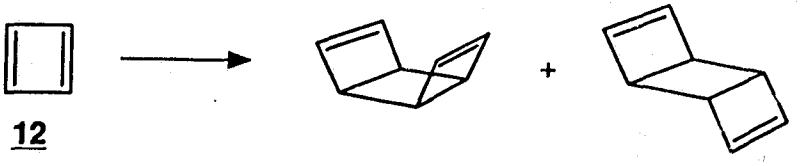

12 (1.8)

However, theoretical calculations of the bond lengths of **11** and **12** in S_0 and S_1 do suggest a change in the properties of these two systems after excitation. One indication of the stability of benzene (**11**) in S_0 is the equivalence of all the C-C bond lengths. Theoretical calculations indicate that in S_1 the bond lengths of

11 are not equivalent, i.e., delocalization of the π electrons is decreased resulting in destabilization of this system[17,22]. Theoretical calculations for 12 indicate a rectangular structure exists in S_0[20,21,23] and a square structure in S_1[17]. These results suggest that the π electrons of 12 are more delocalized in S_1. This in turn may indicate that 12 is relatively more stable in S_1 than in S_0.

1.1.2 Rational for the Behaviour of Aromatic and Antiaromatic Species in the Excited State

Comparison of the electronic configurations of 11 and 12 in S_0 and S_1 has been used to rationalize the behaviour of aromatic and antiaromatic species in different states. Hückel molecular orbital (HMO) theory predicts that the relative energies of the molecular orbitals in 11 and 12 are as shown (Fig. 1.1)[23]. By

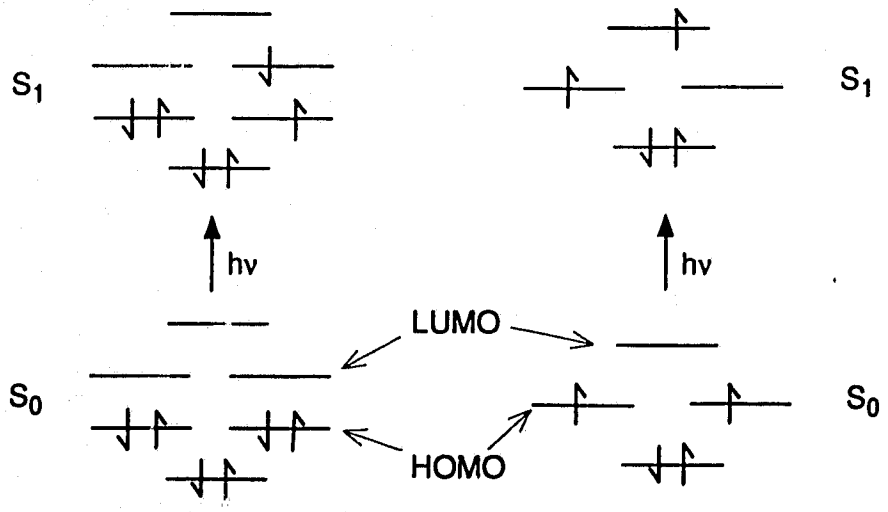

Figure 1.1 The arrangement of π electrons in the molecular orbitals of benzene (11) and cyclobutadiene (12) in S_0 and S_1.

placing the appropriate number of electrons in each set of molecular orbitals (6 for **11** and four for **12**) it can be seen that all the electrons of the former are paired, i.e., **11** has a close-shell arrangement of electrons in S_0. The latter has unpaired electrons, i.e., an open-shell arrangement in S_0[17]. Systems with a close-shell electronic arrangement are believed to be stable whereas species with an open-shell arrangement are unstable.

Excitation of **11** or **12** to S_1 involves promotion of an electron from the highest occupied molecular orbital (HOMO) to the lowest unoccupied molecular orbital (LUMO). The close-shell arrangement of **11** is lost but the open-shell arrangement of **12** remains (Fig. 1.1). The former would therefore be less stable in S_1 than in S_0, whereas the latter would experience no change in stability. The excited state behaviour of aromatic systems can be explained using this argument. However, the behaviour of antiaromatic system such as **12** in excited states requires further reasoning.

The behaviour of **12** can be explained by considering a more accurate molecular orbital representation of this system. By using a "rectangular" representation of **12**, instead of a "square", the distribution of molecular orbitals can be drawn without the degeneracy shown earlier for the two non-bonding orbitals (Fig. 1.2)[23]. Ab initio studies support this molecular orbital configuration since they indicate that **12** has a singlet ground state with all the electrons paired[19] (Fig. 1.2) as opposed to a triplet ground state with unpaired electrons (Fig. 1.1). Excitation of **12** therefore promotes an electron from a non-bonding HOMO to a

non-bonding LUMO. This results in delocalization of the π electrons of 12[24] due to the presence of electrons in both the LUMO and HOMO orbitals.

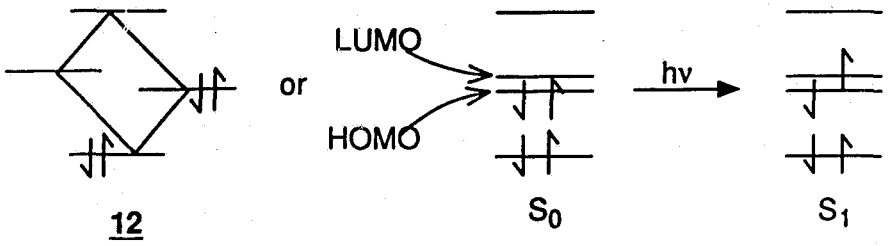

12

Figure 1.2 Corrected molecular orbital distribution for cyclobutadiene (12).

Other antiaromatic systems such as the heptaphenylcycloheptatrienyl anion (24) would be predicted by HMO theory to have a triplet ground state with an open-shell arrangement (unpaired electrons). However, only a singlet ground state (paired electrons) has been detected[25]. The antiaromatic species pentaphenylcyclopentadienyl cation (25) is also predicted by HMO theory to have

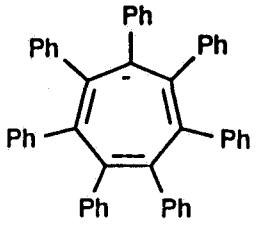

24

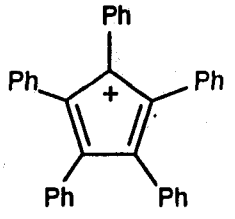

25

a triplet ground state. A triplet is observed but it was found to exist in equilibrium with the singlet ground state[25]. The presence of singlet ground state character in 24 and 25 suggests that the degeneracy of orbitals predicted by HMO theory for these systems does not exist.

The preference for intermediates with ICAs consisting of 4n rather then 4n+2 π electrons in S_1 may therefore be due to the involvement of non-degenerate orbitals as opposed to the degenerate orbitals predicted by simple HMO theory. Therefore, excitation of an electron to a non-bonding rather then antibonding orbital occurs which may stabilize an anti-aromatic species by allowing more delocalization of the π electrons as suggested for 12 in S_1. ICAs consisting of 4n+2 π electrons in S_1 exist with the promoted electron residing in an antibonding orbital and are therefore less delocalized resulting in a less stable species.

1.2 The Brønsted Catalysis Law

Conversion of reactants to products in a chemical reaction involves one or more steps, each with a transition state. By looking at a reactant and the resulting products, several mechanisms may be proposed. In order to determine which mechanism operates, under a given set of conditions, the intermediate species and the transition states involved must be delineated. Transition states are difficult to probe directly and often the intermediates are too short lived. Therefore, indirect methods are frequently required. One method used to probe transition states of chemical reactions involving acid or base catalysis is the Brønsted catalysis law[26] (eq. 1.9 and 1.10).

$$\log k_{AH} = -\alpha pK_a + \text{constant} \qquad (1.9)$$

$$\log k_B = \beta pK_a + \text{constant} \qquad (1.10)$$

The Brønsted catalysis law, developed by Brønsted and Pedersen[27,28] in

1924, involves the correlation of the observed rates (k_{AH} for general acid catalysis and k_B for general base catalysis) of a reaction with the pK_as of the acids or bases used to catalyze it. The Brønsted coefficients α and β are used to indicate the extent of bond formation and breaking in the transition state[26,29]. The following section of the Introduction will include a discussion of general acid and base catalysis and the different facets of the Brønsted catalysis law. The importance of this law with respect to carbon acids and photochemical reactions will be discussed in subsequent sections of this Introduction.

1.2.1 General Acid-Base Catalysis

Many chemical reactions carried out in solution may be sluggish or not proceed at all unless an acid or base catalyst is present. Two types of acid or base catalysis can occur. The type involved depends on the stage in the reaction at which the catalysis takes place[26]. If the proton transfer occurs in the rate limiting step, then general acid or base catalysis is implied. However, if the proton transfer is not involved in the rate limiting step (i.e., it is involved in a rapid pre-equilibrium) then specific acid or base catalysis is implied. This generalization arises from the fact that the strongest acid and base in aqueous solution are H_3O^+ and HO^-, respectively, due to the levelling effect of water[26,30]. Therefore, any reaction in this solvent which involves rapid proton transfer will involve H_3O^+ and HO^- rather then the general Brønsted acid or base. The latter acid or base react at a slower rate and can only catalyze a reaction where the proton transfer

occurs in the slowest step, i.e., the rate limiting step.

A simple technique used to differentiate specific and general acid or base catalysis is to plot the observed rates of a reaction against the acid or base concentration at a constant ionic strength (Fig. 1.3)[26]. If a line with a slope of zero is obtained, specific acid or base catalysis is implied since only H_3O^+ or HO^- catalyze the reaction. However, if a line with a positive slope is obtained with increasing concentrations of the added acid or base then general acid or base catalysis is implied since acids or bases other then H_3O^+ or HO^- can catalyze the reaction.

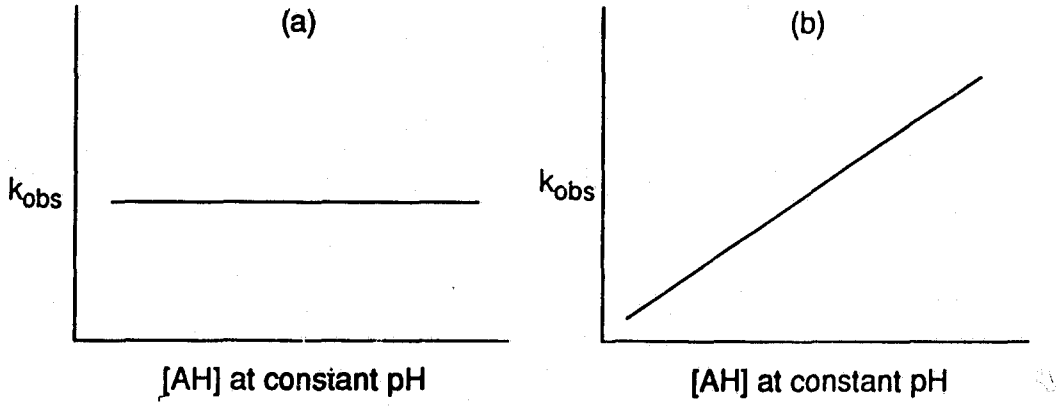

Figure 1.3 Plots of k_{obs} vs [AH] for (a) specific acid catalysis and (b) general acid catalysis.

1.2.2 Linear Free Energy Relationships

In 1924 Brønsted and Pedersen[27] studied the base catalyzed decomposition of nitramide (26) using a series of bases (carboxylates) (eq. 1.11). The mechanism

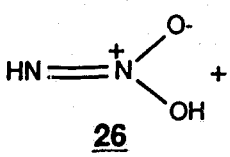

26

$$+ \; B^- \longrightarrow BH + N_2O + HO^- \qquad (1.11)$$

involved in this decomposition is still being studied today[31]. However, in the original work, Brønsted and Pedersen[27] found that the rate of decomposition, when plotted against the pK_a of the bases used for catalysis of the reaction, provided a linear relationship. These results yielded the first example not only of general base catalysis but of a linear free energy relationship (LFER). The Hammett equation and other LFERs developed subsequent to the Brønsted catalysis law[32] have been found very useful in the study of reaction mechanisms. Of these LFERs, the Brønsted catalysis law is believed to be the most accurate[33,34].

The Brønsted catalysis law as presented in equations 1.9 and 1.10 does not involve free energy (ΔG) terms. However, such terms can be substituted in using the relationships between ΔG, reaction rates (eq. 1.12), and equilibrium constants

$$\Delta G^{\ominus\ddagger} = -RT\ln k + \text{constant} \qquad (1.12)$$

$\Delta G^{\ominus\ddagger}$ = standard molar free energy of activation for a reaction.

$k = k_A$ or k_B from equations 1.9 and 1.10.

$$\Delta G^{\ominus} = -RT\ln K \qquad (1.13)$$

$\Delta G^{\ominus}$ = standard molar free energy.

K = equilibrium constant for the acid or base used.

(eq. 1.13)[26]. By converting pK_a in equation 1.9 or 1.10 to $-\log K_a$, differentiating the resulting equation and substituting in $\Delta G^{\ominus\ddagger}$ and $\Delta G^{\ominus}$ the linear standard molar free energy relationship of the Brønsted catalysis law is obtained (eq. 1.14). This

equation now represents a linear relationship between the standard free energy

$$\delta\Delta G^{\ominus\ddagger} = (-\alpha \text{ or } \beta)\delta\Delta G^{\ominus} \qquad (1.14)$$

of activation and the total standard free energy change of a reaction, i.e., a linear free energy relationship.

It is not necessary to use thermodynamic terms in the Brønsted catalysis law, since rates and pK_a are sufficient. As equations 1.9 and 1.10 indicate, Brønsted plots involve the correlation of k_{AH} or k_B and the pK_a of the catalysts utilized (acid or base). The rates plotted must not include a contribution from the specific catalysts (H_3O^+ or HO^-) and, therefore, must be obtained by varying the catalyst's concentration while maintaining a constant pH with buffers[26]. This procedure is repeated for other acids or bases with different pK_a but which have similar structures. Similar structures are required for catalysts to minimize changes in the transition state (i.e., steric interactions). The resulting data can be used to obtain a Brønsted plot, which can be used to obtain the pK_a of very weak carbon acids where dissociation is not directly measurable[29] (*vide infra*). The main use, however, of such data is for the study of transition states in reactions subject to general acid or base catalysis. This is accomplished by determining the magnitude of α or β from the slope of the plot.

1.2.3 Significance of the Brønsted Coefficients α and β

The Brønsted coefficients, α and β are measures of a reaction's sensitivity to general acid or base catalysis[30]. In general values of α and β are found to vary

between 0 and 1. A value between 0 and 0.5 indicates that general catalysis is not significant while a value between 0.5 and 1 indicates that general catalysis is significant. When α or β approaches 0 or 1 then specific acid or base catalysis is inferred. Values outside the range 0 to 1 have also been obtained. The significance of these values will be discussed later.

The magnitude of the Brønsted coefficient is also used to indicate the mean position of the transition state for a series of acids or bases along the reaction coordinate. The Brønsted catalysis law is therefore related to the Hammond Postulate[30], which states that the transition state of an exothermic reaction resembles the reactants and the transition state of an endothermic reaction resembles the products. According to the Brønsted catalysis law, coefficients between 0 and 0.5 indicate the transition state is closer to the reactants and between 0.5 and 1 indicate the transition state is closer to the product. From such data, transition states have been drawn and conclusions made about the charge distribution during bond breakage or formation[35]. However, use of the Brønsted catalysis law for such purposes is considered unsound since the law does not include variables which account for charges. Nevertheless, the law is used extensively in many areas of chemistry including studies involving carbon acids[29].

1.1.3 Carbon Acids and the Brønsted Catalysis Law

The Brønsted catalysis law has been used to study carbon acids and conversely, carbon acids have been used extensively to study the Brønsted

relationship. The following are some of the reasons for the utility of carbon acids:

(i) The pK_a of many carbon acids have been measured in different solvents, which allows for the study of solvent effects on the Brønsted catalysis law[36,37].

(ii) The carbanions formed from conjugated carbon acids are usually stabilized by delocalization of the negative charge. Due to this effect, minor changes in the structure can be made, which in turn causes large changes in pK_a[36]. This is important in Brønsted catalysis studies, since a homogeneous group of acids or bases (such as those obtained by making minor changes in carbon acid structures) is required to ensure that steric factors in the transition state remain constant.

(iii) Deprotonation of most carbon acids involves kinetic acidities[29] (*vide infra*). These kinetic acidities can be related to thermodynamic properties using the Brønsted catalysis law which correlates rate and equilibrium free energies[38,39].

The origin of these properties which make carbon acids useful in the study of the Brønsted catalysis law lie in the difference between these acids and other acids such as oxygen, nitrogen or sulphur based systems. Two types of carbon acids exist, kinetic and equilibrium acids[40]. The latter are similar to other acids since the lone pair of electrons left after deprotonation remains on the atom which lost the proton. Phenylacetylene (27) is an example of such a carbon acid (eq. 1.15)[41]. In kinetic carbon acids the lone pair of electrons is delocalized. This

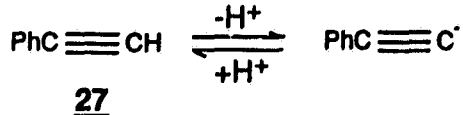

27 (1.15)

delocalization involves rehybridization and rearrangement of the carbanion generated (eq. 1.16). As a result, rates of deprotonation observed for kinetic carbon acids are much slower than for the corresponding oxygen, nitrogen and

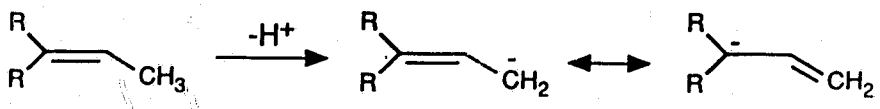

(1.16)

sulphur acids. For example, the rate of deprotonation by ^{-}OH observed for fluorene (9) (a strong kinetic carbon acid, $pK_a \approx 20\text{-}25$)[10] is $\approx 10^4$ $M^{-1}s^{-1}$ in H_2O[42]. Deprotonation of oxygen, nitrogen and sulphur acids under similar conditions occur at rates approaching 10^{10} $M^{-1}s^{-1}$ [41]. Though this behaviour of kinetic carbon acids can facilitate studies of the Brønsted catalysis law it can also lead to problems when using the law to study carbon acids (*vide infra*). Nevertheless, the Brønsted catalysis law has been found useful in the study of carbon acid pK_as.

The pK_as of weak carbon acids have been determined using Brønsted plots[29]. This is accomplished by measuring the rate of exchange of a label such as deuterium or tritium from a carbon acid by a base. The pK_a of the carbon acid is then determined by plotting this rate of label exchange along with rates for similar carbon acids against the known pK_a's of these latter carbon acids. Extrapolation of the pK_a for the desired carbon acid can then be accomplished. However, before this is done one must ensure that the rate of label exchange measured corresponds to the rate of proton loss from the carbon acid[29]. This will not be the case if internal return competes with exchange (reverse of eq. 1.17).

Internal return is important for carbon acids since a solvation shell holds the carbanion and the deuterium that was removed by base (B^- where M^+ is the counterion of B^-), in close proximity. Return of a deuterium to the carbanion before protonation by the solvent (SH) can therefore occur (eq. 1.17). If the system contains an excess of BH compared to substrate RD then the last two steps will not be reversible (eq. 1.18 and 1.19). Using the steady state approximation[29] for R^-M^+ an equation can be obtained for the observed rate of the reaction ($k_{obs} = k_1k_2/[k_{-1} + k_2]$). Two possibilities exist ($k_2 >> k_{-1}$ and $k_2 << k_{-1}$) which can be differentiated using isotope effects[29]. In the former case a primary isotope effect will exist since k_{obs} will equal k_1. A small isotope effect will be observed in the latter case since k_{obs} will equal k_1k_2/k_{-1}.

$$RD + B^-M^+ \underset{k_{-1}}{\overset{k_1}{\rightleftharpoons}} R^-M^+ \cdots\cdots BD \qquad (1.17)$$

$$R^-M^+ \cdots\cdots BD + SH \xrightarrow{k_2} R^-M^+ \cdots\cdots BH + SD \qquad (1.18)$$

$$R^-M^+ \cdots\cdots BH \longrightarrow RH + B^-M^+ \qquad (1.19)$$

The pK_a of many carbon acids have been estimated using the above technique. However, corrections developed using the Eigen model[26,43] and Marcus theory[26,41,44] are often required due to problems associated with the Brønsted catalysis law.

1.2.4 Deviations in the Brønsted Catalysis Law

Two types of deviation occur for the Brønsted catalysis law: 1) anomalous values of α and β, i.e., values outside the range 0-1; and 2) non-linear Brønsted plots. Several reasons have been proposed for the former deviation which is commonly observed for carbon acids. Bordwell and Hughes[45] proposed that delocalization and solvation of the anion formed after deprotonation were responsible for anomalous values of α. These problems occur because rehybridization of the carbon lags behind the deprotonation step and alters the rate of exchange[46] (eq. 1.20). Solvation of the molecule will change since the charge moves from the carbanion onto adjacent groups. These effects are readily observed in the deprotonation of nitroalkanes (28)[37].

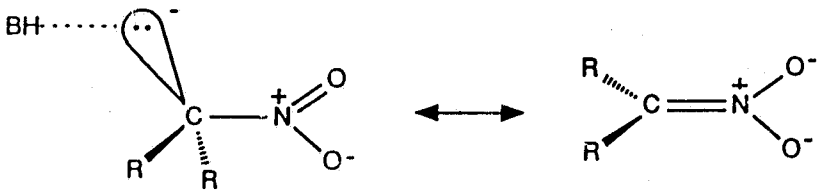

28 (1.20)

The effect of these problems on Brønsted plots can be observed by using Eigen's model of proton transfer[26,29,43] which involves hydrogen bonding steps before (*a* to *b*) and after (*c* to *d*) the proton transfer (eq. 1.21). The transfer of a proton can be represented by reaction coordinate diagrams (with HB as the

$$\underset{a}{HA + B} \rightleftharpoons \underset{b}{AH\cdots B} \rightleftharpoons \underset{c}{A\cdots BH} \rightleftharpoons \underset{d}{A + BH} \qquad (1.21)$$

stronger acid) (Fig. 1.4)[29]. The first curve represents a proton transfer between two atoms which do not require rehybridization, i.e., nitrogen, oxygen or sulphur. In this situation the rate limiting step is *c* to *d*. The second curve proposed by Bordwell and Hughes[45] is for a carbon acid requiring rehybridization. The adjustments made to this reaction profile lead to a new rate determining step (*b* to *c*). However, the equilibrium free energy change of the reaction will be governed by the overall reaction *a* to *d*. The position of *d* relative to *a* is dependent on the rehybridization process and this in turn is affected by factors such as solvent polarity and the substituents present on the carbon acid. The rate of the reaction will not be affected by these two factors to the same extent as the rehybridization process. Therefore, a linear free energy relationship will no longer exist as the rates of the reaction will not correlate with the free energy

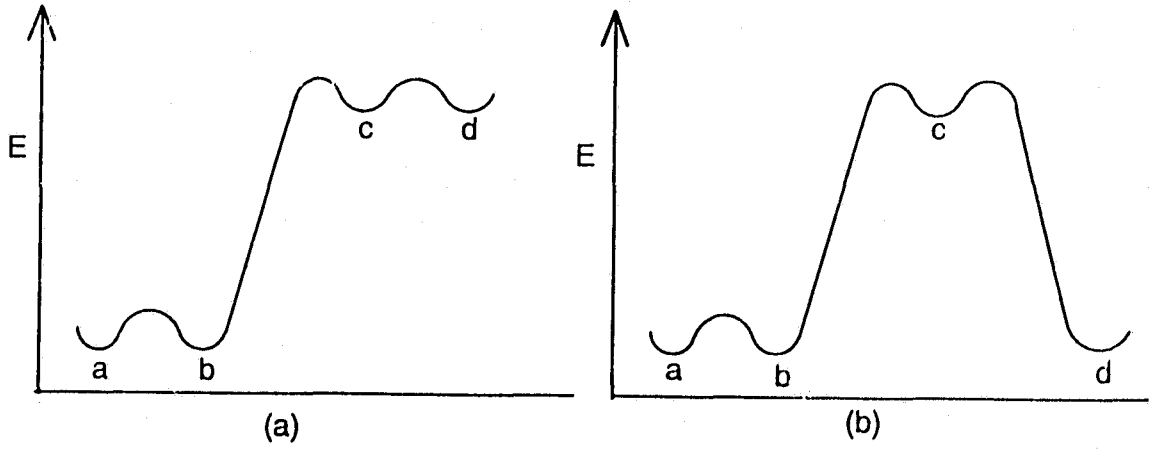

Figure 1.4 Reaction coordinate for proton exchange of (a) an oxygen, nitrogen or sulphur acid and (b) a carbon acid.

changes associated with the reaction. Both anomalous values of α and β and non-linear plots can result from this lack of correlation.

Solvation and rehybridization problems associated with the Brønsted catalysis law are termed "Imbalances" by Jencks and coworkers[46-49]. Imbalances exist when all of the factors involved in a process are not perfectly correlated[46]. Such an occurrence is very likely in the Brønsted catalysis law as it correlates only two factors, rate and equilibria. Various solvation problems[46-48,50], electrostatic effects[49], and resonance effects (rehybridization)[46,47] are factors not correlated by the Brønsted catalysis law. Pross[51] further claims that values of α and β depend largely on the site of reaction not the reaction type. Anomalous values of α and β are obtained when substituents are placed near the reaction site, affecting the rate of the reaction and the equilibrium free energy change differently. A linear correlation of free-energies, therefore, no longer exists resulting in anomalous Brønsted coefficients. As indicated, this is especially true for carbon acids which rehybridize on deprotonation.

Non-linearity in Brønsted plots, as previously mentioned, can result from solvation and rehybridization imbalances. This is why Brønsted plots for carbon acids are generally curved. Non-linearity can also exist in Brønsted plots of reactions not involving carbon acids. The non-linearity observed in these cases is due to changes in the reaction, such as an altering of the mechanism or the relative rates of each step as the pK_a of the general acid or base is changed[26,30]. A plot can also be non-linear due to limitations on the rate of reaction, i.e., the

rate can only be increased to the diffusion limit by the catalysis[26]. This limitation leads to a levelling off of the Brønsted plot. In general all Brønsted plots become non-linear if a sufficient pK_a range of catalysts is used, due to the problems just discussed and due to changes in the catalysts which effect the steric factors in the transition state[26,41].

Despite the controversy surrounding the Brønsted catalysis law, it is used in many studies. More recently the law has been applied to photochemical reactions to gain insight into excited state processes.

1.3 Excited State Acid-Base Chemistry

Acid-base chemistry is very important in photochemical reactions, both as a fundamental process, i.e., excited state proton transfer (ESPT), and as a catalyst for excited state reactions. The latter topic was reviewed recently[52] and numerous reviews[53-57] have appeared on the former topic including two recent reviews concerning intermolecular[58] and intramolecular[59] ESPT. This section will summarize both aspects of acid-base chemistry in the excited state.

1.3.1 Excited State Proton Transfer

In 1931 Weber[60] noted that the fluorescence of 1-naphthylamine-4-sulphonate (29) was shifted when the pH was changed. Eighteen years later Förster[61] attributed this shift to the formation of a *new emissive species* obtained by ESPT. Subsequently Weller[62] proposed a method for determining the excited state

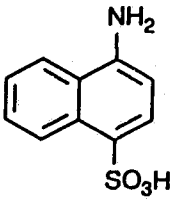

29

pK_a using this shift in the fluorescence spectrum. Since these early studies, ESPT has been shown to be a fundamental process in the photochemistry of numerous substituted aromatic compounds.

The shift in fluorescence with change in pH is clearly shown for 2-naphthol (30) (Fig. 1.5)[53]. In general, deprotonation or protonation of excited state species results in a shift of the fluorescence to longer wavelengths[55,57]. Aromatic systems with electron withdrawing groups (EWGs) (carboxylates, carbonyls and amides) are protonated in the excited state whereas systems with electron donating groups

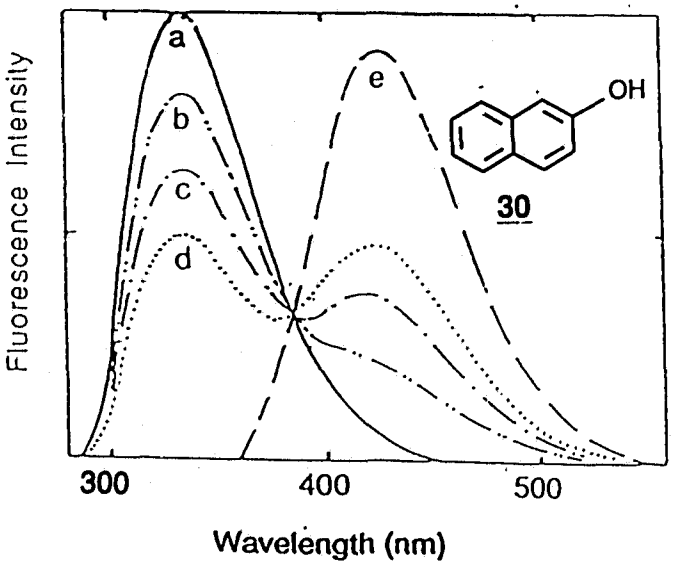

Figure 1.5 Shift in the fluorescence spectrum of 2-naphthol (30) with increasing pH a-e.

(EDGs) (hydroxyls, amines and sulfhydryls) are deprotonated. Both processes result in the formation of a new species which emit fluorescence at longer wavelengths.

Protonation of EWGs in the excited state results from a redistribution of electron density in the molecule as it goes from S_0 to S_1[57]. Substituents such as carboxylates have empty low lying π orbitals which can accept electrons from the π orbitals of the aromatic system when the latter is excited. The increased electron density on the substituent is then stabilized by protonation of this position. Benzoic acid (31) provides an example of this excited state behaviour (Scheme 1.3)[54,55].

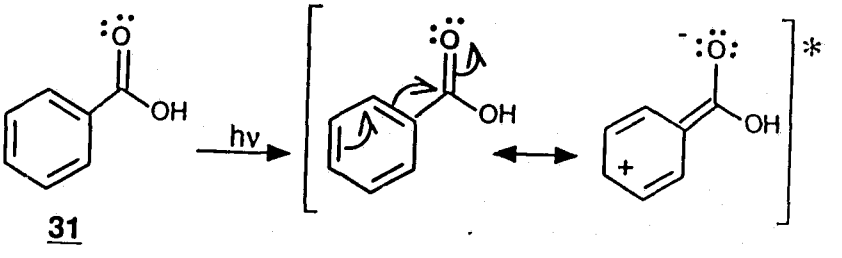

31

Scheme 1.3

Deprotonation of EDGs also results from redistribution of electron density after excitation of the appropriate molecule from S_0 to S_1[57]. However, the direction of electron movement is from the substituent to the π system of the aromatic ring. EDGs such as hydroxyls have a lone pair of electrons which can be donated into the aromatic ring as shown for phenol (32) (Scheme 1.4)[54,55]. The resulting species is stabilized by deprotonation of the hydroxyl group.

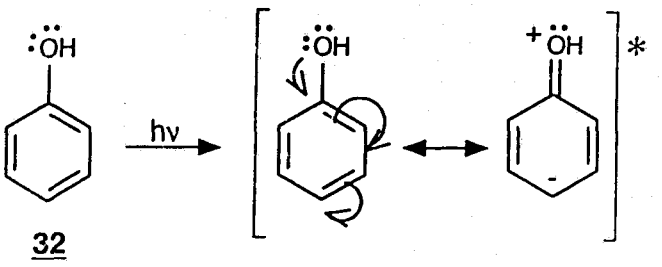

32

Scheme 1.4

The discussion to this point on ESPT has focused on changes between S_0 and S_1. Similar trends are observed for molecules excited to the triplet state (T_1). However, the changes in pK_a between S_0 and T_1 are not as significant as those observed between S_0 and S_1[55]. Molecules excited to T_1 experience a redistribution of electron density but not to the same extent as indicated for molecules in S_1. A better representation of the triplet species is a diradical as drawn for benzoic acid (31) and phenol (32) (Fig. 1.6)[54]. The development of charge on substituents of molecules in T_1 is therefore less than for the same molecules in S_1. Therefore, a molecule excited from S_0 to S_1 will experience a greater change in pK_a than when it is excited to T_1.

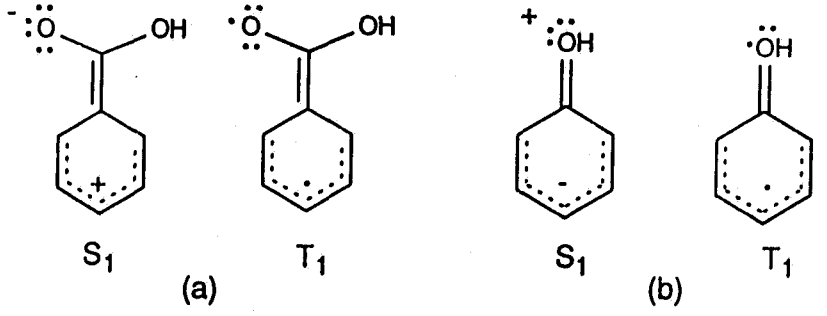

Figure 1.6 Redistribution of electron density in S_1 and T_1 for (a) benzoic acid (31) and (b) phenol (32).

As indicated earlier both protonation of EWGs and deprotonation of EDGs result in a shift of the fluorescence to longer wavelengths or lower energies. This is due to the relative stabilities of the protonated and unprotonated species in S_0 and S_1 (Fig. 1.7)[57]. For example protonation of B (aromatic compounds with EWGs) in S_0 produces BH^+ (Fig. 1.7a). The latter species is less stable and therefore has more energy than B. In S_1 the reverse is true as protonation produces $^*BH^+$ which is more stable than $^*B$. The energy gap between BH^+ and $^*BH^+$ ($\Delta E'$) is smaller than the gap between B and $^*B$ (ΔE). Therefore, transitions between the former two species will occur at lower energies or longer wavelengths. Similar arguments can be used to explain the situation for EDGs (Fig. 1.7b) where AH represents an aromatic compound with an EDG.

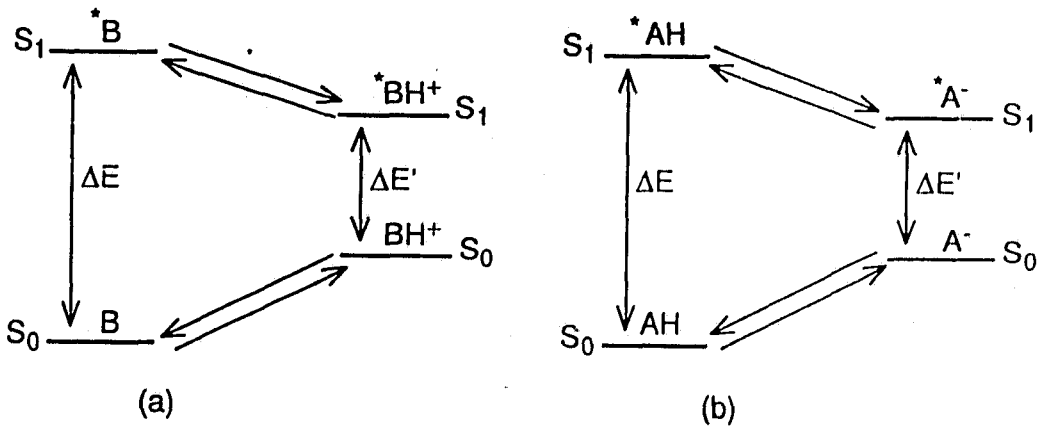

Figure 1.7 Reduction in the energy gap for (a) protonation of EWGs and (b) deprotonation of EDGs.

1.3.2 Carbon Acids in the Excited State

In the previous section the discussion of ESPT dealt only with changes in pK_a for oxygen acids. However, other aromatic compounds containing substituents such as nitrogen and sulphur also exhibit enhanced pK_as in S_1 and T_1. Similar changes in pK_a have been predicted for benzylic carbons. For example the dibenzylic carbon of fluorene (**9**) has been predicted by Förster cycle calculations[57], to exhibit a substantial decrease in pK_a on excitation to S_1 (pK_a of 20.5 in S_0 to -8.5 in S_1)[55]. No such change in pK_a has been observed for **9** after excitation. This lack of confirming experimental results for **9** may arise from the time constraints placed on photochemical reactions. Molecules can only exist in S_1 for a short period of time ($\approx 10^8$ s^{-1})[62] since deactivational processes such as fluorescence, internal conversion and intersystem crossing from S_1 are very rapid (10^9-10^6 s^{-1}, 10^6 s^{-1}, and 10^9-10^6 s^{-1}, respectively)[64]. As indicated, **9** is a kinetic carbon acid, and is deprotonated at a rate of $\approx 10^4$ $M^{-1}s^{-1}$ in the ground state[42]. This deprotonation rate certainly cannot compete with other deactivational processes available in S_1. Deprotonation of oxygen, nitrogen and sulphur occurs at a much faster rate (10^{10} $M^{-1}s^{-1}$)[41] and so ESPT is observed for these acids.

Although deprotonation of kinetic carbon acids cannot compete with deactivational processes from S_1, enhanced acidity can still be observed after excitation of a carbon acid via a diabatic process. A photochemical process is termed *diabatic* if it is initiated in an excited state and completed in S_0. Conversely, a photochemical process initiated and completed in the same excited

state is termed *adiabatic*. Examples of each process are shown in Figure 1.8 for deprotonation of an acid AH. ESPT involving oxygen, nitrogen and sulphur substituted aromatic systems is generally adiabatic as suggested by the fluorescence emitted from the conjugate acids or bases of these systems after excitation of the parent molecule.

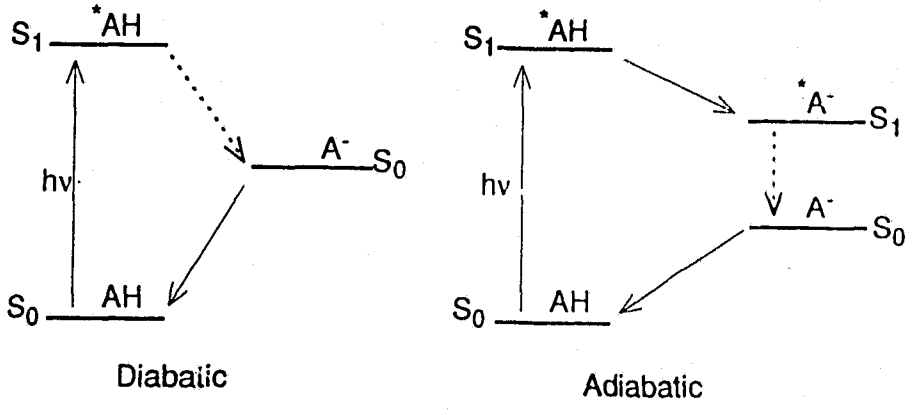

Figure 1.8 Adiabatic vs diabatic deprotonation of an acid AH.

Deprotonation of a carbon acid may occur via a diabatic process if the S_1 and S_0 surfaces of the acid approach each other in the region corresponding to the transition state for loss of a proton (Fig. 1.9). This situation exists when the energy barrier for this transition state in S_1 is smaller than the corresponding barrier in S_0. When the S_1 and S_0 energy surfaces approach each other internal conversion (vibrational relaxation of a molecule from a higher energy singlet state to a lower energy singlet state) can occur[64]. Internal conversion of the carbon acid at the transition state in S_1 to the transition state in S_0 may therefore result.

The carbon acid may then return to starting material or lose a proton to give a carbanion (C^-). Such a carbon acid would exhibit enhanced acidity after excitation to S_1.

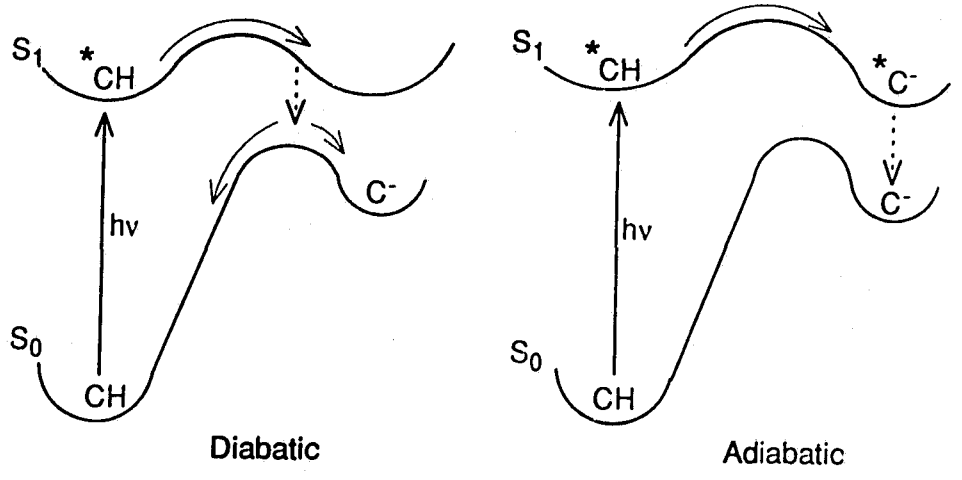

Figure 1.9 Diabatic and adiabatic deprotonation of a carbon acid CH.

An adiabatic deprotonation with formation of the carbanion on the excited state surface can also be envisioned (Fig. 1.9). Transfer of the carbanion to S_0 may occur by internal conversion or fluorescence depending on the distance between the excited and ground state surfaces. However, formation of a carbanion on the excited state surface would be unlikely according to the rates of carbon acid deprotonation observed in the ground state.

Examples of photochemical reactions which take advantage of enhanced excited state acid-base behaviour were recently reviewed by Wan and Shukla[52]. In the following section some of the more significant examples of these

photochemical reactions will be discussed.

1.3.3 Acid-Base Catalysis of Photochemical Reactions

Although the Brønsted catalysis law has been applied extensively to ground state reactions, few examples exist of photochemical reactions involving general acid or base catalysis. Wubbels[65] specified what catalysis of a photochemical reaction involves and provided several examples of photochemical reactions catalyzed by acids and bases. Wan and Shukla[52] and Arnaut and Formosinho[58] also reviewed the literature and examined more recent examples of photochemical reactions catalyzed by acids or bases.

By using a generalized photochemical reaction scheme (Scheme 1.5), an equation similar to that obtained for general acid or base catalysis in the ground

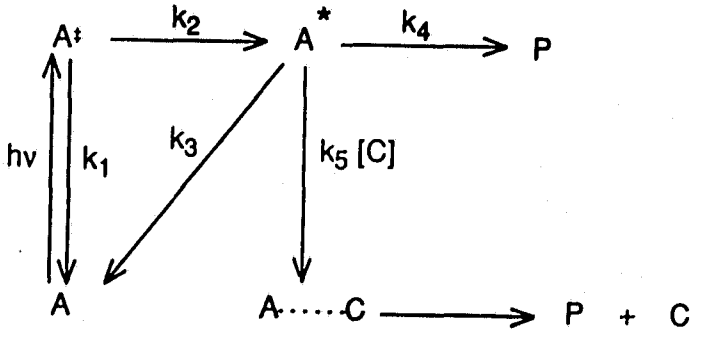

Scheme 1.5

state can be obtained[65] (eq. 1.22) (where $1/\Phi$ represents the efficiency of the conversion A to P). The conversion of A^* to P represents the uncatalyzed reaction and A^* to P + C represents the route promoted by a catalyst (C). The term $1/\Phi_i$

represents the efficiency of the conversion $A^{\ddagger}$ to A^{*}. When $k_4 >> k_5[C]$, a simplified equation (eq. 1.23) can be obtained for this reaction. However, when $k_4 << k_5[C]$, catalysis of the photochemical reaction occurs and the efficiency ($1/\Phi$) can be related directly to the concentration of catalyst (eq. 1.24). Therefore, as the concentration of the catalyst is increased, the efficiency will increase in a linear fashion as expected for general acid or base catalysis.

$$\frac{1}{\Phi} = \frac{1}{\Phi_i}\left(1 + \frac{k_3}{k_4 + k_5[C]}\right) \qquad (1.22)$$

$$\frac{1}{\Phi} = \frac{1}{\Phi_i}\left(1 + \frac{k_3}{k_4}\right) \qquad (1.23)$$

$$\frac{1}{\Phi} = \frac{1}{\Phi_i}\left(1 + \frac{k_3}{k_5[C]}\right) \qquad (1.24)$$

The most common method of obtaining rates for photochemical reactions is through the use of Stern-Volmer analysis[64]. This method relates the change in fluorescence intensity (ϕ_f°/ϕ_f where ϕ_f° is the fluorescence intensity without quencher and ϕ_f is the fluorescence intensity with quencher) to the change in concentration of fluorescence quencher (Q) (eq. 1.25). As the concentration of the quencher, either general acid or base in the present case, is increased more of the excited substrate is diverted to product and less of it is deactivated by

$$\frac{\phi_f^{0}}{\phi_f} = 1 + k_q\tau_0[Q] \qquad (1.25)$$

fluorescence. Using the Stern-Volmer plot and the fluorescence lifetime of the substrate in the absence of quencher (τ_0), the rate of fluorescence quenching (k_q) can be obtained. This quenching rate corresponds to the rate of reaction catalyzed by the general acid or base. Therefore, plots of these rates versus the pK_a of the catalyst yield a Brønsted plot.

A variety of photochemical reactions exhibit acid-base catalysis[52]. However, only a few have been studied using the Brønsted catalysis law. The first well known example of a general base catalyzed photochemical reaction is the rearrangement of ω-anilinoalkyl nitrophenyl ethers (i.e., 33) [65,66] (eq. 1.26). Quantum yields determined for 33 at constant pH with various bases, showed general base catalysis. Brønsted plots were not obtained for this particular reaction. However, a related system ρ-$NO_2C_6H_4O(CH_2)_2NHPh$ exhibits a curved Brønsted plot[66].

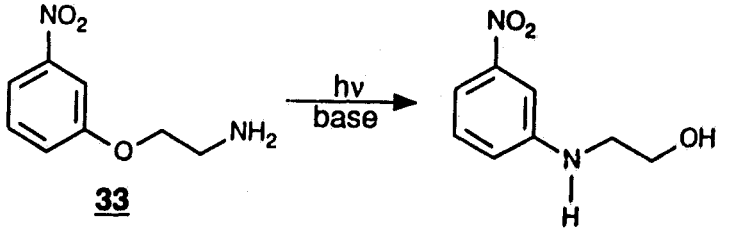

33 (1.26)

Yates[67] indicated that curvature in Brønsted plots is expected for photochemical processes due to the shallowness of excited state energy wells compared to ground state energy wells. This discrepancy is ascribed to the promotion of electrons to anti-bonding orbitals after excitation[64]. In S_0 the free energy change (ΔG^0) associated with proton transfer between similar shaped

energy wells is generally equal to zero. Proton transfer between ground and excited state energy wells with different shapes will therefore lead to curvature in the Brønsted plots since ΔG^0 will not equal zero.

Photohydration of aromatic alkenes and alkynes were the first recognized photochemical reactions which exhibited general acid catalysis[52,58,65] (eq. 1.27 and 1.29). General acid catalysis occurs in the first step which involves irreversible protonation of 34 or 27 in S_1 (or T_1 for nitro derivatives). The initial protonation

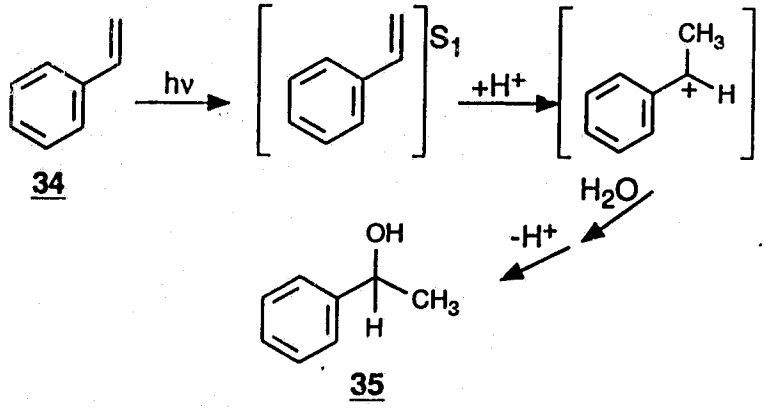

34 35 (1.27)

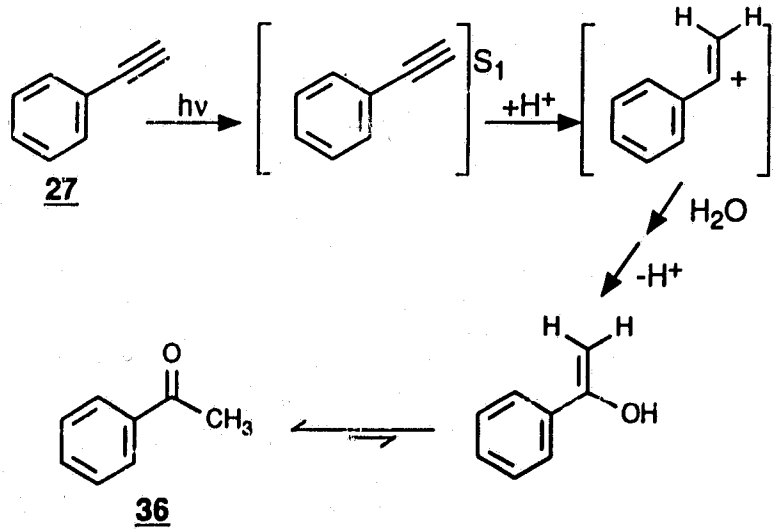

27 36 (1.28)

is facilitated by polarization of the aryl alkene or alkyne moiety in S_1. This in turn increases the basicity of the terminal carbon of the alkene or alkyne (Fig. 1.10). Work by McClelland et al.[68], (using laser flash photolysis) demonstrated that the intermediate formed from this protonation is a benzylic cation. This cation is trapped by water to give the benzyl alcohol 35 for alkenes or a ketone 36 for alkynes. Linear plots of Φ^{-1} vs $[H^+]^{-1}$ and the irreversible nature of the protonation step indicated general acid catalysis[67,69]. The Brønsted plot obtained for these photochemical reactions were linear with α = 0.14-0.18, which implies an early transition state for the protonation step. Similar thermal reactions occur with values of $\alpha > 0.5$ implying a later transition state for the protonation step. Yates[67] attributed the lower value observed in the photochemical process to the shallowness of the excited state energy wells compared to the ground state energy wells. This, as indicated, effects ΔG^0 which leads to errors in the Brønsted catalysis law.

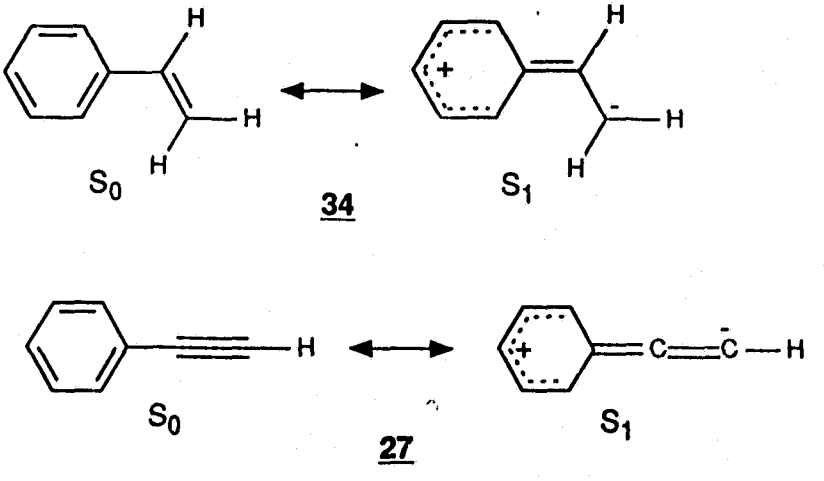

Figure 1.10 Polarization of **34** and **27** in S_1.

Research in our group has indicated that deprotonation of the carbon acids **5** and **6** may involve general base catalysis[7,8]. However, before discussing the results obtained for these two systems, a summary of photochemical sigmatropic shifts and di-π-methane rearrangements will be given since these processes are important in the photochemistry of **6**.

1.4 Excited State Rearrangements

A variety of excited state rearrangements are possible for olefins. Two of the more common reactions observed are sigmatropic shifts and di-π-methane rearrangements. Both are observed in the photochemistry of **6**. In the following section a brief summary of these rearrangements will be given with emphasis on aspects relevant to the photochemistry of **6**.

1.4.1 Photochemical Sigmatropic Shifts

A sigmatropic shift is defined by Woodward and Hoffmann[13] as "the migration of a σ-bond, flanked by one or more π-electron systems, to a new position whose termini are *i* and *j* atoms removed from the original bonded loci, in an uncatalyzed intramolecular process." A Cope rearrangement (eq. 1.29) is

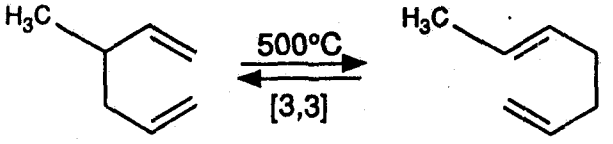

(1.29)

defined as a [3,3] sigmatropic shift since the new position of the σ-bond is located three atoms away from both of the atoms which formed the original bond. Hydrogen shifts are termed [1,*j*]-shifts since the new σ-bond is formed with the same hydrogen which was one of the original termini. Values of *j* are commonly 3, 5, or 7 depending on the π system involved. In the ground state [1,5] hydrogen shifts are observed, whereas, [1,3] and [1,7] hydrogen shifts are observed in the excited state[13].

The preference for certain sigmatropic shifts in the ground state and in the excited state can be demonstrated by looking at the highest occupied molecular orbital (HOMO) and the lowest unoccupied molecular orbital (LUMO) for a π system such as propene (Fig. 1.11)[70]. Transfer of hydrogen between the propene

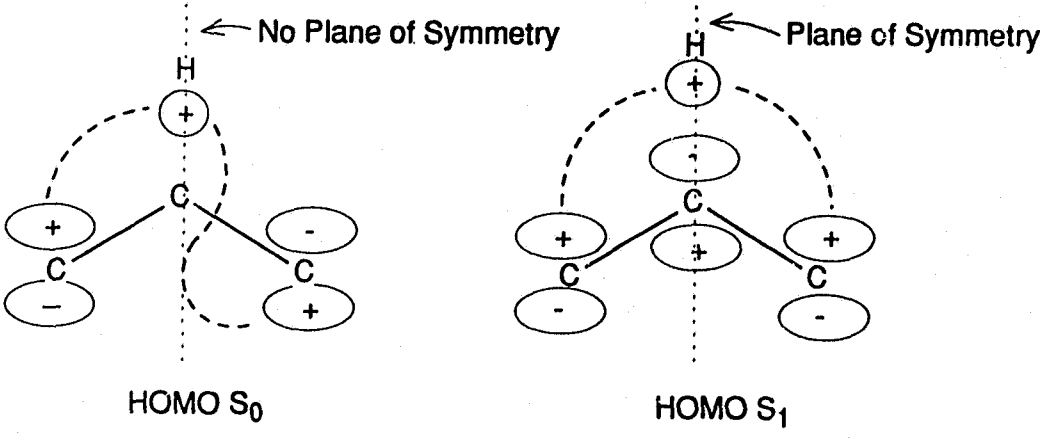

Figure 1.11 S_0 and S_1 HOMOs for a propenyl radical.

termini can only occur between lobes of the same sign. For example, in S_0, the HOMO of the propene radical has lobes at the termini with the same signs on

opposite faces of the molecule. A [1,3]-shift in S_0 would require movement of the hydrogen from one face of the molecule to the other face, i.e., an antarafacial shift. The [1,3]-shift is not observed in S_0 since the hydrogen 1s orbital must overlap with the lobes of both termini for a shift to occur. Such an overlap cannot be achieved in propene. However, excitation of propene to S_1 promotes an electron to the LUMO creating a new HOMO. The lobes at the termini are now the same sign on each face. Therefore, a [1,3]-shift can readily occur, as overlap of the hydrogen 1s orbital with the lobes of the termini is possible. Such a shift, where the hydrogen remains on the same face of the molecule, is termed suprafacial.

By looking at the HOMOs of higher order polyenes[70] it has been shown that a suprafacial [1,5] sigmatropic hydrogen shift is allowed thermally. A thermal [1,7] sigmatropic hydrogen shift is not as facile since it must proceed through an antarafacial pathway. However, it is still possible since distortion of the polyene may occur to allow overlap of the appropriate orbitals. Excitation of the appropriate polyene forces the [1,5]-shift to proceed via an antarafacial pathway and the [1,7]-shift to proceed via a suprafacial pathway. Thus [1,5]-shifts are not commonly observed in photochemical reaction since the required overlap of orbitals is difficult to achieve, whereas [1,7]-shifts readily occur via the suprafacial pathway.

Woodward and Hoffmann[13] developed a set of selection rules to predict the type of sigmatropic shift expected for a given molecule and state. They suggested that a sigmatropic shift of the order [*i*,*j*] is allowed thermally if $i+j = 4n+2$ and

allowed photochemically if $i+j = 4n$. These rules are based on orbital symmetry arguments for the transition states involved. These arguments suggest that transition states with a plane of symmetry (suprafacial shifts) are allowed and transition states lacking this symmetry (antarafacial shifts) are forbidden (Fig. 1.11).

Sigmatropic shifts do still occur in systems which would not be expected to allow such a shift. However, these shifts involve a catalyst (*vide infra*) and according to Woodward and Hoffmann's definition[13] they are not true sigmatropic shifts. Before considering examples of these catalyzed shifts, the photochemistry of cycloheptatriene systems which are related to **6**, will be discussed.

1.4.2 Photochemistry of Cycloheptatrienyl Systems

The photochemical [1,7] sigmatropic shifts of cycloheptatriene (**37**) have been studied extensively[71-76]. Along with a minor electrocyclic ring closure product (**38**), four isomers of **37** exist in equilibrium via [1,7] hydrogen shifts. The latter was demonstrated by photolysis of **39** (Scheme 1.6)[71]. Ter Borg et al.[72] indicated that the ratio of each isomer and the extent of cyclization could be changed dramatically by various substituents. Strong electron donating groups favour ring closure whereas electron withdrawing groups affect the ratios between the four isomers. Phenyl[71] substitution had little effect on the isomer ratios whereas methyl[73] substitution promoted [1,7] hydrogen shifts which placed the methyl group at the saturated position or next to it. On the basis of

theoretical calculations, Tezuka et al.[74] attributed these substituent effects to the existence of a polarized zwitterionic state.

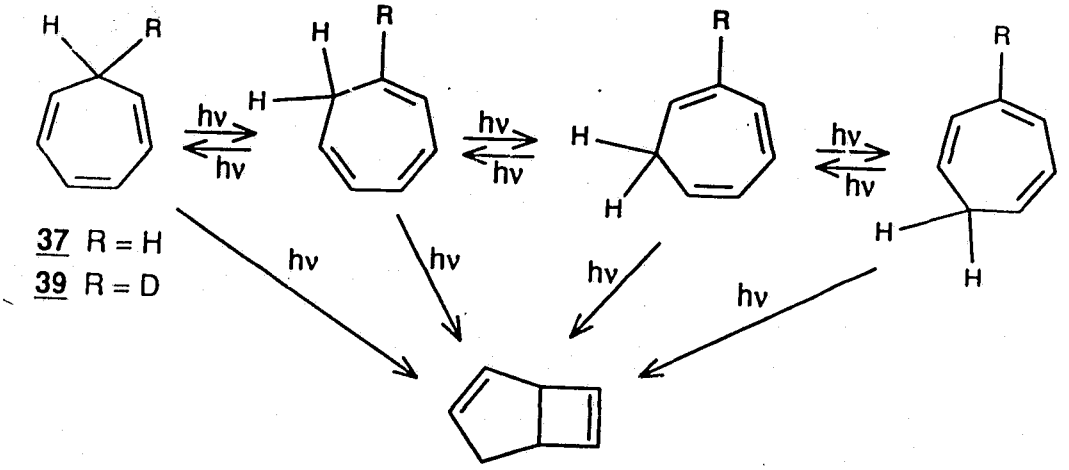

Scheme 1.6

More recent studies by Reid et al.[75,76] focused on the rate of the photochemical [1,7] hydrogen shift and the dynamics of this process for 37. By using picosecond UV resonance raman spectroscopy, it was found that completion of the [1,7] hydrogen shift takes 26 picosecond[75]. This result is similar to that observed for other photochemical pericyclic reactions[77]. Studies of the dynamics of the [1,7]-shift demonstrated that planarization of the excited molecule occurs before the pericyclic reaction proceeds[77]. This planarization would be expected to restrict sigmatropic shifts to molecules able to obtain a planar geometry.

Replacement of one double bond of **37** by a benzene ring as in 1,2-benzotropilidene (**40**) limits the number of stable isomers possible to two but still allows

a minor amount of photochemical electrocyclization. Direct photolysis of **40** produces benzonorcaradiene (**41**) and a trace of **42**. (Scheme 1.7)[78]. Deuterium labelling studies demonstrated that **41** is formed in two steps via a photochemical [1,7] hydrogen shift (producing an isomer of **40** (**43**)) followed by a thermal disrotatory electrocyclic ring closure. The second product (**42**) is formed via a direct photochemical electrocyclization.

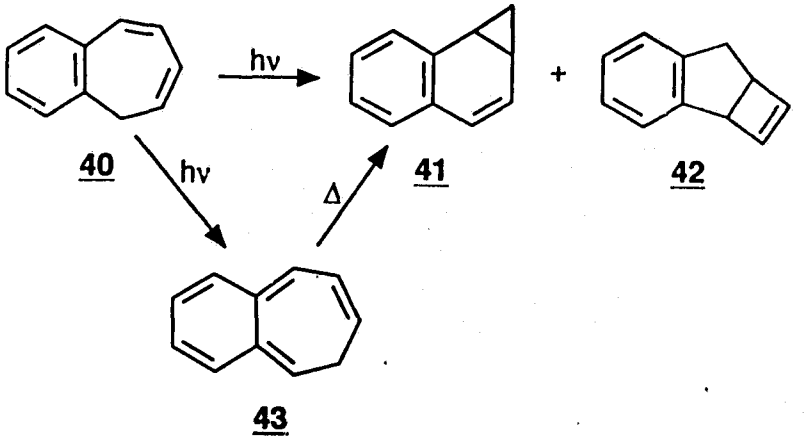

Scheme 1.7

Irradiation of 3,4-benzotropilidene (**44**) also resulted in **41** along with a trace of **40** (eq. 1.30)[78,79]. The former product is formed via a [1,7] hydrogen shift, followed by a thermal disrotatory electrocyclization. The minor product 1,2-benzotropilidene (**40**) is believed to form via a [1,3] sigmatropic hydrogen shift. Burdett et al.[79] indicated that the [1,3]-shift may occur since it does not disrupt the

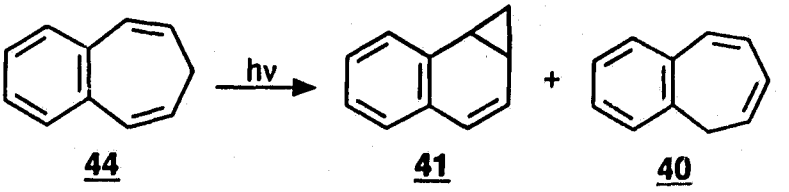

(1.30)

benzene moiety. This result was unexpected since [1,3]-shifts have not been observed in photochemical reactions of other derivatives of **37**.

Reaction of **40** and **44** via the triplet state (T_1) did not result in any rearrangements indicating that the [1,7]-shifts observed occur in S_1[78]. This is expected since both [1,3] and [1,7] sigmatropic shifts in general do not occur in T_1 but in S_1[64].

1.4.3 Base Catalysed [1,3]-Shifts

Numerous examples of photochemical [1,3] sigmatropic hydrogen shifts have been observed for simple alkenes and more complex systems[64,80]. For example, excitation of 1,3-dienes results in a [1,3] rather then a [1,5] hydrogen shift since the latter proceeds through an antarafacial pathway. Alkylphenylcyclopropanes (**45**) can also undergo a photoinitiated [1,3] hydrogen shift to produce an unconjugated alkene (eq. 1.31)[81]. The shift is believed to be very efficient since other processes normally observed in related systems do not

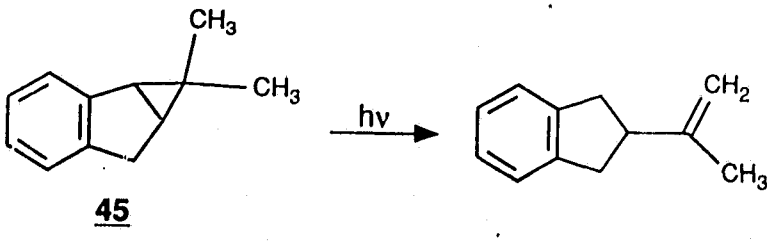

45 (1.31)

occur. However, these ring opening hydrogen migrations are not sigmatropic shifts by definition. In the remainder of this section examples of base catalyzed [1,3]-shifts which are not sigmatropic shifts by definition will be discussed.

Until recently, all pericyclic reactions including sigmatropic hydrogen shifts were believed to be unaffected by solvent polarity[82]. However, numerous papers have been published recently which indicate otherwise. Examples of Diels-Alder reactions[83], Claisen rearrangements[84] and ene reactions[85] have been found which proceed with increased rates in more polar solvents. No evidence has been found to indicate that the rates of sigmatropic hydrogen shifts are enhanced in more polar solvents. However, it has been shown that the rates of product formation from these types of rearrangements can be enhanced in more polar solvents or in the presence of bases by a change of mechanism, i.e., proton rather then hydrogen shifts.

The proton transfer observed in indene (46), by Bergson et al.[86], is a well documented example of a base catalyzed [1,3] proton transfer. Early experimental results[86] and theoretical studies[87] indicate that the proton transfer is intramolecular and stereospecific, i.e., the proton transfer occurs via a suprafacial mechanism (eq. 1.32). Recent theoretical studies[88] show that the base, after proton abstraction, forms an ion-pair with the indenyl carbanion. The protonated base then moves

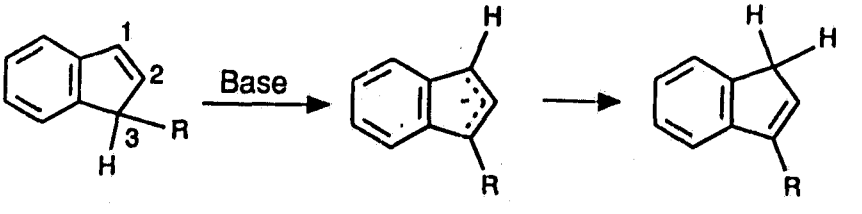

(1.32)

46 R = H
47 R = CH_3

freely between positions 1, 2 and 3 on one face of the carbanion.

Further evidence for the formation of an ion-pair type transition state was obtained by measuring Brønsted coefficients. Meurling[89] obtained a Brønsted coefficient of 0.79 for 1-methylindene (**47**) using a series of tertiary amines in dimethylsulphoxide. More recently Hussénius et al.[90] obtained a value of 0.90 for **47** using a similar set of tertiary amines in o-dichlorobenzene. A direct comparison of these results cannot be made as they were obtained in different solvents. However, both values indicate a late or ion-pair like transition state since the proton involved is more covalently linked to the nitrogen of the base than to the carbon of the indene system (i.e., the transition state resembles the product of the deprotonation which is the carbanion intermediate).

Several examples of base catalyzed photochemical [1,3] proton shifts have also been investigated[91-93]. Lapouyade et al.[91] studied the effect of amine catalysis on the photocyclization of 1,1-diarylethylenes (i.e., **48**) (eq. 1.33). The yield of **49** was found to be dependent on the strength of the base used to catalyze the reaction. Deuterium labelling experiments indicated that a [1,3] proton shift from

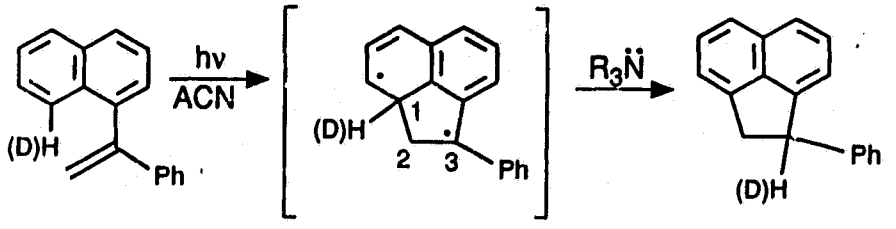

48 **50** **49** (1.33)

the 1-position of the proposed diradical intermediate (**50**) to the 3-position was

occurring. However, further studies were still required to confirm the proposed mechanism.

Laarhoven et al.[92,93] investigated the amine promoted photochemical [1,3] proton shifts of 3-methyl-1,2-dihydronaphthalene (**51**) and 1,2- (**53**) and 3,4-dihydrophenanthrene (**54**). Photolysis of **51** in the presence of a primary amine yields predominantly **52** via a [1,3] proton shift (eq. 1.34)[92]. In the absence of primary amines, photolysis of **51** produces only minor amounts of **52** via a [1,3] hydrogen shift.

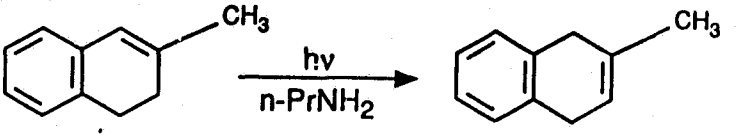

51 **52** (1.34)

A similar base catalyzed [1,3] proton shift was observed for **53** and **54** (eq. 1.35)[93]. Both **53** and **54** are photostable when irradiated in MeOH or hexanes, i.e., no [1,3] hydrogen shift is observed. That a base catalyzed [1,3] proton shift was occurring in **53** and **54** was further suggested by the correlation observed between base strength and quantum yields for the formation of **55**. No correlation was observed between ionization potentials (IP) and product quantum yields.

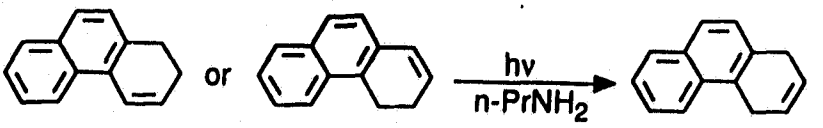

53 **54** **55** (1.35)

Correlation with IP would have indicated a radical ion mechanism involving electron transfer from the amine to the substrate. Such a mechanism is believed to predominate when **53** or **54** are photolyzed in either a secondary or tertiary amine. This was demonstrated by the formation of radical derived products and by the decreased yields of **55** in these amines.

1.4.4 Di-π-methane Rearrangement

The photochemical rearrangement of 1,4-dienes (**56**) to vinylcyclopropanes (**57**) (Scheme 1.8) is formally a [1,2] sigmatropic shift followed by a ring closure[64]. Zimmerman was the first to recognize the generality of this reaction and termed it a di-π-methane rearrangement[94]. It has been shown to occur in arylvinyl-

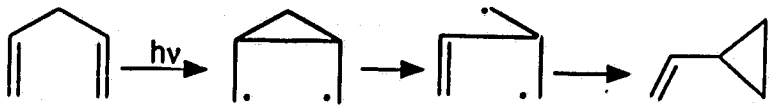

56 **58** **59** **57**

Scheme 1.8

methanes and in systems where one vinyl group is replaced by a carbonyl (oxa-di-π-methane)[95] or a imine (aza-di-π-methane)[96]. The di-π-methane rearrangement continues to attract a considerable amount of interest due to its synthetic utility and the fascinating mechanism involved. Though there are many facets to the rearrangement, the following discussion will concentrate on three aspects, the mechanism, the multiplicity (excited state which the reaction occurs, S_1 or T_1) and

the regioselectivity.

The mechanism outlined in Scheme 1.8 has been examined extensively using a variety of techniques[97] and is believed to commence by formation of a sigma bond between the olefins. This produces a 1,4-diradical (58) which then rearranges to a 1,3-diradical (59). Closure of the latter diradical yields the vinylcyclopropane product (57). As drawn, the reaction can only proceed in a forward direction. However, several examples have been found where vinyl cyclopropanes revert back to 1,4-dienes, as shown for 60 (eq. 1.36)[98].

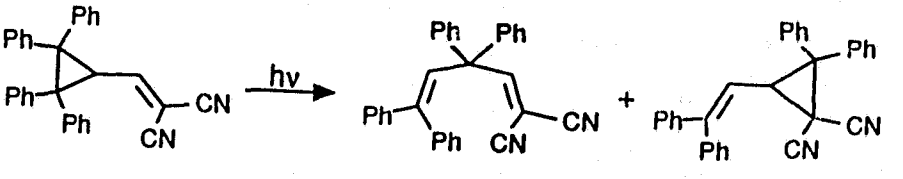

60

(1.36)

The rate limiting step in the mechanism of the di-π-methane rearrangement is dependent on the excited state in which the rearrangement proceeds[97]. In S_1 the rate limiting step occurs prior to cleavage of the cyclopropane ring of the 1,4-diradical. In T_1 the rate limiting step involves cleavage of the cyclopropane 1,4-diradical to produce a 1,3-diradical. The effect of excited state multiplicity on the rate limiting step in the di-π-methane rearrangements was determined by substitution of the 1,4-diene at the 3-position with odd-electron stabilizing groups such as cyano, carbomethoxy or phenyl[98-100]. The state in which the rate limiting step involves the formation of 1,3-diradicals would be expected to have increased rates of di-π-methane rearrangement due to the presence of these substituents.

Increased rates of di-π-methane rearrangement were observed in T_1 and decreased rates in S_1. Therefore, the rate limiting step in T_1 is believed to involve formation of the 1,3-diradical (59).

These results suggest that the energy versus reaction coordinate profile of the di-π-methane rearrangement is not the same in T_1 and S_1. Recent molecular mechanics calculations [101,102] and product studies involving deuterium labelling and azoalkanes[101] point to a concerted mechanism in S_1 with no energy minimum corresponding to the 1,4-diradical. Direct formation of the 1,3-diradical is believed to occur via a 1,2-vinyl or 1,2-aryl shift depending on the system involved. Theoretical calculations[103,104] and structure reactivity studies[104] for the T_1 mechanism suggest that a 1,4-diradical is involved in the triplet state rearrangement. These theoretical studies further suggest an energy minimum for the 1,4-diradical (58), the 1,3-diradical (59) and the 1,2-diradical (61). The 1,2-diradical is believed to be a precursor to the 1,4-diradical in the T_1 rearrangement.

61

The difference between the reaction profiles in S_1 and T_1 does not determine the state in which a particular molecule will rearrange. The state in which the di-π-methane rearrangement occurs, is generally determined by what other photochemical processes are allowable for the molecule being considered. In general acyclic systems rearrange in S_1 and cyclic systems in T_1[97]. Acyclic 1,4-

dienes rearrange in S_1 because of the propensity of these olefins to isomerize in T_1. The photochemical behaviour of **62**, an acyclic 1,4-diene, demonstrates this state selectivity (Scheme 1.9)[105]. Direct irradiation, which excites the molecule to S_1, results in a di-π-methane rearrangement to give **63**. Triplet sensitization, which yields **62** in T_1, results in cis-trans isomerization to give **64**. Acyclic 1,4-dienes can react in the triplet state if either the rate of isomerization is decreased[100] (by using sterically crowded 1,4-dienes) or the rate of rearrangement is increased[98] (by substitution with odd-electron stabilizing groups at the 3-position of the 1,4-diene (*vide supra*)).

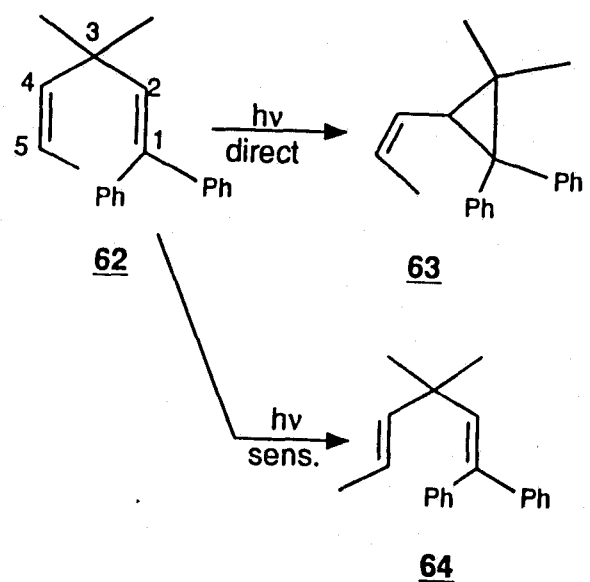

Scheme 1.9

The di-π-methane rearrangement of cyclic 1,4-dienes are affected to a lesser extent by cis-trans isomerization than the acyclic 1,4-dienes due to the restricted motion in the former. Therefore, cyclic compounds generally rearrange in T_1.

Rearrangement in S_1 is not commonly observed since more efficient methods of deactivation exist such as [2+2] cycloaddition. The bicyclic system, barrelene (65), exhibits this behaviour (Scheme 1.10)[106]. Direct irradiation results in an intramolecular [2+2] cycloaddition followed by isomerization to cyclooctatetraene (66). Triplet sensitization, however, produces semibullvalene (67), the di-π-methane product.

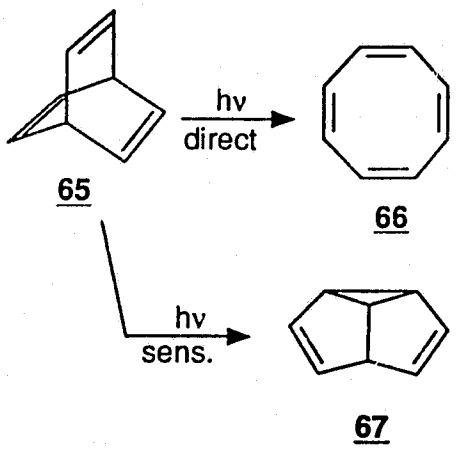

Scheme 1.10

As suggested earlier, substitution at the 3-position of a 1,4-diene can affect the rate of the di-π-methane rearrangement. Substitution at positions 1 or 5 of the 1,4-diene can make this rearrangement highly regioselective depending on the substituents used. An example of this regioselectivity is evident in the photochemical behaviour of **62** (Scheme 1.9)[105]. Only one regioisomer is observed after direct irradiation of **62**. The reason for this regioselectivity can be understood by comparison of the two possible 1,3-diradicals formed (**68** and **69**). The radical at the 1-position of **68** is more stable than the radical at the 5-position

of **69** due to the phenyl substituents. The product formed via **68** will therefore be favoured.

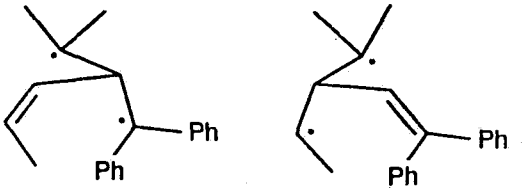

68 **69**

When arylvinylmethanes undergo di-π-methane rearrangements the regioselectivity is controlled by the aryl system. Excitation of 3,3,3-triphenylpropene (**70**) produces **71** (eq. 1.37)[107]. By comparing the two

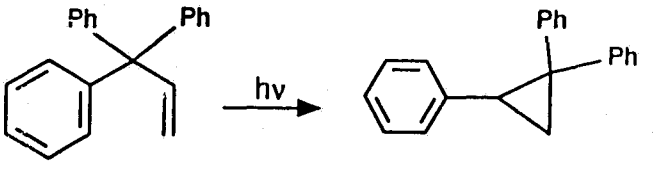

70 **71** (1.37)

possible 1,3-diradicals (**72** and **73**) it can be seen that the diradical with an intact phenyl system would be favoured. Therefore, the regioisomer formed from **72** will be produced. Similar regioselectivities are observed in cyclic systems[94,108].

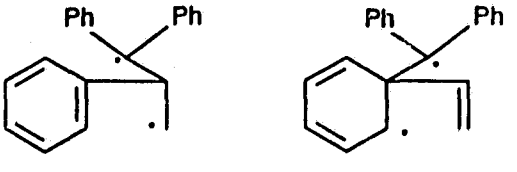

72 **73**

1.5 Excited State Carbon Acids

Examples of neutral hydrocarbons exhibiting enhanced acidity after

excitation were unknown until Wan et al.[7,8] discovered two related compounds which exhibited this behaviour. Excitation of either **5** or **6** in D_2O/ACN resulted in deuterium incorporation at the 5-position of each system, consistent with an increase in the acidity of this position in the excited state. No deuterium incorporation was observed in either compound after the reactions were repeated using the same conditions but without photolysis. The following section is a brief discussion of published work on **5** and **6**.

1.5.1 *5H*-Dibenzo[a,d]cycloheptene (5)

Previous work from our group suggests that reactions proceeding via intermediates containing a 4n ICA are more favourable in the excited state than reactions involving a 4n+2 ICA[15,16] (*vide supra*). It was proposed that the excited state acidity observed for **5** resulted from formation of a carbanion intermediate containing an ICA with 4n π electrons. Support for this theory was found by irradiating fluorene (**9**) and 10,11-dihydro-*5H*-dibenzo[a,d]cycloheptene (**74**) in the presence of D_2O[7]. No deuterium incorporation was observed in either system, both of which are not capable of forming a 4n ICA after deprotonation. However, the benzotropilidene systems **40** and **44** which are capable of forming a 4n ICA after deprotonation, do not exhibit excited state carbon acid behaviour[109]. The efficient photorearrangement observed in **40** and **44**[78,79] (*vide supra*) is believed to prevent these systems from functioning as excited state carbon acids. Comparison of electronic structures of **5** and cycloheptatriene (**37**) in their lowest excited state

(using semiempirical MNDOC-C1 calculations) also suggests a preference for rearrangement in cycloheptatriene systems other then 5[110].

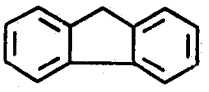

9

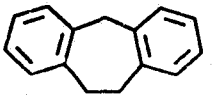

74

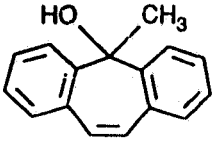

77

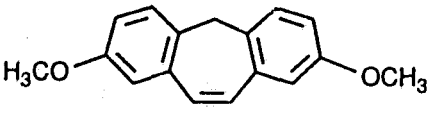

75

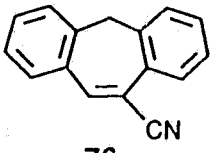

76

The effect of EDGs and EWGs on the photochemistry of 5 was examined by photolysis of 75 and 76 in D_2O/ACN[109]. Compared to 5, the compound with EDGs (75) was shown to be a weaker excited state carbon acid, whereas 76 with EWGs exhibited enhanced acidity after excitation. These results are consistent with photodeuteration of 5 involving the carbanion intermediate 7.

Steady state fluorescence quenching studies demonstrated that water was an efficient quencher of the fluorescence of 5 but had no effect on the fluorescence of 9 and 74[7]. This result was expected since deprotonation by a base of an excited species provides another route for deactivation from the excited state. Both 9 and 74 are unreactive as excited state carbon acids compared to 5 and so their fluorescence is unaffected by water. Similar results were noted for the effect of water on the fluorescence lifetimes of 5 and 9[7]. The lifetime of 5 (4.6 ns) decreased with increasing concentrations of water. However, the lifetime of 9 (6

ns) remained essentially unchanged with increasing water concentrations. In addition, a compound similar to **5** but lacking protons at the 5-position **77** was shown to be unaffected by water in both steady state and time-resolved fluorescence studies[7]. These results indicate that deactivation of excited **5** by a base occurs via interaction of the protons at the 5-position with the base. The fluorescence lifetime data also suggests that lifetimes do not determine the ability of a system to undergo proton exchange since **9** has a similar fluorescence lifetime compared to **5** in solvents where both are incapable of reaction.

The possibility of a radical mechanism was ruled out for the deuterium incorporation observed by photolyzing **5** in CD_3CN[7]. No deuterium incorporation was observed as expected since deuteron abstraction from CD_3CN is difficult, due to the high strength of the C-D bond (86 kcal $mole^{-1}$)[111]. The O-D bond of D_2O is even stronger (119 kcal $mole^{-1}$)[111] suggesting that a radical mechanism cannot be used to explain the deuterium incorporation observed after irradiation of **5** in D_2O.

Photolysis of *5H*-dibenzo[a,d]cyclohepten-5-ol (**78**) in D_2O/ACN resulted in both deuterium incorporation at the 5-position and ketonization (Scheme 1.11)[112]. Photoketonization of **78** proceeds via initial deprotonation of the 5-position to produce carbanion **79**, which can be deuterated to give **80** or deuterated at the 10-position via **81**, to give the final product **83** by subsequent ketonization of enol **82**. These results demonstrate the importance of a carbanion intermediate in the photochemistry of systems related to **5**.

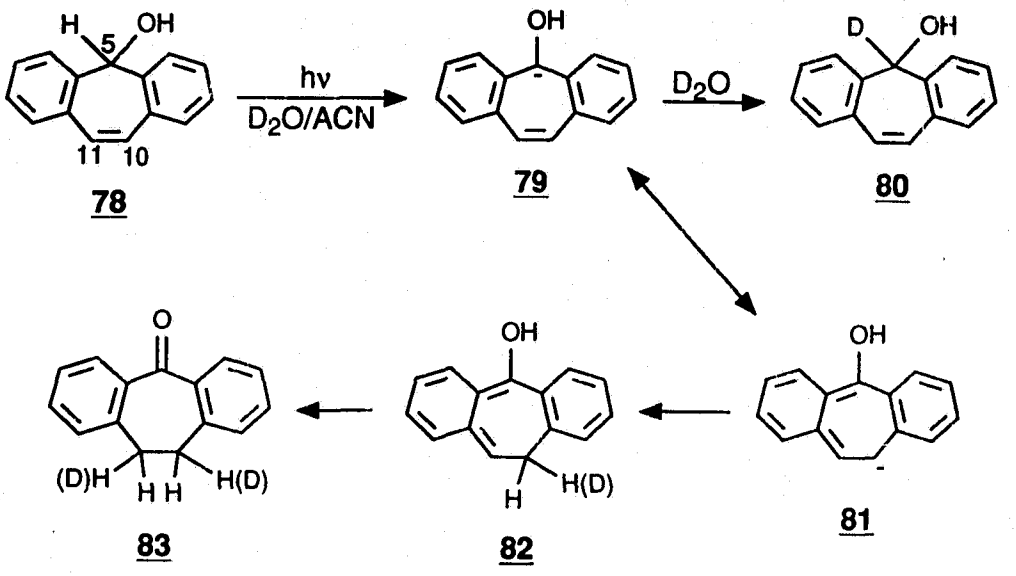

Scheme 1.11

1.5.2 *5H*-Dibenzo[a,c]cycloheptene (6)

Both steady state and time-resolved fluorescence studies performed on **6** demonstrate that the deuterium incorporation observed in this system occurs via a mechanism similar to that described for **5**[8]. As with **5**, photolysis of **6** in CD_3CN did not result in deuterium incorporation, which again rules out a radical mechanism for the proton exchange observed in these systems. The excited state in which deuterium incorporation occurs was examined by triplet sensitization of **6** in D_2O/ACN. No deuterium incorporation was observed which indicates that the carbon acid behaviour of **6** originates from S_1.

In addition to the deuterium incorporation observed for **6**, various rearrangements are also possible. The nature of these rearrangements were studied by performing a series of photolysis on the deuterated system 6-deuterio-

5H-dibenzo[a,c]cycloheptene (**84**)[8]. Direct irradiation and triplet sensitization of **84** demonstrated that two rearrangements occur. In T_1, a di-π-methane rearrangement occurs to yield the deuterated dibenzonorcaradiene (**85**). However, in S_1, a [1,7] hydrogen shift followed by a thermal disrotatory electrocyclic ring closure produces **86**. Photolysis of **84** in H_2O/ACN resulted in **85** only. This suggests that the proton exchange in S_1 effectively competes with the sigmatropic shift, which also occurs in S_1, preventing formation of **86**. The proton exchange also competes with intersystem crossing to T_1 since the yield of **85** is decreased when **84** is irradiated in H_2O/ACN. These results and the proposed mechanism for proton exchange are summarized in Scheme 1.12[8,113].

1.6 Proposed Research

Many questions still remain concerning the photochemistry of **5** and **6**. Further research will provide a better understanding of the factors which influence excited state reactions involving heterolytic bond breakage, such as the significance of a 4n electronic ICA in the excited state.

The excited state carbon acidity of **5** will be quantified first using techniques such as steady state fluorescence, single photon counting (time-resolved fluorescence) and exchange quantum yields. These techniques will also be used to determine the effect of deuterium substitution at the 5-position of **5**. Various bases will be utilized with special attention to amine bases. With these bases, a Brønsted plot will be constructed to determine the importance of general

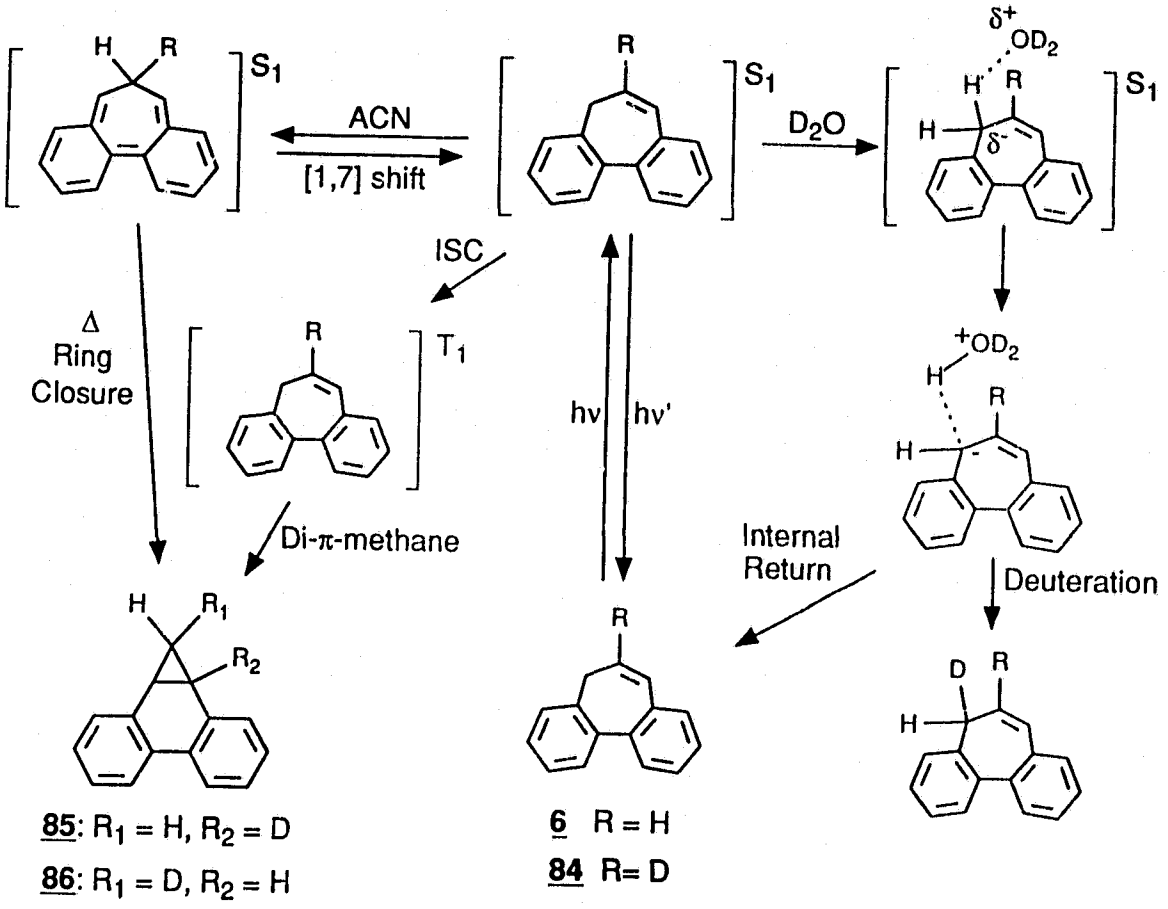

Scheme 1.12

base catalysis in the excited state proton exchange of **5**. Finally the effect of substituents at the 5-position of **5** will be examined.

The photochemistry of **6** will be examined further using 7-deuterio-*5H*-dibenzo[a,c]cycloheptene (**87**). Photolysis of this system in ACN and H_2O/ACN should provide data concerning the possibility of a sigmatropic [1,3] hydrogen shift or a base catalyzed [1,3] proton shift. The results of this study should also reveal more information concerning the [1,7] sigmatropic shift and the di-π-methane rearrangement. Methyl and phenyl derivatives of **6** will be prepared to

examine the effect of substituents on the excited state carbon acid behaviour of this system. The effect of amine bases on the photochemistry of **6** and related systems will also be studied to determine if such bases enhance the excited state proton exchange in these systems. In addition, the effects of electron distribution and conformations on the ICA of **6** will be probed by studying the photochemistry of two related binaphthyl systems **88** and **89**.

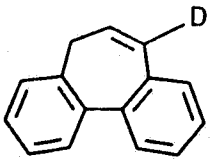

87

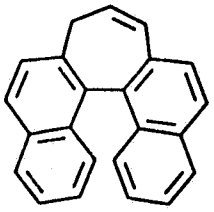

88

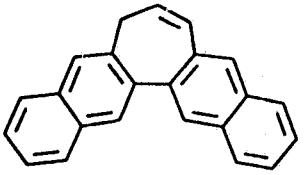

89

CHAPTER 2

EXCITED STATE CARBON ACIDITY OF 5*H*-DIBENZO[a,d]CYCLOHEPTENE

2.1 Introduction

Previous studies[7] of *5H*-dibenzo[a,d]cycloheptene (suberene) (**5**) suggest that excitation of this system results in enhanced carbon acidity at the 5-position. These studies were performed using relatively weak bases such as H_2O or D_2O. The purpose of this Chapter is to examine the excited state acidity of **5** and substituted derivatives using various bases, product studies and steady state and time resolved fluorescence studies. Deuterated derivatives of all the bases used in these studies are not available and so 5,5-dideuteriosuberene (**91**) is prepared along with 5-deuteriosuberene (**90**) to allow for monitoring of the proton-deuterium exchange process using protiated bases. The system **91** is also used to study isotope effects on the excited state proton exchange process observed for **5**. Substituted derivatives of **5** (5-methylsuberene (**93**) and 5-phenylsuberene (**94**)) are prepared to determine the influence of substituents at

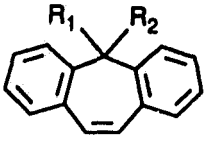

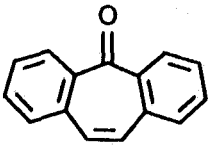

92

5: $R_1 = R_2 = H$

90: $R_1 = D$, $R_2 = H$

91: $R_1 = R_2 = D$

80: $R_1 = OH$, $R_2 = D$

93: $R_1 = CH_3$, $R_2 = H$

94: $R_1 = Ph$, $R_2 = H$

95: $R_1 = CH_3$, $R_2 = D$

96: $R_1 = Ph$, $R_2 = D$

97: $R_1 = Cl$, $R_2 = H$

98: $R_1 = Cl$, $R_2 = D$

the site of proton exchange. The proton exchange observed in 5 and related systems in the presence of various bases are quantified by determination of product quantum yields. A carbene extrusion reaction of a series of alcohols related to 5 is also examined using product studies and product quantum yields.

2.2 Syntheses

2.2.1 Suberene (5), 5-Deuteriosuberene (90) and 5,5-Dideuteriosuberene (91)

Synthesis of 5, 90 and 91 was achieved by reducing suberenone (92) with the appropriate reducing agent. Compound 5 was formed by reducing 92 with $LiAlH_4$ in the presence of $AlCl_3$. The dideuterated derivative 91 was formed in a similar manner with $LiAlD_4$ in the presence of $AlCl_3$. The monodeuterated derivative 90 was achieved by first reducing 92 to the deuterated alcohol 80 with $LiAlD_4$ followed by further reduction with $LiAlH_4$ in the presence of $AlCl_3$. All three products were purified by recrystallization from ethanol. Gas chromatography (GC) and ^1H NMR indicated a purity of > 96% for each.

The identity of the purified products was confirmed by high field ^1H NMR and by analysis of the mass spectrum (MS). The ^1H NMR and MS (M^+ = 192 m/z) of 5 were consistent with the structure shown. The presence of two deuteriums in 91 was confirmed by the absence of a proton resonance at δ 3.75 in the ^1H NMR and by a mass of M^+ = 194 m/z in the MS. One deuterium was shown to be present in 90 by comparison of the integration of the signal at δ 3.73 with the vinyl proton signal at δ 7.04. This comparison indicated a ratio of 1:2 in

favour of the vinyl proton signal. The MS also indicated the required mass (M^+ = 193 m/z). Further confirmation was obtained for both **90** and **91** by ^2H NMR analysis. The ^2H NMR of **90** exhibited a doublet at δ 3.72 for a deuterium coupled to one proton and the corresponding spectrum for **91** exhibited a singlet at δ 3.76.

2.2.2 5-Methylsuberene (93) and 5-Phenylsuberene (94) and Deuterated Derivatives 95 and 96

The derivatives of **5** substituted at the 5-position with methyl (**93**) or phenyl (**94**) were prepared from alcohol **78**. Conversion of **78** to the 5-chloro derivative (**97**) with $SOCl_2$ followed by reaction with either MeMgBr or PhLi provided **93** and **94**, respectively. Repetition of this procedure using the deuterated alcohol **80** (via **98**) gave **95** and **96**. Recrystallization in EtOH yielded products with a purity > 98% according to GC and ^1H NMR analysis.

The compounds were further characterized by high field ^1H (250 and 360 MHz) and ^{13}C NMR and by MS. Two conformations were observed in the ^1H NMR of **93** as indicated by a pair of doublets (representing the methyl protons) at δ 1.42 and 1.96 and by a pair of quartets (due to the methine proton) at δ 3.57 and 4.24. Two signals were also observed for the vinyl protons with singlets at δ 7.00 and 7.21. The ^{13}C NMR of **93** exhibited seventeen signals with one of the aryl signals being much higher in intensity relative to the others. The larger signal suggests the overlap of two ^{13}C resonances. This result also suggests that

93 exists in two conformations since nine signals would be expected based on the symmetrical nature of this system. As expected, the ^{1}H NMR (90 MHz) of the deuterated derivative **95** exhibited a pair of singlets (δ 1.30 and 1.87).

Only one conformation was observed in the ^{1}H NMR (90 MHz) of the phenyl derivative **94**, as indicated by one singlet at δ 5.38 due to the methine proton. However, variable temperature (VT) ^{1}H NMR (90 MHz) demonstrated that at high temperatures (> 55°C) two conformations can exist as the methine signal started to split into two. The ^{1}H NMR (360 MHz) of the deuterated derivative **96** was identical except for the absence of the signal at δ 5.38. The ^{13}C NMR of **96** also indicated one conformation for this system as well as the presence of the deuterium. The latter was demonstrated by the presence of a 1:1:1 triplet at δ 57.07 due to the deuterated methine carbon.

That **93** has two accessible conformations is not unexpected since dibenzo[a,d]cycloheptene systems are known to exist in two conformations[114] (Fig. 2.1). Both conformations are equivalent for **5** as indicated by the single methylene singlet in the ^{1}H NMR of this system. The two conformations of **93** (I and II), however, are not equivalent. According to the ^{1}H NMR of **93** the ratio (2:3) of I and II lies in favour of the latter, which has the methyl signal at δ 1.42. This methyl is believed to belong to II since conformational analysis of similar systems[114] indicate that bulky substituents prefer an axial orientation. Comparison of the chemical shifts for the two conformations also suggest this. It is expected that protons oriented in the equatorial position will experience a deshielding

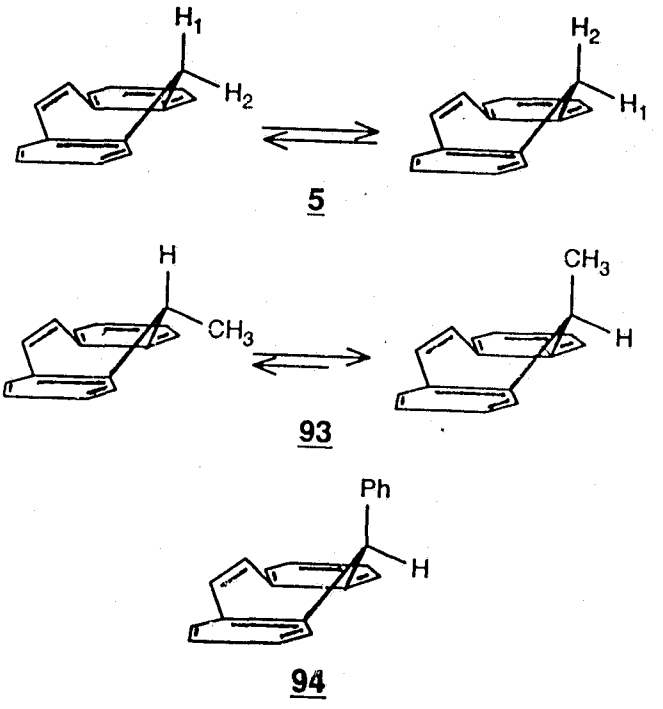

Figure 2.1 Conformations available for **5**, **93** and **94**.

effect since they are in the plane of the aromatic rings. The equatorial methine proton of II is downfield relative to the methine proton of I. Similarly, the methyl protons of I are downfield relative to the methyl protons of II.

Based on the results for **93** it is expected that **94**, with an even bulkier substituent (Ph), would prefer only one conformation, with the bulky group oriented in an axial position. The ^{1}H NMR of **94** indicates only one conformation (at room temperature) which according to the literature[114] has the phenyl oriented axially (Fig. 2.1).

2.2.3 10,11-Dihydro-5*H*-dibenzo[a,d]cyclohepten-5-ol (99) and Related Systems

Reduction of 10,11-dihydro-5*H*-dibenzo[a,d]cycloheptenone (83) with $LiAlH_4$ gave 99. Preparation of the 5-methyl derivative (100) was accomplished by reaction of 83 with MeLi. A third compound, the 5-phenyl derivative (101), was prepared by reaction of 83 with PhLi. Recrystallization of each compound in the appropriate solvent gave products with a purity > 97% by GC and ^1H NMR. The ^1H NMR and MS of each compound were consistent with the structures shown.

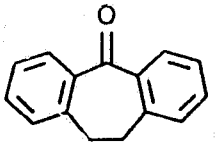

83

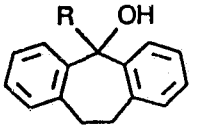

99: R = H **101**: R = Ph
100: R = CH_3 **108**: R = $CH(CH_3)_2$

2.2.4 Dibenzylic Substrates Related to Suberene (5)

Several systems having dibenzylic carbons were synthesized to determine the requirements for excited state carbon acid behaviour. Fluorene (9) was purchased whereas 74 and diphenylmethane (102) were made by reduction of 83 and benzophenone (103) with $LiAlH_4/AlCl_3$, respectively. The deuterated derivative of fluorene (104) was obtained by refluxing 9 in $NaOD/D_2O$/dioxane. The deuterated derivatives of 74 and 102 (105 and 106) were obtained by reducing 83 and 103 with $LiAlD_4/AlCl_3$. Purification by distillation or recrystallization provided products with > 96% purity by GC and ^1H NMR. The identity of each

was confirmed by ^1H NMR and MS.

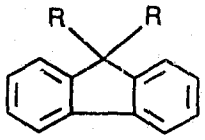

9: R = H
104: R = D

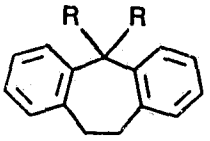

74: R = H
105: R = D

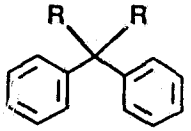

102: R = H
106: R = D

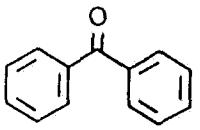

103

2.3 Photolysis of Suberene (5) and Related Systems in ACN/D_2O or H_2O

2.3.1 Extended Photolysis of Suberene (5), 5,5-Dideuteriosuberene (91) and Related Dibenzylic Substrates

Irradiation of ≈100 mg of **5** (Rayonet RPR 100 photochemical reactor; 254 nm lamps; argon purged; at ≈17°C) for 2 h in a 200 mL solution of 50% D_2O/ACN contained in a quartz tube provided the material required for analysis by ^1H NMR. Two signals were noted around δ 3.7, a singlet for the starting material (δ 3.75) and an unresolved triplet (δ 3.73) due to **90**. Comparison of the total integration for these signals with the integration for the vinyl proton signal at δ 7.04 showed ≈40% conversion to **90**. MS analysis further indicated the presence of ≈5% **91** and confirmed the presence of ≈36% of **90**. These results do not rule out the possibility of deuterium incorporation at other positions of **5**. Therefore, a ^2H NMR (360 MHz) was also obtained for the above reaction mixture with the natural abundance of deuterium in CH_2Cl_2 as the reference standard. The resonance at δ 3.7 of this spectrum was too broad to differentiate between **90**

and **91** but the presence of only minor deuterium signals elsewhere in the spectrum indicate that the majority of the deuterium was incorporated at the dibenzylic position. A small deuterium signal (1-2%) was observed at δ 7.05, which corresponds to the vinyl positions of **5**. This suggests that deuterium incorporation occurs at the vinyl position only to a minor extent, either by a photochemical or thermal process.

Repetition of the above reaction with **5** in the absence of light followed by ^{2}H NMR analysis of the resulting reaction mixture indicated only starting material, i.e., no deuterium incorporation at any position. A thermal [1,5] hydrogen shift from the 5-position is possible for **5**, but requires very high temperatures for observable rates (300°C)[115]. The deuterium at the vinyl position must therefore be incorporated via a photochemical route. Repetition of the first photolysis in 50% H_2O/ACN using **91** showed the presence of deuterium only at the dibenzylic position ruling out intramolecular deuterium migration. Therefore, the deuterium observed at δ 7.05 in the initial photolysis must result from a minor proton exchange between D_2O and the vinyl carbons since intramolecular deuterium transfer was ruled out.

A kinetic plot showing the conversion of **5** to **90** and **91** was obtained by photolyzing 200 mg of **5** in a 400 mL 50% D_2O/ACN solution using the same conditions indicated for the initial photolysis. A portion of the reaction mixture was removed at various times and analyzed for percent deuterium incorporation using both ^{1}H NMR and MS. The resulting plot of percent yields for **5**, **90** and

91 versus time is shown in Figure 2.2 clearly showing that **91** is a secondary photoproduct of **90**. For comparison the experiment was repeated using **91** in H_2O/ACN. A similar plot was obtained (Fig. 2.3). However, the growth of the

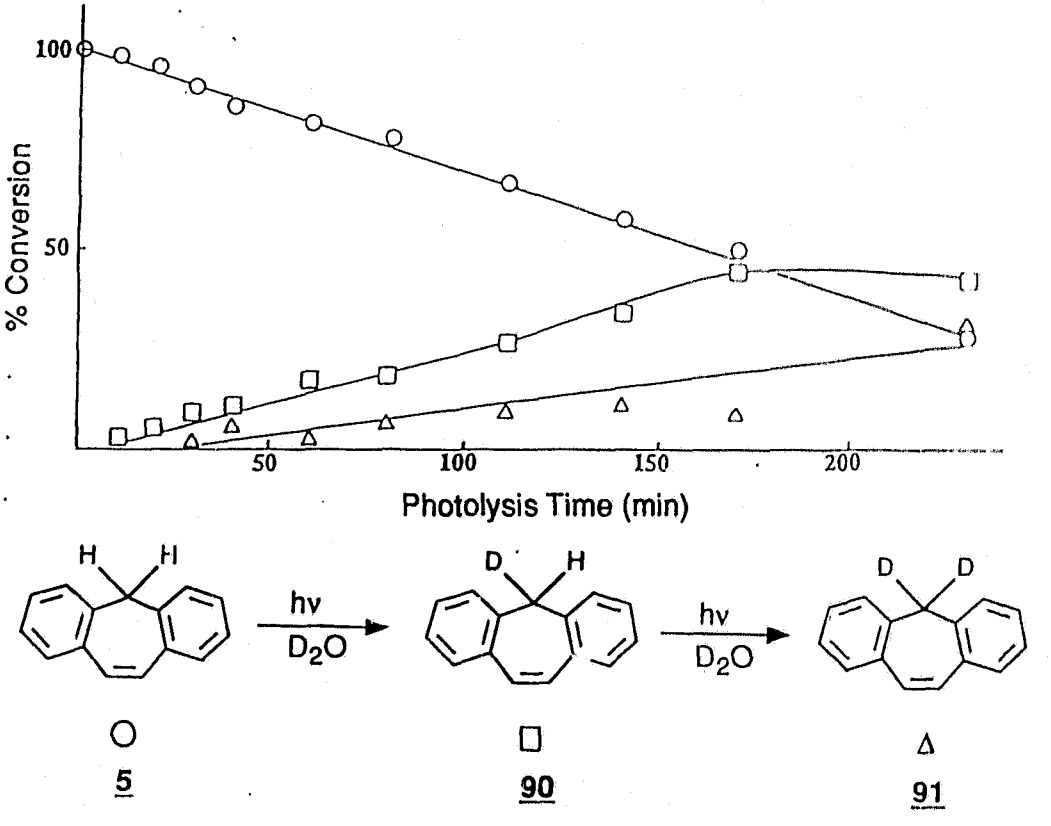

Figure 2.2 Plot of percent conversion of **5** to **90** and **91** versus time of photolysis in D_2O/ACN

secondary photoproduct **5** in this plot was slower than the growth observed for the corresponding photoproduct **91** in the first plot. This is expected since the dibenzylic proton of **90** would be easier to remove than the deuteron (a primary isotope effect), which would favour the formation of **91** in D_2O, and not **5** in H_2O.

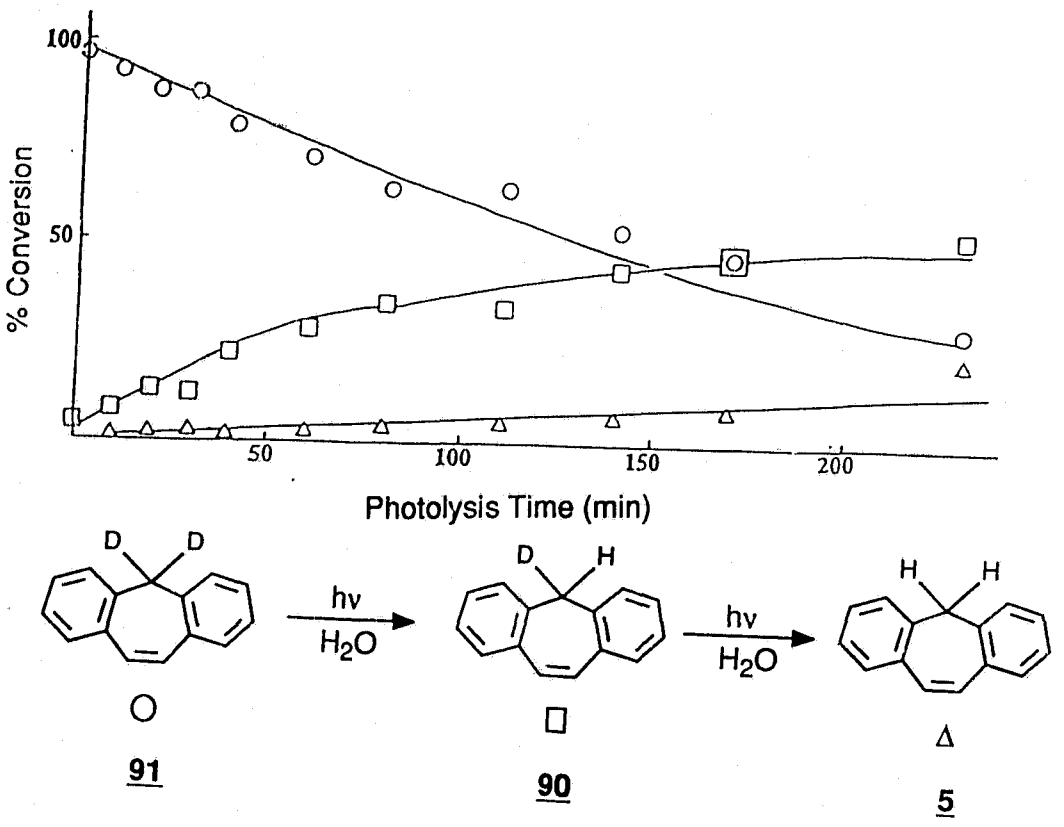

Figure 2.3 Plot of percent conversion of **91** to **90** and **5** versus time of photolysis in H_2O/ACN

Photolysis of fluorene (**9**), **74**, and **102** using the initial conditions indicated for **5** did not result in deuterium incorporation according to analysis of the product mixtures by ^{1}H NMR. Confirmation of these results was achieved by photolyzing the deuterated derivatives **104**, **105** and **106** using the same conditions used to obtain the plot in Figure 2.3. Analysis of the reaction mixture by ^{1}H NMR (360 MHz), after various times of photolysis, indicated that exchange of the deuterium was not occurring since growth of signals due to dibenzylic protons

were not observed in these spectra. These results support the assumption that a 4n electronic ICA is important in the excited state carbon acid behaviour observed for **5**.

2.3.2 Triplet Sensitization of Suberene (5) and 5,5-Dideuteriosuberene (91)

Determination of the reactive state (S_1 or T_1) for proton exchange in **5** was carried out by triplet sensitization of **5** in D_2O/ACN. For successful triplet sensitization of a compound, the triplet energy (E_T) of the donor T_1 state must be greater than the corresponding energy of the acceptor[64] (Fig. 2.4). Intersystem crossing (ISC) of the donor (D) from S_1 to T_1 followed by energy transfer (ET) to the acceptor (A) promotes A to its triplet state. As a result, triplet state reactions of the sensitized species will be observed. By this method, triplet chemistry may be observed selectively.

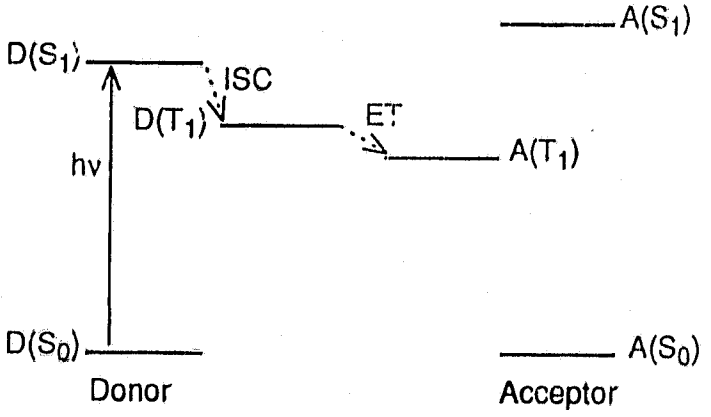

Figure 2.4 Triplet sensitization of an acceptor molecule by irradiation of a donor molecule

2-Benzoylbenzoic acid (**107**) with E_T = 68-71 kcal mol^{-1} [111] was chosen as the donor (triplet sensitizer). The triplet state energy of **5** is estimated to be ≈57 kcal mol^{-1} based on the triplet energy of cis-stilbene (E_T = 57 kcal mol^{-1})[111]. A large excess of **107** (1.0 g) compared to **5** (30 mg) was irradiated for 30 min using a Pyrex tube and 350 nm lamps. The irradiation was carried out in this manner to insure that **5** (which absorbs at < 310 nm) was not directly excited. Analysis of the reaction mixture by ^1H NMR after removal of the sensitizer by base washing indicated no observable deuterium incorporation. As a further check, the triplet sensitization was repeated using **91** in 50% H_2O/ACN. Again no exchange was observed by ^1H NMR analysis. The successful triplet sensitization of **6** ($E_T \approx 60$ kcal mol^{-1} based on styrene (**34**) with E_T = 62 kcal mol^{-1})[111] using the same sensitizer (**107**)[113] suggests that the sensitization carried out for **5** should have also been successful (i.e., energy transfer occurred). Thus, the excited state carbon acid behaviour of **5** must therefore involve S_1, as was demonstrated for **6**[8].

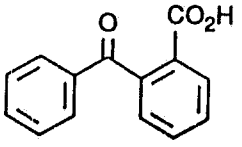

107

2.3.3 Photolysis of 5-Methylsuberene (93) and 5-Phenylsuberene (94)

The excited state carbon acidity of suberene derivatives substituted at the 5-position was investigated by studying **93** and **94**. Irradiation of **93** (70 mg) in 200 mL of 50% D_2O/ACN for 2.5 h using the same conditions as for the initial photolysis of **5** did not result in proton exchange. Photolysis of the deuterated

derivative **95** in 50% 5 M NaOH/EtOH (ethanol is used as a co-solvent since ACN and 5 M NaOH are not miscible) for 2 h resulted in < 5% deuterium exchange by ^{1}H NMR. A similar photolysis of **96** in 50% 5 M NaOH/EtOH also failed to give exchange.

The lack of reactivity observed for these substituted derivatives was unexpected but can be explained by looking at the possible conformations available for **5**, **93** and **94** (Fig. 2.1). The availability of these conformations is believed to play an important role in the lack of excited state proton exchange of **93** and **94**. Wan et al.[116] have shown the effects of conformations on the photosolvolysis of **99** with substituted derivatives **100**, **101** and **108**. A stereoelectronic effect was proposed to account for the relative reactivities observed for the photosolvolysis of these alcohols. It was indicated that heterolysis of the C-O bond, to produce a carbocation, required the assistance of the aryl π orbitals. The π system assists the C-O heterolysis by stabilizing the incipient carbocation. This can only occur if the bond being broken is oriented parallel to the π orbitals of the benzene ring. The systems with a predominance of this conformation (in the ground state) were found to be the most reactive.

A similar requirement for carbanion formation would be expected for **5**, **93** and **94**, i.e., proton exchange depends on the availability of axial protons. Therefore, the 5-methyl derivative (**93**) would be less reactive than **5** towards excited state proton exchange, due to the greater availability of axial protons in the latter. The 5-phenyl derivative (**94**) would be expected to be even less reactive

since it has only a single available conformation, with the proton oriented in the equatorial (hence unfavourable) position. The results observed for **93** and **94** are consistent with this argument. However, the presence of a significant fraction (40%) of the conformer with an axial proton in **93** suggests that this system should be more reactive than what is observed in photolysis in D_2O/ACN. Other factors must therefore be involved which reduce the reactivity of **93** (compared to **5**). The methyl group may hinder abstraction of the dibenzylic proton. Another reason may be the electron donating effect of the methyl group, which will inhibit formation of a carbanion. Results which will be discussed in Chapter 3 add further support that stereoelectronic effects play an important role in determining the reactivity of excited state carbon acids.

2.3.4 Photolysis of Alcohols 99, 100 and 101 in ACN

During the course of the photosolvolysis studies[116] discussed in the last section, a minor unexpected product (2%) was observed, along with the expected product **109** after photolysis of **99** in 50% H_2O/MeOH (eq. 2.1). Compounds **100** and **101** do not react efficiently in photosolvolysis reactions compared to the parent system **99**. The major product observed after irradiation of these substances in H_2O/MeOH or ACN was in fact the minor product observed in the photolysis of **99**.

The origin of this product was investigated by irradiating **99** in ACN (100 mL) using a Rayonet RPR 100 photochemical reactor (254 nm lamps) (eq. 2.2).

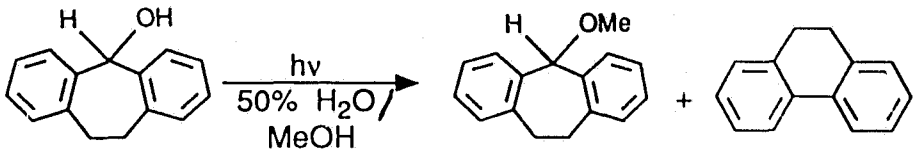

(2.1)

99 **109** **110**

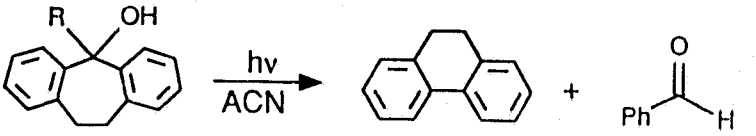

(2.2)

99: R = H
100: R = CH_3
101: R = Ph

110 **111**

Observed when R = Ph

Analysis of the reaction mixture by ^{1}H NMR (90 MHz) indicated that the minor product observed in H_2O/MeOH was now the major product. This product was isolated by preparative thin layer chromatography (TLC) and identified as 9,10-dihydrophenanthrene (**110**) by ^{1}H NMR analysis, by comparison to a spectrum of an authentic sample.

Photolysis of **100** and **101** in ACN using the same conditions noted for **99** also resulted in the formation of **110**. In addition, the ^{1}H NMR of the sample obtained after irradiation of **101** showed a second minor product which was identified as benzaldehyde (**111**) (eq. 2.2). The mechanism proposed to account for **110** involves photoextrusion of a carbene (Scheme 2.1). The first step involves formation of a 1,4-diradical similar to that proposed for di-π-methane rearrangements (*vide supra*). Cleavage of the bonds α to the dibenzylic carbon then regenerates the aromatic rings to give **110**. The benzaldehyde (**111**) observed on irradiation of **101** is derived from rearrangement of the hydroxy phenyl

carbene (or via first addition of water followed by hydrolysis).

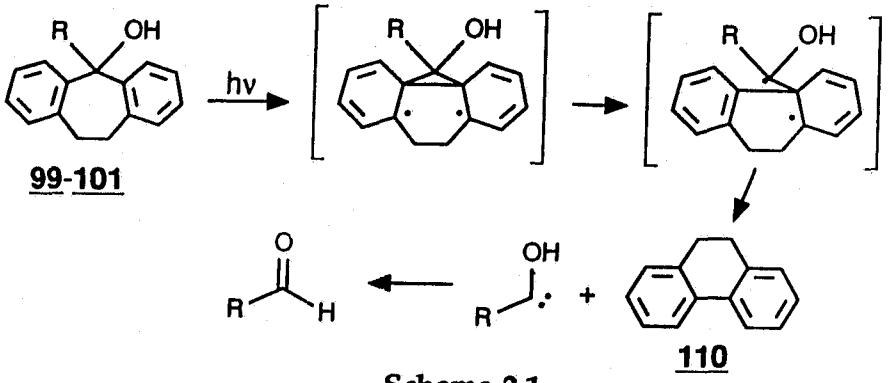

Scheme 2.1

This mechanism, termed an α,α-elimination, was originally proposed by Shi et al.[117] to account for the formation of biphenyl (112) observed in the photochemistry of triphenylmethylphosphonate (113) (eq. 2.3)[118]. Similar reactions have been observed for a variety of triarylmethanes with different substituents at the methyl position (114-119)[117,119]. The α,α-eliminations observed for alcohols 99

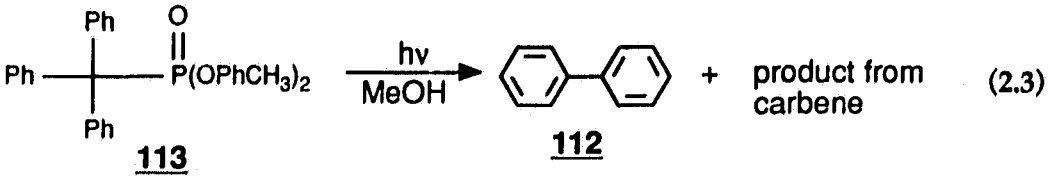

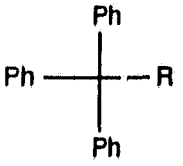

114: R = $N(Et)_2$
115: R = COOH
116: R = $COOCH_3$
117: R = C═CH
118: R = C≡CBu
119: R = CN

101 represent the first examples involving elimination of a hydroxy carbene, as well as the first examples of α,α-elimination of a biaryl system.

The importance of the hydroxyl group at the methyl carbon in promoting

the α,α-elimination was examined by photolyzing **120** and **121** in ACN for 1 h. No reaction was observed. This demonstrates that the hydroxyl substituent does not promote the α,α-elimination to the same extent as the substituents utilized by Shi et al.[117-119]. The linking of the two aryl groups with a carbon chain as in **99**, **100** and **101** must therefore promote the α,α-elimination, by holding the aromatic rings in an arrangement which allows the reaction to proceed. The nature of the chain is also important since photolysis of **122** (obtained by reduction of **92** with PhLi) does not result in an α,α-elimination. Other photochemical reactions, which remain to be delineated, were observed however for **122**.

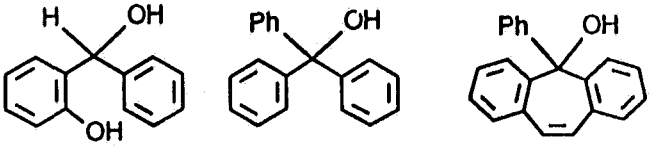

120 **121** **122**

A further check of the generality of the α,α-elimination in systems related to **99** was performed by irradiation of **123** (purchased from Aldrich) in MeOH or ACN. According to GC/MS, the same two products (45%, M^+ = 311 m/z and 5% M^+ = 325 m/z) were formed in each solvent (eq. 2.4). The major product (**124**) was identified by ^{1}H NMR (90 MHz) but the structure of the minor product could

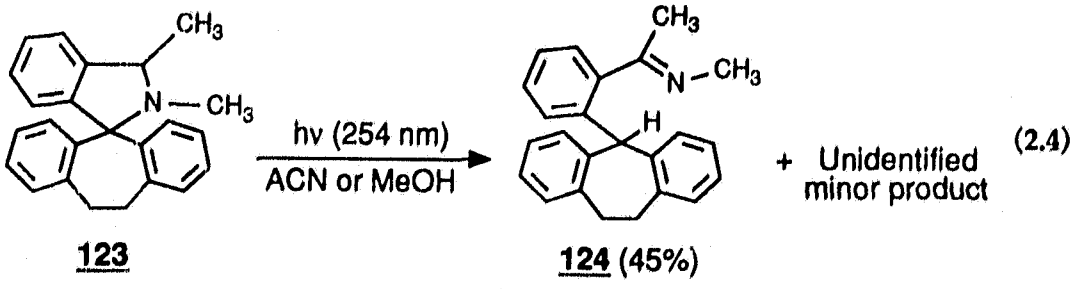

123 **124** (45%) (2.4)

not be determined. However, the α,α-elimination product (**110**) was not observed. This result was not unexpected based on the high yield observed for **124**, which suggests that cleavage of the N-C bond is very efficient.

2.4 Photolysis of Suberene (5) and Related Systems in the Presence of Amines in ACN

In the previous section the base used to investigate the excited state carbon acid behaviour of **5** was H_2O (pK_a (H_3O^+) = -1.7)[15] or D_2O (pK_a (D_3O^+) = -1.8)[120]. A stronger base would be expected to enhance excited state carbon acid behaviour, allowing a better and more efficient study of the factors influencing the proton exchange of **5**. Amine bases were chosen (pK_a (RNH_3^+) = 5 to 11)[121] since they are readily available and have been used extensively in the investigation of carbon acid behaviour in the ground state. The following section examines the effects of tertiary, secondary, and primary amines on the photochemistry of **5** and related systems.

2.4.1 Photolysis of Suberene (5) and Derivatives in the Presence of Et_3N in ACN

Irradiation of **5** (70 mg) for 0.5 h (Rayonet RPR 100 photochemical reactor; 254 or 300 nm lamps; argon purged; at ≈17°C) in 0.01 M Et_3N/ACN (100 mL) resulted in the formation of one major product (20%) and several minor products (total 5%) according to ^1H NMR (90 MHz) and GC analysis of the reaction

mixture (eq. 2.5). The major product was identified as **74** by ^{1}H NMR and

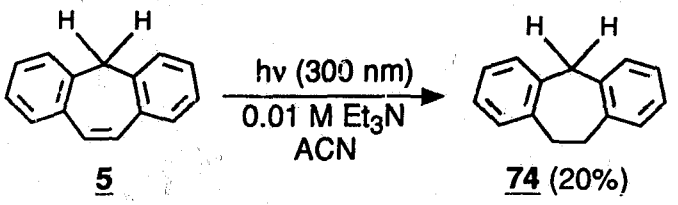

5 **74** (20%) (2.5)

GC/MS (M^+ = 194 m/z) analysis of a sample purified by preparative TLC. The ^{1}H NMR of the major product exhibited two aliphatic signals (singlets at δ 3.12 (4H) and δ 4.08 (2H)) as well as aromatic signals (δ 7.0-7.3) which were identical to the spectrum of authentic **74**.

Photolysis of **91** resulted in the growth of only the δ 3.12 signal which indicates that exchange of the dibenzylic protons (δ 4.08) is not involved during the formation of **74**. This is expected based on the mechanism proposed by Lewis et al.[122] for photoreduction of t-stilbene (**125**) in the presence of tertiary amines (Scheme 2.2). The initial step involves electron transfer (ET) from the ground state tertiary amine to t-stilbene in S_1 resulting in a singlet exciplex **126**. Transfer of a proton from a carbon α to the nitrogen of the amine then occurs to form a radical pair **127**, which can subsequently: a) combine to give adduct **128**, b) disproportionate to give photoreduced product **129**, or c) yield **130**.

The overall yield of these products is dependent on the solvent polarity[123]. For example, in non-polar solvents, isomerization of t-stilbene (**125**) occurs whereas in polar aprotic solvents (ACN) the products derived from **127** predominate. The relative yields of **128**, **129** and **130** were also found to depend

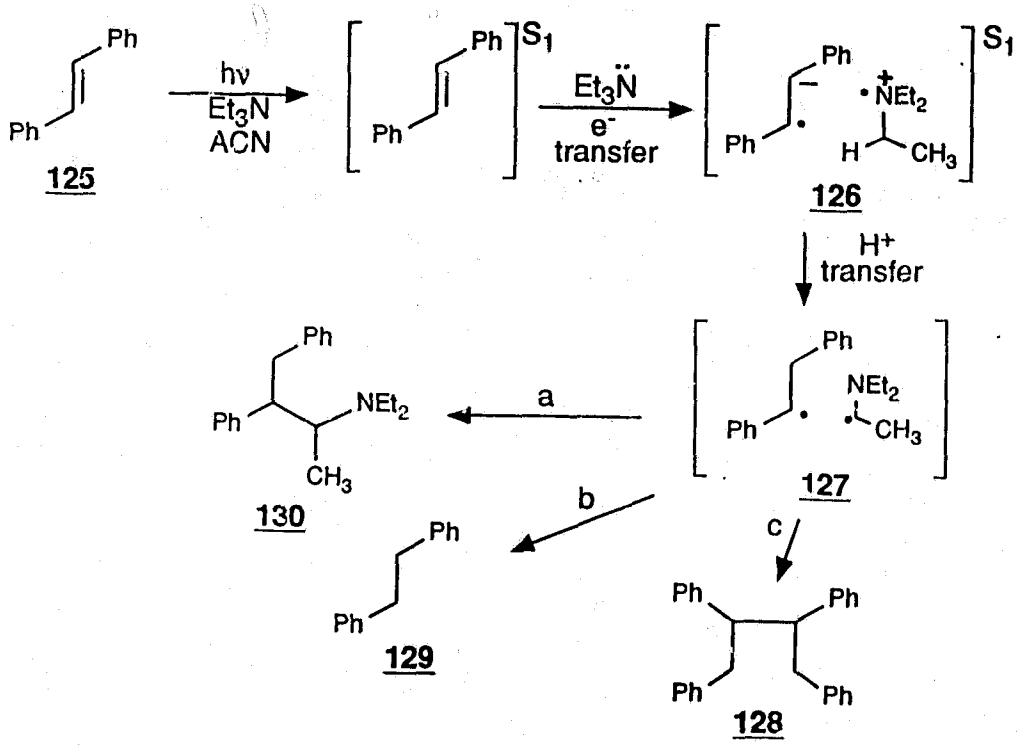

Scheme 2.2

on the structure of the tertiary amine used in the photoreaction[122].

The same mechanism can be used to explain the photoreduction of **5** by Et_3N. Since the major product observed was **74**, disproportionation is the preferred fate of the radical pair formed between Et_3N and **5**. According to the mechanism in Scheme 2.2 the minor products formed along with **74** could be adducts between **5** and Et_3N. The lower rf values of the minor products (relative to **74**) on the TLC of the product mixture is consistent with this conclusion. The complexity of the ^1H NMR of the minor products also suggests adduct formation.

Photolysis of substituted derivatives of suberene **78**, **93** and **94** using the same conditions as for **5** also resulted predominantly in reduction of the vinyl

bond of these compounds. Irradiation of the methyl derivative **93** (50 mg) for 0.5 h resulted in almost complete conversion to the reduced product **131** and several other minor products. The reaction was repeated for 5 min. (eq. 2.6) and analyzed by GC/MS, which confirmed the presence of **131** (9%) (M^+ = 208 m/z), and showed the formation of four adducts with similar retention times (total 8%, ≈ 2% of each) (M^+ = 307 m/z). Four adducts are expected since the radical derived from Et_3N can be attached on either face of the 10- or 11-position of **93**. GC analysis also indicated the presence of dimers (3%) which had much longer retention times. Attempts to analyze these products by MS was unsuccessful, so their exact identity could not be confirmed.

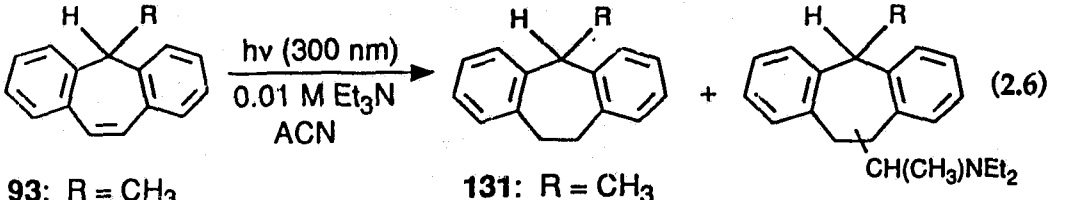

(2.6)

93: R = CH_3
94: R = Ph

131: R = CH_3
132: R = Ph

4 adducts R = CH_3 or Ph

Similar results were obtained for the phenyl derivative **94** (50 mg) when it was photolyzed (10 min.) in 0.01 M Et_3N/ACN (eq. 2.6). The ^1H NMR of the reaction mixture was very complex making identification of products difficult. However, GC/MS analysis indicated formation of the reduced product (**132**) (17%) (M^+ = 270 m/z) and four other adducts with similar retention times (total 11%, ≈ 2-3% of each) (M^+ = 369 m/z). Continuation of the GC for an extended period of time indicated that no dimers were formed from **94**.

Comparison of the photolysis times and yields for **5**, **93** and **94** showed that

the latter two compounds are more reactive in the presence of Et_3N. This difference could result from the presence of a competing reaction available for **5**. One possibility is that Et_3N may actually react as a base and abstract a proton (or deuteron) from the dibenzylic position of excited **5** (or **91**). Since Et_3N has no readily available protons for exchange, the abstracted proton (or deuteron) would be returned to **5** (or **91**) which would result in starting material. This possibility can be investigated by photolyzing alcohol **78**, which ketonizes to **83** when irradiated in the presence of a base, via a carbanion mechanism (*vide supra*).

Photolysis of **78** (102 mg) for 0.5 h in 0.01 M Et_3N/ACN using the same conditions noted for **5** results in one product. Analysis of the reaction mixture by ^1H NMR provided evidence for the formation of the reduction product **99** (26%). No ketonization product (**83**) or adducts were observed. The lack of **83** does not rule out Et_3N functioning as a base, to deprotonate excited **78**, since formation of the ketonization product may require a proton source from solvent (Scheme 1.11). These results do however indicate that **78** has a similar reactivity to that observed for **5** in the presence of Et_3N.

2.4.2 Photolysis of 5,5-Dideuteriosuberene (91) and Related Systems in the Presence of Piperidine in ACN

Photolysis of **91** (100 mg) for 0.5 h in 0.5 M piperidine/ACN resulted in both exchange of the deuterium *and* reduction of the vinyl bond. The yield of each product (**90** and **105**) was less than 10% according to the ^1H NMR (90 MHz).

Unlike the previous photolysis involving Et_3N, a reduction in the concentration of piperidine to 0.05 M had no observable effect on the yields of the two products.

Repetition of the last experiment using the alcohol **78** and 0.1 M piperidine/ACN gave similar results, i.e., the piperidine acted both as a base and an electron donor. This was demonstrated by the presence of both the reduced product (**99**) (14%) and the ketone **83** (2%) in the GC and ^{1}H NMR (90 MHz) of the product mixture.

The results observed for **5** and **78** in the presence of piperidine were expected based on the work of Lewis[123] involving secondary amines. The reduction mechanism involving secondary amines (Scheme 2.3) is similar to that shown for tertiary amines (Scheme 2.2). However, with secondary amines, the proton on the nitrogen is transferred, resulting in a radical pair involving a nitrogen based radical. This radical pair can either: a) combine; b) disproportionate; or c) diffuse apart (Scheme 2.3). According to the products observed for **5** and **78** in the presence of piperidine, disproportionation is preferred, along with deprotonation of the dibenzylic position.

Lewis et al.[124,125] have also demonstrated the usefulness of intramolecular versions of these photoreactions with styrenes[124] and stilbenes[125], which results in nitrogen heterocycles (eq. 2.7). A derivative of **5**, protriptyline (**133**) (provided by Merck Sharp and Dohme Research Labs, U.S.A.), may also react to provide a cyclized product. Photolysis of the hydrochloride salt of **133** in 5% 1.0 M

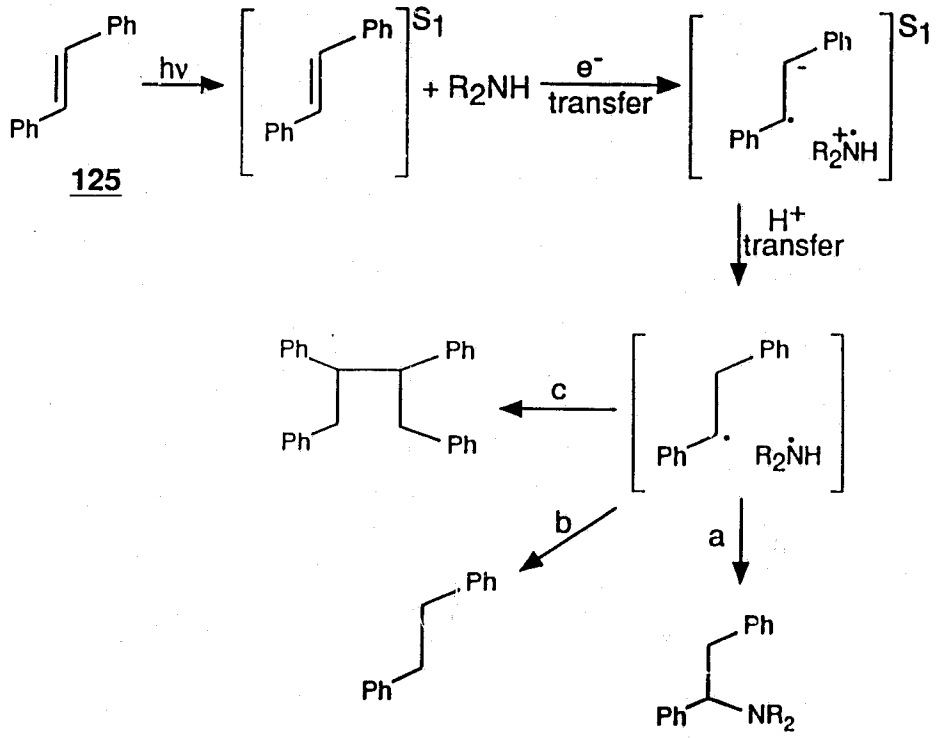

Scheme 2.3

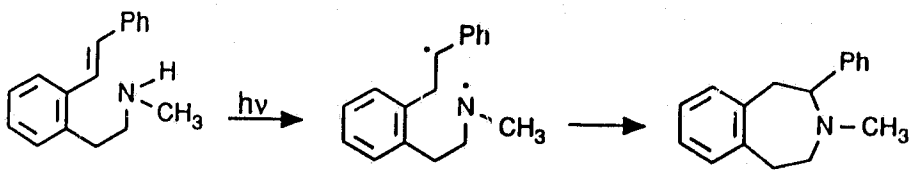

(2.7)

NaOH/ACN for 1.0 h was performed to determine if the amine could react as an electron donor in either an intramolecular or intermolecular fashion. Base was used to insure that the free amine was available for reaction. The results were inconclusive, but formation of approximately 8% of the reduced product **134** was observed (eq. 2.8). This product could be formed via an intramolecular or intermolecular ET process. Based on conformational studies of a related system **135**[126], the latter process is believed to occur since the amine chain is oriented

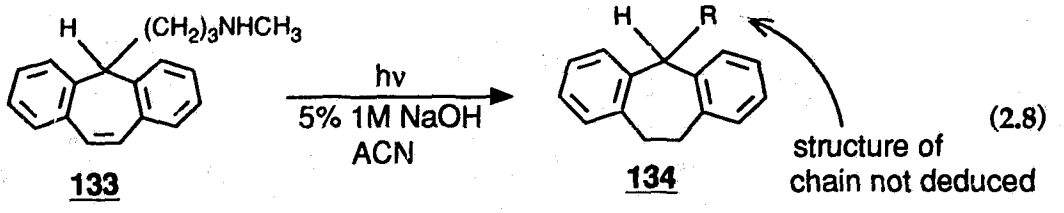

away from the vinyl bond in both of the possible conformations (Fig. 2.5). Confirmation of the formation of **134** and the mechanism involved was obtained by analysis of the reaction by GC/MS.

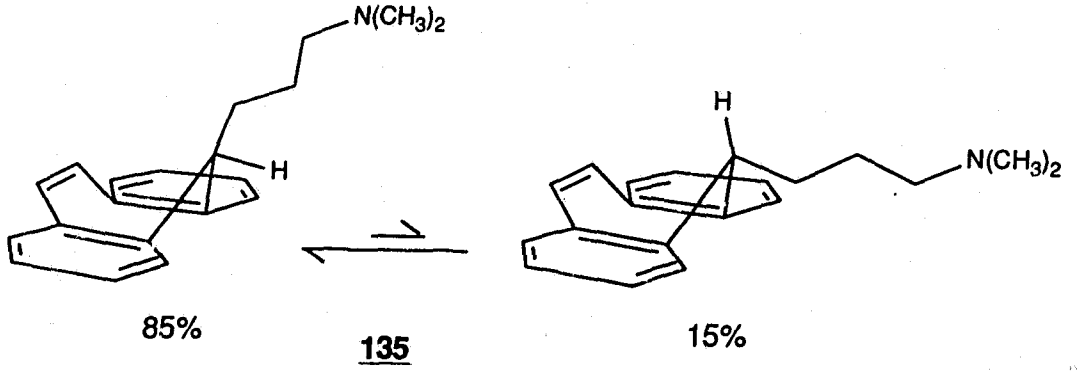

Figure 2.5 Available low energy conformations of **135** showing orientation of the amine chain.

2.4.3 Photolysis of 5,5-Dideuteriosuberene (91) and Derivatives in the Presence of Primary Amines in ACN

As indicated by the photolysis of **5** and related systems in the presence of tertiary and secondary amines, excited state carbon acid behaviour is not enhanced (or at best moderately enhanced) by these bases due to the competing ET process. Primary amines have higher ionization potentials than tertiary or secondary amines (n-propylamine (PA) (8.78 eV) > piperidine (8.04 eV) >

triethylamine (7.82 eV))[127]. Therefore, PA should not donate electrons as readily as the latter two amines. This has been demonstrated in various photochemical studies involving amines as electron donors and as bases[93,128]. In the following studies both ethanolamine (EA) and PA were used to study the effect of primary amines on the photochemistry of **5** and related systems.

Photolysis of **91** (50 mg) in 0.01 M EA/ACN for 0.5 h (same conditions as used for previous photolyses) resulted in exchange of deuterium (**90** (34%) and **5** (5%)) according to a ^{1}H NMR (360 MHz) of the product mixture. Irradiation of **91** in higher concentrations of EA (0.10 M) for 5 min resulted in a substantial amount of deuterium loss (**90** (21%) and **5** (2%)). No reduction products were observed. The greater ability of EA (pK_a (RNH_3^+) = 9.50)[127] to catalyze the excited state deuterium exchange of **91** compared to H_2O (pK_a (H_3O^+) = -1.7)[129] was demonstrated by photolyzing this system in 0.01 M H_2O/ACN for 0.5 h. No deuterium loss could be detected by both ^{1}H NMR and MS.

That the amine portion of EA was responsible for the enhanced exchange of **91** was confirmed by photolyzing this compound in 0.01 M EtOH/ACN and in 0.01 M PA/ACN. No deuterium loss was observed on photolysis in EtOH (pK_a ($EtOH_2^+$) = -2.4)[129]. However, with PA (pK_a ($PrNH_3^+$) = 10.5)[121,130], a similar enhanced exchange was achieved as that observed using EA.

A further check was carried out by photolyzing the deuterated systems **104** and **105** in the presence of primary amines. No deuterium loss was observed in the ^{1}H NMR of either system after a 1 h photolysis of each in the presence of

primary amines (**104** in 1.0 M EA/ACN and **105** in 0.5 M PA/ACN). These results suggest that formation of a carbanion intermediate containing a 4n electronic ICA is still required for observable deprotonation of excited state carbon acids even when stronger bases such as primary amines are used.

Derivatives of **5** (5-methyl (**93**) and 5-phenyl (**94**)) when photolyzed in D_2O/ACN exhibited little or no deuterium incorporation. It would therefore be of interest to measure the amount of exchange observed for these derivatives in the presence of EA and PA. Irradiation of the deuterated 5-methyl derivative **95** (70 mg) in 0.05 M EA/ACN for 0.5 h did not result in loss of deuterium. However, photolysis in 0.10 M EA for 1 h resulted in 15% loss of deuterium. GC analysis of the product mixture indicated only starting material and exchanged product but no photoreduction products. A similar photolysis in 0.50 M EA/ACN resulted in a more substantial loss of deuterium (42%; by MS). Again, GC analysis indicated no additional products.

Photolysis of **95** in 0.5 M PA/ACN for 1 h also resulted in extensive exchange of deuterium (50% by MS) along with products expected via ET from the amine (eq. 2.9). Both the reduced product (deuterated **131**) (3%) and two

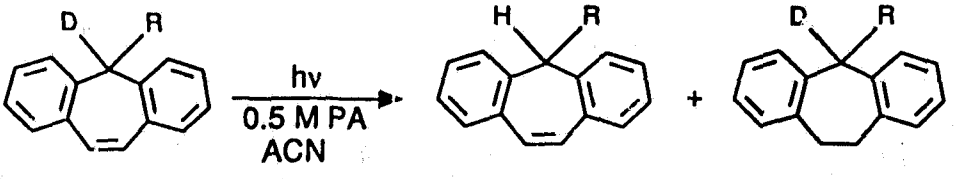

(2.9)

95: R = CH_3
96: R = Ph

93: R = CH_3
94: R = Ph

131: R = CH_3
132: R = Ph

\+ two adducts for each compound

adducts (6%) were formed according to GC. The structures of the adducts were not determined due to their low yields. However, the at best modest yields observed for the ET products indicate that PA functions primarily as a base. The lack of ET products in EA compared to PA was unexpected. The ionization potential of EA would be expected to be somewhat higher than for PA (8.78 eV)[130], due to the presence of the inductively withdrawing hydroxyl group in the former amine, thus making photoreduction less likely.

Photolysis of the deuterated phenyl derivative **96** (99 mg) in 0.5 M EA/ACN for 1 h resulted in only a minor amount of deuterium exchange (< 2% according to ^{1}H NMR. As with **95** no ET products were observed by GC with EA as the base. Photolysis of **96** in 0.5 M PA/ACN resulted in little deuterium exchange (< 2% by ^{1}H NMR). As was observed for **95**, GC analysis of the product mixture showed the formation of products expected via ET (deuterated **132** (5%)) and one adduct (5%)) (eq. 2.9). The presence of both of these products was confirmed by GC/MS but the location of the amine group in the adduct was not determined.

Comparison of the results obtained for photolysis of **91**, **95** and **96** in the presence of primary amines suggests a decrease in reactivity with substitution at the dibenzylic position of **5**. These results agree with those observed for photolysis of **5**, **93** and **94** in D_2O. The relative reactivities observed can be explained by a stereoelectronic argument due to conformational effects (*vide supra*). According to these arguments **96** would be expected to be the least

reactive towards excited state proton exchange with **95** having a reactivity between that of **91** and **96**.

Preliminary studies of the effect of primary amines on the photoketonization of **78** have also been carried out. Photolysis of **78** (100 mg) in 0.01 M EA/ACN for 0.5 h resulted in a minor amount of ketonization to **83** (5%). No ET products were identified in the ^{1}H NMR of the product mixture. When the photolysis was carried out in 0.10 M PA/ACN for 0.5 h the ketonization product (**83**, 3%) as well as the reduction product (**99**, 6%) were formed. Irradiation of **80** (100 mg) in 0.10 M PA/ACN for 0.5 h resulted in a minor amount of **78** (5%) but no ketonization or reduction products.

These results indicate that the photoketonization of **78** is not as efficient as anticipated when primary amines are used. This may be due to the nature of the solvent since previous studies of the photoketonization of **78**[112] were performed in > 50% H_2O/ACN. In the proposed mechanism (Scheme 1.11) water acts both as a base and a proton source. The reaction may therefore be intrinsically less efficient in EA/ACN and PA/ACN due to the lack of water as the proton source. Further studies are required to determine the effect of solvent on the photoketonization process.

2.5 Quantum Yields

When a molecule is placed in an excited singlet state (S_1, S_2, S_3...) by absorption of light with energy hν, it can lose the added energy via several

different pathways, as shown by a Jablonski diagram (Fig. 2.6). The following is a brief description of deactivational pathways from S_1[64]. Deactivation occurs from the lowest vibrational level of S_1 since vibrational relaxation from higher electronic states or vibrational levels occurs more rapidly ($\approx 10^{12}$ sec^{-1})[64] than relaxation from S_1 to S_0.

1) Fluorescence (hν'): Emission of light from a molecule in S_1 resulting in deactivation of the molecule to S_0.

2) Intersystem Crossing (ISC): Change of spin multiplicity, e.g., from singlet to triplet by crossing from S_1 to T_1. Once in T_1 a molecule can

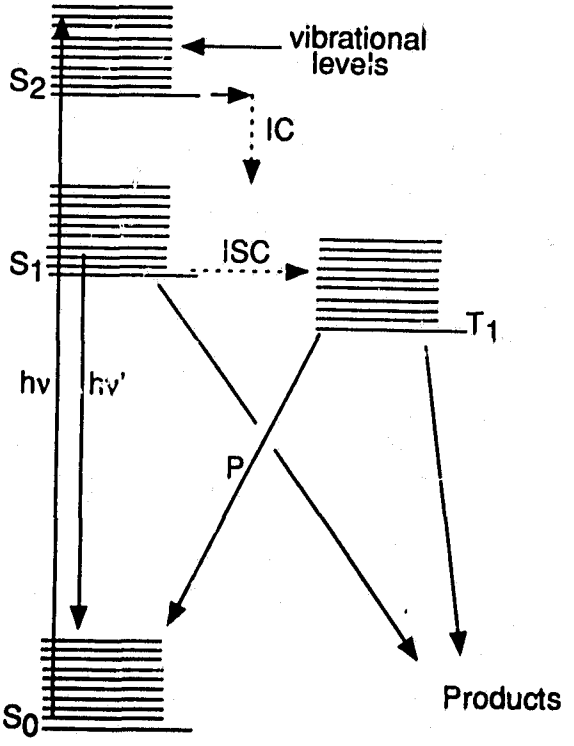

Figure 2.6 Jablonski diagram showing deactivational pathways for an electronically excited molecule.

either (a) emit light to reach S_0 (termed phosphorescence (P)); (b) react to form products; (c) transfer its energy to another molecule (triplet sensitization).

3) Internal Conversion (IC): Non-radiative transition of a molecule from a higher energy state (S_1) to a lower state (S_0). In general IC is more common between higher states (S_3, S_2, and S_1) since the energy gaps between these states are smaller than the corresponding gap between S_1 and S_0.

4) Photochemical Reaction: The molecule in S_1 can react to form products via intramolecular or intermolecular processes.

The relative importance of each of these processes can be determined by the measurement of quantum yields. The quantum yield for a particular process is defined as the percentage of excited molecules which are deactivated via that process. In the following sections two deactivational pathways (photochemical reaction and fluorescence) of **5** and related systems will be quantified by the measurement of their respective quantum yields.

2.5.1 Product Quantum Yields

The product quantum yield may also be defined as the number of moles of a photoproduct produced per mole of photons (Einstein) absorbed by the reactant. This value is a direct measure of the efficiency of the photochemical process involved. Determination of such values allows for the study of factors

which influence the efficiency of a photochemical reaction. In the following section the extent of proton (deuteron) exchange for [illegible] and related systems in various solvents and bases will be quantified by the measurement of exchange quantum yields (Φ_{ex}). Also included in this section will be the product quantum yields (Φ_p) for the α,α-elimination observed on photolysis of the alcohols **99**, **100** and **101**.

All of the product quantum yields reported (Table 2.1 to 2.3 and 2.5) were measured using an optical bench with a mercury arc lamp and a monochromator set at 280 nm as the excitation wavelength. For each quantum yield two or more samples were irradiated separately in UV cuvettes while purging and mixing with argon. Irradiation times were chosen to limit the percent yield of the product to < 20%. Each photolyzed sample was analyzed a minimum of three times by either MS (for Φ_{ex}) or by GC (for Φ_p). The error shown is the standard deviation in the three (or more) analyses performed on each sample. The light intensity (in Einsteins) of the source was determined by use of a potassium ferrioxalate $\{K_3[Fe(C_2O_4)_3]\cdot 3H_2O\}$ actinometry[111,131]. Anhydrous solvents when required were obtained by drying the solvent over molecular sieves, except with ACN which was distilled over CaH.

The values of Φ_{ex} listed in Table 2.4 were measured in a Rayonet photochemical reactor using **91** in 50% H_2O/ACN as a secondary actinometer with analyses by 360 MHz ^1H NMR. The value of Φ_{ex} for **91** in 50% H_2O/ACN was measured on the optical bench. Each sample was irradiated (Rayonet RPR

100 photochemical reactor; 254 nm lamps; argon purged; at ≈17°C) in a 100 mL quartz tube with the indicated solvent. The errors indicated were determined from the error in the standard used and from errors in the measurement of deuterium loss from the starting materials.

Table 2.1 contains values of Φ_{ex} for deuteration of 5 in deuterated solvents. As noted earlier, deuterium incorporation was not observed in CD_3CN (Φ_{ex} = 0.000). Also, as expected the quantum yield decreases as the amount of D_2O is decreased below 50% D_2O/ACN. These quantum yields of exchange are low and indicate that proton exchange is an inefficient process (≈3%), and other deactivational processes must dominate the photochemistry of 5. The value of Φ_{ex} drops even further when MeOD is substituted for D_2O.

Table 2.1 Quantum yields of exchange (Φ_{ex}) for 5 in deuterated solvents[a].

Solvent[b]	Φ_{ex}[c]
100% CD_3CN	0.000
70% D_2O/ACN	0.029 ± 0.004
50% D_2O/ACN	0.030 ± 0.004
20% D_2O/ACN	0.021 ± 0.003
70% MeOD/ACN	0.006 ± 0.001

[a]Ambient temperatures with λ = 280 nm. [b]ACN as cosolvent for solubility reasons. Ratios are v/v. [c]Analyzed by MS of 3 or more independent runs. Errors are standard deviation in these runs.

Table 2.2 shows the corresponding values of Φ_{ex} for protonation of **91** with protiated solvents. Comparison of the results in H_2O with those in D_2O shows that only a small isotope effect for exchange is observed. The isotope effect is also the reverse of that expected based on the relative strengths of the C-H and C-D bonds. Comparison of Φ_{ex} for **5** in 70% MeOD/ACN with **91** in 70% MeOH/ACN also shows a "reverse" isotope effect. An explanation of these results will be presented in a later section dealing with fluorescence quenching

Table 2.2 Quantum yields of exchange (Φ_{ex}) for **91** in protiated solvents[a].

Solvent[b]	Φ_{ex}[c]
100% CH_3CN	0.000
70% H_2O/ACN	0.045 ± 0.006
50% H_2O/ACN	0.035 ± 0.005
20% H_2O/ACN	0.024 ± 0.003
70% MeOH/ACN	0.012 ± 0.002
70% EtOH/ACN	0.008 ± 0.001
70% 2-PrOH/ACN	0.003 ± 0.001
70% t-BuOH/ACN	< 0.002
50% $HCONH_2/H_2O$	0.019 ± 0.005
50% $HCONH_2$/ACN	0.010 ± 0.003

[a]Ambient temperatures with λ = 280 nm. [b]ACN as cosolvent for solubility reasons. Ratios are v/v. [c]Analyzed by MS of 3 or more independent runs. Errors are standard deviation in these runs.

studies (*vide infra*).

Included in Table 2.2 are values of Φ_{ex} using a series of alcohol bases. The trend observed can be explained by considering the pK_as of the protonated alcohols and H_3O^+. The magnitude of these pK_a should affect the value of Φ_{ex} for **91** since the initial step for loss of a deuterium is believed to involve abstraction of a deuterium by the base. The pK_a of H_3O^+ (-1.7)[129] versus alkyl alcohols (ROH_2^+) (-2 to -5)[29,132] suggests that deuterium exchange in water should be higher than in alcohols, i.e., H_2O is more basic. In addition the probability of exchange in water is greater due to the number of available protons in this solvent compared to alcohols. The results confirm these expectations, since a large difference was observed between values of Φ_{ex} measured in 70% H_2O/ACN and 70% alcohol/ACN.

The relative basicity of the alcohols used is not known since literature values were measured using different methods and conditions[132]. Several factors including the nature of the donor acid, the solvent and the temperature influence the basicity of saturated alcohols. These factors are significant since they determine the relative importance of steric and inductive effects on the pK_as of these alcohols. Under certain conditions inductive effects control the relative pK_a, i.e., 2-propanol > ethanol > methanol[132]. This order is reversed when steric effects become important. In the proton transfer being considered **91**, acts as an acid and donates a deuterium to an alcohol. The relatively large size of **91** should increase the importance of steric factors in the proton transfer. The importance of

inductive effects should be less important due to the high polarity of the solvent (70% alcohol/ACN) which should stabilize any protonated alcohol. The trend observed in Table 2.2 for Φ_{ex} using alcohols suggests that steric effects do dominate as the efficiency of the proton exchange decreases in the order MeOH > EtOH > iso-PrOH > t-BuOH.

A comparison of the dielectric constant (ε) of water (78.5)[29] and of several alcohols (MeOH ε = 32.70, EtOH ε = 24.55)[29] indicates that this property of solvents may also play an important role in determining the value of Φ_{ex}. A dielectric constant is a measure of a solvent's ability to stabilize a charged species[29]. Water may enhance the exchange process to a larger extent than the alcohols due to its much higher dielectric constant. An attempt was made to determine the affect of dielectric constants by measuring the value of Φ_{ex} in 50% $HCONH_2/H_2O$. Formamide ($HCONH_2$), with a very high dielectric constant (111.0)[29], should enhance the exchange process. However, as demonstrated by the results in Table 2.2, the value of Φ_{ex} obtained in 50% $HCONH_2/H_2O$ is less than the value obtained in 50% H_2O/CH_3CN (CH_3CN ε = 37.5)[27]. One possible reason for this result may be that exchange of protons is less likely with formamide as protonation preferentially occurs at the amide oxygen where there are no exchangeable protons. This is consistent with the low value of Φ_{ex} found in 50% $HCONH_2/CH_3CN$ (Table 2.2). These results are not completely consistent with the importance of the solvent dielectric constant in the proton exchange of **5** (or **91**). A protic solvent with a higher dielectric constant than water and a similar

pK_a would be required to examine the importance of this solvent property.

Table 2.3 shows values of Φ_{ex} in solutions with various acid (H_2SO_4) and base (NaOH) concentrations. In all cases ethanol was used as a co-solvent rather then ACN since the latter is not miscible with aqueous solutions

Table 2.3 Quantum yields of exchange (Φ_{ex}) for **91** in acidic and basic aqueous solutions[a].

Solvent	Φ_{ex}[b]
70% 1.25 M H_2SO_4/EtOH	0.012 ± 0.002
70% 2.5 M H_2SO_4/EtOH	0.008 ± 0.001
70% 5.0 M H_2SO_4/EtOH	0.002 ± 0.001
50% 0.5 M NaOH/EtOH	0.043 ± 0.006
50% 1.0 M NaOH/EtOH	0.048 ± 0.006
50% 2.0 M NaOH/EtOH	0.064 ± 0.008

[a]Ambient temperatures with λ = 280 nm. [b]ACN as cosolvent for solubility reasons. Ratios are v/v. [c]Analyzed by MS of 3 or more independent runs. Errors are standard deviation in these runs.

containing high acid or base concentrations. As expected, an increase in [H_2SO_4] decreases the value of Φ_{ex} whereas an increase in [NaOH] increases the value of Φ_{ex}. The importance of these results will be discussed in a subsequent section concerned with fluorescence quenching studies.

The results in Table 2.4 also indicate the importance of base strength in determining the value of Φ_{ex}. Primary amines are more basic than H_2O and would be expected to enhance the proton exchange process of **5**. The values shown are for loss of deuterium from **91** using dilute solutions of EA in ACN. Comparison of these values to those obtained in H_2O/ACN solution indicate that primary amines (i.e., EA) are much more efficient at promoting the excited state proton exchange process than H_2O. The result for **95**, which does not exchange

Table 2.4 Quantum yields of exchange (Φ_{ex}) for **91** and related systems in dilute primary amine/ACN solutions[a].

Compound	Solvent	Φ_{ex}[b]
91	0.01 M EA/ACN	0.024 ± 0.006
91	0.10 M EA/ACN	0.08 ± 0.02
95	0.10 M EA/ACN	0.004 ± 0.001
96	0.10 M EA/ACN	0.000

[a]Measured in a Rayonet photochemical reactor (254 nm) at ambient temperatures using **91** in 50% H_2O/ACN as the secondary actinometer (Φ_{ex} = 0.035 ± 0.005). [b]Analysis by 360 MHz ^{1}H NMR. Errors are uncertainties in the secondary actinometer and in peak heights determined from integrations in the ^{1}H NMR.

in water, also indicates the greater ability of primary amines to catalyze the excited state proton exchange process. The low value of Φ_{ex} found for the phenyl derivative **96** was expected based on the conformational effects discussed earlier.

In Table 2.5 product quantum yields (Φ_p) for α,α-elimination observed for alcohols **99, 100** and **101** are presented. The magnitude of these quantum yields indicate that the α,α-elimination proposed for these alcohols is inefficient. It is believed that a fluorescence lifetime effect (*vide infra*) is responsible for the difference in reactivity observed for these compounds.

Table 2.5 Product quantum yields (Φ_p) for α,α-elimination in ACN[a].

Compound	Φ_p[b]
99	0.08 ± 0.02
100	0.015 ± 0.002
101	0.021 ± 0.007

[a]Ambient temperatures with λ = 254 nm in spectroscopic grade ACN. [b]Analyzed by GC of 3 or more independent runs. Errors are standard deviation in these runs.

2.5.2 Fluorescence Quantum Yields

The fluorescence quantum yield (Φ_f) of a compound is the fraction of excited molecules which are deactivated by fluorescence. The fluorescence quantum yield shown in Table 2.6 for **5** was obtained by comparison with two

standards with known Φ_f (2-aminopyridine (136) $\Phi_f = 0.60 \pm 0.05$ and anthracene (137) $\Phi_f = 0.27 \pm 0.03$)[134]. A similar procedure was performed to obtain values of Φ_f for the methyl (93) and phenyl (94) derivatives of 5. However, 5 was used as the secondary standard for these measurements.

Table 2.6 Fluorescence quantum yields (Φ_f) for suberene (5) and related systems[a].

Compound	Φ_f
5	0.89 ± 0.10[b]
93	0.975 ± 0.08[c]
94	0.57 ± 0.05[c]

[a]Determined using areas in fluorescence emissions of indicated compounds at ambient temperatures in dry ACN distilled over CaH. In all cases O.D. were < 0.1. Errors are based on standard deviations in 3 or more independent analysis. [b]Measured against 2-aminopyridine (136) with matching over λ = 262-272 nm and anthracene (137) with matching over λ = 310-311 nm. [c]Measured against 5 with matching over λ = 310-317 nm.

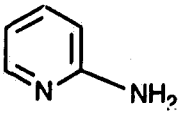

136

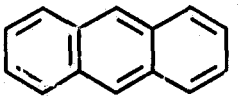

137

Before considering the values of Φ_f, a brief discussion of the fluorescence spectra of 5, 93, and 94 (Fig. 2.7) will be presented. Emission from the methyl derivative 93 is blue shifted relative to the other two systems, whereas the

emission of the phenyl derivative **94** is more structured. A minor amount of structured emission from **5** and **93** is observed by comparison of the respective excitation and emission spectra for each, suggesting a small change in geometry after excitation of each[80]. The proximity of the absorption and emission spectra of **5** and **93** suggests a minor change in geometry for the latter system and a larger change for the former after excitation. The structured emission and red shift observed for the fluorescence emission of **94** both indicate that this system is more rigid in S_1 than in S_0.

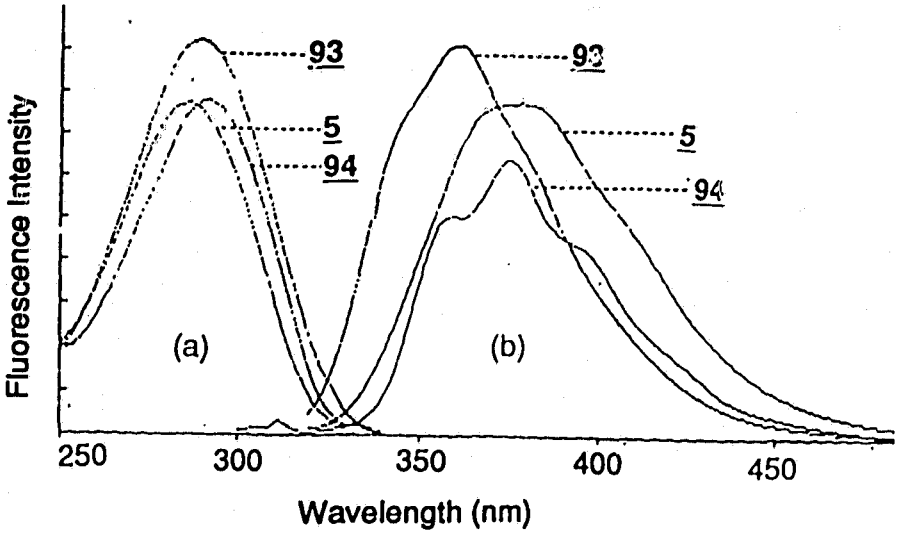

Figure 2.7 Fluorescence excitation (a) and emission (b) spectrum of **5**, **93** and **94**.

The importance of fluorescence as a deactivational pathway for **5** is demonstrated by the magnitude of Φ_f observed for this compound (0.89 ± 0.05).

This result is expected since **5** is fairly rigid, and previous studies of related systems (i.e., locked stilbenes) also indicate fluorescence quantum yields approaching unity[64]. As will be demonstrated in the following section this behaviour of **5** can be used to gain insight into the excited state proton exchange observed for this system.

Comparison of Φ_f for **93** (0.97 ± 0.08) and **94** (0.57 ± 0.05) with the value obtained for **5** suggests that fluorescence is still an important deactivational pathway for these substituted derivatives. The smaller value observed for **94** is due to the greater number of vibrational degrees of freedom introduced into this dibenzannelated system by the phenyl substituent. These additional modes of vibration enhance IC, which reduces the value of Φ_f.

2.6 Fluorescence Lifetimes and Quenching Studies

One of the most common methods of indirectly determining the rates of photochemical reactions is through the use of Stern-Volmer plots[64] (*vide supra*). A Stern-Volmer plot correlates the change in fluorescence intensity with changes in the concentration of a quencher (eq. 1.23). The slope of this plot is equal to the rate of quenching (k_q) multiplied by the fluorescence lifetime of the substrate in the absence of quencher (τ_0). The value of τ_0 must therefore be determined before values of k_q can be derived. In the following section values of τ_0 used in the quenching studies will be measured first. The results obtained in fluorescence quenching studies involving **5**, **93**, **94** and their deuterated derivatives, using

various quenchers, will then be presented and discussed.

2.6.1 Fluorescence Lifetimes

The spontaneous emission of light (fluorescence hν') from an excited species (M^*) (eq. 2.10) is a random process which follows first order kinetics (eq. 2.11)[80] (where k_f represents the rate of the emission in s^{-1}). Integration of equation 2.11 provides the exponential relationship between $[M^*]$ (the concentration of M^* at time = t) and $[M^*]_0$ (the initial concentration of M^* at t = 0) (eq. 2.12). The

$$M^* \longrightarrow M + h\nu' \qquad (2.10)$$

$$-\frac{d[M^*]}{dt} = k_f[M^*] \qquad (2.11)$$

$$[M^*] = [M^*]_0 e^{-k_f t} \qquad (2.12)$$

fluorescence lifetime (τ) of a species such as M^* is inversely related to k_f ($\tau = 1/k_f$). When $t = \tau$ in equation 2.12, $[M^*] = [M^*]_0 1/e$. The time τ required for the original concentration of M^* to decrease by 1/e is defined as the fluorescence lifetime of the excited species.

Single photon counting[135] was the method used to measure fluorescence lifetimes. This technique involves counting of individual photons emitted at certain delay times from a species which is excited by a pulse of light from a hydrogen arc lamp. The delay time between excitation and emission for each

photon is determined by a timer which is started by a pulse from the excitation source and stopped when a photon from the excited species arrives at the photomultiplier. Numerous repetitions of this process produces a histogram which represents the distribution of photons arriving at each delay time being considered (Fig. 2.8). Analysis via deconvolution of this curve provides the

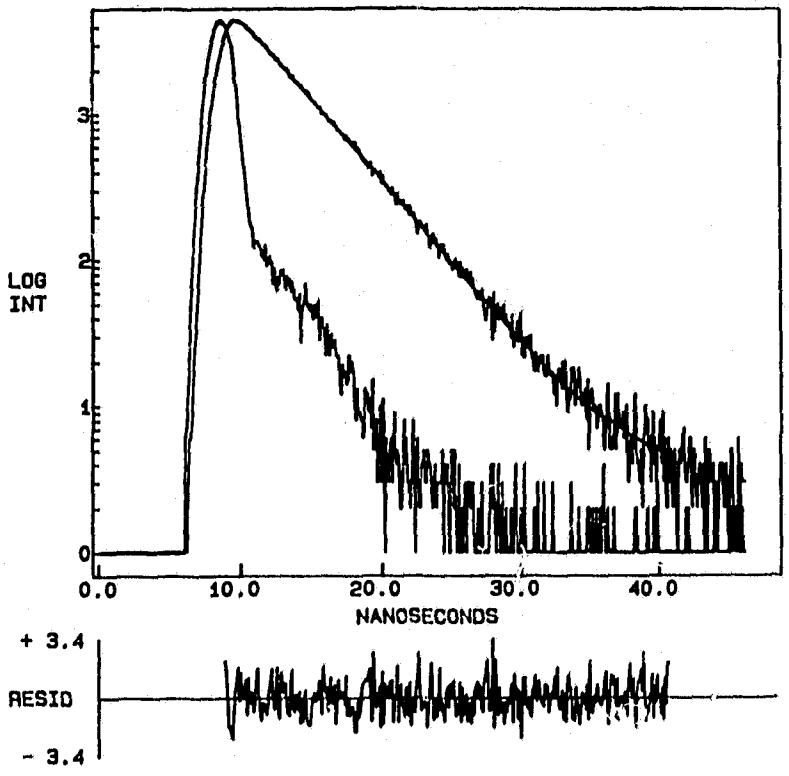

Figure 2.8 Example of a fluorescence decay (upper curve) and the corresponding lamp profile (lower curve) constructed by counting single photons with different delay times. The bottom plot represents the residuals.

required lifetime along with residuals (RESID) which indicate the accuracy of the fit.

The results for **5** and the deuterated derivatives **90** and **91** in ACN suggest a minor isotope effect on the fluorescence lifetime of this system (Table 2.7). Deuteration of an aromatic hydrocarbon has little effect on the fluorescence lifetime[64]. When an effect is observed, the fluorescence lifetime of the aromatic hydrocarbon increases due to a decrease in IC. This decrease in IC is due to the lower frequency of the C-D stretch compared to the C-H stretch. This lower frequency makes vibrational relaxation less favourable. A possible reason for the minor isotope effect noted for the fluorescence lifetimes of **5**, **90** and **91** is a heavy atom effect[64,60]. The deuterium may enhance ISC from S_i to T_1 which would reduce τ. However, such effects are normally significant only for substitution of

Table 2.7 Fluorescence lifetimes of suberene (**5**) and related systems[a].

Compound	τ(ns)[b]
5	5.08 ± 0.05
90	4.85 ± 0.06
91	4.74 ± 0.03
93	2.91 ± 0.06
94	2.03 ± 0.06

[a]At ambient temperatures in dry ACN distilled over CaH, λ_{ex} = 280 nm, λ_{em} = 370 nm. [b]Errors are standard deviations of 3 or more independent runs.

H by halogens (Cl, Br, and I).

A significant decrease in fluorescence lifetimes was observed for the substituted derivatives **93** and **94**, compared to the parent system **5** (Table 2.7). Decreased fluorescence lifetimes are generally observed when non-radiative processes such as IC or ISC compete favourably with fluorescence[64,80]. Enhancement of non-radiative processes may affect the reaction of **93** and **94** with bases such as water, making exchange in these systems less efficient. However, the observed decrease in τ for these systems is not substantial enough to produce the dramatic effect on excited state proton exchange noted in the product studies (*vide supra*).

Table 2.8 gives fluorescence lifetimes for alcohol **99** and substituted

Table 2.8 Fluorescence lifetimes of alcohol **99** and substituted derivatives.

Compound	τ(ns)[b]	$k_{\alpha,\alpha'}$, 10^6 s^{-1} [c]
99	9.79 ± 0.15	8.2 ± 2.2
100	0.00 ± 0.10	16.7 ± 2.4
101	2.87 ± 0.10	27.3 ± 2.7
108	1.58 ± 0.10	-[d]
138	~0.3 ± 0.1	-[d]

[a]At ambient temperatures in dry ACN distilled over CaH, λ_{ex} = 260 nm, λ_{em} = 300 nm. [b]Errors are standard deviations of 3 or more independent runs. [c]Errors from deviation in values of τ and Φ_p. [d]Φ_p not obtained.

derivatives **100** (methyl), **101** (phenyl), **108** (iso-propyl)[136] and **138** (t-butyl)[136] in ACN. The magnitude of τ clearly demonstrates the effect of substitution on the fluorescence lifetime of **99**. All of the substituted systems have lifetimes < 3 ns while the parent system **99** is much longer lived. This decrease in lifetimes limits the quantum yields observed (Table 2.5). However, when relative rates of reactivities are calculated ($k_{\alpha,\alpha}$) by dividing values of Φ_p by the corresponding value of τ it can be shown that **100** is the most reactive followed by **99** and **101**.

2.6.2 Fluorescence Quenching Studies Involving Water and Related Bases

As indicated in previous studies of **5**[7], the fluorescence of this system is efficiently quenched by water. The fluorescence of other systems (**9**, **74** and **102**) which do not function as excited state carbon acids, is not quenched by water. Similarly, when the 5-position of **5** is completely substituted, as in 5-methyldibenzo[a,d]cyclohepten-5-ol (**77**), no fluorescence quenching by water was observed. These results indicate that the fluorescence quenching of **5** by water is due to the photo-initiated exchange of protons at the 5-position of this compound. Quantification of the fluorescence quenching of **5** and related systems by water and other bases should thus provide a direct measure of the rate of this deprotonation process.

The fluorescence quenching rate constants (k_q) tabulated (Table 2.9 and 2.10) were obtained by Stern-Volmer analysis of steady-state fluorescence quenching results. The fluorescence intensities in ACN at various concentrations

of quencher were measured using a Perkin Elmer MPF-66 fluorescence spectrophotometer (Fig. 2.9). Plots of these fluorescence intensities (ϕ_f^0/ϕ_f) against the quencher concentration ([Q]) (Fig. 2.10) provided the required Stern-Volmer plots. In all cases linear plots with intercepts of 1.0 were obtained. Values of k_q were obtained by dividing the slopes obtained from these plots by the appropriate fluorescence lifetime. To minimize effects due to changes in solvent composition the concentration of all quenchers were kept below 1.0 M. Fluorescence quenching by oxygen was minimized by purging each solution for 10 min with Ar prior to measurement. Errors shown are standard deviation observed after three or four repetitions of the fluorescence quenching study concerned.

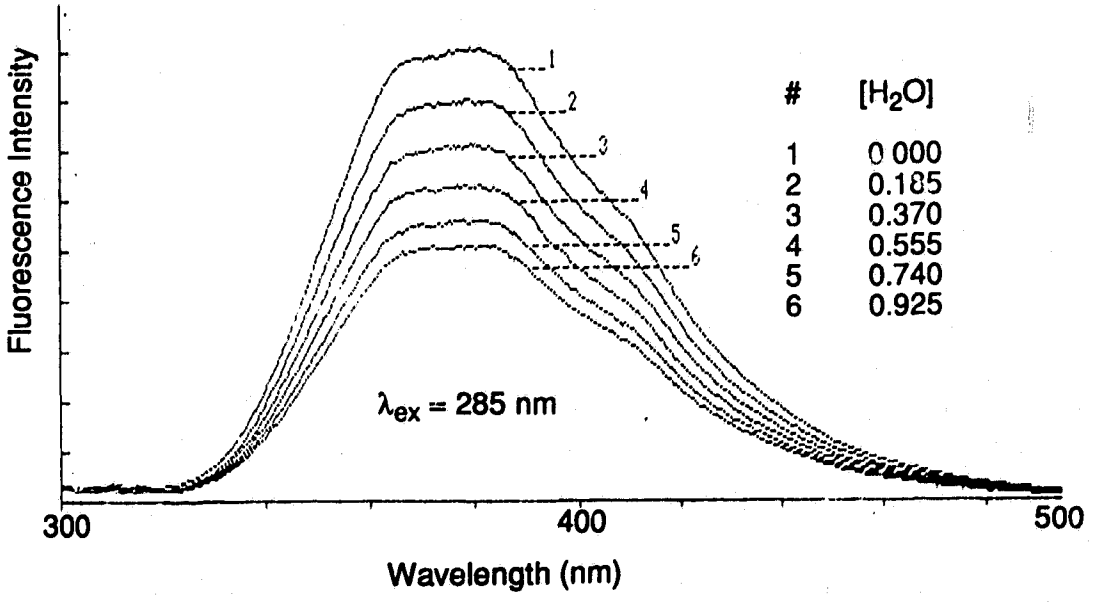

Figure 2.9 Fluorescence emission of **5** in ACN quenched by H_20.

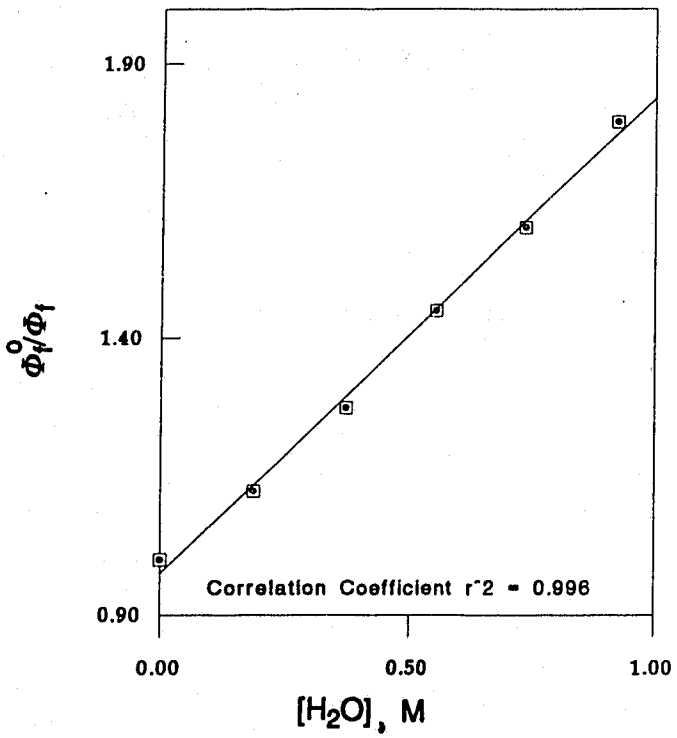

Figure 2.10 Example of a Stern-Volmer plot for quenching of **5** by H_2O.

The magnitude of the fluorescence quenching rates (Table 2.9) are in general large indicating that H_2O is involved in a significant quenching process. Comparison of values of k_q obtained for **5** and **91**, quenched by water, yields a primary isotope effect of $k_q(5)/k_q(91) = 2.8 \pm 0.4$. This primary isotope effect supports the notion that fluorescence quenching of **5** and **91** involves deprotonation of the 5-position in a primary photochemical step. The magnitude of this primary isotope effect (k_H/k_D) is in the range observed in ground state reactions involving proton abstraction from carbon acids by H_2O[137]. Primary isotope effects in these ground state reactions are dependent on the difference in

Table 2.9 Rates of fluorescence quenching (k_q) of suberene (5) and related systems by oxygen bases[a].

Compound	Quencher (base)	k_q , 10^8 $M^{-1}s^{-1}$ [b]
5	H_2O	1.53 ± 0.10
	D_2O	1.47 ± 0.10
	EtOH	8.6 ± 0.4
	THF	21 ± 1
91	H_2O	0.61 ± 0.05
	EtOH	3.2 ± 0.2
93	H_2O	-[c]
94	H_2O	-[d]
78	H_2O	1.20 ± 0.10
80	H_2O	0.42 ± 0.05

[a]At ambient temperatures in dry ACN distilled over CaH, λ_{ex} = 285 nm. [b]Obtained by division of slopes from Stern-Volmer plots by corresponding values of τ_0. Errors are standard deviations of 3 or more independent runs. [c]Weakly quenched. [d]No observable quenching.

pK_a between the carbon acid and the base. Maximum values are observed when these pK_a are about the same[137]. The significance of this pK_a difference in determining values of k_H/k_D will be discussed further in a subsequent portion of

this Chapter.

A similar primary isotope effect was observed by comparison of the values of k_q observed for quenching of alcohols **78** and **80** by water ($k_q(78)/k_q(80) = 2.8 \pm 0.4$)[138]. This result also suggests that fluorescence quenching of **78** involves interaction of the quencher (base) with the proton at the 5-position. A deprotonation similar to that observed for **5**, therefore, plays an important role in the photochemistry of **78**, as already suggested by the mechanism proposed for the photoketonization of this system (Scheme 1.11).

A second primary isotope effect can be obtained for **5** and **91** by comparison of the quenching rates obtained using EtOH. Again a value similar to that observed using water was obtained (2.7 ± 0.4). However, the absolute quenching rates involving EtOH are larger than the rates observed for water. Moreover, the quenching rate observed for THF is even larger. The relative rates of quenching observed for H_2O, EtOH and THF are expected since the quenching studies involve low concentrations of these bases in ACN (< 1.0 M). The relative basicity of these bases in the gas phase (ethers > alcohols > water)[29] is not the same as in protic solvents (water > alcohols > ethers)[29]. The former conditions are approximated by ACN when dilute solutions of the base are used. Therefore, the quenching rates observed for THF and EtOH should be higher than for water, and reflect their relative basicities.

The magnitude of k_H/k_D noted for **5** and **91** quenched by EtOH is expected to be smaller than the value obtained using water based on the difference in pK_a

between **5** and EtOH. A greater difference is believed to exist for this acid-base pair compared to **5** and H_2O and so the primary isotope effect should decrease. However, the change in k_H/k_D is within experimental error. An even stronger base would be required to see a significant change in the primary isotope effects observed in these quenching studies (*vide infra*).

The quantum yield measurements (*vide supra*) indicated a minor isotope effect of $\Phi_{ex}(5)/\Phi_{ex}(91)$ = 0.6 to 0.9 (using D_2O vs H_2O) (Tables 2.1 and 2.2) which is the reverse of the isotope effect observed in the fluorescence quenching studies. These results are not unexpected since the quantum yields of exchange involve both deprotonation and reprotonation of the substrate. The reprotonation process also has a primary isotope effect associated with it, due to the cleavage of O-H versus O-D bonds. The primary isotope effect associated with the deprotonation apparently is more then compensated for. Fluorescence quenching of **5** by base involve only deprotonation and so the larger primary isotope effects observed in these studies are consistent with this mechanism. Quenching of the fluorescence of **5** by D_2O supports this. The basicity of D_2O is similar to that of H_2O[120] and so a similar rate of quenching should be observed. The values measured for H_2O and D_2O (Table 2.9) are within experimental error.

The low isotope effects (as well as the low quantum yields of exchange themselves) observed in the quantum yield studies (Tables 2.1 and 2.2) suggests that internal return dominates the proton exchange observed in **5**. A larger value for $\Phi_{ex}(5)/\Phi_{ex}(91)$, approaching the values obtained in the quenching studies

would, be expected if exchange rather then internal return dominated the carbon acid behaviour of these systems. The extent of the internal return can be estimated by looking at values of Φ_f in the presence and absence of quencher. In pure ACN $\Phi_f = 0.89 \pm 0.05$ for **5**. In 70% D_2O/ACN little fluorescence is observed from **5**, indicating a reduced value for Φ_f of < 0.05. If this reduction in Φ_f results predominantly from proton abstraction from the 5-position by water, then according to the quantum yield of exchange observed in 70% D_2O/ACN ($\Phi_{ex} = 0.029 \pm 0.004$), 3 out of every 84 deprotonations results in exchange. This indicates that internal return is the fate for ≈96% of the deprotonations initiated by D_2O. The higher value of Φ_{ex} observed for **91** in 70% H_2O/ACN suggests that internal return occurs less often, which is expected based on the primary isotope effect associated with return of deuterium versus proton.

The reverse isotope effect observed with MeOH and MeOD ($\Phi_{ex}(5)/\Phi_{ex}(91) = 0.5$) can also be explained by the involvement of a reprotonation step. Reprotonation of **5** by a deuterium from MeOD will be less facile than reprotonation of **91** by a proton from MeOH due to the larger amount of energy required to cleave an O-D vs O-H bond. In the former situation, internal return will be favoured to a greater extent, which will reduce Φ_{ex}.

Confirmation of the k_q values measured for quenching of **5** and **91** by water was obtained by repeating the Stern-Volmer analysis using fluorescence lifetimes[139] (**5**: $k_q = (1.71 \pm 0.04) \times 10^8\ M^{-1}\ s^{-1}$, **91**: $k_q = (0.69 \pm 0.05) \times 10^8\ M^{-1}\ s^{-1}$). The fluorescence lifetime of **5** and **91** both decreased with increasing

concentrations of water. Plots of $1/\tau_f$ (where τ_f is the fluorescence lifetime in the presence of Q) versus [Q] provides a linear plot with slope k_q and intercept $1/\tau_f^0$ (where τ_f^0 is the fluorescence lifetime in the absence of Q) (eq. 2.13). The similarity between these values of k_q obtained for 5 and 91, through different

$$1/\tau_f = 1/\tau_f^0 + k_q[Q] \qquad (2.13)$$

methods, indicate that the quenching observed is dynamic rather then static[139]. The latter quenching process involves association of the quencher and substrate prior to excitation. Dynamic quenching, which is believed to occur in the quenching of 5 by water, involves interaction of the quencher with the excited substrate. If static quenching were occurring, the values of k_q obtained via time resolved and steady-state fluorescence techniques would not agree, since dynamic quenching is only observed in the former technique. However, static and dynamic quenching cannot be readily differentiated in steady-state fluorescence measurements.

In a subsequent section of this Chapter the effect of bases stronger than water (primary amines) will be examined. Before this, the effect of pH (H_0) on the fluorescence of 5 will be presented.

2.6.3 Fluorescence Quenching Studies In Acidic and Basic Aqueous Solutions

The influence of pH (H_0) on the fluorescence of 5 was studied by

comparing the emission due to **5** in the presence of aqueous solutions with differing concentrations of NaOH and H_2SO_4 (1M NaOH (pH 14) to 60% H_2SO_4 ($H_0 \approx -4$). Each sample consisted of 20% ethanol as a co-solvent and 80% aqueous acid or base solution. The resulting plot of Φ_f/Φ_f^0 (where Φ_f^0 represents the sample with the largest fluorescence intensity, which was observed when $H_0 = -2.25$) versus pH (H_0) (Fig. 2.11) is similar to that observed in published studies of **6**[113]. Two trends to note are the significant increase in fluorescence intensity below $H_0 = 0$ and the slight decrease in intensity at pH 14. Between these two pHs the plot is flat.

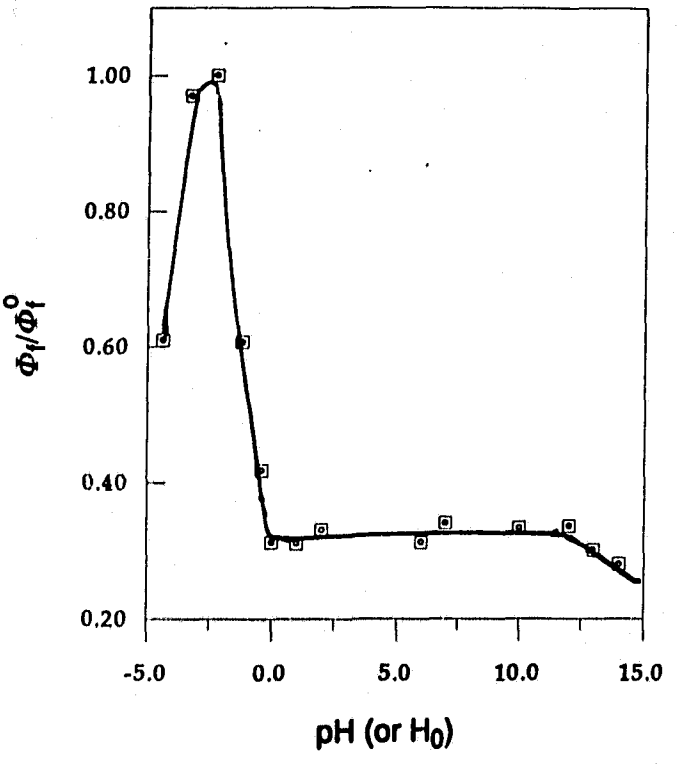

Figure 2.11 Effect of pH (H_0) on the relative fluorescence intensity of **5**.

The increase in fluorescence intensity at $H_0 = 0$ is expected and reflects the increased acidity of the solution, which will retard deprotonation of **5**. This portion of the plot, therefore, resembles a fluorescence titration curve. The exchange quantum yields and fluorescence lifetimes obtained in acidic media corroborate this observation. In H_2SO_4/EtOH solutions, the value of Φ_{ex} is decreased compared to values obtained using neutral conditions (Table 2.3). In addition fluorescence lifetimes are longer in H_2SO_4 solutions (0.41 ± 0.04 ns in H_0 = -1.08) relative to neutral solutions (0.13 ± 0.02 ns in pH 7), which were measured using a picosecond system[140].

The subsequent decrease in fluorescence intensity beyond $H_0 = -3$ is believed to result from either thermal decomposition of **5** or photoprotonation of the aromatic rings. The latter process is known to occur for aromatic systems such as naphthalene and fluorene (**9**) in acidic media and results in fluorescence quenching of these aromatic systems[141,142]. Photoprotonation of **5** may therefore compete with deprotonation of this system, thus not enabling completion of the expected fluorescence titration curve.

At pH 14 a decrease in fluorescence intensity was observed which is believed to result from increased concentrations of HO^-, which deprotonates **5** more efficiently than H_2O. This result agrees with the increase in Φ_{ex} observed with increasing concentrations of NaOH (Table 2.3). However, the change in fluorescence intensity at pH 14 is not as pronounced as expected based on the relative basicity of H_2O and HO^-. This is due to the higher concentration of H_2O

at pH 14 relative to HO^-.

Both of the substituted derivatives of 5 (93 and 94) are not quenched efficiently by water. Additionally, a plot of fluorescence intensity (Φ_f/Φ_f^0) versus pH (H_0) for 93 (Fig. 2.12) is very different from that observed for 5 (Fig. 2.11).

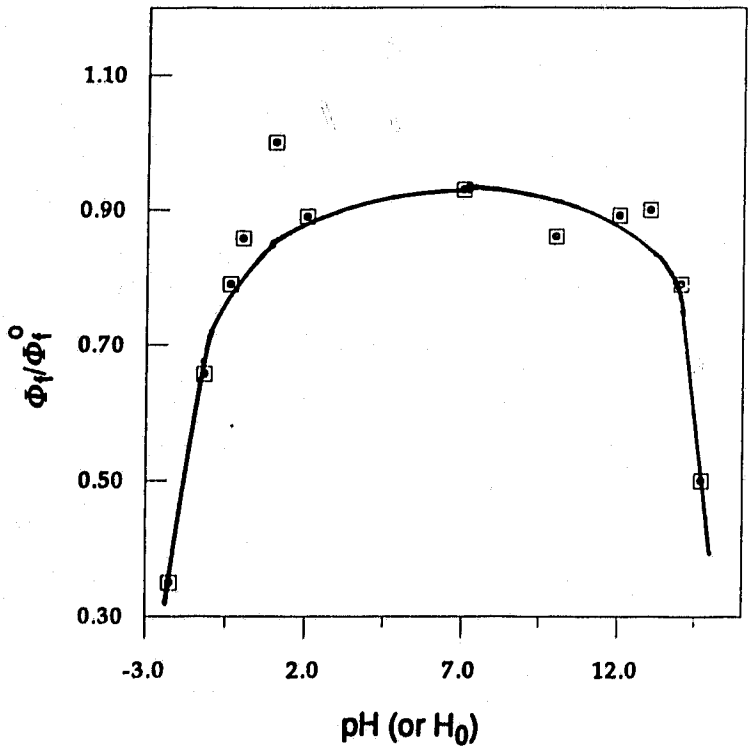

Figure 2.12 Effect of pH (H_0) on the fluorescence intensity of 93.

Below pH 1 and above pH 12 the fluorescence intensity decreases. No increase in intensity was observed below pH 1, as expected based on the inefficient deprotonation of 93 in neutral H_2O. The decrease in intensity below pH 1 can again be attributed to either photoprotonation or thermal reactions. The reason for the decrease in intensity above pH 12 is not known. One would expect this

decrease to be due to the more efficient quenching of the fluorescence of **93** by HO^-. The quenching by HO^- would be expected to be more pronounced in **93** than with **5** since H_2O does not quench the former system very efficiently. This result agrees with the product studies which indicate that the deuterated methyl derivative **95** exhibits observable excited state carbon acid behaviour in basic solutions. However, the fluorescence of **94** and related systems (i.e., **77**), which do not function as excited state carbon acids, are also quenched significantly at pH 14. The fluorescence of fluorene (**9**) and related systems are also quenched above pH 12[142]. It was proposed that fluorescence quenching of fluorene derivatives by HO^- involved deprotonation of the benzylic position. However, such a process is not possible for **77**. Competing electron transfer quenching from HO^- may also operate at these pHs.

2.6.4 Fluorescence Quenching Studies Involving Amines

Product studies of **5** and related systems in the presence of amines indicated that primary amines efficiently catalyze the deprotonation of these systems. Conversely tertiary and secondary amines promote photoreduction of **5** and related systems, via ET. The results of fluorescence quenching of **5** and related systems by amines (Table 2.10) agree with these product studies.

The magnitudes of k_q for **5**, **93** and **94**, with triethylamine as the quencher in ACN, all approach the diffusion limit for ACN (1.9×10^{10} M^{-1} s^{-1})[143]. Lewis et al.[124,128,144] observed similar k_q values for the quenching of styrenes and arenecarbo-

Table 2.10 Fluorescence quenching rate (k_q) for **5** and related systems using amine bases[a].

Compound	Quencher (base)	k_q, 10^9 $M^{-1}s^{-1}$ [b]
5	n-$PrNH_2$	8.34 ± 0.20
	$HOCH_2CH_2NH_2$	6.44 ± 0.20
	$CH_3OCH_2CH_2NH_2$	6.68 ± 0.20
	$NCCH_2CH_2NH_2$	5.07 ± 0.20
	$F_3CCH_2NH_2$	3.47 ± 0.10
	Et_3N	9.16 ± 0.20
91	$HOCH_2CH_2NH_2$	4.70 ± 0.20
93	$HOCH_2CH_2NH_2$	0.47 ± 0.05
	n-$PrNH_2$	0.56 ± 0.05
	Et_3N	10.9 ± 0.2
94	$HOCH_2CH_2NH_2$	0.17 ± 0.05
	n-$PrNH_2$	0.19 ± 0.05
	Et_3N	9.44 ± 0.20

[a]At ambient temperatures in dry ACN distilled over CaH_2, λ_{ex} = 285 nm. [b]Obtained by division of slopes from Stern-Volmer plots by corresponding values of τ_0.

nitriles (ArCN) by triethylamine. This agreement with literature values of k_q

supports a photoreduction mechanism involving initial ET from triethylamine to **5**, **93** or **94**.

Values of k_q obtained for **5** using primary amines are also large but do not approach the diffusion limit of ACN as closely as triethylamine (Table 2.10). Comparison of quenching rates for **5**, **93** and **94** by primary amines suggests that this base may catalyze the excited state proton exchange in all three substrates. However, product studies of these systems indicate that primary amines do promote the photoreduction of **93** and **94**, with proton exchange being a minor process for the latter system. The quenching rates observed for **93** and **94**, therefore, involve both quenching by ET and by deprotonation. No photoreduction products were observed for **5** in the presence of primary amines. Therefore, these values of k_q involve deprotonation exclusively.

As in the fluorescence quenching studies involving water, a primary kinetic isotope effect was observed for quenching of **5** and **91** by EA, ($k_q(5)/k_q(91) = 1.4 \pm 0.2$). The magnitude of this primary isotope effect is smaller than that observed when water was used. As discussed, the difference in pK_a between the acid and base involved in the isotope study determines the magnitude of k_H/k_D, i.e., the smaller the difference, the larger the isotope effect. Therefore, the smaller isotope effect observed using a primary amine to quench **5** and **91** is expected since the difference in pK_a between the base and the excited state carbon acids is believed to be greater when EA, rather then water, functions as the base.

The magnitudes of the primary isotope effects observed using H_2O and EA

to quench the fluorescence of **5** and **91** can be used to indicate the location of a linear transition state involving a given base[29]. A small isotope effect indicates a transition state close to either reactants or products, whereas, a large isotope effect indicates a transition state intermediate to reactants and products. The transition state for deprotonation of excited **5** by primary amines is believed to be closer to the reactants. This is expected since deprotonation of an acid will be more exothermic when a strong base is involved. According to the Hammond postulate[29] the transition state will then be closer to the reactants. Water, a weaker base, will in turn produce a later transition state, as suggested by the larger isotope effect observed using this base.

The position of a transition state can also be examined by the construction of a Brønsted plot (*vide supra*). A plot of $\log k_B$ versus pK_a can be constructed for **5** since k_q represents the rate k_B for the general base catalyzed deprotonation of this excited state carbon acid. The pK_a of the conjugate acid of these bases (primary amines) are not all well established in ACN but they are expected to increase by 7 to 8 pK_a units compared to values obtained in protic solvents[145]. This change results from the inability of ACN, unlike protic solvents such as water, to form hydrogen bonds with the lone pair of electrons on the nitrogen. However, in general the relative basicity of primary amines are maintained in ACN. The trend observed in a Brønsted plot using the pK_as of amines in water should therefore be valid and provide information concerning the transition state for photo-deprotonation of **5** by primary amines.

A plot of $\log k_q$ (with values of k_q obtained from fluorescence lifetime studies since these are believed to be more precise) versus the pK_a of the primary amines used (Table 2.11) provides a Brønsted plot with a slope of $\beta = 0.07 \pm 0.02$ (Fig. 2.13). This low value suggests that deprotonation of excited **5** is not very sensitive to general base catalysis by primary amines and that an early transition state exists. Both of these conclusions agree with the primary isotope effect indicated for quenching of **5** and **91** by EA. Deprotonation of excited **5** would be expected to be insensitive to the base strength of the primary amines since the difference in pK_a between the acid and base is so large. This is especially true when the pK_as of the amines in ACN are considered. An early transition state

Table 2.11 Data used in the Brønsted plot for general base catalysis of the excited state deprotonation of **5** by primary amines[a].

Primary Amines	pK_a[b]	$\log k_q$[c]
$n\text{-}PrNH_2$	10.54	9.92
$HOCH_2CH_2NH_2$	9.50	9.81
$CH_3OCH_2CH_2NH_2$	9.40	9.82
$NCCH_2CH_2NH_2$	8.20	9.70
$F_3CCH_2CH_2NH_2$	5.5	9.54

[a]At ambient temperatures in dry ACN distilled over CaH, $\lambda_{ex} = 285$ nm. [b]From reference 145, in H_2O. [c]Values of k_q obtained from fluorescence lifetime quenching studies.

resembling the reactant will also result from this difference in pK_a between the primary amines and excited **5**.

Deprotonation of **5** probably involves a diabatic photochemical process since no emission was observed from carbanion **7** in steady state fluorescence studies. The minor amount of deuterium incorporation at the vinylic position (*vide supra*) also favours a diabatic mechanism for deprotonation of **5**. This is based on the belief that carbanion **7** is delocalized in S_1 and localized in S_0, due to it's antiaromatic character. Generation of **7** in S_1 would, therefore, result in deuteration of both the vinyl and dibenzylic positions of **5**. Deuteration of the

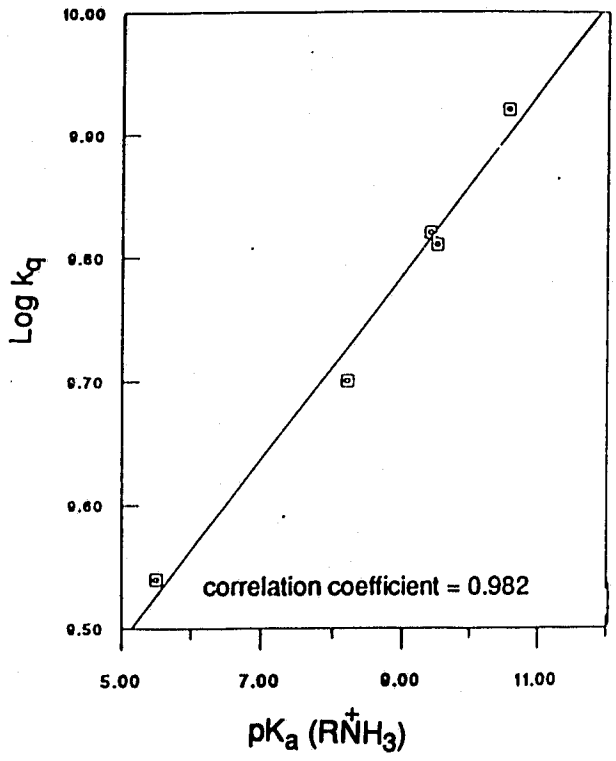

Figure 2.13 Brønsted plot for general base catalysis of the deprotonation of excited **5** by primary amines.

latter position predominates, suggesting diabatic deprotonation.

A diabatic deprotonation, such as the one envisioned in Figure 1.11, could be enhanced by using a stronger base (Fig. 2.14). A stronger base shifts the transition state for deprotonation in S_1 closer to the reactants (*vide supra*). This shift promotes IC from S_1 to a position further over the transition state for deprotonation of **5** in S_0. A weaker base with a later transition state would promote IC from S_1 to the top of the transition state for deprotonation of **5** in S_0. Primary amines may therefore enhance the excited state acidity of **5** by promoting IC from S_1 to a point further along the ground state surface.

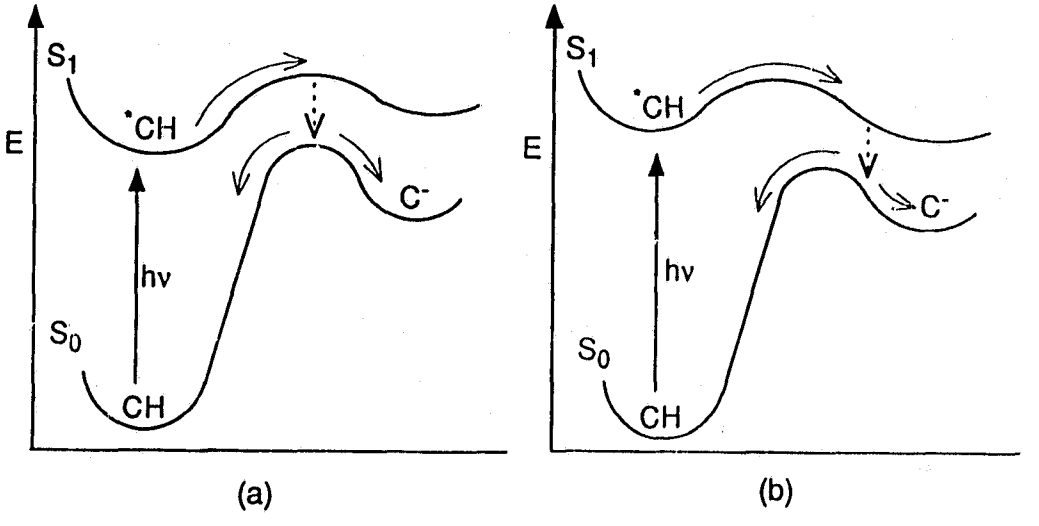

Figure 2.14 Effect of a weak (a) and strong (b) base on the diabatic deprotonation of an excited state carbon acid.

2.7 Summary

Several possible mechanisms can be envisioned to account for deuterium

incorporation at the dibenzylic position of **5**. Mechanisms involving homolysis of the dibenzylic C-H bonds can be ruled out based on the lack of dimerization products and the lack of deuterium incorporation after photolysis of **5** in CD_3CN. Exchange involving radical ions created by ET from the base to excited **5** can be ruled out simply by the fact that the high ionization potential of water (12.59 eV)[130] makes such a process unfavourable. This type of mechanism can also be ruled out based on results from the photolysis of **5** in the presence of Et_3N and on the work of Lewis et al.[122-125]. These studies indicate that ET to systems such as **5** results in photoreduction of double bonds, not in proton exchange.

Another possible mechanism which must be considered involves the photodeuteration of the vinyl bond of **5** (Scheme 2.4). The benzyl cation formed in this process (**139**) can be deprotonated at the dibenzylic position to produce the o-quinone dimethide **140**. A subsequent [1,5] sigmatropic shift of the deuterium in **140** then occurs producing **90**. However, this process would also result in the formation of the alcohol **141** and in significant deuteration of the vinyl position, to yield **142**. Since only a minor amount of the latter product was observed and none of the former, this mechanism is not responsible for the deuterium incorporation observed in **5**. The decrease in fluorescence quenching of **5** with increasing concentrations of H_2SO_4 also suggests that photoprotonation of the vinyl bond is not occurring since enhanced fluorescence quenching in acidic media would be associated with such a process.

The only mechanism consistent with all the experimental data is an acid-

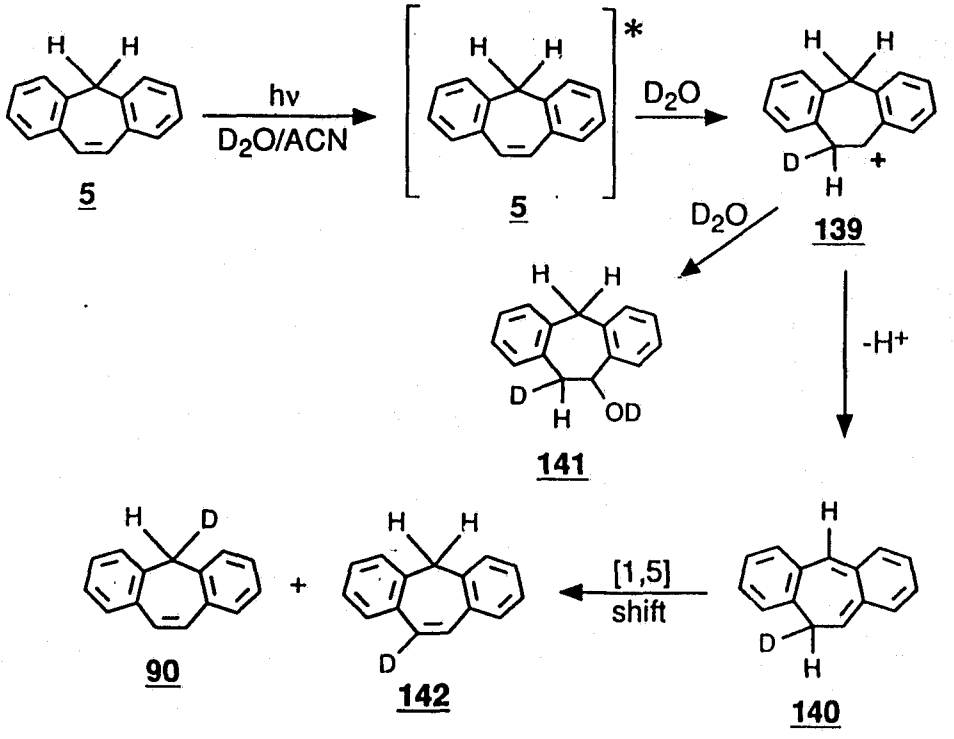

Scheme 2.4

base reaction (Scheme 2.5). Deactivation of excited **5** occurs predominantly via fluorescence in the absence of a base. With a base present, deactivation of excited **5** occurs via diabatic deprotonation of the 5-position, to produce carbanion **143**. Exchange of the proton abstracted, with a deuterium from the solvent, can then occur resulting in **90**. However, deuteration is a minor process for reaction of **143**, as indicated by the estimate for internal return (≈96% in 70% D_2O/ACN). The abstracted proton must therefore remain in close proximity to **143** (via hydrogen bonding) preventing deuteration by other solvent molecules and by the solvent molecule which abstracted the proton. Quantum yields for exchange support this mechanism. These measurements show that the amount of exchange observed

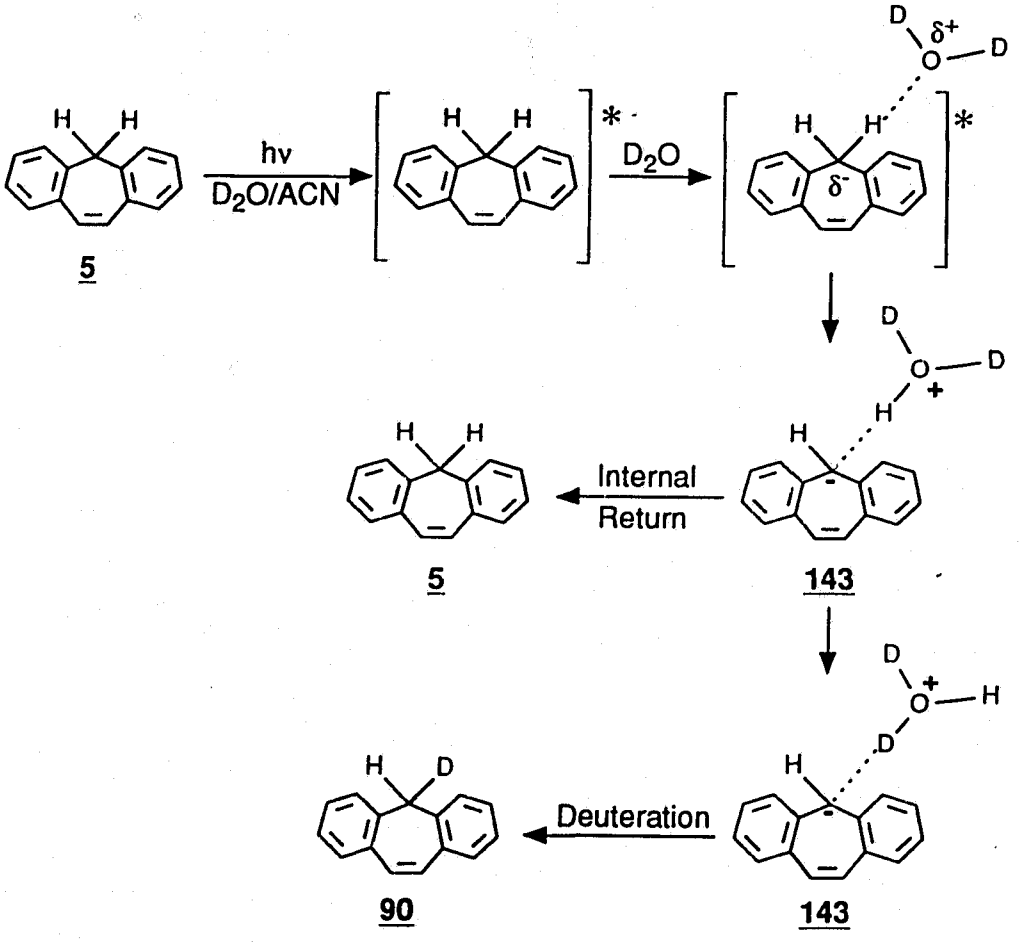

Scheme 2.5

depends on the pK_a of the base used, with primary amines being the most efficient. However, the greatest support was obtained through the fluorescence quenching studies. Rates of fluorescence quenching were initially shown to correspond to rates of proton abstraction from excited **5**, by the lack of quenching for systems not exhibiting excited state carbon acid behaviour. The primary isotope effect observed for **5** and **91** (quenched by either H_2O, EtOH or EA) also support a correspondence between rates of deprotonation and quenching. This correlation was further confirmed by the Brønsted plot obtained using primary

amines, which demonstrated the expected linear correlation between the pK_a of the base used and log k_q.

The pK_a of excited **5** is not known but the effect of pH (H_0) on the fluorescence quenching of this system suggests a value of ≈ -1. Förster cycle calculations[146] also indicate that **5** has a pK_a of < -1 in S_1. These results demonstrate that excitation of **5** from S_0 to S_1 leads to a pK_a change of at least 30 log units. Changes in pK_a observed for other organic molecules after excitation to S_1 range from approximately 1 to 12 log units[55,58] which would make the ΔpK_a observed for **5** the largest observed to date. A large ΔpK_a has been predicted by Förster cycle calculations for fluorene (**9**). However, no evidence has been found to suggest that this change actually occurs.

Addition of substituents to **5** as in **93** and **94** affects the excited state acidity of these systems. Unlike **5**, both **93** and **94** do not incorporate deuterium after photolysis in D_2O. In addition the fluorescence of each is not quenched efficiently by water. Stereoelectronic effects similar to those proposed in the photosolvolysis of **99**, **100**, **101** and **108** are believed to be responsible for this decreased reactivity. The importance of these stereoelectronic effects on the acid-base behaviour of excited state carbon acids will be addressed further in the following Chapter.

The results presented in this Chapter support an acid-base mechanism for the excited state proton transfer involving **5**, confirming that this system is the first example of a neutral excited state carbon acid. Formation of a carbanion with a 4n ICA is believed to be responsible for the enhanced carbon acidity of **5**

in S_1. The importance of the 4n ICA will be examined further in the next Chapter.

CHAPTER 3

EXCITED STATE BEHAVIOUR OF *5H*-DIBENZO[a,c]CYCLOHEPTENE (6)

3.1 Introduction

Photolysis of *5H*-dibenzo[a,c]cycloheptene (6)[8,113] in ACN gives dibenzonorcaradiene (144) via either a di-π-methane rearrangement or a [1,7] sigmatropic shift followed by a thermal electrocyclic ring closure (Scheme 3.1). When photolysis of 6 was carried out in the presence of a base (D_2O) the excited state carbon acid behaviour of this system predominates. The purpose of this

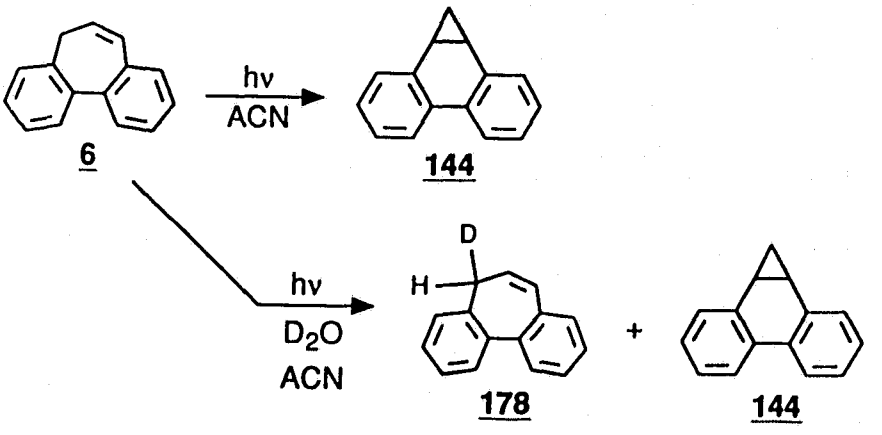

Scheme 3.1

Chapter is to further examine the excited state carbon acid behaviour of 6, by deuterium labelling and by structure-reactivity studies. The deuterium labelled system, 7-deuterio-*5H*-dibenzo[a,c]cycloheptene (87), is prepared and irradiated to study in more detail the photochemistry of 6. Substituted derivatives of 6 (6-methyl-*5H*-dibenzo[a,c]cycloheptene (155) and 6-phenyl-*5H*-dibenzo[a,c]cyclo-heptene (156)) are prepared to probe the effect of substituents on the photochemistry of this excited state carbon acid. Two binaphthyl derivatives of

6 (*3H*-cyclohepta[2,1-a:3,4-a']dinaphthalene (**88**) and *3H*-cyclohepta[2,3-a:3,2-a']dinaphthalene (**89**)) are also prepared to examine the effect of benzannelation on excited state carbon acidity. The geometry of the seven membered ring in these derivatives also allows for an examination of conformational effects on the photochemistry indicated for **6**. Product studies, using water and primary amine bases, in combination with time resolved and steady state fluorescence techniques are used to probe the photochemistry of these compounds.

3.2 Syntheses

3.2.1 7-Deuterio-*5H*-dibenzo[a,c]cycloheptene (87)

In the previous study of **6**, the photochemistry of this system was examined using 6-deuterio-*5H*-dibenzo[a,c]cycloheptene (**84**)[8,113]. Synthesis of **6** was achieved in two steps from ketone **146**, which was prepared from diphenic anhydride (**145**), using the procedure outlined by Tolbert and Ali[147]. Synthesis of the 7-deuterio derivative **87** requires a ketone similar to **146** but with

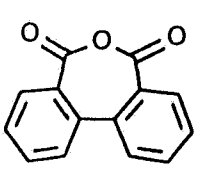

145

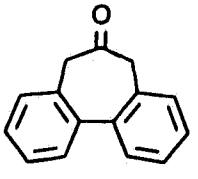

146

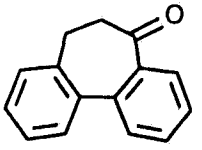

147

the carbonyl functionality situated at the 7-position (**147**). The procedure used to synthesize **147** and **87** is outlined in Scheme 3.2.

The initial step of the synthesis involves addition of dichlorocarbene across

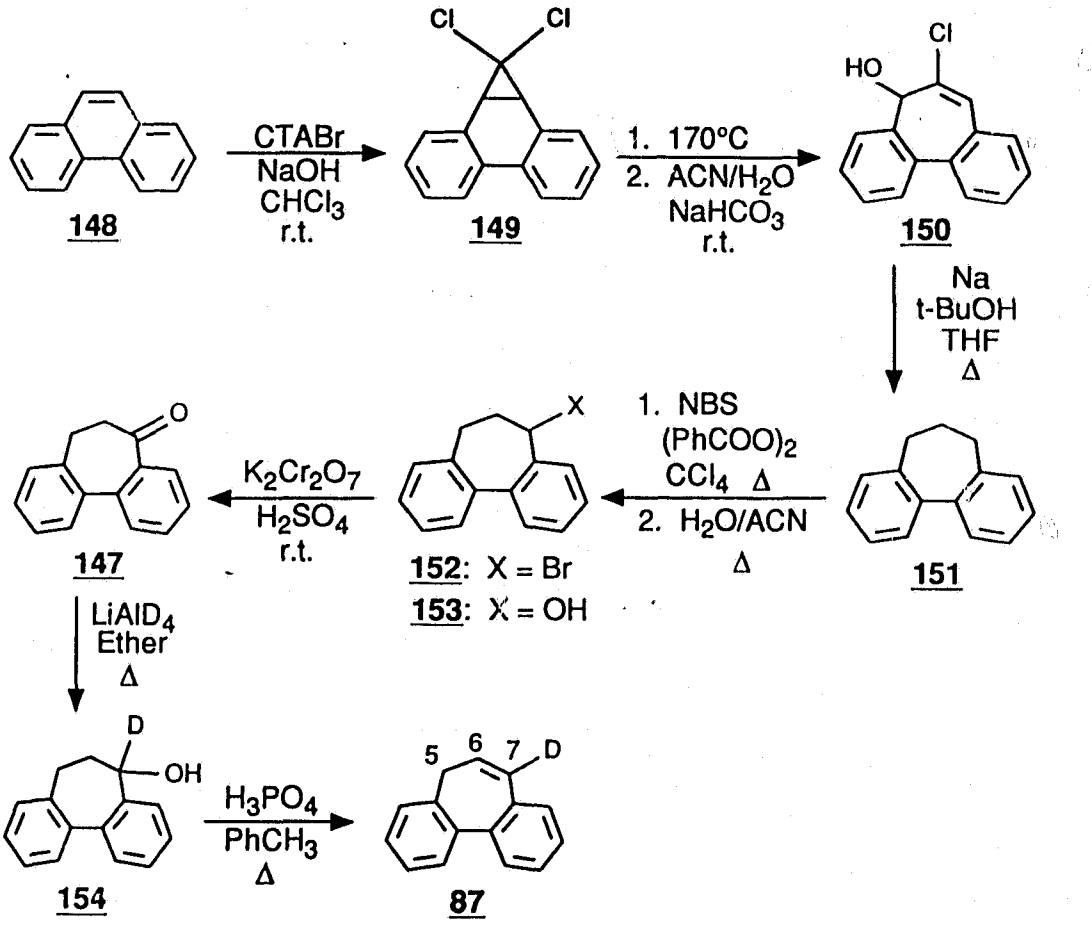

Scheme 3.2

the 9,10-double bond of phenanthrene (**148**) to give **149** (48%)[148,149]. This addition was mediated by CTAB (cetyltrimethylammonium bromide) which acts as a phase transfer catalyst. Thermolysis of **149** followed by suspension in a mixture of ACN and saturated sodium bicarbonate produced **150**[149]. Reduction of **150** with sodium metal in THF with t-butanol present provided hydrocarbon **151** (80% from **149**)[150]. Bromination of the benzylic position of **151** with NBS (N-bromosuccinimide)[151] gave **152**, which was hydrolysed in H_2O/ACN, to give **153** (53%). Oxidation of **153** with Jones reagent[151] gave the required ketone **147** (85% from **152**). The 7-

deuterio derivative of **6** (**87**) was achieved by reduction of **147** to **154** with $LiAlD_4$ (95%), followed by acid catalysed elimination of H_2O (60%). Distillation of the final crude reaction mixture produced **87** with a purity >97% (≈ 9% yield overall).

Both ^1H and ^2H NMR (360 MHz) confirmed that **87** was the product obtained. The former spectrum was similar to the parent system but lacked both the resonance due to the vinyl proton at the 7-position ($\delta \approx 6.7$) and the couplings associated with this proton. The ^2H NMR exhibited one major signal at δ 6.66 with several minor resonances, including a signal at δ 3.05 (≈4%), representing deuterium at the 5-position (Fig. 3.2). MS analysis of the final product achieved via the synthetic route in Scheme 3.2 provided a mass consistent with mono-deuterated **6** ($M^+ + 1$ = 194 m/z).

3.2.2 6-Methyl-5*H*-dibenzo[a,c]cycloheptene (155) and 6-Phenyl-5*H*-dibenzo-[a,c]cycloheptene (156)

The 6-methyl (**155**) and 6-phenyl (**156**) derivatives of **6** were synthesized by reaction of **146** with MeLi and PhLi respectively, according to the procedure of Tolbert and Ali[147] (Scheme 3.3). Several repetitions of the reduction were required since **146** enolizes in the presence of PhLi and MeLi. Elimination of H_2O from the alcohols formed via reaction of **146** (**157** and **158**) provided the crude products **155** and **156**. The former was purified by a flash column (>97% purity) while the latter was purified by column chromatography followed by recrystallization from EtOH (>98% purity).

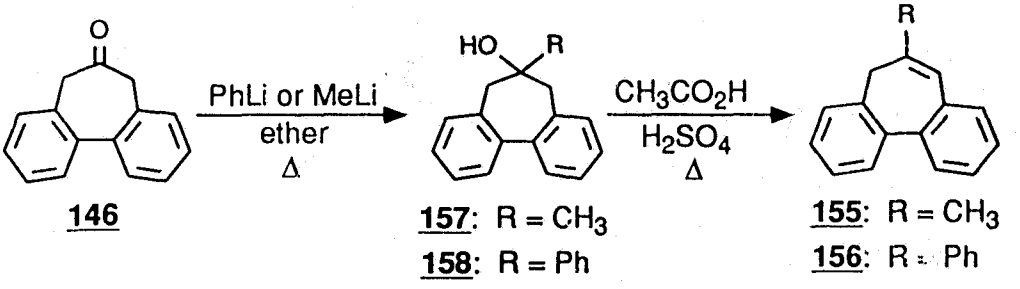

146 **157**: R = CH_3 **155**: R = CH_3

158: R = Ph **156**: R = Ph

Scheme 3.3

Both the MS and ^{1}H NMR (360 MHz) of the purified products confirmed that **155** and **156** were obtained. The ^{1}H NMR of **155** exhibited a doublet at δ 2.11 representing the methyl coupled to the vinyl proton. The vinyl proton appeared as a quartet at δ 6.36. A singlet at δ 3.02 representing the methylene protons at the 5-position. The ^{1}H NMR of **156** exhibited singlets at δ 6.82 and 3.45 confirming the presence of the vinyl proton at the 7-position and the protons at the 5-position. Comparison of the ^{1}H NMR obtained for **156** with the literature spectrum[147] supports these assignments.

3.2.3 *3H*-Cyclohepta[2,1-a:3,4-a']dinaphthalene (88)

Synthesis of *3H*-cyclohepta[2,1-a:3,4-a']dinaphthalene (88) was achieved using the eight step procedure outlined in Scheme 3.4. In the initial step, which starts with commercially available 2-methylnaphthalene (159), bromination of the 1-position[152] was effected (90%) in preparation for the coupling reaction in step two[153]. Coupling of two naphthalene systems via the 1-position was performed by first preparing the Grignard reagent of **160**. This Grignard reagent was then

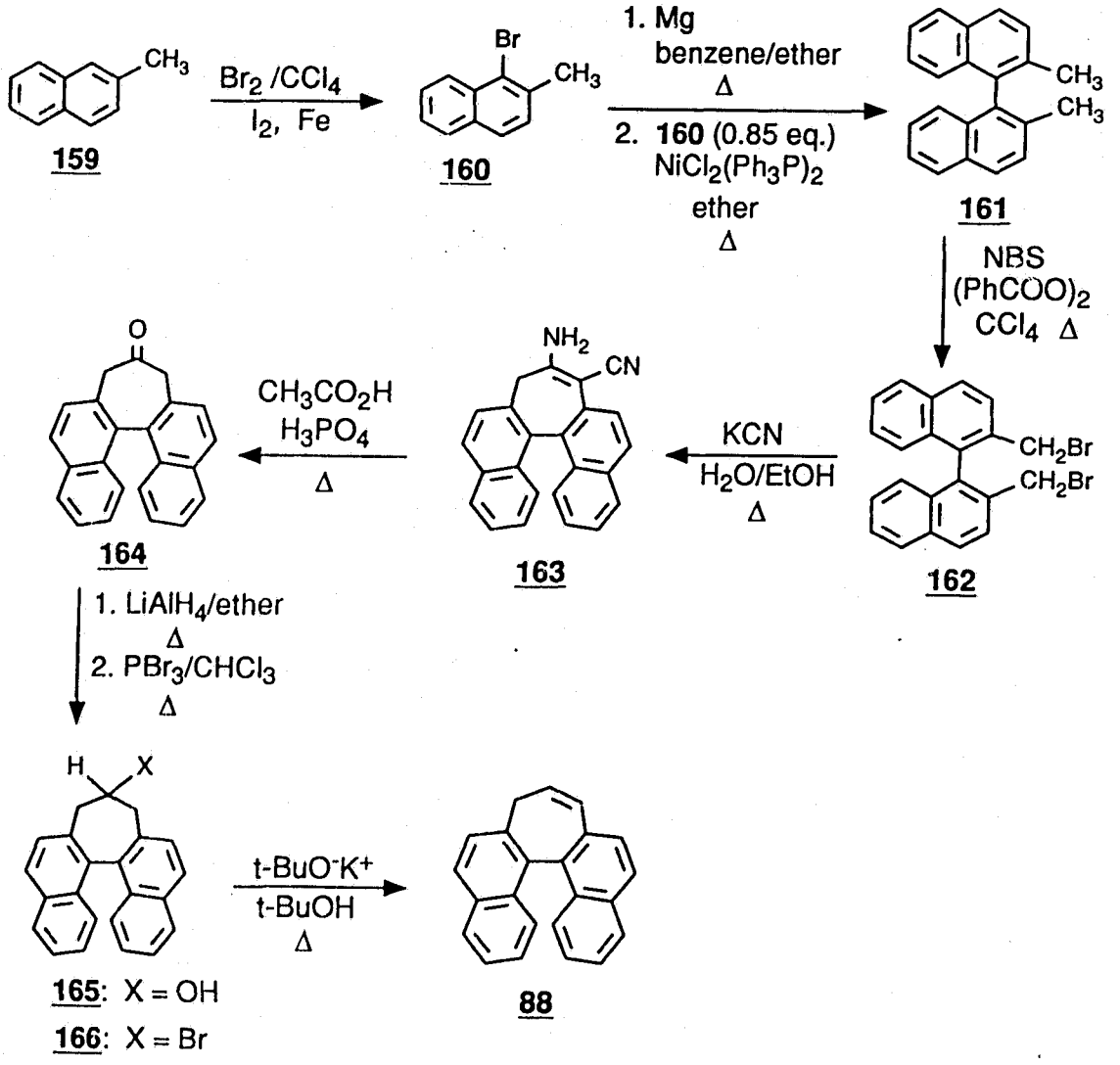

Scheme 3.4

added to another reaction vessel containing $NiCl_2(Ph_3P)_2$ and 0.85 equivalents of **160**, to produce 2,2′-dimethyl-1,1′-binaphthyl (**161**) (40%). Bromination of the methyl groups with NBS gave **162** (85%). Bestmann and Both[154] prepared **88** in two steps from **162**. However, numerous attempts of their procedure were unsuccessful. Therefore, the method outlined by Mislow and McGinn[155] was used

to prepare the precursor **164**, required for synthesis of **88**. This involved cyclization to **163**, by refluxing **162** in a H_2O/EtOH/acetone solution containing KCN. When the reaction was carried out in H_2O/EtOH according to the literature preparation[155] incomplete reaction of **162** occurred. Therefore, acetone was used to dissolve **162** so that it could react more efficiently (60% yield). Formation of **164** (80%) was then achieved by refluxing **163** in H_3PO_4/CH_3COOH. Reduction of **164** to alcohol **165** (90%) followed by bromination with PBr_3 provided **166** (90%) which was converted to **88** (70%) via a base catalyzed elimination using potassium t-butoxide. The resulting product was recrystallized in toluene/anhydrous EtOH to provide **88** with a purity >99% by GC (8% overall yield).

The ^{13}C NMR of **88** exhibited twenty two signals. The structure of **88** requires one secondary (saturated) carbon, fourteen tertiary carbons, and eight quaternary carbons. All of these carbons were observed except for one quaternary carbon signal, which is probably hidden by other resonances.

The ^1H NMR obtained for **88** matched the literature spectrum[154]. Two signals were observed for the protons on the saturated carbon. One for the axial proton (H7B) and one for the equatorial proton (H7A) (see crystal structure Fig. 3.1). The larger allylic coupling constant (J = 2.2 Hz) observed in the former suggests that it is the axial proton since the magnitude of allylic coupling depends on the angle between the allyl and vinyl protons. The magnitude of this coupling is largest when the allyl proton is oriented parallel to the π orbitals of

the vinyl bond[156]. Other signals observed outside the aromatic region of the ^{1}H NMR displayed chemical shifts and coupling constants expected based on the

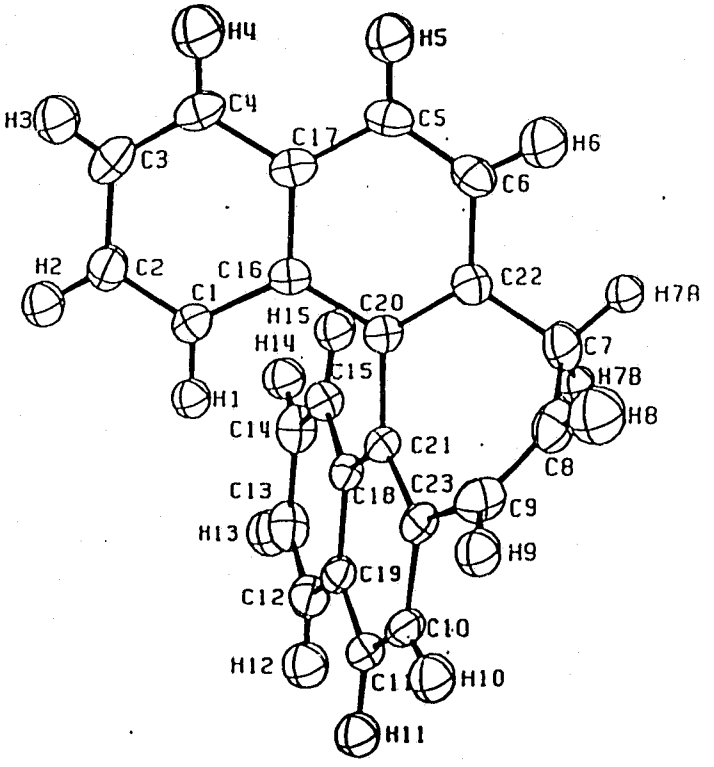

Figure 3.1 ORTEP representation of the X-ray crystal structure of **88**.

structure of **88**. The aromatic region of the ^{1}H NMR consisted of several multiplets which were difficult to interpret. However, the overall integration of this region suggested twelve aromatic protons which is the number expected for **88**. The origin of the coupling observed in the axial and equatorial protons of the saturated carbon were probed further by obtaining a ^{1}H COSY (correlated spectroscopy) NMR of **88**. This NMR technique correlates the coupling observed between various protons and allows for the determination of the origin of the

coupling. The coupling with J = 2.2 Hz in H7B was shown to represent allylic coupling between the axial proton (H7B) and the vinyl proton (H9).

MS analysis of **88** provided the expected mass (M^+ = 292 m/z). Analysis of the crystal structure of **88** by x-ray crystallography also confirmed the structure proposed (Fig. 3.1). The x-ray crystal structure obtained indicates a dihedral angle of $\approx 70^0$ between the naphthyl groups resulting in substantial twisting of the seven membered ring. This twist differentiates the axial and equatorial protons of the methylene carbon, resulting in the two signals observed in the ^{1}H NMR. The crystal structure also indicates that the axial proton is oriented above the plane of a naphthalene ring which results in an upfield shift of this proton relative to the equatorial proton. Bond lengths obtained from the x-ray crystal structure are as expected based on the structure of **88**. The C-C (Table 3.1) and C-H (Table 3.2) bond lengths in the seven membered ring are those expected for

Table 3.1 C-C bond lengths in the seven membered ring of **88** obtained via x-ray crystallography.

Atoms	Distance (Å) †
C(8) - C(7)	1.449(4)
C(22) - C(7)	1.488(4)
C(9) - C(8)	1.332(4)
C(23) - C(9)	1.477(4)
C(21) - C(20)	1.485(3)
C(22) - C(20)	1.390(3)
C(23) - C(21)	1.392(3)

† Estimated Standard Deviation in Parentheses

Table 3.2 C-H bond lengths in the seven membered ring of **88** obtained via x-ray crystallography.

Atoms	Distance (Å) †
H(7A) - C(7)	1.080(3)
H(7B) - C(7)	1.080(3)
H(8) - C(8)	1.017(33)
H(9) - C(9)	0.936(26)

† Estimated Standard Deviation in Parentheses

the proposed structure[130].

3.2.4 *3H*-Cyclohepta[2,3-a:3,2-a']dinaphthalene (89)

Synthesis of *3H*-cyclohepta[2,3-a:3,2-a']dinaphthalene (**89**) involved a synthetic route similar to that used to prepare **88** (Scheme 3.5). However, several modifications were required due to a difference in reactivity between positions one and three of 2-methylnaphthalene (**159**). Bromination of **159** occurs exclusively at the 1-position. Therefore, synthesis of 2-bromo-3-methylnaphthalene (**169**) required the use of **167**[157]. Bromination of **167** using the same conditions noted for bromination of **159**, gave **168** (85%). Thermal decomposition of **168** via distillation produced **169** as an oil (80%). Coupling of two naphthalene rings was then attempted using the procedure used to synthesize **161**. However, only a minor amount of coupling product was observed (5%). This low yield was attributed to the inability of **169** to efficiently form the required Grignard reagent. Therefore, a modification of the procedure

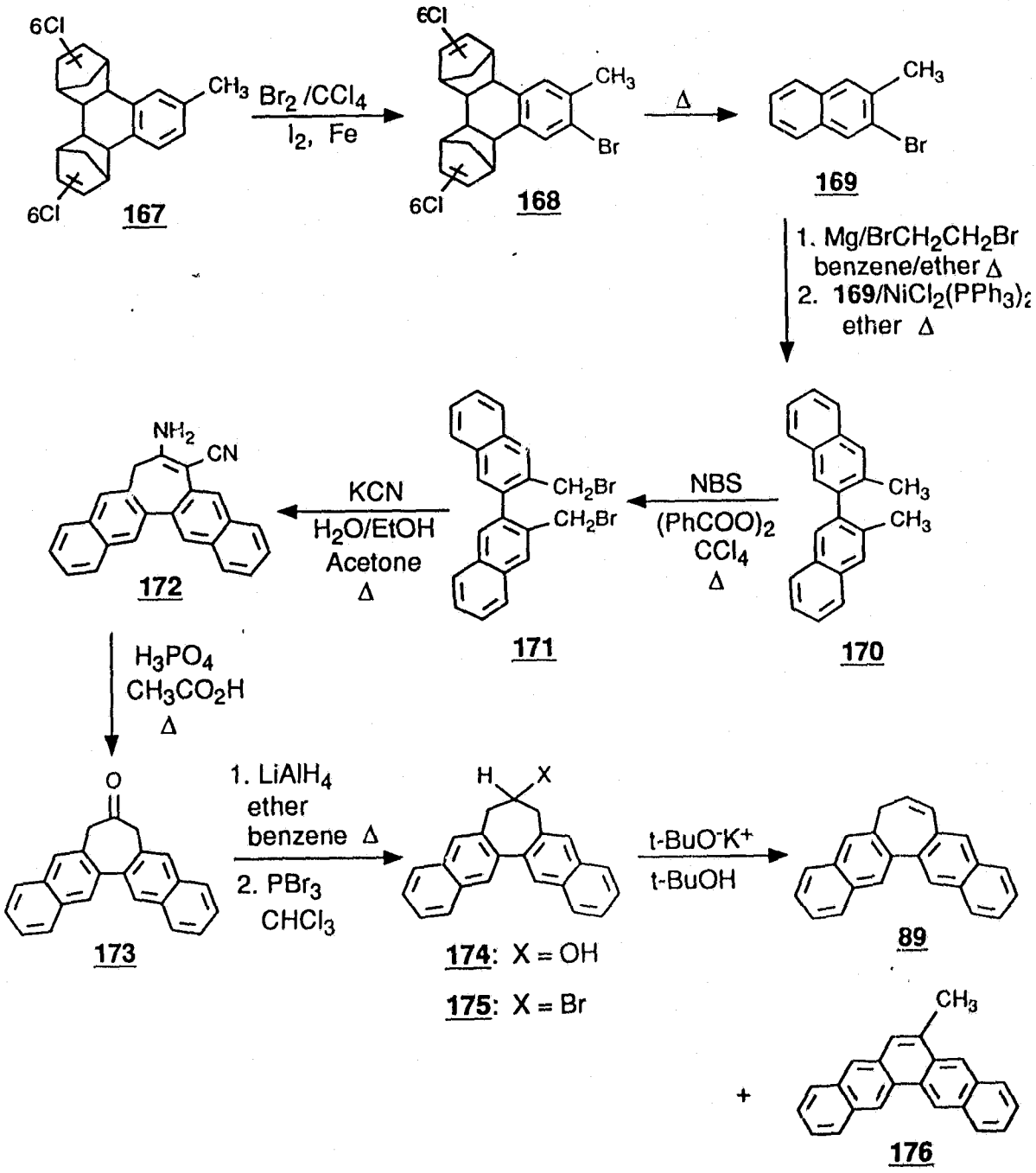
6Cl
CH3
Br2 /CCl4
I2, Fe
6Cl
6Cl
167
6Cl
CH3
Br
168
Δ
CH3
Br
169
1. Mg/BrCH2CH2Br
benzene/ether Δ
2. 169/NiCl2(PPh3)2
ether Δ
NBS
(PhCOO)2
CCl4
Δ
CH3
CH3
170
CH2Br
CH2Br
171
KCN
H2O/EtOH
Acetone
Δ
NH2
CN
172
H3PO4
CH3CO2H
Δ
O
173
1. LiAlH4
ether
benzene Δ
2. PBr3
CHCl3
H
X
174: X = OH
175: X = Br
t-BuO-K+
t-BuOH
89
+
CH3
176

Scheme 3.5

used to prepare the Grignard was employed. This reaction was enhanced by concurrent addition of one equivalent of 1,2-dibromoethane and two equivalents of Mg metal. Addition of 1,2-dibromoethane improves the Grignard reaction since it efficiently reacts with Mg metal and cleans the metal surface allowing for a more efficient reaction between Mg and **169**[158]. The resulting Grignard reagent when reacted with 0.5 equivalents of **169** in the presence of $NiCl_2(Ph_3P)_2$ provided a much greater yield of **170** (45%) compared to the yields observed in previous coupling attempts. Formation of ketone **173** (80%) from **170** via **171** (85% yield) and **172** (40% yield) involved the same synthetic steps used to synthesize **164** from **161**. Reduction of **173** produced alcohol **174** (90%) which was refluxed in toluene/H_3PO_4 with a Dean-Stark trap attached for collection of water formed in the reaction. The product mixture obtained consisted of ≈45% **89** and several unidentified impurities. Purification of **89** obtained via this method was unsuccessful and so the same procedure used to prepare **88** from **164** was attempted, i.e., by bromination of alcohol **174** to give **175** (85%) followed by base catalyzed elimination to give **89** (55%). One major impurity (45%) identified as **176** was obtained along with **89**. Repeated recrystallization of **89** in toluene/EtOH (anhydrous) provided the required product with a purity of >98% by GC (≈ 3.5% yield overall).

Nineteen carbon signals were observed in the ^{13}C NMR of the product which is four less than expected based on the structure of **89**. However, several signals in the aromatic region are larger compared to other signals suggesting the

overlap of signals. When these discrepancies in peak shape were considered, twenty three carbon signals were observed with one being a secondary (saturated) carbon (δ 33.4) and the remainder being aryl or vinyl carbons. This agrees with the structure proposed.

The ^{1}H NMR shows the expected three aliphatic signals (δ 3.37, d, 2H; δ 6.42, m, 1H, and δ 6.81, d, 1H) were observed. The splitting patterns observed in these signals resemble the patterns observed for the parent system **6**. In addition the chemical shifts of these signals indicate two vinyl protons and two protons on a saturated carbon. Close examination of the aromatic region between δ 7.4 and 8.5 reveals four singlets, each representing one proton. The remainder of the aryl protons are split into multiplets representing the remaining eight protons. These aryl proton signals are expected based on the arrangement of the naphthalene rings in **89**.

An exact mass was measured for **89** to determine its molecular formula. A mass of 292.125 m/z (calc. 292.126) was observed which suggests a molecular formula of $C_{23}H_{16}$. This mass measurement considers only ^{12}C and uses a molecular weight for hydrogen of 1.0079.

3.3 Photolysis of 7-Deuterio-*5H*-dibenzo[a,c]cycloheptene (87)

Stabilization of a carbanion at the 5-position of **6** may involve delocalization of the charge to either the aromatic rings or more likely the vinyl bond between positions six and seven. The latter process may result in a formal

base catalyzed [1,3]-shift if a proton were transferred from the 5-position to the 7-position during photolysis of **6** in H_2O/ACN. Such a process has been observed in ground and excited state reactions of allylic systems (*vide supra*). Photolysis of **87** under various conditions should indicate whether or not such a process occurs for **6** in the excited state. Photolysis of this system may also provide more information concerning the [1,7] sigmatropic shift and the di-π-methane rearrangement which competes with the proton exchange at the 5-position.

In the following studies, ^2H NMR was used to analyze the distribution of deuterium in the product mixture obtained from photolysis of **87** under various conditions. In general photolyses of **87** were carried out in a Rayonet RPR 100 photochemical reactor using 254 nm lamps and a quartz container (350 nm lamps and pyrex container in the triplet sensitization experiments).

3.3.1 Photolysis in 100% ACN

Direct photolysis of **87** in ACN resulted in the product distribution shown (eq. 3.1). The percentages indicated were measured from the ^2H NMR (Fig. 3.3)

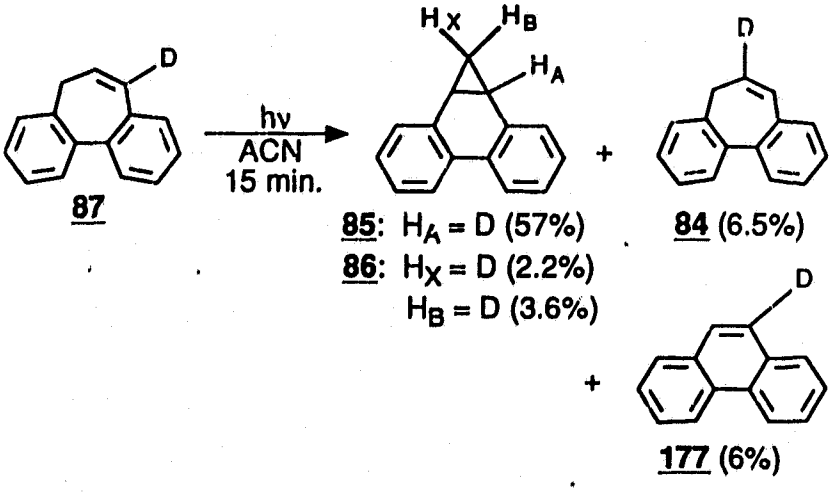

87

85: H_A = D (57%)
86: H_X = D (2.2%)
H_B = D (3.6%)

84 (6.5%)

177 (6%)

(3.1)

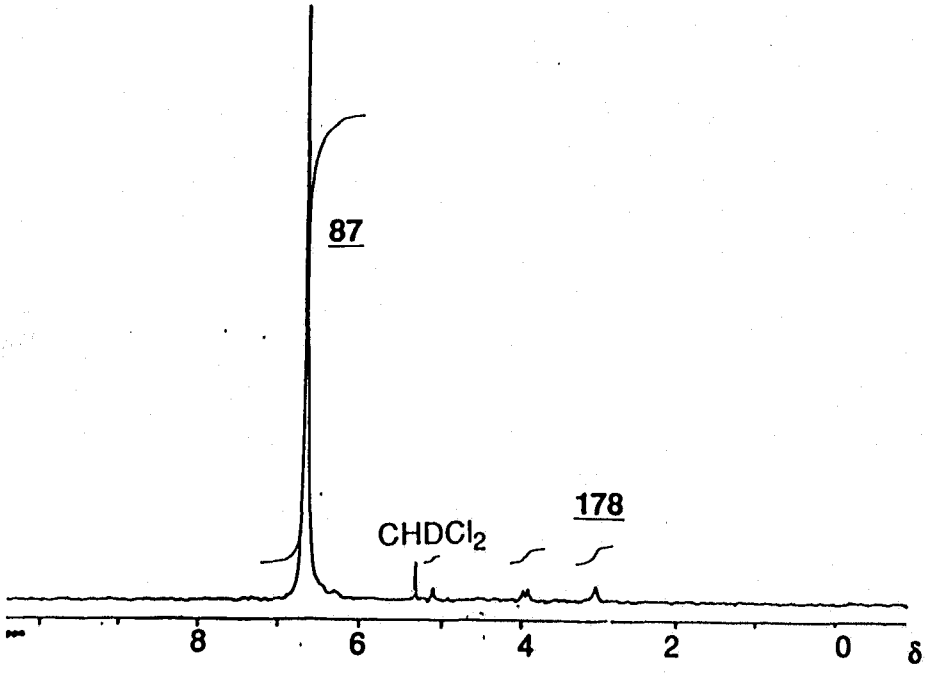

Figure 3.2 ^2H NMR of 87 in CH_2Cl_2

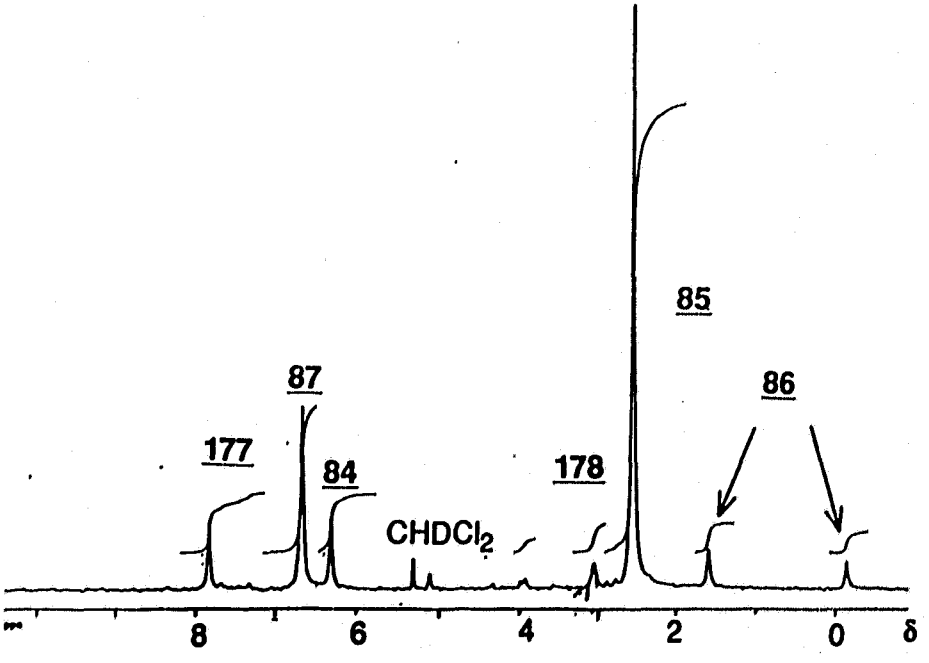

Figure 3.3 ^2H NMR of product mixture formed by photolyzing 87 in ACN.

obtained after evaporation of ACN from the product mixture. Comparison of this ^2H NMR with the one obtained for the starting material (Fig. 3.2) indicates that a [1,3] sigmatropic shift does not occur in ACN since no growth in the signal at δ 3.05 (which represents the 5-position of **87**) was observed. This result was unexpected since previous photochemical studies of 3,4-benzotropilidene (**40**) indicated that [1,3] sigmatropic shifts were possible for benzannelated cycloheptatriene systems[79] (*vide supra*).

Based on previous studies of **6**[8,113] the major product expected after photolysis of **87** in ACN is **85** with a deuterium at the position labelled H_A. This product accounted for 57% of the deuterium label, confirming the previous results. The 9-deuteriophenanthrene (**177**) (6%) observed was also expected based on previous studies of **6** and on the work of Richardson et al.[159]. These studies demonstrated that photolysis of systems such as **85** results in extrusion of a methylene carbon to form phenanthrene systems (i.e., **177**). Previous results can therefore be used to account for the majority of the products observed. However, they do not account for the presence of deuterium at the 6-position (**84**) or for the deuterium observed at positions H_X and H_B (**86**).

Formal di-π-methane rearrangement of **84** would be expected to result in the deuterium observed at positions H_X and H_B of **86**. The formation of **84** itself could be accounted for by a series of [1,7] sigmatropic shifts but such a process would also result in the growth of deuterium at the 5-position. Another mechanism which could be used to account for the formation of **84** is a "reverse

di-π-methane" rearrangement from **85** (Scheme 3.6). Photolysis of **84** in previous studies[113] indicated that a di-π-methane rearrangement produced **85**. The reverse process is possible as indicated by results from the literature (see eq. 1.34)[98]. Such a process, however, was not observed by Richardson et al.[159] but this is to be expected based on the length of photolysis (20 h) performed in these studies and on the high conversions achieved

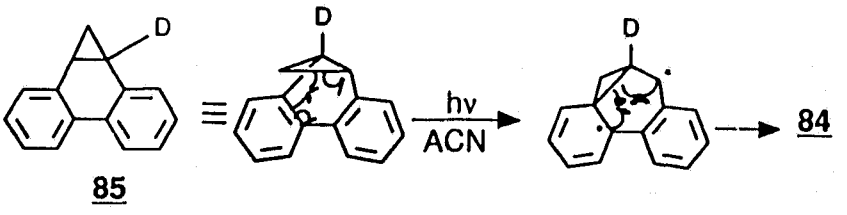

Scheme 3.6

(90% conversion to phenanthrene (**148**)). Long photolysis times would be expected to convert any **6** formed back to starting material and eventually to **148**. By combining the yields for **84** and **86** (≈12%) (eq. 3.1) it can be seen that at short photolysis times the major product observed after photolysis of **85** is **84**, not **177**.

3.3.2 Photolysis in 50% H_2O/ACN

Direct photolysis of **87** in 50% H_2O/ACN resulted in the distribution of deuterium noted in equation 3.2. The percentage of deuterium label observed at each position in the products was measured from the ^2H NMR obtained for this photolysis (Fig. 3.4). These results do not include data for the excited state proton exchange process since a deuterated solvent was not used. However, these results do indicate that in addition to cyclization to **85**, a "base catalyzed" [1,3]-shift

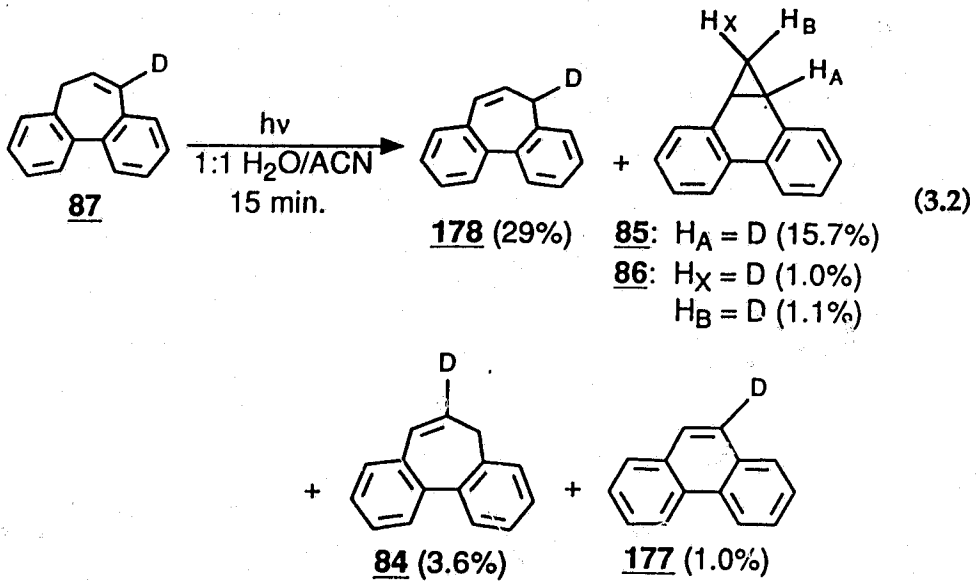

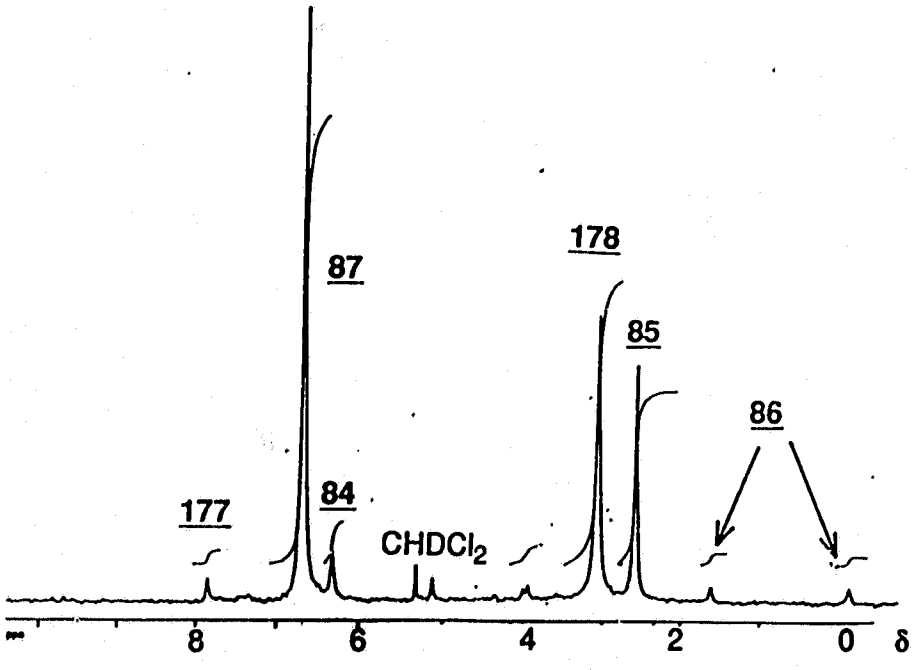

Figure 3.4 ^{2}H NMR of the product mixture formed by photolysis of **87** in 50% H_2O/ACN

occurs to produce **178**. The yield of **85** observed is much less than in the previousphotolysis. This is expected since H_2O quenches S_1 which competes with the [1,7]-sigmatropic shift required for formation of **85**[8,113]. However, ISC to T_1 can still occur to produce (85) (≈16%) via a di-π-methane rearrangement of **87**. The minor deuterium signals, representing **84**, **86** and **177**, can be explained by photolysis of **85**, as discussed in the previous section of this Chapter. In addition, **86** can also be formed via a di-π-methane rearrangement of **178**.

The absence of **178** on photolysis of **87** in ACN suggests that formation of this compound in H_2O/ACN involves a "base catalyzed" [1,3]-shift. A sequence of [1,7] sigmatropic shifts or di-π-methane rearrangements can not be used to account for **178** since these processes would have also resulted in the formation of this product when **87** was photolyzed in ACN. A photochemical base catalyzed hydrogen shift is not unprecedented as demonstrated by the work of Laarhoven et al.[92,93] (*vide supra*).

Based on the quantum yield of cyclization for **6** in H_2O/ACN (≈0.01)[113] and the relative amounts of **85** and **178** observed in Figure 3.4 (roughly two to one), the quantum yield for the base catalyzed [1,3]-shift is estimated to be ≈0.02. Laarhoven et al.[93] demonstrated that roughly one in four of the base catalyzed [1,3]-shifts results in deuterium incorporation into the product. The quantum yield for proton exchange in **6** via a base catalyzed [1,3]-shift is therefore believed to be <0.02 (0.005 according to the results of Laarhoven[93]). Comparison of this value with the quantum yield for deuterium incorporation into **6** using D_2O/ACN

(≈0.034)[113] suggests that the base catalyzed [1,3]-shift accounts for roughly 15% of the deuterium incorporated. These calculations are very rough but they indicate that the base catalyzed [1,3]-shift cannot be used to account for all of the deuterium incorporation observed in **6**. A major portion of the deuterium incorporated into **6** is, therefore, believed to result from the enhanced acidity of this system in S_1.

3.3.3 Triplet Sensitization

To determine the deuterium distribution after reaction of **87** via T_1, triplet sensitization of this system was performed (eq. 3.3). As in previous studies of **6**, 2-benzoylbenzoic acid (**107**) was used as the triplet sensitizer. The resulting product mixture was examined using ^2H NMR (Fig. 3.5). Only **85** was formed via this indirect excitation of **87**. The formation of **85** is expected since previous studies demonstrated that the di-π-methane rearrangement of **6** occurs via T_1[113].

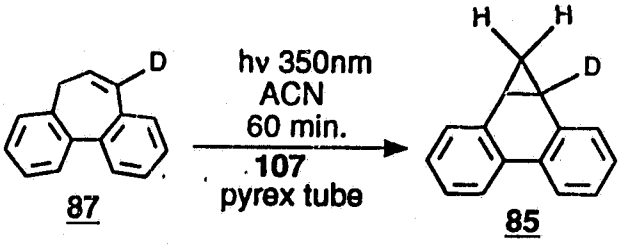

87 → 85 (3.3)

The above triplet sensitization of **87** would have to be repeated with water present to determine in which excited state (S_1 or T_1) the base catalyzed [1,3] proton shift occurs. However, the lack of deuterium incorporation in previous triplet sensitizations of **6** with D_2O[113] present suggests that the base catalyzed

[1,3]-shift occurs via S_1. This conclusion is based on the belief that a base catalyzed [1,3]-shift involves a minor amount of deuterium incorporation when a deuterated base is used.

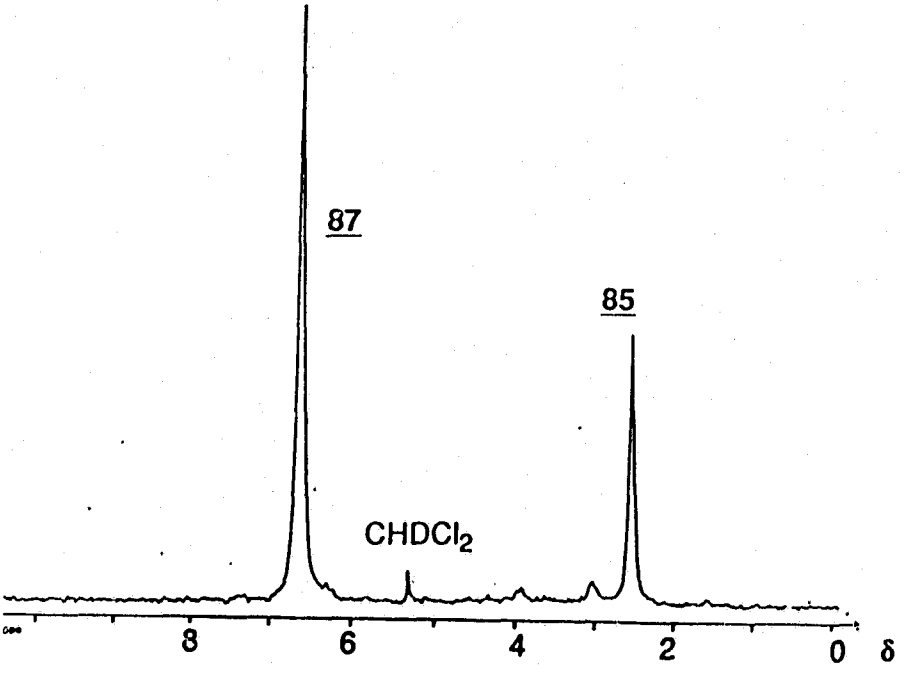

Figure 3.5 ^{2}H NMR of the product mixture formed by triplet sensitization of 87 in ACN.

3.3.4 Modified Mechanism for the Photochemistry of *5H*-Dibenzo[a,c]cycloheptene (6)

The modified mechanism for photochemical reactions of 6 (Scheme 3.7) is similar to the version presented in previous studies[113]. The major difference is the addition of a route involving the base catalyzed [1,3]-shift. As indicated by the mechanism, deuterium incorporation can occur by either the [1,3]-shift or via

exchange with protons at the 5-position. As demonstrated earlier the latter process is believed to account for the majority of deuterium incorporated into 6.

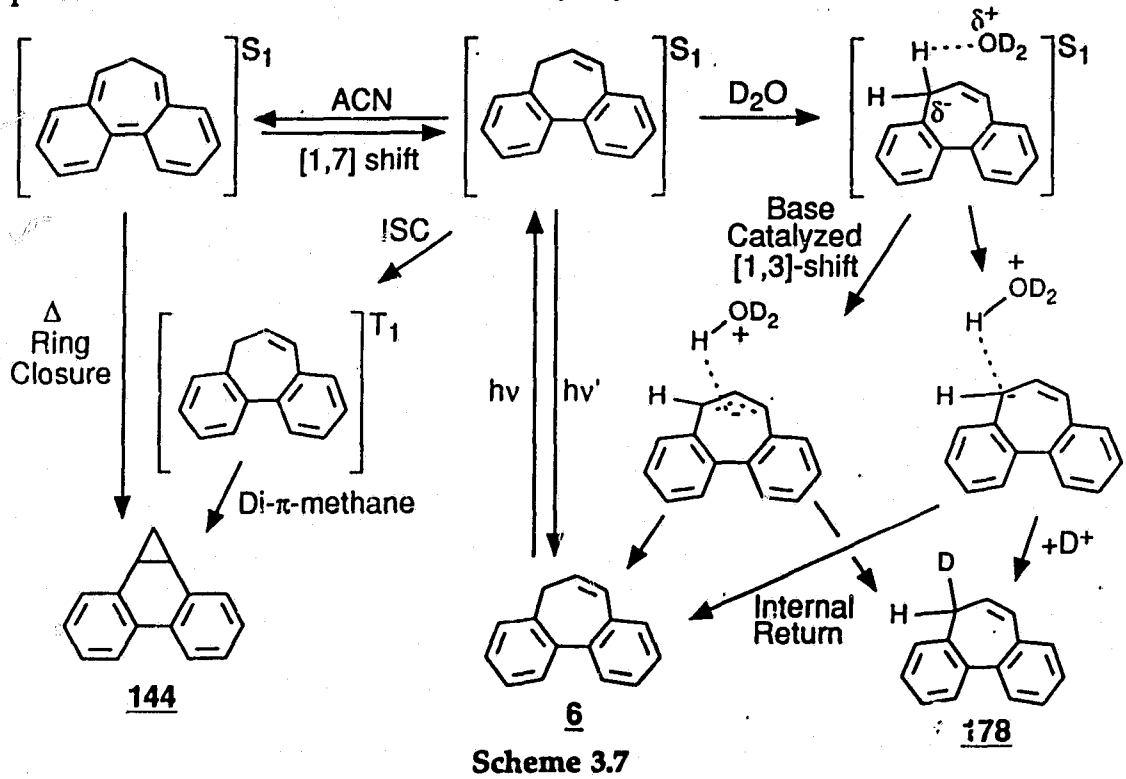

Scheme 3.7

3.4 Photochemistry of 6-Methyl-5*H*-dibenzo[a,c]cycloheptene (155) and 6-Phenyl-5*H*-dibenzo[a,c]cycloheptene (156)

In the previous Chapter it was indicated that substitution of 5 at the 5-position resulted in a substantial decrease in the ability of this system to function as an excited state carbon acid. Substitution of 6 at the 6-position is not expected to have such a dramatic affect on the excited state carbon acid behaviour of 6 since the position where proton exchange occurs is not being changed significantly. Also the presence of substituents at the 6-position should not have

a substantial effect on the conformations available for **6** since this position is not sterically crowded, unlike the 5-position of **5**. The purpose of the following section is to examine the extent to which the photochemistry of **6** is altered by substitution at the 6-position. Included in this section is a brief examination of the effect of primary amines on the photochemistry of **6** and related systems. The photochemical processes covered in this section are also quantified and compared by measurement of quantum yields. These quantum yields were measured using the same procedure outlined for the values listed in Table 2.4 of Chapter 2.

3.4.1 Direct Photolysis of 6-Methyl-5*H*-dibenzo[a,c]cycloheptene (155) in ACN Using 254 nm Lamps

Direct irradiation of **155** (50 mg) in 100 mL ACN for 15 min using 254 nm lamps gave three major products (eq. 3.4) according to both ^{1}H NMR and GC. Minor products were also observed but in quantities (<1% by GC) which made them difficult to identify. The major product observed (**179**) is the product

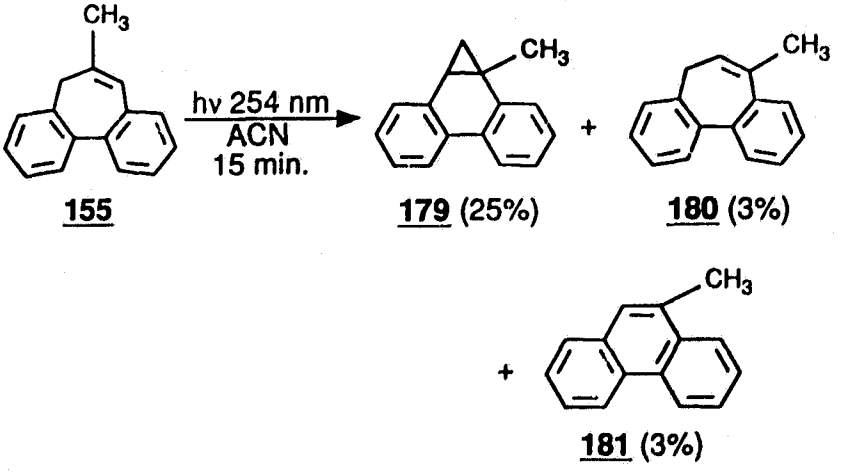

155 **179** (25%) **180** (3%) **181** (3%) (3.4)

expected via a di-π-methane rearrangement (Scheme 3.8). Identification of this product was achieved by analysis of the ^{1}H NMR and by GC/MS of the product mixture (M^+ = 206 m/z). The chemical shifts, splitting patterns, and coupling constants measured for the cyclopropyl protons were all consistent with the proposed structure of **179**. Further verification of the identity of the major product was achieved by obtaining a ^{1}H COSY NMR. By using this NMR technique the origin of the coupling constants observed for various protons were correlated. The correlation observed between the signals believed to represent the cyclopropyl ring protons of **179** confirmed the identity of this product.

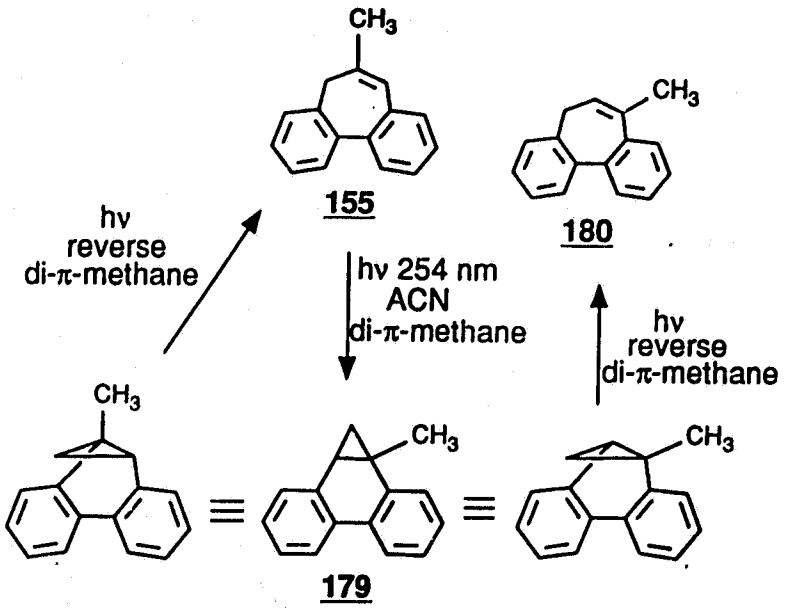

Scheme 3.8

The two other major products observed **180** and **181** were identified in subsequent photolysis since the amounts obtained in the direct photolysis of **155** in ACN provided insufficient material. The chemical shifts, splitting patterns, and

coupling constants observed for these two products were consistent with the proposed structures **180** and **181**. The signals assigned to **181** in the ^{1}H NMR of the product mixture were also consistent with the literature spectrum for this compound[160]. The two methylene protons of **180** exhibit different chemical shifts (δ 2.80 and 3.05) which are believed to result from twisting of the seven membered ring. This twisting results from steric interaction between the methyl at the 7-position and the aryl proton adjacent to it, which forces the seven membered ring into a non-planar conformation similar to that observed for the binaphthyl system **88**. Both GC/MS (**180** M^+ = 206 m/z and **181** M^+ = 192 m/z) and ^{1}H COSY NMR were used to provide further evidence for the formation of **180** and **181**. Both the methyl signal at δ 2.11 and the methylene signals at δ 2.80 and 3.05 correlate with a vinyl proton signal at δ 6.08. The integration and splitting patterns observed in these signals agree with this correlation suggesting the formation of **180** via photolysis of **155**.

The [1,7] sigmatropic shift product (**182**) expected in the direct photolysis of **155** in ACN using 254 nm lamps was not observed in the ^{1}H NMR of this product mixture. The methyl located at the 6-position of **155** may be one reason for the lack of a [1,7]-shift product. As indicated in the Introduction methyl groups do effect [1,7] sigmatropic shifts[73] due to the possible existence of

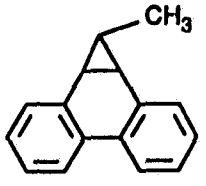

182

polarized zwitterionic states[74].

The three major products observed in eq. 3.4 can be explained based on the results obtained from the photolysis of **87** (*vide supra*). Formation of **179** involves a di-π-methane rearrangement as indicated. Subsequent photolysis of this system is believed to result in the formation of **180** and **181**. The former via a reverse di-π-methane rearrangement and the latter via extrusion of a methylene carbon. As indicated in Scheme 3.8 the reverse di-π-methane rearrangement of **179** results in the formation of **180** and **155**. Formation of the latter compound (**155**) via this route could not be demonstrated as it is the starting material.

3.4.2 Direct Photolysis of 6-Methyl-5*H*-dibenzo[a,c]cycloheptene (155) in ACN Using 300 nm Lamps

Repetition of the previous photolysis of **155** in ACN using 300 nm lamps (15 min.) resulted in the three products (**179-181**) observed in the 254 nm photolysis (eq. 3.5). However, the major product formed was **180** followed by

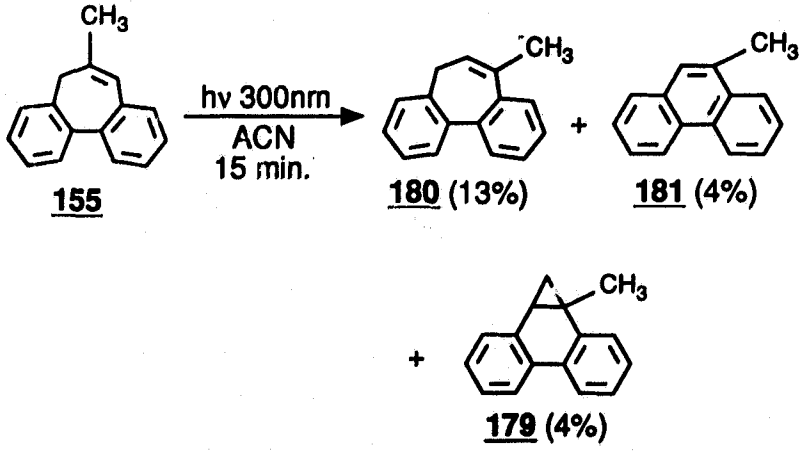

(3.5)

181, then 179. The increased yields of 180 and 181 at 300 nm are expected since cyclopropyl derivatives such as 179 absorb more light at this wavelength than 155[160]. The higher yield of 180 is expected based on the product studies involving 87. These studies indicated that the reverse di-π-methane rearrangement occurs more efficiently than the photoextrusion of a carbene. However, both 155 and 180 should eventually be converted to 181 or phenanthrene (148). As in the 254 nm photolysis of 155, the 300 nm photolysis provided no evidence for the formation of a [1,7] sigmatropic shift product (182).

A 1 h photolysis of 155 at 300 nm in ACN was performed to generate sufficient amounts of 179 and 180 for identification by ^{1}H NMR. The yields obtained were much higher according to GC analysis of the product mixture (43% 180, 22% 181 and 6% 179).

3.4.3 Triplet Sensitization of 6-Methyl-5*H*-dibenzo[a,c]cycloheptene (155)

Triplet sensitization of 155 was carried out, as in previous studies, with 2-benzoylbenzoic acid (107) in ACN. Irradiation of 107 at 350 nm for 60 min. in the presence of 155 (40 mg) resulted in only one product. According to ^{1}H NMR and GC analysis of the product mixture the major product formed was 179. This was as expected since 179 is formed via a di-π-methane rearrangement, which proceeds through the triplet excited state.

3.4.4 Photolysis of 6-Methyl-5*H*-dibenzo[a,c]cycloheptene (155) on the Optical

Bench

Measurement of the product quantum yield for formation of 179 from 155 was attempted on a optical bench using 280 nm light from a mercury arc lamp. Samples made up from a 1.40×10^{-3} M stock solution of 155 in ACN were irradiated in UV quartz cuvettes for various lengths of time. The light source on the optical bench is much less intense than that from Rayonet (>1400 times less intense) so much longer photolysis times were required to achieve measurable conversion to products. However, analysis of the product mixture by GC indicated a new product which was not observed in previous photolyses of 155 using the Rayonet. The quantities irradiated on the optical bench were too small to allow for analysis by ^{1}H NMR so only GC/MS was used to analyze the product mixture. The GC/MS indicated two components for the product peak with masses of 178 (major component) and 222 m/z (minor component). The similar retention times observed for the unknown product 179 suggest that these two compounds may be isomers. One possible isomer of 179 is the product formed via an initial [1,7] sigmatropic shift followed by electrocyclic ring closure (182). This compound (with a mass of 206 m/z) may decompose in the mass spectrometer to produce phenanthrene (148) which has a mass of 178 m/z. The MS (chemical ionization (CI)) indicated a peak at 207 which represents the M+29 peak for the component with a mass of 178 m/z. However, this peak also corresponds to the M+1 signal for 182. This possibility was suggested by a peak at 235 m/z which corresponds to the M+29 signal for 182 (M^+ = 206 m/z). The

compound with a mass of 222 m/z indicates that photooxidation of **155** may have occurred.

To determine if the products formed via photolysis of **155** were wavelength dependent, an irradiation at 254 nm on the optical bench was performed. The same unknown product was observed, suggesting that the product formed depends on the light intensity used, since this is the major difference between the two 254 nm light sources. A photolysis was therefore performed in the Rayonet with all but one of the 254 nm lamps removed. Irradiation of a sample (prepared from the same stock solution used in the optical bench studies) contained in a UV quartz cuvette was performed for various lengths of time to determine if the unknown product was formed then decomposed to **179** or back to starting material. Such a process is possible with a more intense light source. Analysis of the reaction mixture by GC indicated the formation of **179** with no trace of the unknown product. The reason for this difference in photoproducts on the optical bench and in the Rayonet is unknown. However, even with one lamp, the Rayonet still has a much higher light intensity. The identity of the optical bench product would have to be determined first to better understand this dependence on the light intensity.

3.4.5 Photolysis of *5H*-Dibenzo[a,c]cycloheptene (6) and 6-Methyl-*5H*-dibenzo[a,c]cycloheptene (155) in the Presence of Bases

Photolysis of **155** in D_2O/ACN was performed to determine if this system

exhibited excited state carbon acidity similar to that observed for **6**. Direct photolysis of **155** (50 mg) in 25% D_2O/ACN (100 mL), using a rayonet with 254 nm lamps (15 min) gave a similar product mixture (**179** (22%), **180** (3%) and **181** (3%)) as that observed via direct irradiation of this compound in pure ACN. This contrasts with the photochemistry of **6**, where addition of a base (H_2O) decreased the photorearrangement yields. Analysis of the product mixture obtained by photolysis of **155** in D_2O/ACN using ^1H NMR did reveal a minor amount of deuterium incorporation (< 10%). The quantum yield of exchange (Φ_{ex}) and the product quantum yield (Φ_p) measured for this process are presented in Table 3.3. The product distribution and the minor amount of deuterium incorporation observed for **155** suggest that this system does not function as an excited state carbon acid to the same extent as **6**.

In the previous Chapter it was demonstrated that primary amines catalyze the excited state proton exchange of **5** more efficiently than water. The effect of EA on the photochemistry of **6** and **155** was studied by photolyzing these compounds in 10% (5.0 M EA/D_2O)/ACN (100 mL). D_2O was added to provide the source of deuterons. Analysis of the photoproducts formed by photolysis of **6** in the presence of EA using GC and ^1H NMR indicated that the rearrangement processes of this system were effected to the same extent by primary amines and water. This result was confirmed by the product quantum yield (Φ_p) measured for this photolysis (Table 3.3). However, the amount of deuterium incorporation observed in the recovered starting material and in the products suggest that EA

enhances the proton exchange process compared to water. This was confirmed by the value of Φ_{ex} measured for this process (Table 3.3) which is larger than the value measured for **6** in 70% D_2O/ACN ($\Phi_{ex} = 0.034 \pm 0.006$)[113].

Irradiation of **155** (50 mg) for either 5 or 30 min using the same conditions noted for **6** resulted in a product mixture similar to that observed after direct photolysis of the former compound in ACN. Analysis of the reaction mixture from the 30 min. photolysis by GC/MS and by ^1H and ^2H NMR indicated extensive deuterium incorporation in the recovered starting material (73%) and in the product **179** (36%). The ^2H NMR indicated that deuterium was incorporated predominantly into the 5-position with a lesser amount at the 7-position of **155**. The deuterium incorporation into the 7-position could be accounted for by a base catalyzed [1,3] proton shift which was demonstrated in the photolysis of **87**. The ^2H NMR also indicated the presence of deuterium in **179** at all the positions (H_A, H_B and H_X: ratio 1:2:2) of the cyclopropyl ring. A di-π-methane rearrangement of 5-deuterated **155** can be used to rationalize the deuterium observed at H_B and H_X. The deuterium observed at H_A is believed to result via a di-π-methane rearrangement of **155** containing a deuterium at the 7-position.

The quantum yield of exchange (Φ_{ex}) estimated from the 5 min photolysis of **155** is similar to the value measured for **6** (Table 3.3). Primary amines therefore enhance the amount of proton exchange for **6** and **155** and have a similar effect on the rearrangement yields to that observed with water as the base.

Table 3.3 Quantum yields of exchange (Φ_{ex}) and product formation (Φ_p) for **6** and related systems[a].

Compound	Solvent[b]	Φ_{ex}[c]	Φ_p[d]
6	25% D_2O/ACN	0.032 ± 0.009	0.023 ± 0.006
	10% (5M EA/D_2O)/ACN	0.08 ± 0.02	0.029 ± 0.008
155	25% D_2O/ACN	0.006 ± 0.002	0.018 ± 0.006
	10% (5M EA/D_2O)/ACN	0.07 ± 0.02	0.016 ± 0.005
156	40% D_2O/ACN	0.000[e]	-[f]

[a]Measured in a Rayonet photochemical reactor (254 nm) at ambient temperatures using **91** in 50% H_2O/ACN as the secondary actinometer (Φ_{ex} = 0.035 ± 0.005). [b]ACN as cosolvent for solubility reasons. Ratios are v/v. D_2O was added in studies involving EA as a source of deuterium. [c]Analysis by 360 MHz ^1H NMR. Errors are uncertainties in the secondary actinometer and in peak heights determined from integrations in the ^1H NMR. [d]Rearrangement products were quantified by 3 or more injections into a GC. Errors are standard deviation in these injections. [e]No deuterium incorporation was observable by ^1H (360 MHz) NMR. [f]No formal di-π-methane products were observed after photolysis of this compound.

3.4.6 Photolysis of 6-Phenyl-5*H*-dibenzo[a,c]cycloheptene (156)

Direct photolysis of **156** (50 mg) in ACN (100 mL) with 254 nm lamps (30 min) gave only several minor products which could not be identified by ^1H NMR

or GC/MS. However, the ^{1}H NMR did not show signals in the region below δ 0.9, which suggests that cyclopropyl products are not formed. A second photolysis of **156** in 40% D_2O/ACN with 254 nm lamps (15 min) resulted in no deuterium incorporation into the substrate by GC/MS. However, several minor products were observed. Due to the complexity of the product ^{1}H NMR and the lack of deuterium incorporation into **156**, no further attempts were made to identify the products formed on photolysis of this compound.

3.4.7 Fluorescence Studies of 6-Methyl-5*H*-dibenzo[a,c]cycloheptene (155) and 6-Phenyl-5*H*-dibenzo[a,c]cycloheptene (156)

The fluorescence emission and excitation spectra of **155** and **6** are shown in Figure 3.6. Both the emission and excitation spectrum of **155** were essentially

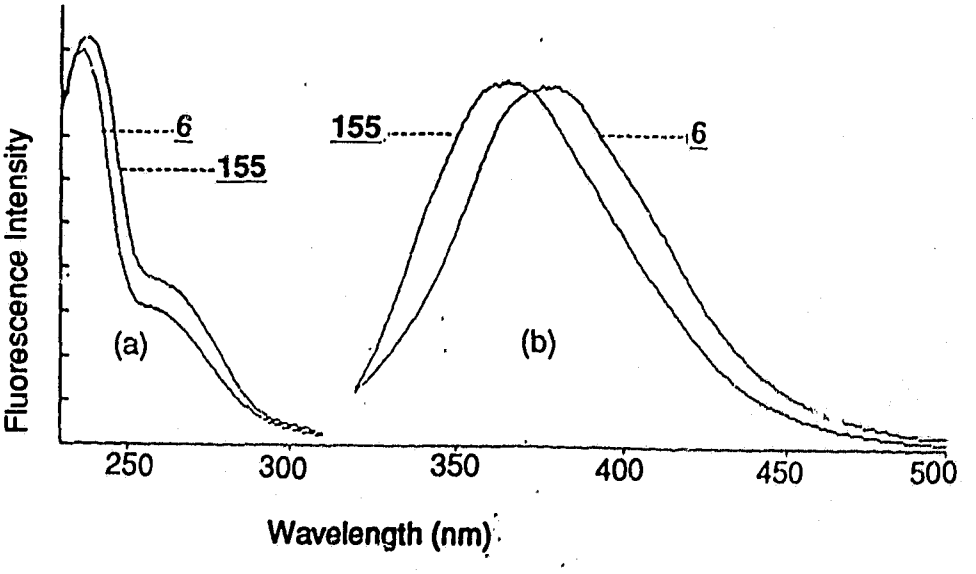

Figure 3.6 Fluorescence excitation (a) and emission (b) spectrum of **6** (λ_{ex} = 260 nm, λ_{em} = 350 nm) and **155** (λ_{ex} = 260 nm, λ_{em} = 350 nm) in ACN.

identical to the corresponding spectra of **6**. This is as expected since introduction of a methyl group at the 6-position of **6** should have little effect on the nature of the chromophore of this compound. However, the fluorescence quantum yield (Φ_f) is affected by addition of a methyl to **6** (Table 3.4). Values of Φ_f were measured for **6** and **155** with **5** as the secondary standard. The value obtained for **6** (0.12 ± 0.02) is larger than the value obtained for **155** (0.07 ± 0.01). A lower fluorescence quantum yield is expected for **155** since the addition of a methyl

Table 3.4 Fluorescence quantum yields (Φ_f) and lifetimes for **6**, **155** and **156**.

Compound	Φ_f[b]	τ(ns)[f]
6	0.12 ± 0.02[c]	4.5 ± 0.1[g]
155	0.07 ± 0.01[d]	1.58 ± 0.07[h]
156	0.006 ± 0.001[e]	4.0 / 20.7[i]

[a]At ambient temperatures in dry ACN distilled over CaH. [b]Determined using areas in fluorescence emissions of indicated compounds. In all cases O.D. were < 0.1. Errors are based on standard deviations in 3 or more independent analysis. [c]Measured against **5** with matching over λ = 307-315 nm. [d]Measured against **5** with matching over λ = 295-310 nm. [e]Measured against **155** with matching at λ = 291 nm. [f]Errors are standard deviations of 3 or more independent runs. [g]λ_{ex} = 280 nm, λ_{em} = 360 nm. [h]λ_{ex} = 270 nm, λ_{em} = 375 nm. [i]Biexponential fit, λ_{ex} = 260 nm, λ_{em} = 370 nm.

group to the 6-position of **6** provides a greater number of vibrational degrees of freedom. IC from S_1 to S_0 is enhanced by these additional modes of vibration and so the value of Φ_f for **155** is decreased.

The fluorescence emission (with two maxima) and excitation spectra of **156** in ACN do not resemble the corresponding spectra of **6** or **155** (Fig. 3.7). Furthermore, as demonstrated by the fluorescence emission obtained using an excitation wavelength of 300 nm (rather than 260 nm), the relative intensity of the two maxima vary with the excitation wavelength. One possible reason for this result is that the fluorescence spectrum of **156** contains emission from two chromophores. This is demonstrated by the changes which occur in the excitation spectrum when the emission wavelength used to monitor this spectrum is changed (Fig. 3.7). The intensity of the emission observed for each chromophore depends on the wavelength chosen to excite the molecule since the absorption

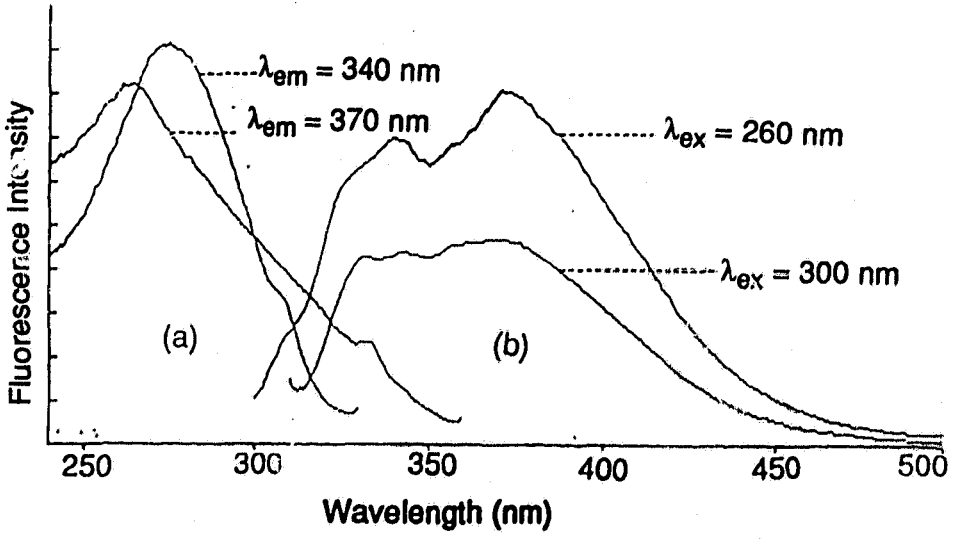

Figure 3.7 Fluorescence excitation (a) and emission (b) spectra of **156**.

spectrum contains absorptions due to each chromophore. The second chromophore may be an impurity, which could be readily observed due to the low fluorescence quantum yield of **156** (0.006 ± 0.001).

Fluorescence lifetimes (τ_f) were measured for **155** and **156** in dry ACN (Table 3.4). A lower value of τ_f was obtained for **155** compared to the value measured for **6**. This difference can be attributed to the greater number of vibrational degrees of freedom available for the former compound.

A biexponential fit was required for the fluorescence decay of **156** (Table 3.4). When monitoring the fluorescence at 370 nm the short lived component accounted for 63% of the emission with the longer lived component making up the remainder of the emission. The percentage of the emission corresponding to each component varied when the emission wavelength was changed. These results support the conclusions made earlier concerning the fluorescence spectrum of **156**, i.e., two or more chromophores (impurities) are present.

Quenching of the fluorescence due to **6** by water has been demonstrated in previous studies[113]. The rate of this quenching process (k_q) involving **6** is comparable to the rate observed for fluorescence quenching of **5** by water. Also, as observed for **5**, the fluorescence of **6** is quenched efficiently by primary amines such as EA and 2-methoxyethylamine (Table 3.5). The fluorescence of **155** is not quenched efficiently by water but is quenched efficiently by EA. These results agree with the quantum yields of exchange presented earlier which showed that **155** required a stronger base than water for efficient incorporation of deuterium.

Table 3.5 Rates of fluorescence quenching for **6**, **155** and **156**[a].

Compound	Quencher[b]	k_q, 10^9 $M^{-1}s^{-1}$ [c]
6	H_2O	0.25 ± 0.01
	$H_2NCH_2CH_2OH$	6.91 ± 0.23
	$MeOCH_2CH_2NH_2$	8.05 ± 0.20
155	H_2O	-[d]
	$H_2NCH_2CH_2OH$	3.21 ± 0.12
156	H_2O	-[e]
	$H_2NCH_2CH_2OH$	-[e]

[a]At ambient temperatures in dry ACN distilled over CaH, λex = 260 nm. [b]H_2O added in directly and EA was diluted in ACN prior to addition. [c]Obtained by division of slopes from Stern-Volmer plots by corresponding values of τ_0. Errors are standard deviations of 3 or more independent runs. [d]Weakly quenched. [e]No observable quenching.

Finally, as expected based on the deuterium exchange studies, the fluorescence of **156** is not quenched by water or EA.

The results observed for **155** and **156** indicate that substitution at the 6-position of **6** has a large effect on the photochemistry of this system. The decrease in excited state acidity observed for **155** and **156** is believed to be due to a combination of effects. The major effect is probably their enhanced deactivation via IC.

3.5 Photochemistry of *3H*-Cyclohepta[2,1-a:3,4-a']dinaphthalene (88) and *3H*-Cyclohepta[2,3-a:3,2-a']dinaphthalene (89)

To further study the effect of the ICA of **6** on efficiency of excited state proton exchange, two naphthalene derivatives **88** and **89** were studied. These systems can be used to probe the importance of the ICA since the position at which the naphthalene rings are fused to the seven membered ring should have and effect on the degree of double bond character in this ring. This results from the well known greater double bond character of the 1,2-bond versus the 2,3-bond of naphthalene[151]. Resonance structures (Scheme 3.9), bond lengths in naphthalene (1,2-bond 1.36 Å, 2,3-bond 1.415 Å) and molecular orbital calculations (which show bond orders of 1.724 and 1.603 for the 1,2 and 2,3 bonds respectively) all demonstrate this difference between the 1,2 and 2,3-bonds.

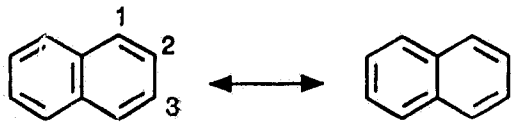

Scheme 3.9

The binaphthyl derivative **88** is expected to react more efficiently as an excited state carbon acid compared to **89** since the naphthalene rings of the former contribute more double bond character to the seven membered ring. This increased double bond character should assist the formation of an ICA by providing more efficient delocalization of the carbanion. Molecular orbital calculations indicate that the bonds of benzene each have a bond order of 1.667[151].

Therefore, the order of reactivity expected based on the ICA available to **6** is **88** > **6** > **89**. However, **88** also exists in a highly twisted conformation, unlike **6** or **89**, which may prohibit formation of a planar ICA.

3.5.1 Photolysis of 3*H*-Cyclohepta[2,1-a:3,4-a']dinaphthalene (88)

Irradiation of **88** (50 mg) in ACN for 4 h (Rayonet RPR 100 photochemical reactor, 254 nm lamps, Ar purged, quartz tube) resulted in no observable reaction according to both ^{1}H NMR (360 MHz) and GC analysis of the reaction mixture. Similarly, repetition of the photolysis in 50% D_2O/ACN for 1 h resulted in no observable deuterium incorporation. The lack of rearrangement of **88** in ACN was expected based on the bent structure of this molecule. Rearrangement of **88** via a di-π-methane or a [1,7] sigmatropic shift followed by electrocyclic ring closure requires that the seven membered ring become more planar, since the product expected and the intermediates involved are essentially planar. The geometry of **88** prohibits any such twisting to planarity as the peri-hydrogens of the naphthalene ring will strongly interact with each other.

The lack of deuterium incorporation into **88** after photolysis in 50% D_2O/ACN was not expected. However, the bent nature of **88** may prohibit formation of a planar 4n ICA, making this system less reactive than **6**. In addition the C-C bond length of the seven membered ring fused with naphthalene is longer (1.39 Å) (Table 3.1) than the 1,2-bond of naphthalene (1.36 Å). Other bond lengths in the naphthalene rings are as expected. This discrepancy may result

from the bent structure of **88** which could distort the naphthalene at the position fused to the seven membered ring. The seven membered ring therefore has less double bond character than expected, which may again hinder the formation of a 4n ICA.

To determine if **88** could exhibit excited state carbon acid behaviour in base, a photolysis (50 mg) was performed in 10% (5.0 M EA/D_2O)/ACN (eq. 3.6). Analysis of the reaction mixture by ^1H NMR indicated a decrease in the resonance due to the axial proton (H7B) (see Fig. 3.1). The equatorial (H7A) and vinyl protons (H8 and H9) of the seven membered ring exhibited little change in their relative intensities. Further analysis of the reaction mixture by ^2H NMR also

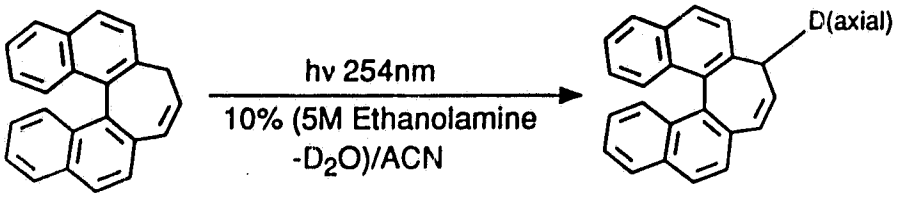

88 **183** (3.6)

indicated deuterium incorporation occurred predominantly at the axial position H7B of **88** to produce **183**. However, a minor deuterium signal was also noted at the position corresponding to H9 (Fig. 3.8).

The origin of the minor signal was investigated by irradiating **88** for various lengths of time and monitoring the change in the percent deuterium at positions H7B, H7A and H9 (using ^1H and ^2H NMR) (Fig. 3.9). Irradiation of **88** in a 0.5 M EA/10% D_2O/ACN (400 mL) solution was performed in a Rayonet using 254 nm lamps. After various intervals of irradiation, samples of **88** were

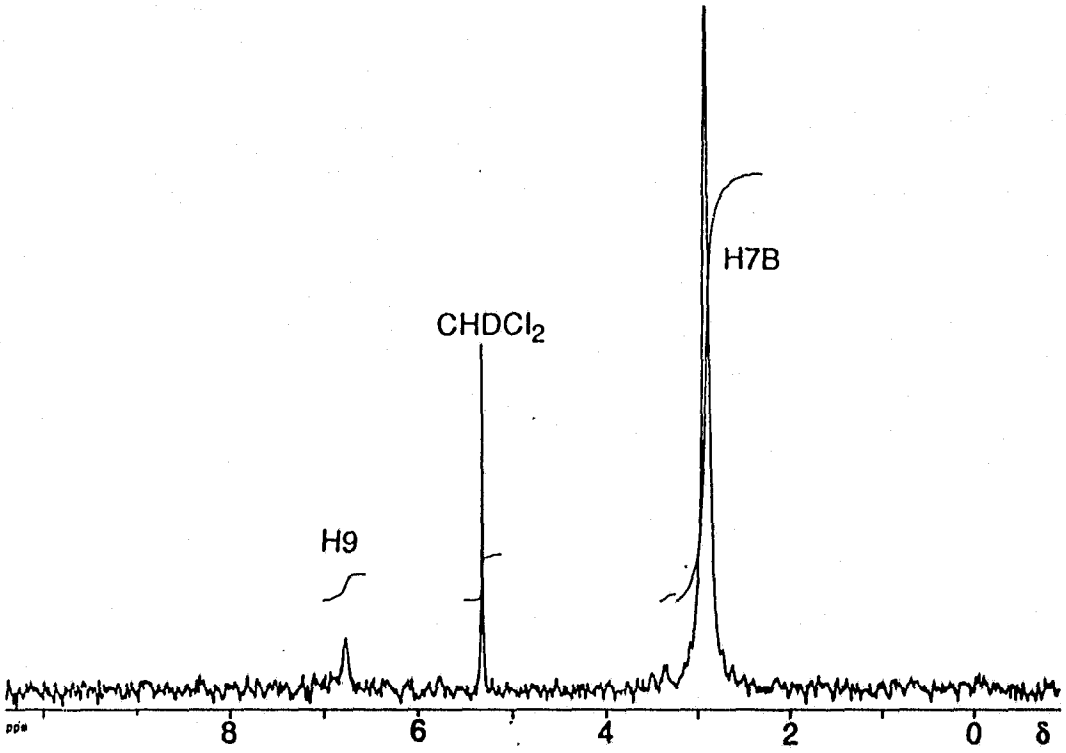

Figure 3.8 ^{2}H NMR of **88** after photolysis in the presence of ethanolamine and D_2O.

withdrawn for analysis. The plot obtained from the resulting data indicates that deuterium incorporation occurs predominantly at H7B with minor amounts at H9 and H7A.

Deuterium incorporation at the axial position is believed to occur via a proton exchange process similar to that proposed for **5** and **6**. EA, deuterated by D_2O, is believed to catalyze the exchange since photolysis of **88** in 50% D_2O/ACN did not result in deuterium incorporation. The delayed growth of deuterium at the equatorial (H7A) and vinyl (H9) positions relative to the axial position (H7B)

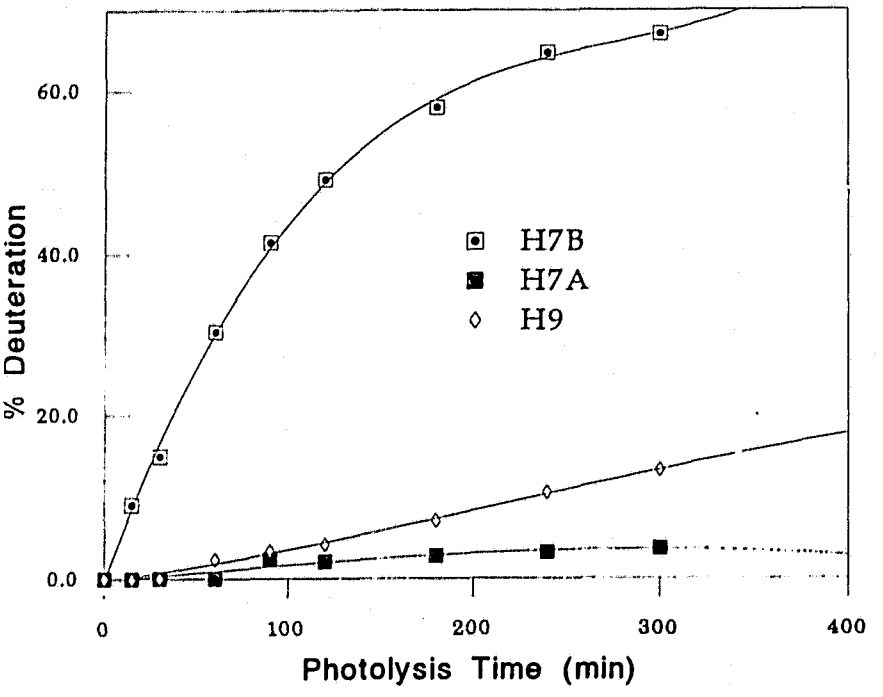

Figure 3.9 Percent deuterium observed at positions H7A (equatorial), H7B (axial) and H9 (vinyl) after various irradiation times.

suggests that initial exchange does not occur at these positions. Deuteration of H7A and H9 is believed to involve excitation of **183** followed by a [1,3]-shift similar to that proposed for **6** (*vide supra*). A shift of H7A results in deuterium growth at H9 whereas a shift of H7B results in deuterium growth at H7A (Scheme 3.10). Both shifts are mechanistically similar but the latter shift involves a deuterium and would, therefore be expected to be slower due to a primary isotope effect. This expectation is borne out by comparison of the plots corresponding to deuterium incorporation at the positions labelled H7A and H9

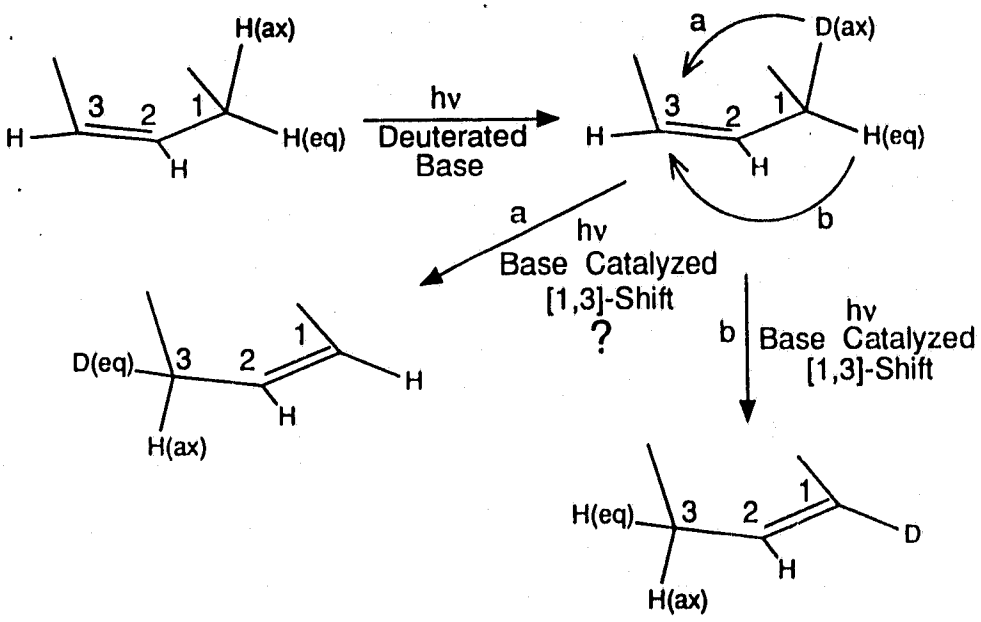

Scheme 3.10

(Fig. 3.9), in which growth of deuterium at H7A is the least efficient.

The nature of the [1,3]-shift was examined further by irradiation of a mixture of **88** and **183** in ACN for 6 h (separation of **88** and **183** was not possible). No deuterium growth was observed at H9 but a minor amount was observed at H7A (13%) according to ^{2}H NMR. These results suggest that deuteration of H9 involves base catalysis whereas deuteration of H7A does not. The latter shift may not involve a [1,3]-shift as conformation equilibration could exchange the axial and equatorial protons via a photochemical process (no thermal exchange of H7A and H7B is observed). However, this process is very sluggish compared to the exchange observed at H7B.

The results obtained for the photolysis of **88** suggest that excited state

proton exchange occurs only at the axial position (H7B) and not the equatorial position. This preference for exchange of the axial proton (H7B) is believed to result from the alignment of the axial proton with the π orbitals of the adjacent naphthalene ring and the vinyl group, i.e., a stereoelectronic effect. Alignment of the bond being broken with a π orbital is believed to facilitate carbanion formation, by allowing conjugation of the developing charge with the π orbital. Similar stereoelectronic effects have been noted for ground state reactions involving proton[162] and hydrogen[163] abstraction from carbons. The stereoelectronic effect, noted for the excited state proton exchange in **88** is the first example to our knowledge in which the axial proton is shown to be selectively exchanged.

3.5.2 Photolysis of *3H*-Cyclohepta[2,3-a:3,2-a']dinaphthalene (89)

Photolysis of **89** in ACN, using the same conditions as for **88** resulted in one product (eq. 3.7) according to both ^{1}H NMR (360 MHz) and GC analysis of the reaction mixture. The ^{1}H NMR exhibited three new aliphatic proton resonances at δ 0.18 (1H), 1.63 (1H) and 2.77 (2H). The chemical shifts of these three signals and the splitting patterns observed in each signal (doublet of triplets, doublet of triplets and a doublet of doublets, respectively) are similar to the chemical shifts and splitting patterns observed for the cyclopropyl protons of dibenzonorcaradiene (**144**). This similarity suggests that the product formed after irradiation of **89** is the cyclopropyl product **184**. GC/MS analysis of the reaction mixture also indicated the required mass for **184** (M^+ = 292 m/z).

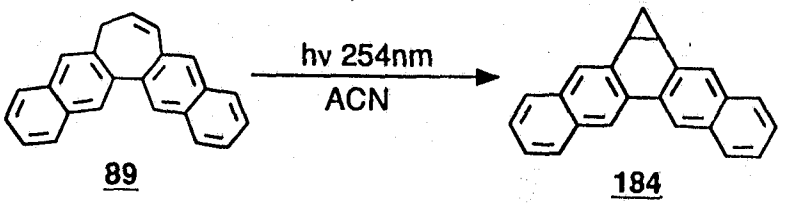

89 184 (3.7)

The overlay of UV spectra obtained after irradiation of **89** for various lengths of time are shown in Figure 3.10. Several clear isobestic points can be seen which suggest a clean reaction. The short photolysis times required for the changes observed in Figure 3.10 suggest that formation of **184** is efficient. The product quantum yield measured for this reaction ($\Phi_p = 0.47 \pm 0.02$) supports this belief. According to the photochemical mechanism proposed for rearrangement of **6**, the formation of **184** from **89** may occur via a di-π-methane rearrangement or a [1,7] sigmatropic shift followed by a thermal electrocyclic ring closure. One reason for the efficient nature of the rearrangement of **89** to **184** compared to the

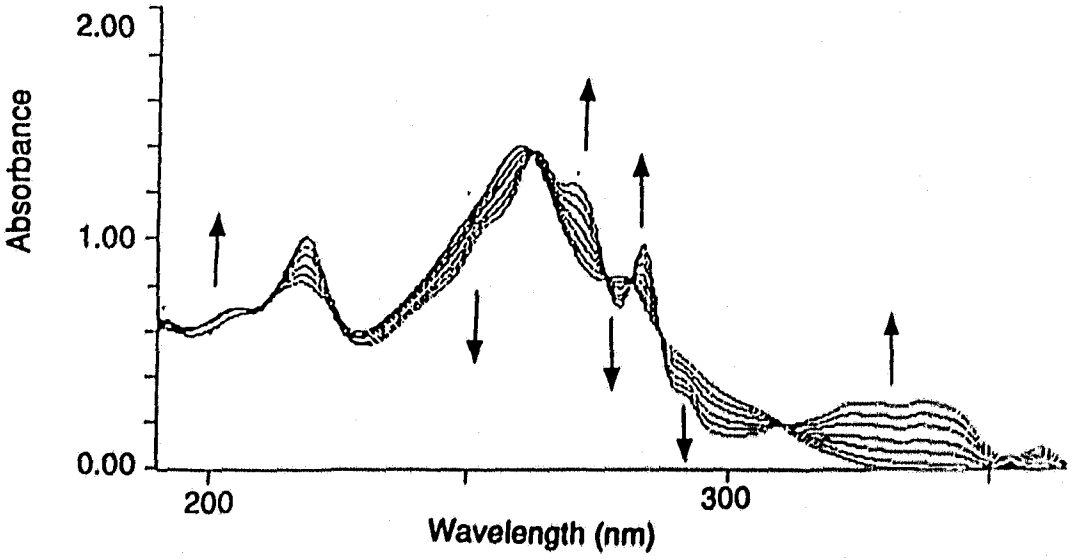

Figure 3.10 UV traces of **89** at various times of irradiation in ACN.

rearrangement of **6** to **144** is that naphthalene systems prefer to ISC to T_1 rather then fluoresce from S_1[64]. In T_1 **89** may undergo an efficient di-π-methane rearrangement to give **184**.

To determine if **89** exhibited excited state carbon acid characteristics a sample (≈$2x10^{-5}$ M) was irradiated in 10% (5 M EA in D_2O)/ACN in a 3 mL quartz cuvette with 254 nm lamps. No deuterium incorporation was observed according to a GC/MS of the resulting product mixture. Comparison of the GC of this reaction mixture with a GC of a similar reaction in pure ACN also indicated that the rearrangement process was unaffected by the added base, unlike the rearrangement of **6**, which is decreased in the presence of water. This result is expected based on the efficiency of the rearrangement process.

3.5.3 Fluorescence Studies of *3H*-Cyclohepta[2,1-a:3,4-a']dinaphthalene (88) and *3H*-Cyclohepta[2,3-a:3,2-a']dinaphthalene (89)

The fluorescence spectrum of both **88** and **89** in ACN are fairly broad and structureless and exhibit a significant Stokes shift (Fig. 3.11). This shift suggests that the geometry of both **88** and **89** are altered in S_1 compared to S_0. No decrease in fluorescence intensity was observed for either **88** or **89** after addition of water to the sample. Addition of EA causes a minor decrease in the fluorescence intensity of **88** but no decrease was observed for **89**. A value of k_q was obtained for the fluorescence quenching of **88** by EA ($(8.6 \pm 0.2) \times 10^8$ M^{-1} s^{-1}). This value is much less than the rate obtained for **6** using EA ($(6.91 \pm 0.25) \times 10^9$ M^{-1} s^{-1}). The

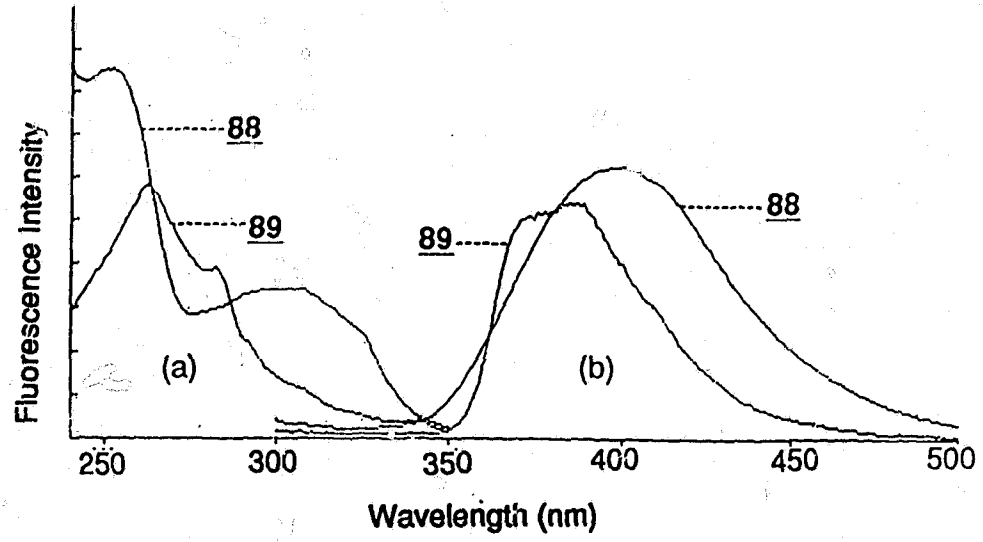

Figure 3.11 Fluorescence excitation (a) and emission (b) spectra of **88** (λ^{ex} = 270 nm, λ_{em} = 360 nm) and **89** (λ_{ex} = 270 nm, λ_{em} = 380 nm).

insignificant or lack of fluorescence quenching observed for **88** and **89** support the product studies which indicated that these binaphthyl systems do not function as excited state carbon acids to the same extent as **5** or **6**.

The fluorescence quantum yields (Φ_f) of **88** and **89** were measured in ACN using **5** as the secondary standard. Both values are similar to the fluorescence quantum yield observed for **6** (Table 3.6).

Fluorescence lifetimes of **88** and **89** measured in ACN differ from each other and from the value observed for **6** (Table 3.6). These differences are expected since binaphthyl systems joined via the 1-position, as in **88**, are short lived (≈2 ns) compared to binaphthyls joined via the 2-position as in **89** (30 ns)[111]. The short lifetime of **88** may be one reason why this system is less reactive as an

Table 3.6 Fluorescence quantum yields (Φ_f) and lifetimes of **6** compared to values obtained for **88** and **89**[a].

Compound	Φ_f[c]	τ (ns)[f]
6[b]	0.12 ± 0.02	4.5 ± 0.1
88	0.13 ± 0.02[d]	2.37 ± 0.06[g]
89	0.14 ± 0.02[e]	15.0 ± 0.3[h]

[a]At ambient temperatures in dry ACN distilled over CaH. [b]Added for comparison. [c]Determined using areas in fluorescence emissions of **88** and **89**. In all cases O.D. were < 0.1. Errors are based on standard deviations in 3 or more independent analysis. [d]Measured against **5** with matching over λ = 277-284 nm. [e]Measured against **5** with matching over λ = 297-301 nm. [f]Errors are standard deviations of 3 or more independent runs. [g]λ_{ex} = 270 nm, λ_{em} = 400 nm. [h]λ_{ex} = 270 nm, λ_{em} = 380 nm.

excited state carbon acid compared to **6**. However, the bent configuration of **88** is believed to be the main factor controlling the reactivity of this system.

The long fluorescence lifetime and magnitude of Φ_f observed for **89** would be expected to make this system susceptible to quenching by bases. The lack of such quenching suggests that deprotonation of **89** is not a favoured process. Such a conclusion is plausible based on the decrease in double bond character in the seven membered ring of **89** compared to **6**. As indicated this decrease may hinder the formation of a 4n ICA in **89** making quenching by bases inefficient. The long singlet lifetime of **89** may in turn provide a greater chance for

rearrangement of **89** which would contribute to a higher quantum yield of rearrangement for this system compared to **6**. Further studies of **89** are required to determine the reason for the efficient rearrangement of this system and for the lack of excited state carbon acidity. For example triplet sensitization would indicate the importance of ISC for **89** and the state in which the rearrangement occurs.

3.6 Summary

Examination of the photochemistry of various derivatives of **6** has revealed additional information on the rearrangement processes and excited state acidity of this system. Photolysis of the 7-deuterio derivative **87** indicated the existence of a base catalyzed [1,3] proton shift, which competes with the proton exchange and rearrangement of **6**. In addition extensive photolysis of **87** demonstrated that dibenzonorcaradiene (**85**) when irradiated can revert back to starting material via a "reverse di-π-methane" rearrangement. Irradiation of the 6-methyl derivative **155** in ACN with 254 nm lamps also suggests the existence of a reverse di-π-methane rearrangement for the cyclopropyl product **179**.

The photochemistry observed for **155** in the presence of bases demonstrated that substitution of **6** (at the 6-position) reduces the ability of this system to function as an excited state carbon acid. However, in this system, unlike in **93** and **94**, substitution is believed to hinder the proton exchange process by promoting IC. This was suggested by comparison of the fluorescence quantum

yields and lifetimes obtained for **155** with those of the parent system **6**.

The presence of a base catalyzed [1,3] proton shift in systems related to **6** was confirmed by irradiation of the binaphthyl derivative **88** in the presence of EA and D_2O. More importantly the photolysis of **88** in the presence of EA and D_2O revealed that only exchange of the axial proton occurs. This result demonstrates the significance of stereoelectronic effects in the excited state proton exchange process. Such effects were originally proposed to account for the decreased reactivity of the 5-methyl (**93**) and 5-phenyl (**94**) derivatives of **5**.

Comparison of the photochemistry observed for the two binaphthyl derivatives (**88** and **89**) with the photochemistry of **6** did not reveal the results expected. The rigid nature of **88** and the efficient rearrangement of **89** decreased the excited state carbon acidity of these systems. Other binaphthyl derivatives which are not highly twisted and do not undergo photorearrangments (i.e., **185-187**) may provide examples of efficient excited state carbon acids.

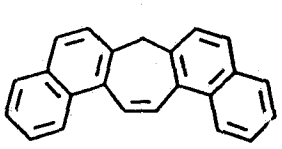

185

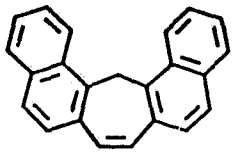

186

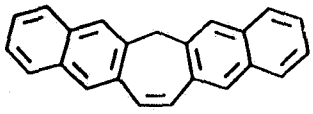

187

The results of this Chapter indicate that the photochemistry of **6** is even more complicated than originally proposed[113]. However, excited state proton exchange is still an important aspect of this systems photochemistry when a base is present. As with **5** an acid-base mechanism involving a carbanion intermediate

with a 4n ICA of π electrons is believed to be responsible for the proton exchange observed in **6**. Also, as indicated in previous studies the pK_a of **6** is decreased by ≈30 units after excitation to S_1[113] which is similar to the change in pK_a observed for **5**. To date, **5** and **6** and their derivatives are the only known neutral hydrocarbons which exhibit such a large change in carbon acidity after excitation to S_1.

CHAPTER 4

EXPERIMENTAL

4.1 Instrumentation

^{1}H NMR analysis were performed using either a Perkin-Elmer R32 (90 MHz) or Bruker WM250 (250 MHz) or AM360 (360 MHz) spectrometers in $CDCl_3$. Tetramethylsilane (TMS) was used as an internal standard in studies requiring the 90 MHz instrument. The trace of $CHCl_3$ present in $CDCl_3$ provided the standard required for the ^{1}H NMR obtained on the 250 and 360 MHz instruments. ^{2}H NMR spectra were obtained on the Bruker AM360 (360 MHz) spectrometer using CH_2Cl_2 as the solvent. The natural abundance of deuterium in CH_2Cl_2 provided the required deuterated standard for the ^{2}H NMR. ^{13}C NMR were acquired on either the Bruker WM250 (250 MHz) or Bruker AM360 (360 MHz) spectrometer using $CDCl_3$ as the solvent and standard.

MS analyses were performed using a Perkin-Elmer Hitachi RMU-7 mass spectrometer and GC/MS were obtained using a Finnigan 3300 gas chromatography mass spectrometer using methane as a carrier gas and for chemical ionization (CI). High resolution MS (HRMS) were obtained on a Kratos Concept 1H instrument using electron impact (EI). GC analysis were performed on a Varian 3700 gas chromatograph using a SE-54 capillary column and a Hewlett-Packard 3390A integrator for recording of the data. Melting points were measured using a Koefler hot stage microscope. A Corning pH meter 140 was utilized to measure the pH of buffered solutions. Preparative thin layer

chromatography (TLC) were performed on 20 x 20 cm silica gel GF Uniplate (1000 μm) from Analtech.

Infrared (IR) spectra were determined using a Perkin-Elmer 283 spectrophotometer with NaCl solution cells. UV spectra were obtained on either a Pye Unicam SP8-400 or Perkin-Elmer Lambda 4B or Cary 5 UV-Vis-NR spectrophotometer. Steady state fluorescence studies were performed on a Perkin-Elmer MPF-66 fluorescence spectrometer. Fluorescence lifetimes were measured on a PTI LS-1 using a single photon counting technique. Preparative photolysis were performed in a Rayonet RPR 100 photochemical reactor using either 254, 300 or 350 nm lamps. Reaction mixtures for these photolysis were contained in a 100, 200 or 400 mL quartz tube. Reaction mixtures prepared for triplet sensitization were contained in 100 mL pyrex tubes. GC scale photolysis were performed in 3 mL Suprasil quartz cuvettes. Quantum yields were acquired on a optical bench using an Oriel 200W Hg arc lamp and an Applied physics monochromator set at either 254 or 280 nm with 5 nm slits.

X-Ray diffraction studies involving **88** were performed using a Nonius diffractometer with $\omega/2\Theta$ scan for collection of data (1613 reflections). Of these reflections 1372 were used to refine the structure. NRC Solver[164] was the program used to solve the crystal structure with a SHELX least square program[165] used to refine the structure. Other experimental aspects of the x-ray diffraction study of **88** are listed in Table 4.1.

Table 4.1 Crystallographic data for **88**.

Formula	$C_{16}H_{23}$
Molecular Weight	292.38 g/moi)
Crystal System	monoclinic
Space Group	P 2 1/n (no. 14)
Cell Dimensions	
a(Å)	8.5545(6)
b(Å)	18.8395(17)
c(Å)	9.7556(6)
α(deg)	90
β(deg)	94.960(7)
(deg)	90
V(Å^3)	1566.347
Z	4
T(°C)	20
λ(Å)	Cu (1.540562)
ρ_{obsd} (g mL^{-1})	1.225
ρ_{calc} (g mL^{-1})	1.240
μ(cm^{-1})	4.97
$R(F_o)$	0.0508
$R_w(F_o)$	0.0499

4.2 Solvents and Reagents

Solvents required during the completion of this research were used without

purification except CH_2Cl_2 which was distilled. Anhydrous solvents required such as ACN (dried over CaH), EtOH (dried over Mg turnings), diethyl ether (dried over Na metal), tetrahydrofuran (THF) (dried over K or Na metal) and benzene (dried over Na metal) were refluxed over the indicated drying agent for greater than two days before distillation. When anhydrous ACN was not required spectrophotometric grade ACN (Fischer Chemicals) was used directly. GC analysis were performed using spectrophotometric grade acetone (Aldrich). Deuterated solvents D_2O (MSD 99.9% purity), CH_3OD (Aldrich 99.5% purity), CD_3CN (Cambridge Isotope Laboratories (CIL)) and $CDCl_3$ (CIL) were used without purification. The amines utilized (triethylamine (BDH), piperidine (BDH), ethanolamine (EA) (Aldrich), n-propylamine (PA) (Aldrich), 2-methoxyethylamine (Aldrich), 2-aminoethylnitrile (Lancaster) and 2,2,2-trifluoroethylamine (Aldrich)) were used as purchased.

Buffer solutions (Fisher Chemicals) with pHs of 1, 2, 7, 10, 12, 13 and 14 were used for the fluorescence quenching studies. More acidic solutions with H_0 of 0.04, -0.45, -1.18 and -2.25 were prepared by dilution of H_2SO_4 solutions (Fisher Chemicals). Solutions requiring an even lower H_0 value (50% or 60% by volume H_2SO_4) were prepared using concentrated H_2SO_4 (Fisher Chemicals).

Reagents required in the following experimental procedures were used as purchased from Aldrich except thionyl chloride ($SOCl_2$) which was distilled prior to it's use.

4.3 Syntheses

4.3.1 Suberene (5) and Related Systems

Suberene (5) and 5,5-Dideuteriosuberene (91): Preparation of **5** and **91** both involved reduction of *5H*-dibenzo[a,d]cycloheptenone (**92**) using the following general procedure. To a two-neck r.b. flask (500 mL) fitted with a condenser, purged with N_2 and cooled in a dry ice/acetone bath was added anhydrous THF (200 mL) with 2.0 g $LiAlH_4$ ($LiAlD_4$) (0.048 mole) and 9.7 g $AlCl_3$ (0.073 mole). Ketone **92** 5.0 g (0.024 mole) dissolved in anhydrous THF (100 mL) was added dropwise via an addition funnel to the solution which was stirred with a magnetic stirrer. The resulting solution was allowed to warm up to r.t. and refluxed for 2 h. Work up with 5% HCl (100 mL) (2x) followed by washing of the organic layer with water allowed for isolation of the required product. Drying of the organic layer over $MgSO_4$ followed by evaporation of the THF provided crude **5** (**91**) (>95% yield) which was recrystallized in 95% ethanol to give colourless crystals (mp = 134°C, lit. mp = 133-4°C)[166]. Both **5** and **91** were achieved with >99% purity by GC; (**5**) ^1H NMR (360 MHz) δ (ppm): 3.75 (s, 2H, CH_2), 7.08 (s, 2H, vinyl), 7.2-7.4 (m, 8H, arom.); MS (CI) m/z: 193 (M^++1), 221 (M^++29), 233 (M^++41); (**91**) ^1H NMR (360 MHz) δ (ppm): 7.08 (s, 2H, vinyl), 7.2-7.4 (m, 8H, arom.); ^2H NMR (360 MHz) δ (ppm): 3.76 (s, 2D); MS (CI) m/z: 195 (M^++1), 223 (M^++29), 235 (M^++41). The same UV spectrum (ACN) was achieved for each; λ_{max} (nm) (in ACN): 210 (29000), 218 (sh, 25000), 285 (13700).

10,11-dihydro-5*H*-dibenzo[a,d]cycloheptene (74), Diphenylmethane (102) and Dideuterated Derivatives 105 and 106: Reduction of the appropriate ketones (83 and 103) using $LiAlH_4/AlCl_3$ and the above procedure provided both 74 (colourless crystals) and 102 (clear liquid) (both > 90% yield). Use of $LiAlD_4/AlCl_3$ provided 105 (colourless crystals) and 106 (clear liquid) (both > 90% yield). The ^1H NMR of each were consistent with literature[167] spectra with the dibenzylic protons being absent in the spectra of 105 and 106. MS (CI) indicated the required mass; m/z (74): 195 (M^++1), 223 (M^++29), (102): 169 (M^++1), 197 (M^++29), (105): 197 (M^++1), 225 (M^++29) and (106): 171 (M^++1), 199 (M^++29).

9,9-Dideuteriofluorene (104): Deuteration of fluorene (9) was performed by dissolving 9 (5.0 g) in dioxane (200 mL) in a two-neck r.b. flask purged with Ar and fitted with a condenser. To this solution was added D_2O (100 mL) and NaOD (≈12 drops). The resulting mixture was then stirred and refluxed gently for 2 h. Cooling of the reaction mixture resulted in precipitation of the product (104) which was collected by filtration. Recrystallization of 104 in 95% EtOH provided colourless crystals (quantitative) with a purity > 98% according to GC and ^1H NMR analysis. The ^1H NMR (360 MHz) was identical to that of fluorene (9) except for the absence of a resonance at 3.85 ppm which is where the dibenzylic protons of 9 resonate. The MS (CI) indicated >97% deuteration of fluorene (9); m/z: 169 (M^++1), 197 (M^++29), 209 (M^++41).

5*H*-Dibenzo[a,d]cyclohepten-5-ol (78) and Deuterated Derivative 80: To a suspension of $LiAlH_4$ ($LiAlD_4$) (2.0 g) in anhydrous ether (400 mL) contained in a 500 mL two-neck r.b. flask purged with Ar and fitted with a condenser (cooled in a dry ice/acetone bath) was added ketone **92** (35 g) as a solid. The resulting solution was warmed up to r.t. and refluxed for 1 h then poured into a 5% HCl ice solution (200 mL). Washing of the organic layer with water (200 mL) followed by drying over $MgSO_4$ and evaporation of the solvent provided crude **78** (80). Recrystallization in hexanes provided colourless needles with >98% purity according to GC (>90% yield) (mp = 222°C, lit mp 122°C?)[166]; (**78**) ^{1}H NMR (90 MHz) δ (ppm): 2.38 (s, 1H, OH), 5.38 (s, 1H, CH), 7.09 (s, 2H, vinyl), 7.2-7.7 (m, 8H, arom.); MS (CI) m/z: 191 (M^++1 after loss of H_2O), 209 (M^++1), 219 (M^++29 after loss of H_2O), 237 (M^++29); (**80**) ^{1}H NMR (90 MHz) δ (ppm): 2.38 (s, 1H, OH), 7.09 (s, 2H, vinyl), 7.2-7.7 (m, 8H, arom.); MS (CI) m/z: 192 (M^++1 after loss of H_2O), 210 (M^++1), 220 (M^++29 after loss of H_2O), 238 (M^++29).

5-Deuterio-5*H*-dibenzo[a,d]cycloheptene (90): Alcohol **80** (3.0 g) dissolved in anhydrous ether (50 mL) was added dropwise via an addition funnel to a suspension of $LiAlH_4$ (0.9 g) and $AlCl_3$ (5.0 g) in anhydrous ether (100 mL) under Ar in a two-neck r.b. flask (250 mL) fitted with a condenser and cooled in a dry ice/acetone bath. The resulting mixture was allowed to warm up to r.t., refluxed (2 h) and poured into a 5% HCl/ice solution. Isolation of the organic layer followed by washing with water, drying over $MgSO_4$ and evaporation of the

solvent provided the required product **90** (>90% yield). A purity of >98% according to GC was achieved by recrystallization in 95% EtOH which provided colourless crystals. The ^{1}H NMR (360 MHz) was identical to that of **5** except the intensity of the signal at 3.75 ppm was decreased by half. The ^{2}H NMR (360 MHz) exhibited one signal at 3.72 ppm (d, J = 1.7 Hz, 1D). MS (CI) analysis indicated the formation of mono-deuterated suberene **90** with a purity of >97%; m/z: 194 (M^++1), 222 (M^++29), 234 (M^++41).

5-Methylsuberene (93) and 5-Phenylsuberene (94) and Deuterated Derivatives 95 and 96: Synthesis of **93** and **94** (and the deuterated derivatives **95** and **96**) required two steps from alcohol **78** (or **80** for deuterated derivatives). In the first step alcohol **78** (or **80**) (5.0 g) was added as a solid over a 15 min. period to $SOCl_2$ (15 mL) stirred in a two-neck r.b. flask fitted with a condenser. Stirring and heating of the resulting mixture for 10 min. produced **97** (or the deuterated derivative **98**). The $SOCl_2$ was removed by distillation and the resulting residue was taken up in ether and washed with water. Drying of the organic layer over $MgSO_4$ followed by evaporation of the solvent produced crude **97** (or **98**); ^{1}H NMR (90 MHz) δ (ppm): 6.20 (s, 1H, CH) (absent in **98**), 7.14 (s, 2H, vinyl), 7.2-7.6 (m, 8H, arom.). This crude material was used directly in the next step.

Formation of **93** and the deuterated derivative **95** was achieved by addition of the appropriate chlorine derivative (**97** or **98**) (3.0 g) to MeMgBr in anhydrous ether. The grignard reagent was prepared by reaction of Mg turnings (0.4 g) with

MeBr (7.9 mL of a 2 M solution) in anhydrous ether (100 mL) contained in a two-neck r.b. flask (250 mL) fitted with a condenser and purged with Ar. Dropwise addition of the MeBr was performed using a syringe at a rate sufficient to maintain a gentle reflux without heating. After complete addition of the MeBr the reaction mixture was gently refluxed for another 30 minutes. The appropriate chorine derivative (97 or 98) (3.0 g) dissolved in anhydrous ether (50 mL) was then added via an addition funnel over a period of 30 minutes. The resulting solution was gently refluxed for a further 30 minutes and then poured into a 5% HCl/ice solution. Separation of the organic layer followed by washing with water, drying over $MgSO_4$ and evaporation of the solvent produced crude 93 (or 95) as an oil which solidified after several days on the bench. Recrystallization in 95% EtOH provided the required product 93 (or 95) as colourless crystals (mp = 58-59°C) with a purity >97% by GC (both >80% overall yield); (93) ^{1}H NMR (250 MHz) δ (ppm) more abundant conformation: 1.42 (dd, J = 7.2, 0.8 Hz, 3H, CH_3), 4.24 (q, J = 7.2 Hz, 1H, CH), 7.00 (s, 2H, vinyl); less abundant conformation: 1.96 (d, J = 7.3 Hz, 3H, CH_3), 3.57 (q, J = 7.3 Hz, 1H, CH), 7.21 (s, 2H, vinyl) for both 7.1-7.6 (m, 8H, arom.); ^{13}C NMR (250 MHz) δ (ppm): 15.4, 17.3 (CH_3), 38.0, 49.3 (CH), 123.1, 125.3, 126.2, 127.6, 128.3, 128.8, 129.9, 130.8, 131.4 (CH, arom. or vinyl), 133.9, 135.3, 141.7, 142.6 (C, arom.); MS (CI) m/z: 207 (M^++1), 235 (M^++29), 247 (M^++41); (95) ^{1}H NMR (360 MHz) δ (ppm) more abundant conformation: 1.31 (s, 3H, CH_3), 6.91 (s, 2H, vinyl); less abundant conformation: 1.86 (s, 3H, CH_3), 7.12 (s, 2H, vinyl) for both 7.1-7.4 (m, 8H, arom.); MS (CI) m/z: 208 (M^++1), 236

(M^++29), 248 (M^++41); UV (ACN) λ_{max} (nm): 211 (25600), 220 (sh, 20700), 288 (12200).

Preparation of **94** (and the deuterated derivative **96**) was performed by addition of PhLi (6.5 mL of a 1.9 M solution) with a syringe to a solution of **97** (or **98**) (2.0 g) dissolved in anhydrous ether (200 mL) contained in a two-neck r.b. flask (500 mL) fitted with a condenser, cooled in a dry ice/acetone bath and purged with Ar. Warming and refluxing of the stirred reaction mixture for 2 h provided the required product **94** (or **96**). Isolation of the product was performed as in previous work ups and recrystallization in 95% EtOH provided colourless crystals with a purity >98% by GC (both > 80% yield) (mp = 143-144°C); (**94**) ^{1}H NMR (90 MHz) δ (ppm): 5.38 (s, 1H, CH), 6.6-7.5 (m, 15H, arom. and vinyl); MS (CI) m/z: 269 (M^++1), 297 (M^++29), 309 (M^++41); (**96**) ^{1}H NMR (250 MHz) δ (ppm): 6.6-6.7 (m, 2H, arom.), 6.75 (s, 2H, vinyl), 7.0-7.1 (m, 3H, arom.), 7.3-7.5 (m, 8H, arom.); MS (CI) m/z: 270 (M^++1), 298 (M^++29), 310 (M^++41); ^{13}C NMR δ (ppm): 57.1 (t, 19 Hz, CD), 125.8, 126.7, 127.1, 127.2, 128.5, 129.8, 130.3, 130.8 (CH, arom. or vinyl), 134.7, 140.3, 141.8 (C arom.); UV (ACN) λ_{max} (nm): 205 (sh, 38900), 292 (12100).

10,11-dihydro-5*H*-dibenzo[a,d]cyclohepten-5-ol (99), 5-Methyl-10,11-dihydro-5*H*-dibenzo[a,d]cyclohepten-5-ol (100) and 5-Phenyl-10,11-dihydro-5*H*-dibenzo[a,d]-cyclohepten-5-ol (101): Alcohol **99** was prepared from 10,11-dihydro-5*H*-dibenzo[a,d]cycloheptenone (**83**) by following the procedure outlined for the

synthesis of **78**. Recrystallization in hexanes yielded colourless needles with a purity >97% according to both GC (>90% yield); ^{1}H NMR (90 MHz) δ (ppm): 2.24 (broad s, 1H, OH), 2.9-3.6 (m, 4H, CH_2CH_2), 5.93 (s, 1H, CH), 7.1-7.5 (m, 8H, arom.); MS (CI) m/z: 193 (M^++1 after loss of H_2O), 211 (M^++1), 221 (M^++29 after loss of H_2O), 239 (M^++29).

Both **100** and **101** were synthesized via the same route by reduction of **83** with the appropriate lithium reagent. For example **101** was prepared by addition of PhLi (15.2 mL of a 1.9 M stock solution) dropwise with a syringe to **83** (5.0 g) dissolved in anhydrous THF (300 mL) contained in a two-neck r.b. flask (500 mL) fitted with a condenser, cooled in a dry ice/acetone bath and purged with Ar. The resulting reaction mixture was allowed to warm up to r.t. and then refluxed overnight. Isolation of the crude product was achieved using the same procedure outlined in previous synthesis. Recrystallization in hexane provided brown crystals which were recrystallized a second time in 10% benzene/hexanes to obtain colourless crystals of **101** (>90% yield). A purity of >97% was achieved according to GC; ^{1}H NMR (90 MHz) δ (ppm): 2.23 (s, 1H, OH), 2.42-3.03 (m, 4H, CH_2CH_2), 6.9-7.4 (m, 11H, arom.), 8.0-8.2 (m, 2H, arom.); MS (CI) m/z: 269 (M^++1 after loss of H_2O), 287 (M^++1), 297 (M^++29 after loss of H_2O), 315 (M^++29).

Synthesis of **100** following this procedure provided colourless crystals with a purity >97% according to GC (>90% yield); ^{1}H NMR (90 MHz) δ (ppm): 1.84 (s, 3H, CH_3), 2.2 (broad s, 1H, OH), 3.4-3.8 (m, 4H, CH_2CH_2), 7.0-7.3 (m, 6H, arom.), 7.8-8.0 (m, 2H, arom.); MS (CI) m/z: 207 (M^++1 after loss of H_2O), 225 (M^++1), 235

(M^++29 after loss of H_2O), 253 (M^++29).

4.3.2 7-Deuterio-*5H*-dibenzo[a,c]cycloheptene (87)

***7,7-Dichlorodibenzo[a,c]bicyclo[4,1,0]heptane* (149):** Phenanthrene (148) (Aldrich) (35.6 g) was dissolved in $CHCl_3$ (300 mL) and placed in a two-neck r.b. flask (1000 mL) fitted with a guard tube and equipped with a magnetic stirrer. To this solution was added cetyltrimethylammonium bromide (CTABr) (1.2 g) and 50% w/w of NaOH/H_2O (100 mL). The resulting mixture was stirred for three days at r.t. then poured into a mixture of water (1000 mL) and $CHCl_3$ (250 mL). The organic layer was separated out and washed with water then passed through basic alumina (200 g) using a flash column. Washing of the alumina was performed with an additional 200 mL of $CHCl_3$. Both the initial solution passed through the alumina and the washings were combined and the solvent evaporated off to obtain crude **149**. This material was first recrystallized in 95% EtOH then in hexanes to achieve ≈25 g (48% yield) of **149** with a purity >95% by ^{1}H NMR (90 MHz). The ^{1}H NMR was consistent with the literature spectrum[148]. The MS also confirmed the required product by the presence of peaks with relative intensities corresponding to the isotopes of the two chlorine present.

***6-Chloro-5H-dibenzo[a,c]cyclohepten-5-ol* (150):** The dichloro derivative (149) (2.5 g) was placed in a two-neck r.b. flask (250 mL) under N_2 and thermolyzed

by heating the material to 170°C for 30 min. using an oil bath. The resulting residue was cooled to r.t. and taken up in ACN (50 mL). To this solution was added a saturated aqueous solution of sodium bicarbonate (70 mL). This mixture was then stirred at r.t. for 1 h then diluted with 50 mL of H_2O prior to extracting the product (150) with CH_2Cl_2 (2 x 100 mL). The combined organic layers were dried over $MgSO_4$ and the solvent evaporated off to obtain crude 150 (quantitative) with a purity of ≈96% by GC. The ^1H NMR obtained was consistent with the literature spectrum[149]. The material was used without purification in the following step.

6,7-Dihydro-5*H*-dibenzo[a,c]cycloheptene (151): The choro alcohol 150 (2.4 g) was dissolved in anhydrous THF (300 mL) with sodium metal (6 g) and t-butanol (6.5 g) under N_2. The reaction, contained in a two-neck r.b. flask (500 mL) fitted with a condenser was refluxed for 24 h. The resulting solution was cooled and the solvent decanted off to allow for removal of excess sodium metal. Evaporation of the solvent produced an oil which was taken up in ether (200 mL) and washed first with a 5% HCl solution (100 mL) then with a 10% sodium bicarbonate brine solution (100 mL). The ether layer was then dried over $MgSO_4$ and the solvent evaporated off to achieve crude 151 as an oil. Purification was performed using a silica column (40 cm by 4 cm) with 20% CH_2Cl_2/hexanes as the eluting solvent. A clear oil (1.5 g, ≈80% from 149) with a purity of 99% by GC; ^1H NMR (90 MHz) δ (ppm): 1.9-2.6 (m, 6H, $(CH_2)_3$), 7.1-7.4 (m, 8H, arom.); MS

(CI) m/z: 195 (M^++1), 223 (M^++29), 235 (M^++41).

5-Bromo-6,7-dihydro-*5H*-dibenzo[a,c]cycloheptene (152): Approximately 0.5 g of **151** was dissolved in CCl_4 (100 mL) in a two-neck r.b. flask (250 mL) equipped with a magnetic stirrer. To this solution was added N-bromosuccinimide (NBS) (0.55 g, 1.2 eq.) and benzoyl peroxide (50 mg). The reaction mixture was then refluxed overnight cooled down and the succinimide formed filtered off. Evaporation of the solvent provided a crude product mixture containing the required monobrominated product **152** (≈53% yield by GC/MS). Starting material was also present but attempts at pushing the reaction further resulted in dibrominated products. The ^{1}H NMR (90 MHz) of the product mixture suggested that **152** was achieved due to the growth of a multiplet at 5.0 ppm, which is believed to correspond to the benzylic proton attached to the carbon substituted with a bromine. This crude product mixture was carried on to the next step without purification.

6,7-Dihydro-*5H*-dibenzo[a,c]cyclohepten-5-ol (153): The monobrominated species **152** was dissolved in 1:1 H_2O/ACN (40 mL) in a two-neck r.b. flask (100 mL) fitted with a condenser and equipped with a magnetic stirrer. The reaction mixture was gently refluxed and stirred for 1 h and then saturated with NaCl. Extraction of the organic portion of the mixture was performed using CH_2Cl_2. Drying of the organic extract with $MgSO_4$ and evaporation of the solvent

provided the crude alcohol 153. The ^{1}H NMR (90 MHz) differed from the starting material by a multiplet due to the methine proton at 4.6 ppm instead of at 5.0 ppm.

6,7-Dihydro-5*H*-dibenzo[a,c]cyclohepten-5-one (147): The crude alcohol (153) (1.0 g) was then dissolved in ether (40 mL) in a two-neck r.b. flask (100 mL) fitted with a guard tube and equipped with a magnetic stirrer. A solution of chromic acid[168] (20 mL) was then added dropwise to the reaction mixture over a 10 min. period. After stirring the solution overnight the organic layer was separated and the aqueous layer washed with ether (2 x 50 mL). All the organic layers were combined and washed with a sodium bicarbonate solution then with an NaCl solution. Drying of the organic layer with $MgSO_4$ and evaporation of the solvent produced the crude ketone 147. Partial purification of 147 was performed by eluting the sample through a flash column (silica 50 g) first with hexanes (600 mL) to wash out non-polar components of the product mixture (i.e., hydrocarbon 151) then with 50% CH_2Cl_2/hexanes to wash off the ketone 147 (85% from 152). A purity >90% was achieved according to both GC and ^{1}H NMR (90 MHz). The ^{1}H NMR ($CDCl_3$) was consistent with the literature spectrum[149]; ^{1}H NMR (90 MHz) δ (ppm): 2.90 (s, 4H, CH_2CH_2), 7.19-7.72 (m, 8H, arom.).

5-Deuterio-6,7-dihydro-5*H*-dibenzo[a,c]cyclohepten-5-ol (154): The ketone 147 was then reduced using the procedure outlined (*vide supra*) for reduction of a

ketone to an alcohol using $LiAlD_4$. The crude product formed (154) (90% yield) provided a ^1H NMR (90 MHz) which resembled the spectrum obtained for the alcohol **153**. However, the signal due to the methine proton at 4.6 ppm was absent along with the coupling associated with this proton.

7-Deuterio-5*H*-dibenzo[a,c]cycloheptene (87): The deuterated alcohol 154 (200 mg) was dissolved in toluene (50 mL) contained in a r.b. flask fitted (250 mL) with a Dean Stark trap, a condenser and equipped with a magnetic stirrer. After addition of 85% H_3PO_4 (20 mL) the reaction mixture was refluxed for 3 h while collecting water in the Dean Stark trap. The reaction mixture was then poured onto ice and the organic layer separated off. The remaining aqueous solution was washed with hexanes (2 x 50 mL). All the organic extracts were then combined, washed with a sodium bicarbonate solution and dried over $MgSO_4$. Evaporation of the solvent provided crude **87** as an oil. Distillation using a kugelrohr produced a clear oil (110 mg, 60% yield) with a purity >97% by GC (96% deuterium at the 7-position by ^2H NMR); ^1H NMR (360 MHz) δ (ppm) at ambient temperature: 3.08 (broad s, 2H, CH_2), 6.27 (t, J = 6.9 Hz, 1H, vinyl), 7.22-7.32 (m, 1H, arom.), 7.35-7.44 (m, 5H, arom.), 7.53-7.62 (m, 1H, arom.), 7.71-7.77 (m, 1H, arom.); at -40°C δ (ppm): 2.93 (dd, J = 5.4 and 13.1 Hz, 1H), 3.29 (dd, J = 8.3 and 13.2 Hz, 1H), 6.32 (dd, J = 5.5 and 8.2 Hz, 1H, vinyl), aromatic region unchanged; ^2H NMR (360 MHz) δ (ppm): 3.05 (s, 4%, D at the 5-position), 6.66 ppm (s, 92%, D at the 7-position); MS (CL) m/z: 194 (M^++1), 222 (M^++29), 243 (M^++41).

4.3.3 6-Methyl-5*H*-dibenzo[a,c]cycloheptene (155) and 6-Phenyl-5*H*-dibenzo-[a,c]cycloheptene (156)

The 6-methyl (155) and 6-phenyl (156) derivatives of 6 were synthesized in two steps from ketone 146 which was prepared from diphenic anhydride (145)[147]. Reduction of 146 was accomplished with MeLi or PhLi using the same method outlined by Tolbert and Ali[147]. The ^{1}H NMR (90 MHz) of the crude methyl alcohol 157 was consistent with the structure shown; δ (ppm): 1.31 (s, 3H, CH_3), 2.32 (broad s, 1H, OH), 2.45 (s, 4H, $2CH_2$), 7.1-7.5 (m, 8H, arom.). The ^{1}H NMR (90 MHz) of the crude phenyl alcohol (158) was difficult to interpret due to the presence of starting material, however, the spectrum exhibited a multiplet (2.4-3.2 ppm) due to the protons α to the alcohol.

Formation of 155 and 156 from the alcohols 157 and 158 respectively was achieved using the procedure of Tolbert and Ali[147]. Purification of 155 was achieved using a flash column (50 g silica) and hexanes. A clear oil was obtained with a purity of >97% by GC (60% overall yield); ^{1}H NMR (360 MHz) δ (ppm): 2.10 (d, J = 1.6 Hz, 3H, CH_3), 3.02 (s, 2H, CH_2), 6.36 (q, J = 1.6 Hz, 1H, vinyl), 7.23-7.41 (m, 6H, arom.), 7.54-7.59 (m, 1H, arom.), 7.69-7.73 (m, 1H, arom.); MS (CI) m/z: 207 (M^++1), 235 (M^++29), 247 (M^++41); UV (ACN) λ_{max} (nm): 238 (36700), 254 (11600), 292 (1330).

Purification of 156 was achieved using column chromatography (silica, 40 x 4 cm). Elution with hexanes (200 mL) followed by a 10% $CHCl_3$/hexanes solution allowed for isolation of the product (purity >98% by GC) (60% overall

yield) (mp = 82-83°C, lit. mp = 92-94°C)[147]; ^{1}H NMR (250 MHz) δ (ppm): 3.28 (broad s, 1H, CH), 3.76 (broad s, 1H, CH), 6.88 (s, 1H, vinyl), 7.25-7.78 (m, 13H, arom.); MS (CI) m/z: 269 (M^++1), 297 (M^++29), 309 (M^++41); UV (ACN) λ_{max} (nm): 228 (21400), 250 (28500), 293 (16300).

4.3.4 3*H*-Cyclohepta[2,1-a:3,4-a']dinaphthalene (88)

1-Bromo-2-methylnaphthalene (160): Bromination of 2-methylnaphthalene (159) (Aldrich) (50 g) at the 1-position was carried out using the procedure of Adams and Binder[152]. Distillation of the crude product mixture provided **160** as a clear oil (90% yield); ^{1}H NMR (90 MHz) δ (ppm): 2.56 (s, 3H, CH_3), 7.2-7.8 (m, 5H, arom.), 8.2-8.3 (m, 1H, arom.); MS (CI) m/z: 221 (M^++1, ^{79}Br), 223 (M^++1, ^{81}Br), 249 (M^++29, ^{79}Br), 251 (M^++29, ^{81}Br), 261 (M^++41, ^{79}Br), 263 (M^++41, ^{81}Br). These results are consistent with the literature for **160**[169]

2,2'-Dimethyl-1,1'-binaphthyl (161): Coupling of **160** to form **161** was achieved via the method of Maigrot and Mazaleyrat[153]. The two major impurities **159** and **160** were distilled off using a Kugelrohr to provide partially purified **161**. Further purification was achieved by elution of this material through a flash column (silica, 50 g) with hexanes to achieve **161** with a purity of >95% by GC (40% yield); ^{1}H NMR (90 MHz) δ (ppm): 2.01 (s, 6H, $2CH_3$), 6.9-7.6 (m, 8H, arom.), 7.8-8.0 (m, 4H, arom.); MS (CI) m/z: 283 (M^++1), 311 (M^++29), 323 (M^++41). The ^{1}H

NMR (90 MHz) is consistent with the literature spectrum[169].

2,2′-Bis[bromomethyl]-1,1′-binaphthyl (162): Bromination of the methyl of **161** was performed using NBS and the procedure outlined for the synthesis of **158** (*vide supra*). Recrystallization of the crude product in 1:3 benzene/hexanes provided yellowish crystals with a purity of >95% (85% yield); ^{1}H NMR (90 MHz) δ (ppm): 4.20 (s, 4H, $2CH_2$), 7.0-8.1 (m, 12H, arom.). This ^{1}H NMR is consistent with the literature spectrum[169].

4-Cyano-5-imine-3*H*-cyclohepta[2,1-a:3,4-a′]dinaphthalene (163): In a three-neck r.b. flask (500 mL) fitted with a condenser and equipped with a magnetic stirrer and heating mantle was added a solution of KCN (40 g) in 30% H_2O/EtOH (160 mL). This solution was heated and **162** (20 g) dissolved in acetone (200 mL) added in dropwise via an addition funnel over 2 h. The third neck of the r.b. flask was left open to allow for evaporation of acetone which was used only to allow addition of **162** to the reaction vessel. After complete addition of **162** the flask was stoppered and left overnight to reflux. The reaction mixture was then poured into 2 L of water and the precipitate formed was filtered off to achieve **163** (60% yield) with a purity >90% by ^{1}H NMR (90 MHz) δ (ppm): 3.11 (d, J = 12 Hz, 1H), 3.37 (d, J = 12 Hz, 1H), 5.07 (broad s, 2H, NH_2), 7.0-8.1 (m, 12H arom.); MS (CI) m/z: 333 (M^++1), 361 (M^++29), 373 (M^++41); IR (CH_2Cl_2) (cm^{-1}): 3495, 3390 (two sharp s, NH_2 str.), 2163 (sharp s, CN str.). This material was

carried on into the next step without purification.

***3H*-Cycloheptan-4-one[2,1-a:3,4-a']dinaphthalene (164)**: Preparation of ketone **164** from **163** was accomplished using the procedure of Mislow and McGinn[155]. Recrystallization of **164** in acetone provided a brown powder (80% yield) with a purity >95% by ^{1}H NMR (90 MHz) δ (ppm): 3.61 (two overlapping d, both J = 15 Hz, 4H, $2CH_2$), 7.1- 7.6 (m, 8H, arom.), 7.8-8.0 (m, 4H, arom.); MS (CI) m/z: 309 (M^++1), 337 (M^++29), 349 (M^++41); IR (CH_2Cl_2) (cm^{-1}): 1710 (s, carbonyl str.).

***3H*-Cycloheptan-4-ol[2,1-a:3,4-a']dinaphthalene (165)**: Reduction of **164** (2 g) with $LiAlH_4$ using the procedure indicated for formation of **78** (*vide supra*) produced alcohol **165** (90% yield). The product was shown to be sufficiently pure for the next step by ^{1}H NMR (90 MHz) δ (ppm): 1.55 (s, 1H, OH), 2.1-3.1 (m, 4H, $2CH_2$), 4.3-4.7 (m, 1H, CH), 7.1-7.6 (m, 8H, arom.), 7.8-8.0 (m, 4H, arom.); MS (CI) m/z: 293 (M^++1 after loss of H_2O), 311 (M^++1), 321 (M^++29 after loss of H_2O), 339 (M^++29), 333 (M^++41 after loss of H_2O), 351 (M^++41).

4-Bromo-*3H*-cyclohepta[2,1-a:3,4-a']dinaphthalene (166): The alcohol **165** (2 g) was dissolved in $CHCl_3$ (100 mL) in a two-neck r.b. flask (250 mL) fitted with a condenser and equipped with a magnetic stirrer and heating mantle. To this reaction mixture was added PBr_3 (2 g) dropwise with a pipette. The resulting mixture was refluxed overnight and then poured into 200 mL of water. The

organic layer was separated out and the aqueous portion washed with CH_2Cl_2. The combined organic extracts were dried over $MgSO_4$ and the solvent evaporated off to obtain crude **166** (90% yield); ^1H NMR (90 MHz) δ (ppm): 2.5-3.4 (m, 4H, $2CH_2$), 4.5-4.8 (m, 1H, CHBr), 6.9-8.1 (m, 12H, arom.). This material was carried on directly into the next step.

***3H*-Cycloheptan[2,1-a:3,4-a']dinaphthalene (88):** The bromo compound (**166**) was dissolved in t-BuOH (150 mL) in a two-neck r.b. flask (250 mL) fitted with a condenser and equipped with a heating mantle and magnetic stirrer. To this solution was added t-BuO$^-$K$^+$ (2 g). After an overnight reflux the reaction mixture was poured into water (100 mL) and the resulting solution washed with CH_2Cl_2 (2 x 100 mL). The organic extracts were dried over $MgSO_4$ and evaporation of the solvent provided crude **88**. Recrystallization in toluene and anhydrous EtOH provided colourless crystals with a purity >99% by GC (70% yield) (mp = 166-168°C, lit. mp = 163-164°C)[166]; ^1H NMR (360 MHz) δ (ppm): 2.96 (ddd, J = 12.8, 5.6, 2.2 Hz, axial CH), 3.33 (ddd, J = 12.9, 7.9, 0.6 Hz, equatorial H), 6.42 (ddd, J = 9.8, 7.9, 5.6 Hz, 1H, vinyl), 6.72 (dd, J = 9.7, 2.3 Hz, 1H, vinyl), 7.09-7.11 (m, 2H, arom.), 7.19-7.24 (m, 1H, arom.), 7.29-7.35 (m, 1H, arom.), 7.41-7.56 (m, 4H, arom.), 7.84-7.83 (m, 4H, arom.); ^{13}C NMR (360 MHz) δ (ppm): 33.9 (CH_2), 124.3, 125.3, 125.4, 125.5, 125.6, 126.5, 127.1, 127.8, 127.9, 128.1, 128.6, 128.8, 129.5, 134.8 (CH, arom. or vinyl), 130.3, 131.5, 132.0, 133.0, 135.4, 143.6 (C, arom.); MS (EI) m/z: 292 (M^+); UV (ACN) λ_{max} (nm): 208 (sh, 38900), 225 (77600), 251 (35300), 303 (10600).

4.3.5 *3H*-Cyclohepta[2,3-a:3,2-a']dinaphthalene (89)

2-Bromo-3-methylnaphthalene-bis(hexachlorocyclopentadiene) adduct (168): Bromination of **167** (Aldrich) was performed using the literature preparation used to brominate 2-methylnaphthalene[152,157]. The product achieved (**168**) was carried onto the next step without purification (85% yield); ^{1}H NMR (90 MHz) δ (ppm): 2.39 (s, 3H, CH_3), 3.48 (d, J = 9 Hz, 2H, 2CH), 3.89 (d, J = 9 Hz, 2H, 2CH), 7.58 (s, 1H, arom.), 7.93 (s, 1H, arom.); MS (EI) m/z: 766 (M^+).

2-Bromo-3-methylnaphthalene (169): The brominated product (**168**) was placed in a r.b. flask (100 mL) and attached to a collection bulb and a rotoevaporater. While under aspiration the sample was rotated and heated vigorously with a heating gun. An oily white solid was collected in the cooled collection bulb. Recrystallization of this solid in hexanes provided white flaky crystals (80% yield); ^{1}H NMR (90 MHz) δ (ppm): 2.49 (s, 3H, CH_3), 7.3-7.8 (m, 5H, arom.), 8.01 (s, 1H, arom.); MS (EI) m/z: 220 (M^+ for ^{79}Br), 222 (M^+ for ^{81}Br).

3,3'-Dimethyl-2,2'-binaphthyl (170): Formation of **170** was accomplished using the procedure outlined by Maigrot and Mazaleyrat[153], however, during preparation of the grignard one equivalence of 1,2-dibromoethane was added in along with an additional equivalence of Mg. The former material was added in to react with Mg activating it and allowing for a cleaner reaction with **169**. After

completion of the reaction, unreacted starting material (**169**) and the major byproduct **159** were distilled off using a kugelrohr set up to achieve a purity of >90% for **170** (yield 45%). Further purification was performed by eluting the product through a flash column (silica 50 g) using hexanes to achieve a yellowish brown solid; ^{1}H NMR (90 MHz) δ (ppm): 2.17 (s, 6H, $2CH_3$), 7.3-7.9 (m, 12H, arom.); MS (CI) m/z: 283 (M^++1), 311 (M^++29), 323 (M^++41).

3,3′-Bis[bromomethyl]-2,2′-binaphthyl (171): Bromination of **170** with NBS according to the procedure outlined for the synthesis of **152** (*vide supra*). An oil was achieved which solidified under vacuum (85% yield). The product obtained (**171**) was sufficiently pure for the next step by ^{1}H NMR (90 NHz) δ (ppm): 4.2-4.6 (m, 4H, CH_2Br), 7.3-8.1 (m, 12H, arom.). The MS (CI) exhibited a series of peaks around 441 (M^++1) and 469 (M^++29) indicating the presence of the two bromine in **171**. This was further confirmed by a MS obtained using EI which exhibited a series of peaks around 440.

4-Cyano-5-imine-3*H*-cyclohepta[2,3-a:3,2-a′]dinaphthalene (172): Cyclization of **171** was performed using the method outlined for the synthesis of **163** (*vide supra*). Compound **172** was obtained as a brown solid (yield 40%) with a purity of >90%; ^{1}H NMR (90 MHz) δ (ppm): 2.15 (d, J = 13 Hz, 1H), 2.66 (d, J = 13 Hz, 1H), 5.00 (broad s, 2H, NH_2), 7.1- 8.2 (m, 12H, arom.); IR (CH_2Cl_2) (cm^{-1}): 3500, 3400 (m, str. of NH_2), 2190 (m, str. CN); MS (CI) m/z: 333 (M^++1), 361 (M^++29), 373 (M^++41).

3*H*-Cycloheptan-4-one[2,3-a:3,2-a′]dinaphthalene (173): Ketone **173** was prepared from **172** following the procedure of Mislow and McGinn[155] for the synthesis of **164**. The product formed was fairly pure (>90%) (80% yield); ^{1}H NMR (250 MHz) δ (ppm): 3.4-3.9 (m, 4H, overlapping doublets, $2CH_2$), 7.5-7.6 (m, 4H, arom.), 7.74 (s, 2H, arom.), 7.8-8.0 (m, 4H, arom.), 8.13 (s, 2H, arom.); IR (CH_2Cl_2) (cm^{-1}): 1720 (s, carbonyl str.); MS (CI) m/z: 309 (M^++1), 337 (M^++29), 349 (M^++41).

3*H*-Cycloheptan-4-ol[2,3-a:3,2-a′]dinaphthalene (174): Conversion of **173** to alcohol **174** was performed using $LiAlH_4$ and the procedure outlined for the synthesis of **78**. Partial purification of **174** was achieved by use of a flash column (silica 50 g) with hexanes then CH_2Cl_2 as the eluting solvents to remove any non-polar impurities (90% yield). A purity of >95% was achieved for **174**; ^{1}H NMR (90 MHz) δ (ppm): 2.1-3.1 (m, 5H, $2CH_2$ and OH), 4.32 (quintet, J = 6 Hz, 1H), 7.2-8.0 (m, 12H, arom.).

4-Bromo-3*H*-cyclohepta[2,3-a:3,2-a′]dinaphthalene (175): Replacement of the hydroxyl group of **174** with a Br as in **175** was achieved using PBr_3 and the method used to synthesize **176** (*vide supra*). Partial purification was carried out using a flash column (silica 50 g) with hexanes as the eluting solvent to remove any polar impurities (85% yield). A purity of >95% was achieved for **175**; ^{1}H NMR (90 MHz) δ (ppm): 2.8-3.5 (m, 4H, $2CH_2$), 4.6-4.9 (m, 1H, CHBr), 7.3-8.4 (m, 12H, arom.).

***3H*-Cyclohepta[2,3-a:3,2-a']dinaphthalene (89):** As in the synthesis of **88** elimination of HBr from **175** using t-BuO$^-$K$^+$ provided **89**. However, with a purity of 55% **89** and 45% **176** by GC and ^{1}H NMR. Purification of **89** was performed by repeated recrystallization in toluene/EtOH (anhydrous) until a purity of >99% (by GC) was achieved (mp = 169-170°C); ^{1}H NMR (360 MHz) δ (ppm): 3.37 (d, J = 6.9 Hz, 2H, CH_2), 6.42 (dt, J = 10.2, 6.9 Hz, 1H, vinyl), 6.81 (d, J = 10.3 Hz, 1H, vinyl), 7.47-7.58 (m, 4H, arom.), 7.68 (s, 1H, arom.), 7.81 (s, 1H, arom.), 7.83-8.01 (m, 4H, arom.), 8.09 (s, 1H, arom.), 8.25 (s, 1H, arom.); ^{13}C NMR (360 MHz) δ (ppm): 33.4 (CH_2), 124.3, 125.4, 126.1, 126.3, 126.8, 127.4, 127.7, 127.9, 129.1, 129.8, 130.1, 132.3 (CH, arom. or vinyl), 132.0, 132.4, 132.7, 134.5, 138.2, 142.0 (C, arom.); HRMS (EI) m/z: 292.125 (calc. 292.126); UV (ACN) λ_{max} (nm): 209 (sh, 24700), 219 (40100), 260 (59500), 280 (sh, 36100), 303 (sh, 13600).

The major impurity was isolated out of the first recrystallization in toluene/EtOH (anhydrous) with a purity of >97% by GC; ^{1}H NMR (90 MHz) δ (ppm): 2.63 (s, 3H, CH_3), 7.3-7.7 (m, 5H, arom.), 7.8-8.2 (m, 5H, arom.), 8.30 (s, 1H, arom.), 9.08 (s, 1H, arom.), 9.13 (s, 1H, arom.); MS (CI) m/z: 293 (M^++1), 321 (M^++29), 333 (M^++41).

4.4 General Procedures for Direct Photolyses

Samples (30-100 mg) used in direct photolysis were dissolved in ACN (30-200 mL depending on the amount of other reagents used) then if required a second reagent (i.e., H_2O, D_2O, amines) was added. The resulting solution was

placed in a quartz tube (100 or 200 mL), cooled with a cold finger (≈17°C) and purged with Ar. The purging was started 10-15 min. prior to photolysis and continued through the photolysis along with the cooling. The length of photolysis varied from 5 min. to several hours depending on the efficiency of the photochemical process involved.

Photolysis performed in solvents with low boiling points were worked up by simply evaporating off the solvent followed by drying under vacuum. Reactions involving H_2O or D_2O were saturated with NaCl and extracted with CH_2Cl_2. The organic extracts were then dried over $MgSO_4$ and the solvent evaporated off followed by drying under vacuum. Reactions involving amines such as EA were worked up by addition of 1 M NaOH. The resulting solution was washed with CH_2Cl_2. If required an additional portion of NaOH was added to the organic extracts and the separation repeated to insure that all the EA was removed. The organic extracts were then dried over $MgSO_4$, the solvent evaporated and the resulting material placed on a vacuum pump. Photolysis involving the monitoring of product yield with photolysis time required the removal of samples (10-30 mL) at various times. The method used to work up each sample was dependent of the reagents involved as in the previous examples. Photoproducts were then analyzed by ^1H NMR, GC and GC/MS. If possible photoproducts were isolated using preparative thin layer chromatography (ptlc) and analyzed further by ^1H NMR and MS.

All photolysis were repeated in the absence of light using the same

conditions present in the photoreaction to determine if any thermal reactions took place. In the following photoreactions all of the substrates were shown to be thermally inert under the conditions used to perform the photolysis.

4.4.1 Suberene (5) and Related Systems in Aqueous Solutions

Suberene (5) in 50% D_2O/ACN and 5,5-Dideuteriosuberene (91) in 50% H_2O/ACN: Irradiation of **5** (100 mg) in 50% D_2O/ACN (100 mL) for 2 h with 254 nm light produced **90** (36%) and **91** (5%) by MS. These percentages were obtained by comparison of the MS of the starting material with the MS of the photoproduct. Changes noted in the NMR (360 MHz) of the photoproduct compared to starting material are as follows; ^{1}H NMR δ (ppm): 3.73 (growth of a t, **90**, 40%), 3.75 (decrease in a s, **5**, 60%); ^{2}H NMR δ (ppm): 3.7 (growth of a s, **90** and **91**), 7.05 (growth of a s, **142**, 1-2% compared to deuterium at the dibenzylic position).

Repetition of the photolysis of **5** (200 mg) in 50% D_2O/ACN (400 mL) with 254 nm light provided the data listed in Table 4.2. At the time intervals indicated 30 mL samples of the photoreaction were syringed out and analyzed by ^{1}H NMR (360 MHz) and MS. The data for the NMR analysis was used to prepare the graph shown in Figure 2.2. A similar photolysis of **91** (200 mg) in 50% H_2O/ACN (400 mL) with 254 nm provided the data listed in Table 4.3. Both ^{1}H NMR (360 MHz) and MS were used to analyze the samples withdrawn. The data

Table 4.2 Percent deuterium incorporation for **5** vs photolysis time.

Photolysis time (min.)	% Conversion		
	5	**90**	**91**
0	100	0	0
10	98	2	0
20	95	5	0
30	90	9	1
40	85	10	5
60	81	17	2
80	77	18	6
110	66	26	8
140	57	33	10
170	49	44	7
230	28	42	30

from the former analysis was used to prepare the graph in Figure 2.3.

Dibenzylic Substrates 9, 74, 102 in 50% D_2O/ACN and 104, 105, 106 in 50% H_2O/ACN: Photolysis of the protonated derivatives **9, 74** and **102** using the same conditions noted for **5** did not result in any visible changes in both the $_1$H NMR (360 MHz) and MS (CI). Photolysis of the deuterated derivatives **104** to **106** using the conditions noted for photolysis of **91** also did not result in any visible changes in the ^{1}H NMR (360 MHz).

Table 4.3 Percent deuterium loss from **91** vs photolysis time.

Photolysis time (min.)	% Conversion		
	91	**90**	**5**
0	96	4	0
10	92	7	1
20	87	12	1
30	87	11	2
40	78	21	1
60	71	27	2
80	63	34	3
110	63	33	4
140	52	42	6
170	46	46	8
230	28	58	20

5-Deuterio-5-methylsuberene (95) and 5-Deuterio-5-phenylsuberene (96) in 50% 5M NaOH/EtOH: Irradiation of **95** (50 mg) in 50% 5M NaOH/EtOH (100 mL) for 2 h with 254 nm lamps produced **93** (<5%); ^{1}H NMR (90 MHz) δ (ppm): 3.52 (growth of a quartet, **93**, very minor), 4.18 (growth of a quartet, **93**, very minor).

Photolysis of **96** using the same conditions noted for photolysis of **95** did not result in any visible changes in the ^{1}H NMR (90 MHz).

4.4.2 Derivatives of Suberene (5) in Non-aqueous Solutions

10,11-dihydro-*5H*-dibenzo[a,d]cyclohepten-5-ol (99), 5-Methyl-10,11-dihydro-*5H*-dibenzo[a,d]cyclohepten-5-ol (100) and 5-Phenyl-10,11-dihydro-*5H*-dibenzo[a,d]-cyclohepten-5-ol (101) in ACN: Irradiation of **99** (78 mg) in ACN (100 mL) for 1 h with 254 nm light produced one major product **110** (≈11%). Isolation of **110** by ptlc provided a product with a purity of >95%; ^{1}H NMR (90 MHz) δ (ppm): 2.82 (s, 4H, $2CH_2$), 7.1-7.4 (m, 6H, arom.), 7.6-7.8 (m, 2H, arom.); MS (CI) m/z: 181 (M^++1), 209 (M^++29), 221 (M^++41).

Irradiation of **100** and **101** using the same conditions resulted in **110**. An additional product benzaldehyde (**111**) was observed in the photolysis of **101** by the presence of a singlet at 9,92 ppm.

2'-Methyl-2',3',10,11-tetrahydrospiro[*5H*-dibenzo[a,d]cycloheptene-5,1:[*1H*]isoindole] (123) in ACN or CH_3OH: Photolysis of **123** (100 mg) in either ACN or MeOH (200 mL) for 1 h with 254 nm lamps produced one major product **124** (45%) and a minor product (5%) which was not identified. The changes due to **124** noted in the product mixture's ^{1}H NMR (90 MHz) were; δ (ppm): 2.3-3.3 (m, 4H, $2CH_2$), 3.1 (broadening of singlet from **123** by CH_3 in **124**), 5.53 (s, 1H, CH), 7.6-7.8 (m, 1H, arom.), 8.5 (broad s, 1H, imine); MS (from GC/MS) (CI) m/z: 312 (M^++1), 340 (M^++29), 352 (M^++41). The minor product was not observed in the ^{1}H NMR but a MS was obtained using GC/MS; (CI) m/z: 326 (M^++1), 354

(M^++29), 366 (M^++41).

4.4.3 Photolysis of Suberene (5) and Related Systems in the Presence of Amines in ACN

Suberene (5) and 5,5-Dideuteriosuberene (91) in the Presence of Et_3N: Irradiation of **5** (100 mg) (or **91** (70 mg)) in 0.01 M Et_3N/ACN for 30 min. with 254 or 300 nm lamps resulted in one major product **74** (21% at 300 nm) (or **105** (24% at 300 nm)) and several minor products by GC and ^1H NMR. The minor products were not identified. However, isolation of the major product by ptlc allowed for it's characterization; ^1H NMR (90 MHz) δ (ppm): 3.12 (s, 4H, $2CH_2$), 4.08 (s, 2H, CH_2, absent for **105**), 7.0-7.3 (m, 8H, arom.); MS (CI) m/z (**74**): 195 (M^++1), 223 (M^++29), 235 (M^++41); (**105**): 197 (M^++1), 225 (M^++29), 237 (M^++41).

5-Methylsuberene (93) in the Presence of Et_3N: Excitation of **93** (49 mg) in the presence of 0.01 M Et_3N in ACN (100 mL) for 5 min. with 254 nm lamps produced **131** (9%) four adducts (2% each) by GC/MS. Other products were visible in the GC with much longer retention times but they were not identified. A longer photolysis (30 min.) using the same conditions provided sufficient amounts of product for isolation by ptlc; ^1H NMR (90 MHz) δ (ppm) (**131**): 1.70 (d, J = 7 Hz, 3H, CH_3), 3.19 (s, 4H, $2CH_2$), 4.42 (q, J = 7 Hz, 1H, CH), 7.0-7.3 (m, 8H, arom.); MS (CI) m/z: 209 (M^++1), 237 (M^++29), 249 (M^++41); ^1H NMR (90

MHz) δ (ppm) (adducts): 1.4-2.0 (methyl signals of adducts), 2.2-5.0 (protons of other saturated carbons in adducts), 6.8- 7.4 (aromatic protons of adducts); MS (CI) m/z: 308 (M^++1), 336 (M^++29).

5-Phenylsuberene (94) in the Presence of Et_3N: Photolysis of **94** (50 mg) in 0.01 M Et_3N/ACN (100 mL) for 10 min. with 254 nm lamps provided **132** (17%) and four adducts (total 11%) according to GC/MS; MS (CI) m/z (**132**): 271 (M^++1), 299 (M^++29), 311 (M^++41); (adducts): 270 (M^++1), 398 (M^++29). The ^{1}H NMR (90 MHz) had numerous new signals which could not be identified and no attempt was made at isolation of each product.

Suberenol (78) in the Presence of Et_3N: Irradiation of **78** (102 mg) in the presence of 0.01 Et_3N in ACN (100 mL) with 300 nm lamps for 30 min. resulted in one major product **99** (26%) ^{1}H NMR. The product mixture was purified by ptlc to isolate **99** along with starting material; ^{1}H NMR (90 MHz) δ (ppm): 2.52 (broad s, 1H, OH of **78** and **99**), 2.8-3.5 (m, 4H, $2CH_2$), 5.31 (s, 1H, CH of **78**), 5.88 (s, 1H, CH of **99**), 7.0-7.7 (m, 8H of **78** and **99**).

5,5-Dideuteriosuberene (91) in the Presence of Piperidine: Photolysis of **91** (100 mg) in 0.5 M piperidine/ACN (100 mL) for 30 min. with 254 nm lamps provided **90** (≈10%) and **105** (≈7%) by ^{1}H NMR. Other minor products were visible but they were not identified; ^{1}H NMR (90 MHz) δ (ppm): 3.10 (s, 4H, $2CH_2$ of **105**),

3.71 (s, 1H, CH of **90**), 6.9-7.7 (m, aromatic and vinyl H of **91**, **90** and aromatic H of **105**).

Suberenol (78) in the Presence of Piperidine: Excitation of **78** (101 mg) in a solution of 0.10 M piperidine/ACN (100 mL) for 30 min. with 300 nm lamps produced **99** (14%) and **83** (2%) by GC. The ketone **83** was not visible in the ^{1}H NMR since the positions where it resonates was obscured by other signals; ^{1}H NMR (90 MHz) δ (ppm): 2.6-3.4 (m, $2CH_2$ of **99** and possibly **83**), 5.31 (s, 1H, CH of **78**), 5.88 (s, 1H, CH of **99**), 6.8-7.8 (m, aromatic and vinyl H of **78** and aromatic H of **99** and **83**).

5,5-Dideuteriosuberene (91) in the Presence of Ethanolamine or n-Propylamine: Excitation of **91** (50 mg) in 0.01 M EA/ACN (100 mL) with 254 nm lamps for 30 min. resulted in the growth of proton resonances in the ^{1} H NMR (360 MHz) at 3.77 and 3.79 ppm due to **90** (34%) and **5** (5%) respectively. Repetition of the photolysis in 0.10 EA/ACN for 5 min. also resulted in the growth of signals at 3.77 and 3.79 ppm due to **90** (21%) and **5** (2%). Irradiation of **91** (55 mg) in 0.01 M PA/ACN (100 mL) for 30 min. with 300 nm lamps resulted in formation of **90** (40%) and **5** (6%) according to both ^{1}H NMR (90 MHz) and MS (CI). The percentages of **90** and **5** formed in the last photolysis were determined by comparison of the product MS with the MS of the starting material **91**.

5-Deuterio-5-methylsuberene (95) in the Presence of Ethanolamine or n-Propylamine: Excitation of **95** (52 mg) in 0.10 M EA/ACN (100 mL) for 1 h with 254 nm lamps resulted in the formation of **93** (15%); ^{1}H NMR (360 MHz) δ (ppm): 1.36 and 1.91 (singlets from **95** overlapping doublets from **93**), 3.52 and 4.18 (quartets due to CH of **93**). Repetition of this photolysis in 0.50 M EA/ACN resulted in loss of 42% of the deuterium in **95** according to comparison of the MS (CI) obtained for the starting material and the product.

Irradiation of **95** (100 mg) in 0.50 M PA/ACN (100 mL) for 1 h with 254 nm lamps produced **93** (50%), deuterated **131** (3%) and two adducts (6%). The latter two quantities were determined by GC and the first quantity by comparison of MS. The adducts were also visible in the ^{1}H NMR (90 MHz) (2.0-4.3 ppm) along with the reduced product (deuterated **131**) (3.17 ppm (s, 4H, $2CH_2$)).

5-Deuterio-5-phenylsuberene (96) in the Presence of Ethanolamine or n-Propylamine: Photolysis (254 nm) of **96** (99 mg) in 0.50 M EA/ACN (100 mL) for 1 h resulted in one product **94** (<2%) by growth of a minor signal in the ^{1}H NMR (90 MHz) at 5.32 ppm (s, 1H, CH of **94**). A repeat of this photolysis in 0.50 M PA/ACN produced **94** (<2%), deuterated **132** (5%) and one major adduct (5%). The ^{1}H NMR (90 MHz) with a signal at 5.32 ppm (s, 1H, CH of **94**) indicated the presence of **94** while GC/MS was used to determine the quantities of the other two products; MS (CI) m/z (deuterated **132**): 272 (M^++1); (adduct): 329 (M^++1), 357 (M^++29).

Suberenol (78) and 5-Deuteriosuberenol (80) in the Presence of Ethanolamine or n-Propylamine: Excitation of **78** (100 mg) in the presence of 0.01 M EA/ACN (100 mL) for 30 min. with 300 nm lamps resulted in ketone **83** (5%) according to the growth of a resonance at 3.04 ppm (s, 4H, $2CH_2$). Irradiation of **78** (100 mg) in 0.10 M PA/ACN for 30 min. with 300 nm lamps provided **83** (3%) and **99** (6%) according to growth of resonances at 3.06 (s, 4H, $2CH_2$) and 5.85 ppm (s, 1H, CH) for each respectively in the ^1H NMR of the product mixture. These results were confirmed by GC.

Photolysis of **80** (100 mg) in 0.10 M PA/ACN with 300 nm lamps for 30 min. produced **78** (5%) according to the growth of a resonance at 5.30 ppm (s, 1H, CH) in the ^1H NMR (90 MHz) of the product mixture.

4.4.4 *5H*-dibenzo[a,c]cycloheptene (6) and Related Systems

7-Deuterio-*5H*-dibenzo[a,c]cycloheptene (87) in ACN and 50% H_2O/ACN: Excitation of **87** (50 mg) in ACN (100 mL) with 254 nm lamps (15 min.) provided the products indicated in the ^2H NMR (360 MHz) (Fig. 3.3); δ (ppm): -0.14 (**86** H_X, 2.2%), 1.59 (**86** H_B, 3.6%), 2.57 (**85** H_A, 58.7%), 3.05 (**178**, 3.1%), 5.32 ($CDHCl_2$), 6.31 (**84**, 6.5%), 6.67 (**87**, 19.6%), 7.83 (**177**, 5.9%). Photolysis of **87** (50 mg) in 50% H_2O/ACN using the same conditions resulted in the products indicated in the ^2H NMR (360 MHz) (Fig. 3.4); δ (ppm): -0.12 (**86** H_X, 1.1%), 1.60 (**86**, H_B, 1.0%), 2.58 (**85** H_A, 16.1%), 3.08 (**178**, 29.3%), 5.32 ($CDHCl_2$), 6.32 (**84**, 3.7%), 6.68 (**87**, 47.4%),

7.85 (177, 1.4%).

6-Methyl-5*H*-dibenzo[a,c]cycloheptene (155) in ACN: Irradiation of 155 (50 mg) in ACN (100 mL) with 254 (15 min.) or 300 nm (15 min.) lamps provided the same 3 major products 179 (25% at 254 nm and 4% at 300 nm), 180 (3% at 254 nm and 13% at 300 nm) and 181 (3% at 254 nm and 4% at 300 nm) according to GC/MS and ^{1}H NMR. The signals which could be isolated for each product in the ^{1}H NMR (360 MHz) of either the 254 nm or 300 nm (1 h photolysis) are as follows; δ (ppm) (179): 0.07 (dd overlapped by a singlet, J = 4.5 Hz visible, H_X), 1.45 (dd, J = 9.0, 3.8 Hz, H_B), 1.65 (s, 3H of CH_3), 2.34 (dd, J = 9.0, 5.0 Hz, H_A); (180): 2.11 (m, J = 1.3 Hz visible, 3H of CH_3), 2.80 (m partially obscured and not all of the coupling is resolved, axial H of CH_2), 3.05 (dd partially obscured, J = 13.1, 8.2 Hz, equatorial H of CH_2), 6.08 (m all of coupling not resolved, vinyl H); (181): 2.75 (d, J = 1.0 Hz, 3H of CH_3), 6.68 (m, aryl H). The correlation between signals believed to represent each product was verified using ^{1}H COSY NMR; (179): signals at 0.07 (H_X), 1.45 (H_B) and 2.34 ppm (H_A) are coupled; (180): signals at 2.11 (CH_3), 2.80 (axial H of CH_2) and 6.08 ppm (vinyl H) are all coupled and the signal at 3.05 ppm (equatorial H of CH_2) is coupled to signals at 2.80 (axial H of CH_2) and 6.08 ppm (vinyl H); (181): signal at 2.75 ppm coupled to an aryl signal around 7.6 ppm.

5*H*-dibenzo[a,c]cycloheptene (6) in D_2O/ACN and in the Presence of

Ethanolamine in D_2O/ACN: A sample of **6** (30 mg) was dissolved in a 25% D_2O/ACN solution, purged with Ar, and irradiated for 15 min. in a rayonet with 254 nm lamps. After removal of the solvent the product mixture was analyzed by GC and ^1H NMR. Both **144** (30%) and **148** (5%) were achieved as in previous photolysis of **6** in D_2O/ACN[8,113]. Comparison of the integration for protons located in the vinyl and 5-position of **6** in the ^1H NMR (360 MHz) suggested a percent deuterium incorporation of 49%.

A solution of 5 M EA in D_2O (100 mL) was prepared and a portion of the mixture (10 mL) added to a solution of **6** (30 mg) in ACN (90 mL). The resulting solution was purged and irradiated (5 min.) as in the previous photolysis. Analysis (GC) of the isolated product mixture indicated the presence of **144** (14%) and **148** (1%). The ^1H NMR (360 MHz), of the product mixture, indicated a total of 40% deuterium incorporation.

6-Methyl-5*H*-dibenzo[a,c]cycloheptene (155) in the Presence of Bases: Irradiation of **155** (32 mg) in 25% D_2O/ACN with 254 nm lamps (15 min.) produced **179** (22%), **180** (3%) and **181** (3%) according to GC and ^1H NMR (360 MHz) analysis of the product mixture. Integration and comparison of the ^1H NMR signals due to the proton at the vinyl and 5-position of **155** indicated a percent deuterium incorporation of 9%.

Compounds **179** (29%), **180** (4%) and **181** (12%) along with starting material (36%) were observed by GC analysis of the product mixture achieved after

irradiation of **155** (50 mg) in 10% (5 M EA/D_2O)/ACN (100 mL) with 254 nm lamps (30 min.). GC/MS and ^2H NMR analysis of the product mixture indicated extensive deuterium incorporation in the starting material and products: **155** (73% at the 5-position including deuterium at vinyl position), **179** (36% at positions H_A, H_B and H_X). A shorter photolysis (5 min.) with 32 mg of **155** and the same conditions just noted produced **179** (5%), **180** (2%) and **181** (1%) and resulted in less deuterium incorporation (36%) into recovered starting material.

6-Phenyl-5*H*-dibenzo[a,c]cycloheptene (156) in ACN and D_2O/ACN: The product mixture obtained after irradiation of **156** (50 mg) in either ACN or 50% D_2O/ACN was very complex according to both GC and ^1H NMR studies. The latter exhibited signals throughout the region of 1 to 7 ppm. GC/MS analysis of recovered starting material indicated that deuterium incorporation did not occur in the photolysis involving D_2O. Due to the complexity of the product mixture and the lack of excited state carbon acid behaviour, no further photolysis of **156** were performed to delineate the photochemistry of this system.

3*H*-Cyclohepta[2,1-a:3,4-a']dinaphthalene (88) in the Presence of Ethanolamine in D_2O/ACN: Approximately 50 mg of **88** was dissolved in ACN (90 mL) and 10 mL of a 5 M EA in D_2O added. Irradiated of this solution with 254 nm lamps (60 min.) resulted in deuterium incorporation at the positions labelled H7B (30%), H7A (< 1%) and H9 (≈2%) according to ^1H and ^2H NMR (360 MHz). Repetition

of this photolysis using 300 mg of **88** in 40 mL 5 M EA in D_2O and 360 mL ACN for various lengths of times provided the data listed in Table 4.4. At the times indicated ≈45 mL samples were withdrawn from the quartz tube and the solvent removed. Analysis by ^1H and ^2H NMR (360 MHz) provided the percent deuterium incorporation at positions H7A, H7B and H9. This data was used to generate the plot shown in Figure 3.8

Table 4.4 Incorporation of deuterium at position H7A, H7B and H9 of **88** vs photolysis time in 10%(5M EA/D_2O)/ACN.

Photolysis Time (min.)	% Deuterium at		
	H7B	H7A	H9
0	0	0	0
15	9.1	0	0
30	14.9	0	0
60	30.3	0	2.4
90	41.4	2.4	3.4
120	49.1	2.1	4.2
180	57.9	2.8	7.1
240	64.6	3.2	10.5
300	67.0	3.7	13.2

Deuterated *3H*-Cyclohepta[2,1-a:3,4-a']dinaphthalene (183) in ACN: The deuterated product from samples 2, 3 and 4 of the extended photolysis of **88** were combined (total ≈100 mg of **88** (82%) and **183** (18%)) and irradiated in ACN (140

mL) with 254 nm lamps (6 h). Comparison of the ^2H NMR of the sample before and after photolysis indicated only a minor growth of deuterium at position H7A (≈13% of the quantity at position H7B).

***3H*-Cyclohepta[2,3-a:3,2-a']dinaphthalene (89) in ACN and in the Presence of Ethanolamine in D_2O/ACN:** Approximately 30 mg of **89** was dissolved in ACN (100 mL) and irradiated for 30 min. with 254 nm lamps. The GC and ^1H NMR of the photolyzed material indicated the formation of one product (44%) identified as **184**; ^1H NMR (360 MHz) δ (ppm): 0.18 (td, J = 5.4, 4.2 Hz, H_X of cyclopropyl ring), 1.63 (td, J = 8.9, 4.1 Hz, H_B of cyclopropyl ring), 2.77 (dd, J = 8.9, 5.0 Hz, $2H_A$ of cyclopropyl ring), 7.89 (s, 2H, arom.), 8.63 (s, 2H, arom.), remaining eight aromatic protons were mixed with aromatic protons from **89**; GC/MS (CI) m/z: 293 (M^++1), 321, (M^++29), 333 (M^++41).

Formation of **184** was monitored by taking UV spectrum after irradiation of **89** (≈2 x 10^{-5} M in ACN) in a 3 mL quartz cuvette on the optical bench with 254 nm light for various lengths of time (15 to 60 sec). Overlap of the UV spectrum obtained provided Figure 3.10.

Irradiation of **89** (≈2 x 10^{-5} M) in 10% (5M EA in D_2O)/ACN (3 mL) using a quartz cuvette and the rayonet (254 nm lamps) for 15 min. followed by GC analysis indicated the formation of **184** (25%). A GC/MS of the product mixture indicated no deuterium incorporation into the starting material (**89**). Repetition of the last photolysis in ACN also resulted in the formation of **184** (25%)

according to GC.

4.5 General Procedures for Triplet Sensitizations

The sensitizer 2-benzoylbenzoic acid **107** was used in large excess to insure that all the light from the 350 nm lamps was absorbed by the sensitizer and not the compound under study. To confirm this UV absorption spectrum were taken of the compound being sensitized and of **107** at the concentrations being used. Both **5** and **6** do not absorb above 320 nm whereas **107** absorbs light at 350 nm. The compound to be sensitized was then dissolved in 100 mL of the required solvent mixture along with **107** and placed in a pyrex tube (100 mL). This solution was cooled with a cold finger and purged for >10 min. with Ar prior to irradiation in a rayonet RPR 100 photochemical reactor with 350 nm lamps. Cooling and purging were continued during the photolysis which were carried out for various lengths of time depending on the system being studied. The resulting solution was washed with 0.1 M NaOH (4x) to remove **107**. After washing the remaining organic layer with water and drying it over $MgSO_4$ the solvent was evaporated off to obtain the products required for analysis by GC, ^1H and ^2H NMR, and GC/MS.

4.5.1 Suberene (5) in D_2O/ACN and 5,5-Dideuteriosuberene (91) in H_2O/ACN

Both **5** (50 mg) and **107** (1.0 g) were dissolved in ACN (50 mL) then D_2O was added in well sonicating the reaction mixture. This solution was placed in

a pyrex tube and irradiated (30 min.). Analysis of the material recovered by ^1H NMR (250 MHz) indicated only starting material with no deuterium incorporation. The same result was obtained after irradiation of **91** (30 mg) and **107** (1.0 g) in 50% H_2O/ACN for 1 h.

4.5.2 7-Deuterio-*5H*-dibenzo[a,c]cycloheptene (87) in ACN

A mixture of **87** (30 mg) and **107** (1.0 g) was dissolved in ACN (100 mL) and placed in a pyrex tube for irradiation (1 h). Analysis of the recovered material by ^2H NMR (360 MHz) suggested the formation of **85** (≈31%); δ (ppm): 2.57 (s, D at position H_A of cyclopropyl ring).

4.5.3 6-Methyl-*5H*-dibenzo[a,c]cycloheptene (155) in ACN

A solution of **155** (40 mg) and **107** in ACN (100 mL) was placed in a pyrex tube and irradiated for 1 h. According to GC and ^1H NMR analysis of the recovered material **179** (10%) was the major product formed; ^1H NMR (360 MHz) δ (ppm): 0.06 (m, H_X of cyclopropyl ring overlapped by other signals), 1.46 (dd, J = 9.0, 3.7 Hz, H_B of cyclopropyl ring), 1.65 (s, 3H of CH_3), 2.35 (dd, J = 8.9, 5.0 Hz, H_A of cyclopropyl ring).

4.6 Product Quantum Yields

The product quantum yields listed in the previous two Chapters were determined either on an optical bench or in a rayonet. This section describes the

procedure used to obtain quantum yields with these two set ups.

4.6.1 Quantum Yields on the Optical Bench

The product quantum yields in Tables 2.1, 2.2, 2.3 and 2.5 and the value measured for **89** were all measured on the optical bench using an Oriel 200W mercury arc lamp and an Applied Physics Monochromator. The quantum yields of exchange (Table 2.1 to 2.3) and the product quantum yield for **89** were obtained using the monochromator set to 280 nm with slits of 5 nm whereas the product quantum yields in Table 2.5 were obtained with settings of 254 nm and 7 nm slits. Samples were irradiated in suprasil quartz cuvettes (3.00 mL) fitted with a two hole stopper. Through one hole was passed a needle which was used to purge the sample with Ar for 10 min. prior to photolysis. Purging was continued during the photolysis to exclude oxygen and to stir the sample. Photolysis times ranged from 2 min. to 2.5 h depending of the conversion which was kept below 20% to prevent formation of secondary photoproducts.

Samples of **5** were prepared by addition of 0.300 mL of a 2.10×10^{-3} M stock solution of **5** in ACN to the appropriate solvent mixture (2.70 mL) contained in a cuvette. Samples of **91** were prepared by addition of 0.30 mL of a 2.07×10^{-3} M stock solution of **91** in ACN or EtOH (for Table 2.3) to the appropriate solvent mixture (2.70 mL) in a cuvette. Samples of **99-101** were prepared by addition of the required volume of stock solution to make up 3.00 mL samples in ACN with 1.44×10^{-5} moles of the required compound. The sample required for **89** was

prepared by the addition of 0.30 mL of a 1.37×10^{-3} M stock solution in ACN to a cuvette with 2.70 mL of ACN. Prior to photolysis the absorption at 280 or 254 nm was measured to determine the portion of the light being absorbed by the sample.

Samples in ACN were worked up by evaporation of the solvent whereas samples with non-volatile components (i.e., water, formamide, salts) required a more extensive work up. Solutions of H_2O or D_2O/ACN were worked up by saturating the sample with NaCl followed by extraction of the organic layer with added CH_2Cl_2. The organic layer was then dried over $MgSO_4$ and the solvent evaporated. Samples involving formamide were washed with 0.1 M NaOH and the required material extracted out with CH_2Cl_2. The organic extracts were dried over $MgXO_4$ and the solvent evaporated. Solutions containing acids or bases were saturated with NaCl and washed with CH_2Ci_2. The organic layer was washed with water saturated with NaCl and then dried over $MgSO_4$ before evaporation of the solvent. In all cases the resulting samples were taken up in acetone (spec. grade) and analyzed by GC or GC/MS depending on the reaction under study. Each sample was injected three or more times in the GC to achieve reasonable data. For each quantum yield determined three or more samples were prepared, irradiated and analyzed to obtain an average quantum yield. Percent deuterium loss or gain in the samples required for exchange quantum yields was measured by comparison of the MS (CI) obtained for the starting material and for the irradiated samples. Both the natural abundance of ^{13}C and ^{2}H were taken into

consideration using this comparison.

A chemical actinometer, potassium ferrioxalate (PF) ($K_3Fe(C_2O_4)_3$)[111,131] was used to measure the light intensity on the optical bench. A stock solution of PF (0.0060 M in 0.05 M H_2SO_4 (250 mL)) was prepared along with a 1,10-phenanthroline (188) solution (0.2% by weight in distilled H_2O) in the presence of a red light since the former is light sensitive. The procedure used to measure the light intensity involved placing 3.00 mL of the PF solution two different cuvette. One cuvette was irradiated on the optical bench using the same conditions used for quantum yield samples (including purging with Ar). The second cuvette was placed next to the optical bench to provide a blank.

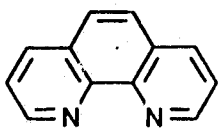

188

The irradiated PF was reacted with 188 by placing 1.00 mL of cuvette sample in a 10 mL volumetric with 2.00 mL of the stock solution of 188, 0.50 mL of a buffer NaOAc3H_2O) solution and 6.5 mL of H_2O. Aluminum foil was then wrapped around the volumetric and the sample left for 1 h to react. This procedure was repeated with the blank sample of PF. After the 1 h period 3 mL of each sample were placed in cuvettes and their absorption at 510 nm recorded. This procedure was repeated every day that the optical bench was in use. The values measured (ex. at 280 nm, 5 nm slits, I = 1.95×10^{-7} Einsteins/min./3 mL) remained constant over periods of time where no adjustments were made to the

optical bench.

Irradiation of PF results in conversion of Fe^{3+} to Fe^{2+} (eq. 4.1). The quantity of reduced iron formed is measured by reacting it with **188** to form a complex which absorbs at 510 nm. By measuring the absorption at 510 nm, due to this complex, the light intensity (I) can be calculated using the following equation (eq. 4.2).

$$2Fe^{3+} + C_2O_4^{2-} \longrightarrow 2Fe^{2+} + 2CO_2 \qquad (4.1)$$

$$I = \frac{\Delta A V_2 V_3 \times 10^{-3}}{\epsilon \phi_\lambda t V_1} \qquad (4.2)$$

Where:

ΔA difference between absorption of reacted sample and blank at 510 nm.

v_1 is the volume of irradiated actinometer withdrawn (1.00 mL).

v_2 is the volume of actinometer irradiated (3.00 mL).

v_3 is the volume of the volumetric flask (10.00 mL).

ϵ is the extinction coefficient for the F^{2+} 1,10-phenanthroline (**188**) complex at 510 nm (1.11×10^4 $Lmol^{-1}cm^{-1}$).

Φ_λ is the known quantum yield for Fe^{2+} formation at the wavelength used for photolysis, 254 or 280 nm (≈1.25).

t is the time of photolysis (5 min.).

This light intensity in Einsteins/min./3 mL was then adjusted to take into

account the absorption due to the sample being quantified. The resulting value was plugged into the following equation (eq. 4.3) for quantum yields (Φ) along with the moles of product formed and the time of photolysis (t_p).

$$\Phi_{ex} \text{ or } \Phi_p = \frac{\text{(moles of product)}}{It_p} \qquad (4.3)$$

4.6.2 Quantum Yields in the Rayonet

The quantum yields listed in Tables 2.4 and 3.1 were measured using preparative scale photolysis and the procedure outlined at the start of section 4.4. In each photolysis 2.60×10^{-4} mole of starting material was dissolved in the appropriate solvent and irradiated (254 nm lamps, quartz tube) for a time sufficient to produce a product yield of between 5 and 20%. Product yields were measured from ^{1}H NMR (for loss or gain of deuterium) and GC (for formation of products). The absorption of each sample was also measured to insure that similar amounts of light were being absorbed.

Light intensity in the rayonet was measured by irradiating 91 (50.0 mg) (15 min.) in 50% H_2O/ACN. Using equation 4.3 and the known quantum yield of exchange for 91 (Φ_{ex} = 0.035 ± 0.005) in 50% H_2O/ACN and the percent deuterium loss in the rayonet photolysis, the light intensity in this apparatus was calculated. The value obtained (I = 1.57×10^{-4} Einsteins/min ± 20.5%) is

consistent with earlier measurements of the light intensity in the rayonet with 254 nm lamps. To insure a standard set of conditions for the quantum yields measured using this technique all of the subsequent photolysis were performed in the same rayonet with the quartz tube used for the standard.

4.7 Fluorescence Quantum Yields

The fluorescence quantum yield of **5** was determined using two standards (2-aminopyridine (**136**) $\Phi_f = 0.60 \pm 0.05$ and anthracene (**137**) $\Phi_f = 0.27 \pm 0.03$)[134]. These standards were chosen since they both fluoresce in the same region as **5**. Fluorescence in the same region is required to insure that the energy of the light being emitted is the same for the standard and the unknown[134].

Dilute solutions of **5** (ACN) and the standards **136** (0.05 M H_2SO_4) were prepared. UV spectrum were then recorded (using the Pye Unicam SP8-400) for each in four sided suprasil quartz cuvettes to find a point in the spectrum where a match of absorption curves existed (with an absorption <0.10). A match was required to insure that each solution absorbed the same number of photons and an absorption of <0.10 was required to prevent self quenching which occurs at high concentrations[134]. If no match was achieved then one or both of the solutions in the cuvettes were diluted or concentrated to find a match. For **5** and **136** a match was achieved from 262 to 272 nm. Each sample was then purged with Ar (10 min.) and the fluorescence spectrum recorded (using the Perkin-Elmer MPF-66 fluorescence spectrometer) at several wavelengths over the region where a match

was achieved. The area under each fluorescence curve for **5** and **136** at each wavelength were then placed into equation 4.4 to calculate the fluorescence quantum yield (Φ_f).

$$\Phi_f^u = \Phi_f^n \frac{\phi^u}{\phi^n} \left(\frac{\eta^u}{\eta^n}\right)^2 \qquad (4.4)$$

Where:

ϕ^u and ϕ^n are the areas under the sample (unknown) and standard (known) fluorescence curves respectively.

Φ_f^u and Φ_f^n are the fluorescence quantum yields of the sample and standard respectively.

η^u and η^n are the refractive indexes of the solvent used for the sample (ACN $\eta = 1.3$)[131] and the standard (0.05 M H_2SO_4 $\eta = 1.33$)[170] respectively.

This procedure was repeated using **5** and **137** to verify the fluorescence quantum yield obtained with **136** as a standard. Fluorescence quantum yields required for **93, 94, 155, 156, 88** and **89** were measured using the procedure outlined for **5** and **136** but with the former compound as the standard. In addition the fluorescence quantum yield of **6** was remeasured with **5** as the standard. This was done to allow for a more accurate comparison of Φ_f values for **6** and related systems.

4.8 Fluorescence Lifetimes

The fluorescence lifetimes (τ) measured were determined using the single photon counting technique[135] described earlier. Materials required for the analysis were purified to a purity of >99% since the technique is very sensitive and biexponential fits would result if an impurity were present. Samples were prepared in ACN and placed in four sided quartz cuvettes. The absorption of each sample was kept below 0.10, at the excitation wavelength chosen, to prevent self quenching which occurs at higher concentrations[134]. Purging with Ar was then performed for 10 min. prior to measurement of τ to prevent quenching of the fluorescence by oxygen[64,135].

Samples which were used to measure the lifetimes required in the quenching studies were prepared using a dilute stock solution of unknown concentration. To insure consistency the same amount of stock solution was used each time. This sample was added to ACN (3.00 mL) along with the required volume of quencher (primary amines) in a four sided cuvette. The sample was then purged and the fluorescence lifetime measured.

4.9 Fluorescence Quenching Studies

Fluorescence quenching studies were performed on a Perkin-Elmer MPF-66 fluorescence spectrophotometer. As in the fluorescence lifetime studies dilute samples were required to prevent self quenching. For each compound studied a stock solution was prepared and a measured amount taken with a syringe and injected into a four sided cuvette containing the appropriate solvent with

quencher. The quenching studies involving H_2O, D_2O, EtOH, THF, Et_3N and primary amines were performed in ACN which was dried over CaH and distilled when required. Quenching studies involving H_2SO_4 and NaOH were performed in 10% EtOH/H_2O with the water portion containing the appropriate acid or base concentration.

Prior to each quenching study the purity of the solvent and substrate were investigated by obtaining a fluorescence spectrum of each to check for any unusual behaviour, i.e., extra peaks. A blank run with the solvent and highest concentration of quencher to be used were also ran to determine if the quencher produced any fluorescence signals in the region of interest. The substrates purity was also investigated by obtaining an excitation spectrum. This spectrum should resemble the absorption spectrum of the substrate[64]. Once the purity of all the components involved in the study had been confirmed the instrument was left for 2 to 3 hours (which is the time required before the fluoremeter readings became constant).

Quenching studies resulting in a Stern-Volmer plot involved the preparation of >6 samples each with different concentrations of quencher. Studies involving H_2O, D_2O, EtOH and THF used the quencher directly without dilution. However, when primary amines or Et_3N were used as quenchers they were diluted so that the volumes injected into the cuvette could be measured out accurately (i.e., in the 10 to 100 μL range). In all cases the concentration of the quencher was kept below 1.0 M to minimize solvent changes which could effect

the fluorescence spectrum. Each sample was then purged for 10 min. with Ar and the fluorescence intensity taken at a fixed wavelength using an excitation wavelength dependent on the substrate involved. The fluorescence intensity at a fixed wavelength was used since not all of the substrates studied provided stable fluorescence spectrum (i.e., the fluorescence spectrum of **6** and related systems gradually decreased in intensity over time). Each series of samples were ran three or more times and the average rates of quenching from the Stern-Volmer plots taken. All samples in each series were ran on the same day right after each other to minimize any changes in the instrument and surroundings.

Quenching studies involving examination of pH and H_0 effects on the fluorescence intensity of different substrates were performed in the same manner. Samples with different pH (1, 2, 7, 10, 12, 13, 14) and H_0 (0.04, -0.45, -1.18, -2.25, -3.3, -4.4) were prepared in 10% EtOH/ACN with added substrate and their fluorescence intensity recorded. However, plots of fluorescence intensity against pH and H_0 (Fig. 2.10 and 2.11) were obtained rather then Stern-Volmer plots. Again all samples were ran in as short a time span as possible to minimize changes in the instrument and surroundings. In addition the fluorescence spectrum of each sample was obtained to check for the formation of any new peaks which would suggest formation of a new emissive species and possible decomposition of the substrate.

REFERENCES AND NOTES

1. Horspool, W.; Armesto, D. *Organic Photochemistry: A Comprehensive Treatment*; Ellis Horwood and Prentice Hall: Toronto, 1992.

2. Cristol, S. J.; Bindel, T. H. *Organic Photochemistry*; Padwa, A., Ed.; Marcel Dekker, Inc.: New York, 1983; vol. 6.

3. Das, P. K. *Chem. Rev.* **1993**, *93*, 119.

4. Margerum, J. D.; Petrusis, C. T. *J. Am. Chem. Soc.* **1969**, *91*, 2467.

5. Childs, R. F.; Shaw, G. B. *Organic Photochemistry*; Padwa, A., Ed.; Marcel Dekker, Inc.: New York, 1991; vol. 11.

6. Tolbert, L. M. *Organic Photochemistry*; Padwa, A., Ed.; Marcel Dekker, Inc.: New York, 1983; vol. 6.

7. Wan, P.; Krogh, E.; Chak, B. *J. Am. Chem. Soc.* **1988**, *110*, 4073.

8. Wan, P.; Budac, D.; Earle, M.; Shukla, D. *J. Am. Chem. Soc.* **1990**, *112*, 8048.

9. This pK_a was estimated by noting values for other cycloheptatriene derivatives in the literature: (a) Dauben, H. J., Jr.; Rifi, M. R. *J. Am. Chem. Soc.* **1963**, *85*, 3041. (b) Doering, W. V. E.; Gaspar, P. P. *J. Am. Chem. Soc.* **1963**, *85*, 3043. (c) Staley, S. W.; Ordeval, A. W. *J. Am. Chem. Soc.* **1973**, *95*, 3384. (d) Staley, S. W.; Ordeval, A. W. *J. Am. Chem. Soc.* **1974**, *96*, 1618.

10. Streitwieser, A., Jr.; Hammons, J. H. *Progress in Physical Organic Chemistry*; Cohen, S. G., Streitwieser, A., Jr., Taft, R. W., Eds.; Interscience Publishers: New York, 1965; vol. 3.

11. Dewar, M. J. S. *Angew. Chem., Int. Ed. Engl.* **1971**, *10*, 761.

12. Zimmerman, H. E. *Acc. Chem. Res.* **1971**, *4*, 272.

13. Woodward, R. B.; Hoffmann, R. *J. Am. Chem. Soc.* **1965**, *87*, 2511.

14. Breslow, R. *Acc. Chem. Res.* **1973**, *6*, 393.

15. Wan, P.; Krogh, E. *J. Am. Chem. Soc.* **1989**, *111*, 4887.

16. Krogh, E.; Wan, P. *J. Am. Chem. Soc.* **1992**, *114*, 705.

17. Fratev, F.; Monev, V.; Janoshek, R. *Tetrahedron* **1982**, *38*, 2929.

18. Gorelik, M. V. *Russian Chem. Rev.* **1990**, *59*, 116.

19. Scott, L. T.; Jones, M., Jr. *Chem. Rev.* **1972**, *72*, 181.

20. Bally, T.; Masamune, S. *Tetrahedron* **1980**, *36*, 343.

21. Lloyd, D. *Non-Benzenoid Conjugated Carbocyclic Compounds*; Elsevier: Amsterdam, 1984.

22. Cundall, R. B.; Robinson, D. A.; Pereira, L. C. *Advances in Photochemistry* **1977**, *10*, 147.

23. Streitwieser, A., Jr. *Molecular Orbital Theory for Organic Chemists*; Wiley: New York, 1961.

24. Padma, E. J.; Jug, K. *Tetrahedron*, **1986**, *42*, 417.

25. (a) Breslow, R.; Chang, H. W. *J. Am. Chem. Soc.* **1965**, *87*, 2200. (b) Breslow, R.; Chang, H. W.; Hill, R.; Wasserman, E. *J. Am. Chem. Soc.* **1967**, *89*, 1112.

26. Maskill, H. *The Physical Basis of Organic Chemistry*; Oxford University Press: New York, 1985.

27. Brϕnsted, J. N.; Pedersen, K. J. *Z. Phys. Chem. (Leipzig)* **1924**, *108*, 185.

28. Brϕnsted, J. N. *Chem. Rev.* **1928**, *5*, 23.

29. Lowry, T. H.; Richardson, K. S. *Mechanism and Theory in Organic Chemistry 3rd ed.*; Harper and Row: New York, 1987.

30. Isaacs, N. S. *Physical Organic Chemistry*; Longman Scientific and Technical: Essex, 1987.

31. Arrowsmith, C. H.; Kresge, A. J.; Tang, Y. C. *J. Am. Chem. Soc.* **1991**, *113*, 179.

32. Hammett, L. P. *Chem. Rev.* **1935**, *17*, 125.

33. Bordwell, F. C.; Cripe, T. A.; Hughes, D. L. *Advances in Chemistry: Nucleophilicity* **1987**, *215*, 137.

34. Bordwell, F. C.; Zhang, X.-M. *Acc. Chem. Res.* **1993**, *26*, 510.

35. For an example see Bowden, K.; Chana, R. S. *J. Chem. Soc. Perkin Trans. 2* **1990**, 2163.

36. Streitwieser, A., Jr.; Kaufman, M. J.; Bors, D. A.; Murdoch, J. R.; MacArthur, C. A.; Murphy, J. T.; Shen, C. C. *J. Am. Chem. Soc.* **1985**, *107*, 6983.

37. Bernasconi, C. F.; Kliner, D. A. V.; Mullin, A. S.; Ni, J. K. *J. Org. Chem.* **1988**, *53*, 3342.

38. (a) Gronert, S.; Streitwieser, A., Jr. *J. Am. Chem. Soc.* **1988**, *110*, 2836. (b) Gronert, S.; Streitwieser, A., Jr. *J. Am. Chem. Soc.* **1988**, *110*, 2843.

39. Bowden, K.; Nadvi, N. S.; Ranson, R. J. *J. Chem. Res.* **1990**, 299.

40. Buncel, E., Durst, T., Eds. *Comprehensive Carbanion Chemistry*; Elsevier: Amsterdam, 1984; Part A.

41. (a) Kresge, A. J. *Chem. Soc. Rev.* **1973**, *2*, 475. (b) Kresge, A. J. *Acc. Chem. Res.* **1975**, *8*, 354.

42. Bernasconi, C. F.; Terrier, F. *J. Am. Chem. Soc.* **1987**, *109*, 7115.

43. Eigen, M. *Angew. Chem., Int. Edn.* **1964**, *3*, 1.

44. Bunting, J. W.; Stefanidis, D. *J. Am. Chem. Soc.* **1989**, *111*, 5834.

45. Bordwell, F. G.; Hughes, D. L. *J. Am. Chem. Soc.* **1985**, *107*, 4737.

46. Jencks, W. P. *Chem. Rev.* **1985**, *85*, 511.

47. Jencks, W. P.; Brant, S. R.; Gandler, J. R.; Fendrich, G.; Nakamura, C. *J. Am. Chem. Soc.* **1982**, *104*, 7045.

48. Jencks, W. P. *Advances in Chemistry: Nucleophilicity* **1987**, *215*, 155.

49. Jencks, D. A.; Jencks, W. P. *J. Am. Chem. Soc.* **1977**, *99*, 7948.

50. Bunting, J. W.; Stefanidis, D. *J. Am. Chem. Soc.* **1990**, *112*, 779.

51. (a) Pross, A. *J. Org. Chem.* **1984**, *49*, 1811. (b) Pross, A.; Shaik, S. S. *New J. Chem.* **1989**, *13*, 427.

52. Wan, P.; Shukla, D. *Chem. Rev.* **1993**, *93*, 571.

53. Weller A. *Prog. React. Kinet.* **1961**, *1*, 189.

54. Vander Donckt, E. *Prog. React. Kinet.* **1970**, *5*, 273.

55. Ireland, J. F.; Wyatt, P. A. H. *Adv. Phys. Org. Chem.* **1976**, *12*, 131.

56. Martynov, I. Y.; Demyoshkevich, A. B.; Uzhimov, B. M.; Kuzmin, M. G. *Russian Chem. Rev.* **1977**, *46*, 1.

57. Kelly, R. N.; Schulmann, S. G. *Molecular Luminescence Spectroscopy: Methods and Applications-Part II*; Wiley: New York, 1988.

58. Arnaut, L. G.; Formosinho, S. J. *J. Photochem. Photobiol. A: Chem.* **1993**, *75*, 1.

59. Formosinho, S. J.; Arnaut, L. G. *J. Photochem. Photobiol. A: Chem.* **1993**, *75*, 21.

60. Weber, K. *Z. Phys. Chem.* **1931**, *B15*, 18.

61. (a) Förster, T. *Naturwiss.* **1949**, *36*, 186. (b) Förster, T. *Z. Elektrochem.* **1950**, *54*, 42. (c) Förster, T. *Z. Elektrochem.* **1950**, *54*, 531.

62. (a) Weller, A. *Z. Elektrochem.* **1952**, *56*, 662. (b) Weller, A. *Z. Physik. Chem.* **1955**, *3*, 238. (c) Weller, A. *Z. Physik. Chem.* **1958**, *15*, 438.

63. Mason, S. F.; Smith, B. E. *J. Chem. Soc. (A)* **1969**, 325.

64. Turro, N. J. *Modern Molecular Photochemistry*; Benjamin/Cummings: Menlo Park, 1978.

65. Wubbels, G. G. *Acc. Chem. Res.* **1983**, *16*, 285.

66. Wubbels, G. G.; Sevetson, B. R.; Kaganove, S. N. *Tetrahedron Lett.* **1986**, *27*, 3103.

67. (a) Yates, K. *J. Am. Chem. Soc.* **1986**, *108*, 6511. (b) McEwen, J.; Yates, K. *J. Am. Chem. Soc.* **1987**, *109*, 5800.

68. (a) McClelland, R. A.; Cozens, F.; Steenken, S. *Tetrahedron Lett.* **1990**, 3821. (b) Cozens, F. L.; Mathivanan, N.; McClelland, R. A.; Steenken, S. *J. Chem. Soc., Perkin Trans.* 2 **1992**, 2083. (c) McClelland, R. A.; Chan, C.; Cozens, F.; Modro, A.; Steenken, S. *Angew. Chem., Int. Ed. Engl.* **1991**, *30*, 1337.

69. Wan, P.; Yates, K. *J. Org. Chem.* **1983**, *48*, 869.

70. Fukui, K. *Acc. Chem. Res.* **1971**, *4*, 57.

71. Ter Borg, A. P.; Kloosterziel, H. *Recueil* **1965**, *84*, 241.

72. Ter Borg, A. P.; Razenberg, E.; Kloosterziel, H. *Chem. Commun.* **1967**, 23, 1210.

73. Ter Borg, A. P.; Kloosterziel, H. *Recueil* **1969**, *88*, 266.

74. Tezuka, T.; Kikuchi, O.; Houk, K. N.; Paddon-Row, M. N.; Santiago, C. M.; Rondan, N. G.; Williams, J. C., Jr.; Gandour, R. W. *J. Am. Chem. Soc.* **1981**, *103*, 1367.

75. Reid, P. J.; Wickham, S. D.; Mathies, R. A. *J. Phys. Chem.* **1992**, *96*, 5720.

76. Reid, P. J.; Lawless, M. K.; Wickham, S. D.; Mathies, R. A. *J. Phys. Chem.* **1994**, *98*, 5597.

77. (a) Reid, P. J.; Doig, S. J.; Mathies, R. A. *Chem. Phys. Lett.* **1989**, *156*, 163. (b) Reid, P. J.; Doig, S. J.; Mathies, R. A. *J. Phys. Chem.* **1990**, *94*, 8396.

78. Pomerantz, M.; Gruber, G. W. *J. Am. Chem. Soc.* **1971**, *93*, 6615.

79. Burdett, K. A.; Shenton, F. L.; Yates, D. H.; Swenton, J. S. *Tetrahedron* **1974**, *30*, 2057.

80. Gilbert, A.; Baggott, J. *Essentials of Molecular Photochemistry*; Blackwell Scientific Publications: Oxford, 1991.

81. Hixson, S. S. *Organic Photochemistry*; Padwa, A., Ed.; Marcel Dekker, Inc.: New York, 1979; vol. 4.

82. Reichardt, C. *Solvents and Solvent Effects in Organic Chemistry*; VCH: Weinheim, 1988.

83. (a) Rideout, D. C.; Breslow, R. *J. Am. Chem. Soc.* **1980**, *102*, 7816. (b) Breslow, R. *Acc. Chem. Res.* **1991**, *24*, 159. (c) Blokzijl, W.; Blandamer, M. J.; Engberts, J. B. F. N. *J. Am. Chem. Soc.* **1991**, *113*, 4241.

84. (a) White, W. N.; Wolfarth, E. F. *J. Org. Chem.* **1970**, *35*, 2196. (b) Coates, R. M.; Rogers, B. D.; Hobbs, S. J.; Peck, D. R.; Curran D. P. *J. Am. Chem. Soc.* **1937**, *109*, 1160. (c) Gajewski, J. J.; Jurazj, J.; Kimbrough, D. R.; Grande,

M. E.; Ganem, B.; Carpenter, B. K. *J. Am. Chem. Soc.* **1987**, *109*, 1170. (d) Brandes, E.; Greico, P. A.; Gajewski, J. J. *J. Org. Chem.* **1989**, *54*, 515. (e) Severance, D. L.; Jorgensen, W. L. *J. Am. Chem. Soc.* **1992**, *114*, 10966.

85. Desimoni, G.; Faita, G.; Righetti, P. P.; Sfulcini, A.; Tsyganov, D. *Tetrahedron*, **1994**, *50*, 1821.

86. Bergson, G.; Weidler, A.-M. *Acta Chem. Scand.* **1963**, *17*, 1798.

87. Wold, S; Bergson, G. *Ark. Kemi* **1967**, *28*, 245.

88. Alvarez-Idaboy, J. R.; Lunell, S.; Matsson, O.; Bergson, G. *Acta Chem. Scand.* **1994**, *48*, 423.

89. Meurling, L. *Chem. Scr.* **1975**, *7*, 23.

90. Hussénius, A.; Matsson, O.; Bergson, G. *J. Chem. Soc., Perkin Trans. 2* **1989**, 851.

91. Lapouyade, R.; Koussini, R.; Bouas-Laurent, H. *J. Am. Chem. Soc.* **1977**, *99*, 7374.

92. (a) van Arendonk, R. J. F. M.; Fornier de Violet, Ph.; Laarhoven, W. H. *Recl. Trav. Chim. Pays-Bas* **1981**, *100*, 256. (b) Laarhoven, W. H.; Berendsen, N. *Recl. Trav. Chim. Pays-Bas* **1986**, *105*, 367. (c) Cuppen, Th. J. H. M.; Berendsen, N.; Laarhoven, W. H. *Recl. Trav. Chim. Pays-Bas* **1990**, *109*, 168.

93. (a) Somers, J. B. M.; Couture, A.; Lablache-Combier, A.; Laarhoven, W. H. *J. Am. Chem. Soc.* **1985**, *107*, 1387. (b) Woning, J.; Weisenborn, P. C. M.; Varma, A. G. O.; Laarhoven, W. H. *J. Photochem. Photobiol. A: Chem.* **1990**, *55*, 169.

94. Hixson, S. S.; Mariano, P. S.; Zimmerman, H. E. *Chem. Rev.* **1973**, *73*, 531.

95. (a) Swenton, J. S. *J. Chem. Ed.* **1969**, *46*, 217. (b) Givens, R. S.; Oettle, W. F. *Chem. Commun.* **1969**, 1164. (c) Dauben, W. G.; Kellogg, M. S.; Seeman, J. I.; Spitzer, W. A. *J. Am. Chem. Soc.* **1970**, *92*, 1786.

96. (a) Armesto, D.; Horspool, W. M.; Apoita, M.; Gallego, M. G.; Ramos, A. *J. Chem. Soc. Perkin Trans. 1* **1989**, 2035. (b) Armesto, D.; Gallego, M. G.; Horspool, W. M. *Tetrahedron Letts.* **1990**, 2475.

97. Zimmerman, H. E. *Organic Photochemistry*; Padwa, A., Ed.; Marcel Dekker, Inc.: New York, 1991; vol. 11.

98. Zimmerman, H. E.; Armesto, D.; Amezua, M. G.; Gannett, T. P.; Johnson, R. P. *J. Am. Chem. Soc.* **1979**, *101*, 6367.

99. Zimmerman, H. E.; Boettcher, R. J.; Braig, W. *J. Am. Chem. Soc.* **1973**, *95*, 2155.

100. Zimmerman, H. E.; Factor, R. E. *Tetrahedron* **1981**, *37*, Supplement 1, 125.

101. Adam, W.; De Lucchi, O.; Dörr, M. *J. Am. Chem. Soc.* **1989**, *111*, 5209.

102. Reguero, M.; Bernardi, F.; Jones, H.; Olivucci, M.; Ragazos, I. N.; Robb, M. A. *J. Am. Chem. Soc.* **1993**, *115*, 2073.

103. Quenemoen, K.; Borden, W. T.; Davidson, E. R.; Feller, D. *J. Am. Chem. Soc.* **1985**, *107*, 5054.

104. Zimmerman, H. E.; Sulzbach, H. M.; Tollefson, M. B. *J. Am. Chem. Soc.* **1993**, *115*, 6548.

105. (a) Zimmerman, H. E.; Pratt, A. C. *J. Am. Chem. Soc.* **1970**, *92*, 1409. (b) Zimmerman, H. E.; Pratt, A. C. *J. Am. Chem. Soc.* **1970**, *82*, 6267.

106. (a) Zimmerman, H. E.; Grunewald, G. L. *J. Am. Chem. Soc.* **1966**, *88*, 183. (b) Zimmerman, H. E.; Binkley, B. W.; Givens, R. S.; Sherwin, M. A. *J. Am. Chem. Soc.* **1967**, *89*, 3932. (c) Zimmerman, H. E.; Binkley, B. W.; Givens, R. S.; Grunewald, G. L.; Sherwin, M. A. *J. Am. Chem. Soc.* **1969**, *91*, 3316.

107. (a) Griffin, G. W.; Marcantonio, A. F.; Kristinsson, H. *Tetrahedron Lett.* **1965**, 2951. (b) Hixson, S. *Tetrahedron Lett.* **1972**, 1155.

108. Morrison, H. *Organic Photochemistry*; Padwa, A., Ed.; Marcel Dekker, Inc.: New York, 1979; vol. 4.

109. Shukla, D. *Ph. D. Dissertation*, University of Victoria, 1994.

110. Steuhl, H.-M.; Klessinger, M. *Angew. Chem., Int. Ed. Engl.* **1994**, *33*, 2431.

111. Murov, S. L.; Carmichael, I.; Hug, G. L. *Handbook of Photochemistry*; Marcel Dekker: New York, 1993.

112. Wan, P.; Budac, D.; Krogh, E. *J. Chem. Soc., Chem. Commun.* **1990**, 255.

113. Budac, D. *M.Sc. Thesis*, University of Victoria, **1990**.

114. (a) Downing, A. P.; Ollis, W. D.; Nógradi, M.; Sutherland, I. O. *The Jerusalem Symposia on Quantum Chemistry and Biochemistry Vol. III: Aromaticity, Pseudo-aromaticity, Anti-aromaticity*; The Israel Academy of Sciences and Humanities: Jerusalem, 1971, 296. (b) Young, S. D.; Baldwin, J. J.; Cochran, D. W.; King, S. W.; Remy, D. C.; Springer, J. P. *J. Org. Chem.* **1985**, *50*, 339. (c) Cioranescu, E.; Voicu, A.; Elian, M. *Revue Roumaine de Chimie* **1989**, *34*, 87.

115. Pomerantz, M.; Fink, R. *J. Org. Chem.* **1977**, *42*, 2788.

116. Budac, D.; Shukla, D.; Krogh, E.; Wan, P. *J. Photochem. Photobiol. A: Chem.* **1992**, *67*, 33.

117. Shi, M.; Shouki, K.; Okamoto, Y.; Takamuku, S. *J. Chem. Soc. Perkins Trans. 1* **1990**, 2443.

118. (a) Shi, M.; Okamoto, Y.; Takamuku, S. *J. Chem. Soc. Chem. Commun.* **1989**, 151. (b) Shi, M.; Okamoto, Y.; Takamuku, S. *Bull. Chem. Soc. Jpn.* **1990**, *63*, 453. (c) Shi, M.; Okamoto, Y.; Takamuku, S. *Bull. Chem. Soc. Jpn.* **1990**, *63*, 1269.

119. (a) Shi, M.; Okamoto, Y.; Takamuku, S. *J. Chem. Research (S)* **1990**, 131. (b) Shi, M.; Okamoto, Y.; Takamuku, S. *Chem. Lett.* **1990**, 1079. (c) Shi, M.; Okamoto, Y.; Takamuku, S. *Bull. Chem. Soc. Jpn.* **1990**, *63*, 3345. (d) Shi, M.; Okamoto, Y.; Takamuku, S. *J. Chem. Research (S)* **1990**, 346.

120. Studies of the keto-enol interconversion of 2-acetylcyclohexanone involving D_2O and H_2O indicate that the latter is 1.2 times more basic and 5 times more acidic than the former. See: Riley, T.; Long, F. A. *J. Am. Chem. Soc.* **1962**, *84*, 522.

121. Albert, A.; Serjeant, E. P. *The Determination of Ionization Constants: A Laboratory Manual*; Chapman and Hall: London, 1984.

122. (a) Lewis, F. D.; Ho, T.-I. *J. Am. Chem. Soc.* **1977**, *99*, 7991. (b) Lewis, F. D.; Ho, T.-I.; Simpson, J. T. *J. Org. Chem.* **1981**, *46*, 1077.

123. Lewis, F. D. *Advances in Photochemistry* **1986**, *13*, 165.

124. (a) Lewis, F. D.; Reddy, G. D.; Schneider, S.; Gahr, M. *J. Am. Chem. Soc.* **1991**, *113*, 3498. (b) Lewis, F. D.; Bassani, D. M.; Reddy, G. D. *J. Org. Chem.* **1993**, *58*, 6390. (c) Lewis, F. D.; Reddy, G. D.; Bassani, D. M.; Schneider, S.; Gahr, M. *J. Am. Chem. Soc.* **1994**, *116*, 597.

125. Lewis, F. D.; Reddy, G. D. *Tetrahedron Lett.* **1992**, *33*, 4249.

126. Hofer, O.; Weissensteiner, W. *Monatshefte für Chemie* **1992**, *123*, 1045.

127. Watanabe, K.; Mottl, J. R. *J. Chem. Phys.* **1957**, *26*, 1773.

128. Lewis, F. D.; Correa, P. E. *J. Am. Chem. Soc.* **1984**, *106*, 194.

129. Ege, S. N. *Organic Chemistry*; D. C. Heath and Co.: Toronto, 1984.

130. (a) Streitwieser, A., Jr. *Progress in Physical Organic Chemistry*; Cohen, S. G., Streitwieser, A., Jr., Taft, R. W., Eds.; Interscience Publishers: New York, 1974; vol. 1. (b) Jones, F. M., III; Arnett, E. M. *Progress in Physical Organic Chemistry*; Streitwieser, A., Jr., Taft, R. W., Eds.; Interscience Publishers: New York, 1974; vol. 11.

131. Kuhn, H. J.; Braslavsky, S. E.; Schmidt, R. *Pure and Appl. Chem.* **1989**, *61*, 187.

132. Arnett, E. M. *Progress in Physical Organic Chemistry*; Cohen, S. G., Streitwieser, A., Jr., Taft, R. W., Eds.; Interscience Publishers: New York, 1963; vol. 1.

133. Kolthoff, I. M.; Bruckenstein, S. *J. Am. Chem. Soc.* **1956**, *78*, 1.

134. Eaton, D. F. *Pure and Appl. Chem.* **1988**, *60*, 1107.

135. Birch, D. J. S.; Imhof, R. E. *Topics in Fluorescence Spectroscopy: Vol. 1 Techniques*; Lakowicz, J. R., Ed.; Plenum Press: New York, 1991.

136. Both **108** and **138** used in the fluorescence lifetimes studies were obtained from Dr. Erik Krogh.

137. Hope, D. J.; Pohl, E. R. *J. Am. Chem. Soc.* **1984**, *106*, 5634.

138. The fluorescence quenching rates obtained for **78** and **80** were derived using fluorescence lifetimes measured by Dr. Erik Krogh.

139. Eftink, M. *Topics in Fluorescence Spectroscopy: Vol. 2 Principles*; Lakowicz, J. R., Ed.; Plenum Press: New York, 1991.

140. These fluorescence lifetimes were measured on a picosecond laser system by Dr. Erik Krogh at the Center for Fast Kinetics Research (CFKR) in the University of Texas at Austin.

141. (a) Stevens, C. G.; Strickler, S. J. *J. Am. Chem. Soc.* **1973**, *95*, 3922. (b) Shizuka, H. *Acc. Chem. Res.* **1985**, *18*, 141. (c) Wan, P.; Wu, P. *J. Chem. Soc., Chem. Commun.* **1990**, 822.

142. Manoharan, R.; Dogra, S. K. *J. Photochem. Photobiol. A: Chem.* **1988**, *43*, 81.

143. Zhang, X.; Yeb, S.-R.; Hong, S.; Freccero, M.; Albini, A.; Falvey, D. E.; Mariano, P. S. *J. Am. Chem. Soc.* **1994**, *116*, 4211.

144. Lewis, F. D.; Bassami, D. M. *J. Photochem. Photobiol. A: Chem.* **1994**, *81*, 13.

145. (a) Coetzee, J. F. *Progress in Physical Organic Chemistry*; Streitwieser, A., Jr., Taft, R. W., Eds.; Interscience Publishers: New York, 1967; vol. 4. (b) Serjeant, E. P. *Chemical Analysis: Vol. 69 Potentiometry and Potentiometric Titrations*; Elving, P. J., Winefordner, J. D., Kolthoff, I. M., Eds.; John Wiley and Sons: New York, 1984.

146. Förster cycle calculations were performed by Dr. Peter Wan using an $E_{0,0}$ value of ≈ 34 kcal mol^{-1} obtained from the absorption spectrum of 7 generatedy in THF using n-BuLi.

147. Tolbert, L. M.; Ali, M. Z. *J. Org. Chem.* **1982**, *47*, 4793.

148. Halton, B.; Officer, D. L. *Aust. J. Chem.* **1983**, *36*, 1167.

149. Coburn, T. T.; Jones, W. M. *J. Am. Chem. Soc.* **1974**, *96*, 5218.

150. Griffen, G. W.; Horn, K. A. *Org. Prep. Proceed. Int.* **1985**, *17*, 187.

151. March, J. *Advanced Organic Chemistry*; John Wiley and Sons: New York, 1985.

152. Adams, R.; Binder, L. O. *J. Am. Chem. Soc.* **1941**, *63*, 2773.

153. Maigrot, N.; Mazaleyrat, J.-P. *Synthesis*, **1985**, 317.

154. Bestmann, H. J.; Both, W. *Chem. Ber.* **1974**, *107*, 2926.

155. Mislow, K.; McGinn, F. A. *J. Am. Chem. Soc.* **1958**, *80*, 6036.

156. Lambert, J. B.; Shurvell, H. F.; Lightner, D. A.; Cooks, R. G. *Introduction to Organic Spectroscopy*; Macmillan Publishing Company: New York, 1987.

157. Smith, J. G.; Dibble, P. W.; Sandborn, R. E. *J. Org. Chem.* **1986**, *51*, 3762.

158. Personal communication with Dr. V. Iyer.

159. Richarson, D. B.; Durrett, L. R.; Martin, J. M., Jr.; Putnam, W. E.; Slaymaker, S. C.; Duoretzky, I. *J. Am. Chem. Soc.* **1965**, *87*, 2763.

160. (a) Clar, E.; McAndrew, R. A.; Zander, M. *Tetrahedron* **1967**, 23, 985. (b) Lambert, J. B.; Fabricius, D. M.; Hoard, J. A. *J. Org. Chem.* **1979**, *44*, 1480.

161. Müller, E.; Kessler, H.; Suhr, H. *Tetrahedron Lett.* **1965**, 423.

162. (a) Hine, J.; Dalsin, P. D. *J. Am. Chem. Soc.* **1972**, *94*, 6998. (b) Bordwell, F. G.; Bares, J. E.; Bartmess, J. E.; McCollum, G. J.; Van Der Puy, M.; Vanier, N. R.; Matthews, W. S. *J. Org. Chem.* **1977**, *42*, 321. (c) Grossert, J. S.; Hoyle, J.; Cameron, T. S.; Roe, S. P.; Vincent, B. R. *Can. J. Chem.* **1987**, *65*, 1407. (d) Bernasconi, C. F.; Ohlberg, D. A. A.; Stronach, M. W. *J. Org. Chem.* **1991**, *56*, 3016. (e) Bordwell, F. G.; Vanier, N. R.; Zhang, X. *J. Am. Chem. Soc.* **1991**, *113*, 9856.

163. (a) Hayday, K.; McKelvey, R. D. *J. Org. Chem.* **1976**, *41*, 2222. (b) Malatesta, V.; Ingold, K. U. *J. Am. Chem. Soc.* **1981**, *103*, 609. (c) Beckwith, A. L. J.; Easton, C. J. *J. Am. Chem. Soc.* **1981**, *103*, 615.

164. Larson, A.; Lee, F.; Page, Y.; Webster, M.; Charland, J.; Gabe, E. J. *NRC Solver: A program for crystal structure determination*, Chemistry Division, NRC, Ottawa, Canada, 1985.

165. Sheldrick, G. M. *SHELX: A program for crystal structure determination*, Anorganish-Chemisches Institut der Universitat Gottingen, Germany, 1976.

166. *Dictionary of Organic Compounds 5th ed.*; Chapman and Hall: Toronto, 1982.

167. Pouchert, C. J.; Campbell, J. R. *The Aldrich Library of NMR Spectra* Aldrich Chemical Company Inc., Milwaukee, 1974.

168. The chromic acid solution used was prepared according to the procedure outlined in: Vogel, A. *Vogel's Textbook of Practical Organic Chemistry*; Furniss, B. S., Hannaford, A. J., Rogers, V., Smith, P. W. G., Tatchell, A. R., Eds.; Longman Inc.: New York, 1978; 4th edition.

169. Hayashi, T.; Hayashizaki, K.; Kiyoi, T.; Ito, Y. *J. Am. Chem. Soc.* **1988**, *110*, 8153.

170. *Handbook of Chemistry and Physics 48th ed.*; Weast, R. C., Selby, S. M., Eds.; The Chemical Rubber Co.: Cleveland, 1967.

VITA

Surname: Budac Given Names: David Patrick

Place of Birth: Fort St. John, B. C. Canada

Educational Institutes Attended:

University of Victoria 1983-1995

Degrees Awarded:

B.Sc. (Honours)	University of Victoria	1988
M.Sc.	University of Victoria	1990

PUBLICATIONS

7. D. Budac and P. Wan, Recent Advances in Photochemical Reactions Involving Carbanions, submitted to *Advances in Carbanion Chemistry*, **1993**.

6. P. Wan and D. Budac, Photodecarboxylation of Acids and Lactones, *Handbook of Organic Photochemistry*, **1995** in press.

5. D. Budac and P. Wan, Photodecarboxylation: Mechanisms and Synthetic Utility, *J. Photochem. Photobiol., A*, **1992**, *67*, 135-166.

4. D. Budac, D. Shukla, E. Krogh and P. Wan, Photosolvolysis of 5-Substituted Dibenzosuberol Derivatives: A Stereoelectronic Requirement for Carbocation Photogeneration, *J. Photochem. Photobiol., A*, **1992**, *64*, 33-40.

3. D. Budac and P. Wan, Excited State Carbon Acids. Facile Benzylic C-H Bond Heterolysis of Suberene on Photolysis in Aqueous Solution: A Photogenerated Cyclically Conjugated Eight π Electron Carbanion, *J. Org. Chem.*, **1992**, *57*, 887-894.

2. P. Wan, D. Budac, M. Earle and D. Shukla, Photochemical C-H Bond Heterolysis vs. Formal Di-π-Methane Rearrangement of 5*H*-Dibenzo[a,c]cycloheptene and Related Compounds, *J. Am. Chem. Soc.*, **1990**, *112*, 8048-8054.

1. P. Wan, D. Budac and E. Krogh, Excited State Carbon Acids: Base Catalyzed Photoketonization of Dibenzosuberenol to Dibenzosuberone via Initial C-H Bond Heterolysis from S_1, *J. Chem. Soc., Chem. Commun.*, **1990**, 255-257.

PARTIAL COPYRIGHT LICENSE

I hereby grant the right to lend my dissertation to users of the University of Victoria Library, and to make single copies only in such cases or in response to a request from the Library of any university or similar institution, on its behalf or for one of its users. I further agree that permission for extensive copying of this dissertation for scholarly purposes may be granted by me or a member of the University designated by me. It is understood that copying or publication of this thesis for financial gain shall not be allowed without my written permission.

Title of Dissertation: Excited State Carbon Acidity of the Benzylic Position of Dibenzannelated Cycloheptatrienes

Author: _____

David Patrick Budac

Date: July 19, 1995